

Modelling and Development of Process Control for a Vascular Tissue Engineering Bioreactor

Thesis submitted for the degree of

Doctor of Philosophy
In
Biochemical Engineering

By
Matthew William Scutcher
MEng ACGI

The Advanced Centre for Biochemical Engineering
Department of Biochemical Engineering
University College of London

To my parents, William and Anthea

Acknowledgements

I would like to thank all the people who have helped me work towards this thesis: Within the Department of Biochemical Engineering at UCL my principal supervisor, Dr. Yuhong Zhou and my co-supervisor Dr. Chris Mason as well as Prof. Mike Hoare and Prof. Nigel Titchener-Hooker for all of their enthusiasm, help, encouragement and support as well as gentle pressure at times.

I would also like to thank Dr. Spyridon Gerontas for his assistance with Comsol Multiphysics, Alfred Ding for his help with the bioreactor and the entire Regenerative Medicine Bioprocessing (ReMeBio) group for help with cell culture and a positive working environment with special mention for Meg Gillett for persuading me that the skies were not falling down on more than one occasion.

Outside of work, I would like to acknowledge the contribution all those friends whose birthdays were missed over the years and all my housemates who have endured my oscillatory moods, particularly Ian, Fran, Ed, Megan, Annie, Rayno and Lize Marie.

I would like to thank Adam Stonier for all the coffee and associated, at times, decidedly odd conversations; Simon Edwards Parton for bailing me out once or twice with computer disasters; John, Rich, and Andy for not letting us die up a mountain in Slovenia; and Lucy, Marcel and Dave for all the beers.

I would also like to gratefully thank the EPSRC and the department of Biochemical Engineering for their financial support that allowed me to perform this work.

Finally, and most importantly, I would like to thank my parents who have at times lived my PhD vicariously through me. I could have completed this without their love and support.

Table of Contents

1.	Introduction.....	15
1.1	Traditional treatment of coronary artery disease.....	19
1.1.1	Autologous graft.....	20
1.1.2	Synthetic graft.....	21
1.2	Tissue engineering bypass grafts.....	22
1.3	Tissue engineering process.....	27
1.3.1	Raw materials.....	27
1.3.1.1	Mature cells.....	28
1.3.1.2	Mesenchymal stem cells.....	30
1.3.1.3	Embryonic stem cells.....	31
1.3.2	Cell culture media.....	35
1.3.3	Polymeric scaffolds for tissue engineering.....	37
1.3.4	Key stages within a tissue engineering process.....	42
1.3.4.1	Biopsy.....	44
1.3.4.2	Purification.....	46
1.3.4.3	Culture.....	48
1.3.4.4	Harvest and implantation.....	49
1.4	Bioreactors in tissue engineering.....	49
1.4.1	Small-scale cell proliferation.....	50
1.4.2	Generation of three dimensional tissue constructs.....	51
1.4.3	Direct organ support devices.....	54
1.4.4	Traditional bioprocessing.....	55
1.5	Control parameters within tissue engineering bioreactors.....	60

1.5.1	pH.....	61
1.5.2	Temperature.....	64
1.5.3	Substrates and metabolism.....	65
1.5.4	Dissolved oxygen tension.....	66
1.5.5	Representing acceptable ranges of environmental parameters.....	67
1.6	Existing manufacture of tissue engineering products.....	68
1.6.1	Blood vessels.....	69
1.6.2	Skin.....	69
1.6.3	Cartilage.....	72
1.6.4	Summary.....	73
1.7	Conclusions.....	74
1.8	Project Aims.....	75
2.	Materials and methods.....	77
2.1	Mesenchymal stem cell culture.....	77
2.1.1	Isolation.....	77
2.1.2	Culture vessel.....	78
2.1.3	Culture medium.....	79
2.1.4	Passaging MSC.....	79
2.1.5	Refeeding MSC.....	80
2.1.6	Cell counting and viability.....	81
2.2	Yeast Culture.....	81
2.2.1	Yeast extract peptone dextrose (YEPD) broth.....	81
2.2.2	Initial Culture.....	81
2.3	Bioreactor system.....	82

2.3.1	Pumps.....	83
2.3.2	Tubing.....	84
2.3.3	Oxygenator.....	85
2.3.4	Media and waste storage.....	86
2.3.5	Bioreactor.....	86
2.3.5.1	Alginate preparation.....	87
2.3.5.2	Preparation of cells for mixing with alginate.....	87
2.3.5.3	Hydrogen perfusion media preparation.....	88
2.3.5.4	Alginate tube extrusion.....	88
2.3.6	Bioreactor containment and thermal insulation.....	90
2.3.7	Cooling of fresh feed.....	91
2.3.8	Oxygen measurement.....	92
2.4	Computer modelling.....	93
2.4.1	MATLAB.....	93
2.4.2	Comsol Multiphysics.....	95
3.	Modelling the vascular tissue engineering bioreactor (VTEB).....	98
3.1	Introduction.....	98
3.2	Model variables.....	99
3.2.1	Batch sheet data.....	101
3.2.2	Descriptive data.....	103
3.2.3	Expert comments.....	104
3.2.4	Forming equations.....	104
3.3	Modelling the oxygenator.....	107
3.4	Modelling the bioreactor.....	110

3.4.1	Modelling the alginate scaffold.....	111
3.4.2	Modelling cell growth in the bioreactor.....	114
3.4.3	Modelling substrate uptake in the bioreactor.....	116
3.5	Modelling system flows.....	120
3.6	Overall model.....	122
3.7	Conclusions.....	125
4.	The control of oxygen tension within the VTEB.....	127
4.1	Introduction.....	127
4.1.1	Human mesenchymal stem cells.....	128
4.1.2	Yeast.....	129
4.1.3	Measurement of dissolved oxygen tension (DOT).....	129
4.2	Method of controlling DOT within the VTEB.....	130
4.2.1	Control mechanism and manipulation of variables.....	132
4.2.2	Types of controller.....	132
4.3	Determining the capacity of the system and the acceptable range of flow rates.....	136
4.3.1	Oxygen uptake rate model.....	136
4.3.2	Window of operation for dissolved oxygen tension.....	143
4.4	Designing process controllers.....	152
4.4.1	Two-step controller.....	153
4.4.2	Proportional-Integral controller.....	155
4.4.3	Testing the control system.....	162
4.5	Conclusions.....	162

5.	Considering pH within the VTEB system.....	165
5.1	Cell media buffers.....	165
5.2	Bicarbonate Buffer.....	167
5.3	HEPES buffering system.....	168
5.4	Calculating the window of operation for pH versus lactic acid concentration.....	168
5.5	Single pass pH window of operation.....	173
5.6	Continuous pH window of operation.....	175
5.7	Conclusions.....	178
6.	Process control of respiratory metabolites.....	179
6.1	Glucose.....	179
6.2	Lactate.....	182
6.3	Glutamine.....	184
6.4	Ammonia.....	187
6.5	Combination of metabolic windows of operation.....	190
6.6	Process Control.....	192
6.7	Conclusions.....	196
7.	Overall process control.....	197
7.1	Introduction.....	197
7.2	Comparing windows of operation.....	198
7.3	Modification of operating conditions.....	199
7.4	Integrated control model.....	205
7.5	Conclusions.....	210

8.	Conclusions and further work.....	212
8.1	Bioreactor system.....	212
8.2	Dissolved oxygen tension (DOT) process control.....	213
8.3	Metabolic compound process control.....	214
8.4	Overall system control model.....	215
8.5	Future work.....	217
Appendices.....		219
Appendix 1 – Oxygen model level 1.....		220
Appendix 1 – Oxygen model level 2 (oxygenator).....		221
Appendix 1 – Oxygen model level 2 (bioreactor).....		222
Appendix 2 – Substrate model level 1.....		223
Appendix 2 – Substrate model level 2.....		224
Appendix 3 – Overall top model.....		225
References.....		226

List of Figures

Figure 1.1	Coronary artery bypass graft.....	17
Figure 1.2	Human artery structure.....	18
Figure 1.3	L'heurueux's tissue engineered artery after 9 weeks maturation.....	24
Figure 1.4	Tissue engineering process.....	44
Figure 1.5	Qualitative operating boundaries for an aerobic bacterial fermentation.....	67
Figure 2.1	General layout of the bioreactor system.....	82
Figure 2.2	OX miniature gas exchange oxygenator by living systems.....	86
Figure 2.3	Extrusion of alginate scaffold tube.....	90
Figure 2.4	Partitioned bioreactor system container.....	91
Figure 2.5	Flow chamber for oxygen spots designed by Ding and Town.....	93
Figure 2.6	Screenshot of a simple Simulink program.....	94
Figure 2.7	Reduction of Comsol model from 2D to 3D.....	96
Figure 2.8	A simple example of finite element modelling (FEM).....	96
Figure 3.1	Sub-Division of fermentation data.....	99
Figure 3.2	Relationship between bulk flow through the oxygenator and the oxygen uptake coefficient.....	109
Figure 3.3	Length of alginate tube based upon the priming volume of alginate solution.....	111
Figure 3.4	Length of alginate tube based upon priming volumes of 1% and .2% alginate solution.....	113

Figure 3.6	Phases of the cell cycle.....	117
Figure 3.7	Flows within the VTEB system.....	121
Figure 3.8	Changes in oxygen concentration within the system.....	123
Figure 4.1	Process control feedback loop for DOT.....	135
Figure 4.2	Final yeast cell number within the alginate scaffold.....	138
Figure 4.3	Yeast cell composite growth curves.....	139
Figure 4.4	Yeast cell oxygen uptake rate curves.....	139
Figure 4.5	Theoretical model determining cell number within the scaffold based upon oxygen uptake rate.....	142
Figure 4.6	Oxygen gradients within the alginate scaffold.....	146
Figure 4.7	Initial window of operation (WOO) relating the flow rate of the recycle stream to the cell concentration within the scaffold.....	147
Figure 4.8	Enhanced window of operation incorporating shear stress.....	148
Figure 4.9	Window of operation for relating cell concentration and feed rate....	152
Figure 4.10	Location of DOT sensor within the system.....	153
Figure 4.11	Two step control of DOT at the exit of the tissue engineered artery support scaffold.....	154
Figure 4.12	Flow rate of two step controlled recycle stream.....	155
Figure 4.13	Linearization of the relationship between overall oxygen transfer coefficient within the oxygenator and the recycle rate.....	157
Figure 4.14	Proportional control of DOT at the exit of the tissue engineered artery support scaffold.....	159
Figure 4.15	Cell growth within alginate support scaffold related to Fig. 4.14.....	159
Figure 4.16	Flow rate of proportionally controlled recycle stream.....	160

Figure 4.17 Proportional and integral control of DOT at the exit of the tissue engineered artery support scaffold.....	161
Figure 4.18 Flow rate of PI controlled recycle stream.....	161
Figure 4.19 Proportional and integral control of DOT at the exit of the tissue engineered artery support scaffold.....	163
Figure 4.20 Flow rate of controlled recycle stream.....	171
Figure 5.1 Window of operation for pH versus lactic acid concentration.....	171
Figure 5.2 Single pass pH change across the alginate support scaffold containing Mesenchymal Stem Cells.....	173
Figure 5.3 Logarithmic plot of mesenchymal stem cell number present in scaffold and minimum recycle flow rate required to ensure pH change across the bioreactor falls with an acceptable range.....	175
Figure 5.4 Controlled flow rates within the VTEB system.....	176
Figure 5.5 Continuous window of operation for pH for mesenchymal stem cells	177
Figure 6.1 Window of operation for glucose concentration 4-6 mmol.L ⁻¹	181
Figure 6.2 Window of operation for lactate concentration 0-3 mmol.L ⁻¹	183
Figure 6.3 Window of operation for glutamine concentration 3-4 mmol.L ⁻¹	187
Figure 6.4 Window of operation for ammonia concentration 0-6 mmol.L ⁻¹	189
Figure 6.5 Overall metabolic window of operation.....	190
Figure 6.6 Glutamine v Glucose domination.....	191
Figure 6.7 Glucose control achieved with untuned PI controller.....	193
Figure 6.8 Feed flow rate associated with Fig. 6.7.....	194

Figure 6.9	Glucose concentration achieved by tuned proportional integral feed rate controller.....	194
Figure 6.10	Proportional integral feed rate controller action associated with the glucose concentration in figure 6.9.....	195
Figure 6.11	Instability of glucose concentration due to excessive gain of feed rate controller.....	195
Figure 7.1	Minimum fresh feed rates required to maintain glucose and glutamine concentrations for feed of composition glucose, 12mmol.L ⁻¹ and glutamine, 8mmol.L ⁻¹	200
Figure 7.2	Concentration of lactate and ammonia for decreased feed rates.....	201
Figure 7.3	Minimum concentration of glutamine required in the fresh feed.....	202
Figure 7.4	Minimum flow rate required to maintain concentration restraints for richer culture medium.....	203
Figure 7.5	Windows of Operation (WOOs) relating recycle rate to feed flow rate for a variety of oxygen concentration.....	204
Figure 7.6	Integration of oxygen model (see chapter 4) and substrate model (see chapter 6) into a single model.....	206
Figure 7.7	Controlled dissolved oxygen (DOT) trends, at exit of bioreactor, within overall combined model.....	208
Figure 7.8	Controlled recycle flow rate, in overall control system, into bioreactor system.....	209
Figure 7.9	Controlled glucose concentration trends, at exit of bioreactor, within overall combined model.....	209

Figure 7.10 Controlled fresh feed flow rate, in overall control system, into bioreactor system.....	210
--	-----

List of tables

Table 3.1	Time variant data for the VTEB.....	100
Table 3.2	Batch sheet data item.....	102
Table 3.3	Descriptive data items.....	103
Table 3.4	Alginate scaffold parameters for modelling.....	114
Table 3.5	Constants within the overall model.....	125
Table 4.1	Comparing methods of controlling DOT within the VTEB.....	132
Table 4.2	Assumptions of model to represent oxygen mass transfer in a prototype bioreactor.....	144
Table 5.1	Phenol red colour variation with solution pH.....	168
Table 5.2	Data required for calculating lactate production rate by cells.....	172
Table 7.1	Modifications to system operating conditions to allow models developed in chapters 4 and 6 to be integrated.....	205

Chapter 1 Introduction

The loss or failure of an organ or tissue is one of the most frequent, devastating, and costly problems in human health care. The cost of such failures to the US healthcare system is estimated at \$400 billion annually (Langer and Vacanti, 1993). Replacement of damaged organs has historically been carried out using either material from other non-damaged (and normally less sensitive) parts of the body such as with skin grafts, or using organs taken from either living or deceased donors. Both strategies give rise to issues. In the case of autologous material (self-donated), the removal of such material often brings greater complexity to an already highly traumatic procedure and can lead to risk of secondary infections. Autologous donation is also limited by the finite nature of the supply; only a limited number of blood vessels or skin may be donated without causing a problem of equal severity to that of the original trauma or disease. Allogeneic donation (donation from another individual) carries with it the risk that the organ will be rejected as the new host's immune system recognises the material as foreign and attacks and destroys it. Immune suppressing drugs may be taken to limit the immune response and allow the organ to survive, such drugs however must be taken for life and carry a number of side effects such as a greater risk of infection due to the immune response being reduced. Additionally their non-specificity cannot exert full control of the individual's immune response and hence the graft will ultimately be rejected (Boyd et al, 2005). Allogeneic vessels have an added disadvantage that demand normally hugely outstrips supply (Niklason and Langer, 1997), with the waiting lists in most western nations massively exceeding the number of available organs.

In recent years a variety of techniques have been explored as methods for either growing *in-vitro* replacement organs or by encouraging the regeneration of the damaged tissue through the use of growth factors and stem cells. These would provide an attractive alternative if available as a clinical level treatment.

Cardiovascular disease is a disease of the coronary arteries, those vessels that carry the blood supply to the heart. Symptoms consist of gradual accumulation of fatty plaque deposits within the cells forming the wall of the coronary arteries (Fig. 1.1). If a plaque grows to a size where it occludes flow or becomes damaged and a section breaks off leading to an occlusion downstream then death of heart tissue may occur. If the blockage remains blocked and there is no alternative route for blood to reach the heart tissue then death will ultimately ensue. Normal causal and risk factors for such a disease are related to lifestyle with a genetic component.

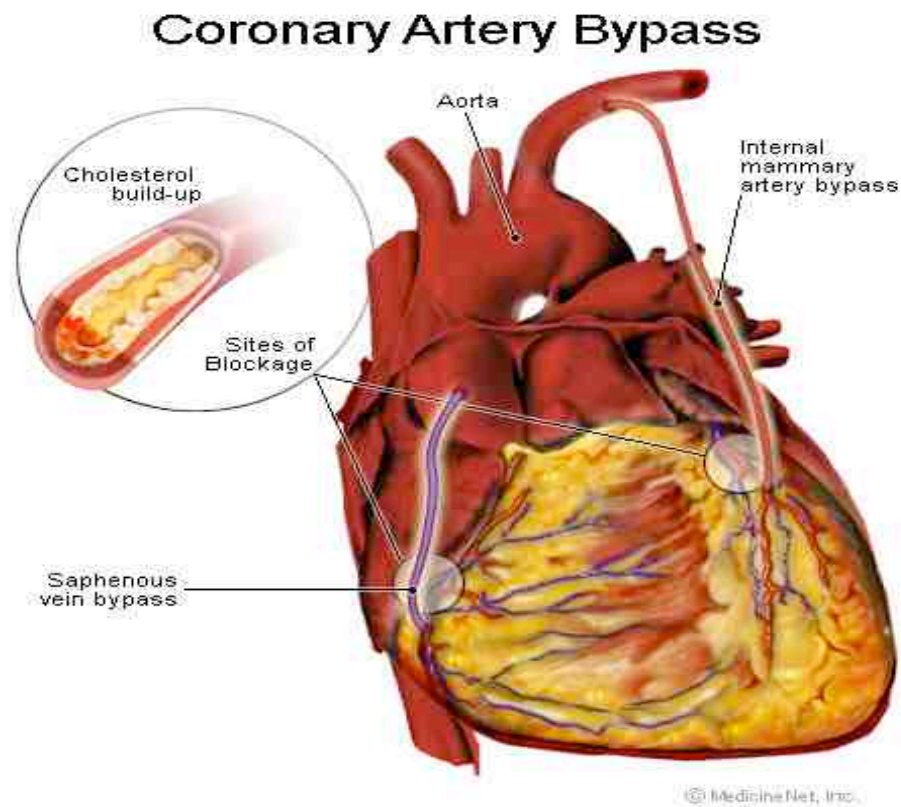


Figure 1.1 Coronary Artery Bypass Graft (intensivecare.hsnet.nsw.gov.au)

A cholesterol build up in one or more of the coronary arteries (as shown inset) reduces blood flow to the heart muscle. This reduced blood flow can result in damage and normally requires surgical intervention. Standard procedure is to bypass blockages using grafts created from veins in the leg (saphenous) or from arteries in the thorax (internal mammary artery).

An artery is composed of three layers (Fig. 1.2). The *intima*, the section closest to the blood flow is formed of a single layer of endothelial cells, which are responsible for recognising chemical and physical signals and regulating vascular tone (Davies, 1995). The second layer, the *media* is composed of smooth muscle cells, which are specialised contractile cells that respond to endothelial cells and cause dilation or contraction of the artery (Owens, 1995). The third and final layer is composed of a support structure of collagen and fibroblasts and is called the *adventis*. Fibroblasts are dispersed throughout connective tissue within the body and can differentiate to form

smooth muscle cells. Their presence in the artery lends structural support and the ability to form new cells in the event of damage (Alberts et al, 1994).

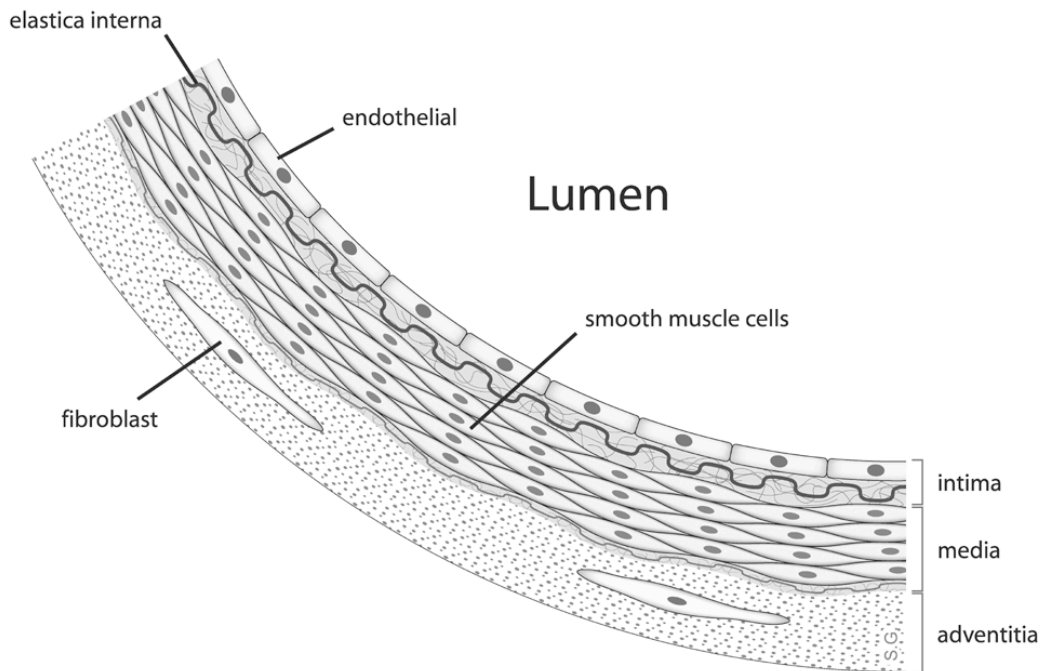


Figure 1.2 Human artery structure

The artery is composed of three main layers. The innermost layer, the intima, is in contact with blood flow and is composed of a single layer of endothelial cells. These endothelial cells respond to physical stimuli (mechanotransduction) and chemical stimuli (chemotransduction). The media is the middle layer of the artery and is composed predominantly of smooth muscle cells (SMC). These SMC control the vasoconstriction (contracting) and the vasodilation (expanding) of the artery in response to stimuli from the endothelial cells. The final layer, the adventitia, consists of connective tissue interspersed with periodic fibroblasts.

Within the United States alone 58 million people suffer cardiovascular disease. This has led to around 550,000 vascular bypass surgeries being carried out within the United States each year (Xue and Greisler, 2000). In terms of all operations occurring where vascular conduits are required (includes Arterial-venous shunts for dialysis) and autologous, allogenic or synthetic small calibre conduit is required, the estimate is 1.4 million per year (Langer and Vacanti, 1993).

The aim of this chapter is to provide an overview of the need for new treatments for cardiovascular disease, one of the largest causes of morbidity within western nations. This literature review will extend to current engineering and regenerative medicine strategies for treating cardiovascular diseases and the devices within which this takes place. Particular attention will be given to automation of these devices and the methods employed to maintain and control the environmental conditions required to sustain cellular growth. Consideration will also be given to the use of bioreactors and similar devices both within tissue engineering, for treatment of other conditions and within different but related fields such as industrial fermentation. These systems will be analysed to determine how existing technology may assist in advancing and improving automation in a device designed for producing a tissue engineered artery.

1.1 Traditional treatment of coronary artery disease

1.1.1 Autologous graft

The usual treatment for coronary artery disease is an autologous therapy using veins from alternative parts of the patient's own body to bypass the blockages. Surgeons remove a segment of a healthy and accessible blood vessel from a number of possible parts of the body and use it to make a detour of blood flow around the blocked part of the coronary artery. Most operations of this nature use vessels <5-6mm in diameter (Niklason and Langer, 1997; L'heureux, 1998).

A piece of long vein from the patient's leg (saphenous vein) may be taken. One end is sewn onto the large artery connecting the heart to the aorta. The other end of the vein is attached or "grafted" to the coronary artery below the blocked area. Alternatively and more unusually an artery may be detached from the chest wall and the open end

attached to the coronary artery below the blocked area. In both case the graft provides a new pathway by which blood may reach the heart muscle. Patients may receive one, two, three or an even greater number of such bypass grafts, depending on how many coronary arteries are blocked.

The disadvantages of autologous transplants are significant. The procedure requires an additional operation to harvest the vessel, which may lead to further complications. The side branches of the extracted vein must be stitched closed which is an intricate procedure and often the pain arising from the extraction of such a vessel is generally excruciating and is often the greatest source of complaint from the recovering patient

Harvested veins used are structurally adapted for a low-pressure environment and are being used to replace an artery carrying high-pressure blood flow a change that does not come without consequence (Cox et al, 1991). Problems relating to difference in vessel compliance between the graft and in-situ artery can occur, aneurysms can form where the lumen dilates due to the vein being insufficiently adapted to deal with arterial pressures (Teebken and Haverich, 2002) and even in extreme cases rupture (Nwasokwa, 1995). More gradual failures can also take place, *ex-vivo* experiments mimicking the early effects of native conditions compared with the environment experienced by vascular grafts were shown to lead to reduced matrix metalloproteinase by half and stimulate cell proliferation rates of 220-750% of normal leading to thicker vessel walls in response to the increased pressure. This may lead eventually to intimal hyperplasia (uncontrolled cell growth) that could contribute to an occlusion of the graft. (Mavromatis et al, 2000).

Saphenous veins have been shown to have long-term limitations due to occlusion of the graft. The most common cause for this occlusion is a progression of

atherosclerosis. After 10-12 years 40% of vessels are blocked, 18.9% contain blockages obstructing at least half of the cross sectional area of the artery and 8.1% showed some evidence of atherosclerosis (Bourassa, 1984). These occlusions lead to further operations that carry increasing risk to the patient but also may result in a shortage of useful autologous vessels. Internal mammary arteries from the chest have been shown to have a significantly longer lifespan (Grodin et al, 1984). The disadvantage of using these vessels is that they are significantly shorter in length and thus they may only be used to bypass blockages arising at the initial (proximal) length of the coronary artery. Additionally a more complex operation is required to harvest an internal mammary artery and hence they are inappropriate for emergency surgery (Angelini and Newby, 1989, Markusen, 2005). In order to compensate for the finite supply of autologous vessels attempts to use vessels derived from animals (xenogenic) have been made (Rosenborg et al, 1966), although the use of animal products risks transmission of animal borne diseases (Fishman, 2006) and long term patency is poor due to rejection or formation of thromboses (Stock and Vacanti, 2001). Allogeneic vessels from cadavers have also been tested however unsuccessful results similar to xenografts have been attained with rejection and a higher risk of aneurysm than synthetic vessels (Madden et al, 2006).

1.1.2 Synthetic graft

Vorhees developed the first synthetic graft more than half a century ago in 1952, called Vinyon and composed of fabric (Vorhees et al, 1952). Currently the most widely used synthetic materials are poly-ethylene-terephthalate (Dacron) and expanded poly-tetra-fluoroethylene (e-PTFE). These materials although originally designed to be chemically inert are not capable of passively transporting blood flow without reaction.

Some of these reactions are beneficial, whilst others are damaging, however no reaction would be preferable (Xue and Griesler, 2000). Synthetic grafts while demonstrating long term function for more than 10 years when used as large diameter grafts (Hoerstrup et al, 2001) have been shown to have particularly poor patency for smaller diameter grafts (<5-6mm). This is especially so for grafts used below the knee, where low blood flow and high resistances increase the risk of thromboses (Yeager, 1982). Adaptations have been made to these vessels to try and make them more biologically compliant including coating the internal surfaces of the vessels with proteins, particularly components of the extra cellular matrix, usually containing the RGD tripeptide (Deutsch, 1999). Such vessels have even been coated with autologous endothelial cells (Lamm et al, 2001) which may potentially be obtained from peripheral flow within the patient (Mooney, 2001), although it appears that no surface treatment will entirely eliminate the low level immune response caused by recognising the graft as a foreign body (Greisler, 1990).

1.2 Tissue engineering bypass grafts

A major new initiative in the treatment of coronary artery disease is to grow grafts *in-vitro* within an environmentally controlled device (bioreactor) from small quantities of biological material that may be harvested from the human body. Such a procedure is referred to as tissue engineering, the use of the biological material as a raw material to create necessary tissues and organs to replace those that are damaged or failing.

The term “tissue engineering” is generally credited to the use by Y.C. Fung at the University California, San Diego in 1985 and was proposed at the National Science Foundation (NSF) meeting within the United States in 1987 for wider use. A further 6 years were required before the term had entered the scientific zeitgeist sufficiently that

the first major review publication (Langer and Vacanti, 1993) occurred. Tissue engineering was defined as an interdisciplinary field involving the application of the principles of biology and engineering to the development of functional substitutes for damaged tissue. The usual interpretation involves placement of cells on or within scaffold matrices to encourage tissue growth into a suitable structure that may be implanted into the patient to fulfil either the same role or an analogous one as was carried out by the original *in-vivo* tissue or organ.

The first attempt at developing a tissue-engineered artery or graft used a Dacron mesh as a support scaffold for seeded fibroblasts and smooth muscle cells. The lumen of this vessel was subsequently coated in endothelial cells. The graft produced by this method, although healthy did not possess sufficient strength to withstand arterial pressure, possessing a burst pressure of 318mmHg compared with approximately 2000mmHg in a native artery (Weinberg and Bell, 1986).

Recent attempts have considered burst pressure to be a key parameter within their work (L'heureux et al, 1998) and developed a vessel that could withstand arterial pressures by a “sheet based method” (L'heureux et al, 2007) without the use of a synthetic support. A sheet of vascular smooth muscle cells was formed into a sheet, rolled around a tubular support and subsequently wrapped with a second sheet consisting of fibroblasts. Following maturation and the removal of the central support scaffold, endothelial cells were seeded into the lumen to provide the third key component of an *in-vivo* artery (Fig. 1.3).

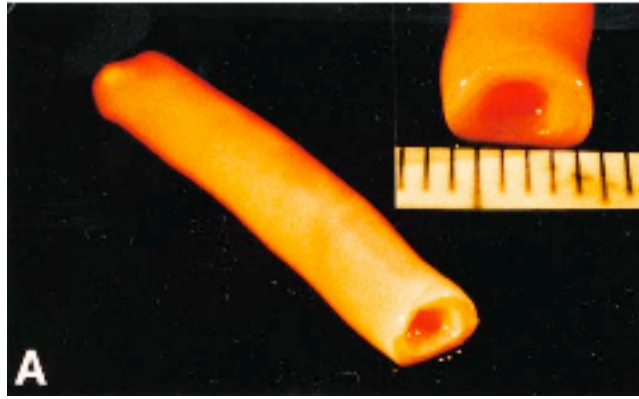


Figure 1.3 Engineered artery at 9 weeks maturation (L'heureux et al, 1998).

L'heureux's tissue engineered artery is composed of a fibroblast sheet rolled into a tube and coated in endothelial cells. L'heureux et al, excluded smooth muscle cells (SMC) from their design due to the limited number of divisions such cells proved capable of performing. The presence of gradually increased amounts of smooth muscle actin (SMA), a marker of SMC, indicated that such cells may develop naturally through the differentiation of fibroblasts.

L'heureux's group recognised that the thickness of the fibroblast sheet and hence the culture time of this component was the key parameter in developing a vessel by this method that possessed a bursting pressure that compared favourably with in-vivo arteries (~ 2000 mmHg) and was superior to the saphenous vein (1680 ± 307 mmHg). Subsequent work by this research group eliminated smooth muscle cells due to their low proliferative capacity and has led to improved vessel burst pressure of 3468 ± 500 mmHg for vessels of 4.5 mm diameter and 3688 ± 1865 mmHg for 1.5 mm diameters. Despite the absence of this SMC layer, the presence of a SMA positive cell population indicates remodelling may be regenerating the vascular media. One disadvantage of such tissue engineered vessels is that a 28 week production time prevents the use of these vessels in an emergency situation. Work has demonstrated the effectiveness of such grafts as arteriovenous shunts for human patients receiving dialysis due to kidney failure. The first six patients in such a study at the time of publishing the results had been followed up for 13 months and were performing well (L'heureux et al, 2007). This work followed studies testing the vessels in rats as

abdominal interpositional graft, a study that also yielded successful results (L'heureux et al, 2006).

(Niklason et al, 1999) were also able to grow arbitrary lengths of vascular graft from smooth muscles endothelial cells. These cells were obtained from bovine vascular biopsies and possessed a rupture strength $>2000\text{mmHg}$. Smooth muscle cells (SMC) were obtained from the medial layer and pipetted onto treated tubular biodegradable polystyrene scaffolds. Following thirty minutes to permit adhesion, pulsatile flow (165 beats per second) was applied to the seeded scaffolds sited within a bioreactor system consisting of four parallel perfusion bioreactors containing the developing grafts. These bioreactors were sited on a hot plate maintained at 37°C with flow gradually being increased from 0.033 to 0.1 ml.s^{-1} (equivalent to a shear stress of 1×10^{-2} and $3 \times 10^{-2}\text{ N.m}^{-2}$).

The translation of this technique into humans posed problematic due to species and age differences, SMC from elderly people possess a limited proliferative capacity. Gong and Niklason (2008) explored the potential of human mesenchymal stem cells (hMSC) as a replacement for smooth muscle cells based upon their autologous nature, high proliferative capacity and a multipotent nature that allows differentiation into multiple cell lineages including fat, muscle, bone and connective tissue progenitors (Pittenger, 1999). They showed that factors such as $\text{TGF}\beta 1$ could be used to induce these hMSC into early stage smooth muscle cells. It was also shown that while cyclical strain enhanced proliferation smooth muscle cells, it inhibited proliferation of hMSC although it did increase smooth muscle actin (SMA) expression in existing hMSC of in the presence of PDGF-BB, possibly indicating differentiation down a

SMC lineage. These results led Gong and Niklason (2008) to develop an optimised protocol of operating the bioreactor in two separate operational forms, four weeks for proliferation of cells throughout the scaffold and four weeks for differentiation of the cells into smooth muscle, followed by seeding the resulting smooth muscle tube with endothelial cells (EC). The successful proliferation of these seeded cells was taken as an indication that by deriving EC as well as SMC from hMSC, the goal of a marrow derived vascular replacement may soon be achieved.

Shinoka's group in Japan, initially used saphenous veins harvested from the leg. These veins were minced and seeded onto scaffolds to form grafts (Shinoka et al, 2001). Such an approach was discontinued as harvesting the cells could induce infection just as with standard bypass grafts and there was the possibility that the cells obtained would have insufficient proliferative capacity. Additionally these cells required animal serum to grow, which raises concerns about the use of the vessels in humans. These concerns led to the use of bone marrow cells, which in addition to not having many of the disadvantages listed above, require less cell culture media and other reagents which reduces the financial cost of the procedures. These cells were seeded into a tube-shaped biodegradable polymeric scaffold by pipetting and this scaffold was kept in culture for 2-4 hours until implantation into the patient. Four implantations into patients have been demonstrated to date – two using saphenous veins and two using bone marrow cells. In all instances the implanted vessels have demonstrated excellent post-operative flow (Matsumura, 2003).

The successes of these groups indicate that the hope of developing tissue engineered arteries to solve many of the problems associated with more conventional treatments

based on autologous harvesting or use of synthetic materials may soon be a possibility. Many of these techniques are still at a very low scale, with small numbers of patients receiving treatment. Given the scale of the patient body, consideration of the potential for scale out to a manufacturing level is required, as this will be the ultimate goal. Such scale out requires detailed consideration of the process and the key stages that make up a tissue engineering process.

1.3 Tissue Engineering Processes

The process involved in engineering a graft has great relevance on the potential for scaling out. Any process has two key aspects, firstly the raw materials required (for a tissue engineered artery - cells, culture medium and support scaffold) and the steps that make up the process.

1.3.1 Raw Materials

The main raw material of cell culture is the cell themselves, the types used within the development of tissue engineered arteries range from mature cells (those with limited proliferative capacity present in the human body) to embryonic stem cells (cells derived from early stage embryos). Each cell type has varied culture conditions and that are commonly related to the conditions they would experience within the microenvironment within which they reside in-vivo. Cells will often react to different culture conditions in different ways that are not limited to the health of the cell. This is most noticeable with progenitor cells, which can often be driven down particular differentiation pathways by modifying chemical and physical conditions.

1.3.1.1 Mature Cells

Mature cells used for engineering arteries tend to be those that are present natively in the mammalian artery and include endothelial, smooth muscle cells and fibroblasts in order of layer from the lumen outwards. Endothelial cells form the lining of all blood vessels within the mammalian body (Alberts et al, 1994). They are responsible for regulating vascular tone, arterial tone, arterial structure and remodelling through a process known as mechanotransduction (Davies, 1995). One of the responses to these transduced signals is the release of vasoactive substances such as nitric oxide synthase (NOS), which causes an increase in the synthesis and release of nitric oxide to produce vasodilatation or trophic changes in the artery (Burnstock, 1998). In addition to shear stress, endothelial cells respond to multiple chemical factors within the blood flow. Indeed the general health of the arterial wall is directly linked to the shear and chemical impulses experienced by the endothelium and the resulting mechanotransduction and linked responses (Davies, 2005).

Platelet endothelial cell adhesion molecule (PECAM-1 or CD-31) a surface glycoprotein represents a common method of identifying a cell as endothelial. It is known to regulate calcium signals (Ji et al, 2002), control the passage of materials and white blood cells (Alberts et al, 1994) as well as apparently being part of a mechanosensory complex (Tzima et al, 2005). This marker has the added advantage as an endothelial marker as it is not present on fibroblasts, muscle or other non-vascular cells (Newman, 1997). In a similar way endothelial cells may be identified by VE-Cadherin (CD-144) a strictly endothelial specific adhesion molecule that is found at

junctions between endothelial cells. It is directly involved in regulating permeability through the endothelium and is implicated in the same mechanotransductory pathway as CD31 (Vestweber, 2008, Tzima et al, 2005).

The dependence of the artery's health upon the endothelium means that it must form a key part of any tissue engineered arterial graft that is intended to be truly analogous to the arteries found natively *in-vivo*.

The second layer of the artery is formed from vascular smooth muscle cells (VSMC). VSMC are highly specialised cells with the primary function of contraction. The cell is so specifically designed once mature and fully differentiated that its proliferation rate is very low, as the majority of its energy and resources are reserved for contraction (Owens, 1995). The key markers for positive identification of VSMC are the SMA (Smooth Muscle Actin) Proteins which are directly associated with the cells' contractile properties. Matrix GLA Protein is also expressed preferentially in late passage de-differentiated VSMC and is particularly strongly expressed in aortic VSMC but not in other smooth muscle cells (Shanahan et al, 1993).

The final and outer layer of the artery is composed of fibroblasts within an extra-cellular matrix. Fibroblasts are dispersed within connective tissue within the body, and are responsible for secreting a non-rigid extra cellular matrix that is rich in collagen. At injury these cell will migrate to the site of the wound and secrete this collagen to isolate and repair the wound (Alberts et al, 1994).

Mature cells, although an obvious source of material for forming tissue engineered arteries, have disadvantages, particularly in the case of smooth muscle cells, which possess a limited proliferative capacity, particularly when extracted from ageing donors (Owens, 1995, Gong and Niklason , 2008).

1.3.1.2 Mesenchymal stem cells (MSC)

Mesenchymal stem cells (MSC) are multipotent cells found within adult humans (and other mammalian species). Multipotent cells are stem cells, which are capable of differentiating (becoming after a number of cell divisions) to form a number of mature cells. In the case of MSC, which are normally located within the mammalian bone marrow at a proportion of between 1 in 10,000 and 100,000 (Deans and Moseley, 2000, Galotto, 1999) this capability manifests itself as the potential to form into connective tissue, fat, muscle or bone (Pitinger et al, 1999). Such cell lines are often referred to as adult stem cells as they can be found in mature individuals of a species and are responsible for the continual regeneration and repair of the organism's body.

MSC have been shown to be capable of differentiating down a pathway towards smooth muscles cells and have been used in the growth of vascular grafts (Gong and Niklason, 2008). They have also been differentiated into endothelial cells in the presence of 2% fetal calf serum (FCS) and vascular endothelial growth factor (VEGF) (Oswald et al, 2004). Transplantation studies have even been performed and the results show that MSC appear to enter circulation from the bone marrow and engraft other tissues. It also appears that MSC may be normally present within arterial vessel walls. Such a presence indicates their role in vascular regeneration and regeneration may be extensive (Abedin et al, 2004).

As with many stem cells, there is no single test that identifies MSC with complete confidence and they tend to be identified using a panel of surface antigens including CD13, CD29, CD44, CD90, CD105, SH-3 and STRO-1 and by not possessing haemopoietic markers such as CD45, CD34, CD11 and CD14 (Koc and Lazarus, 2001). The murine monoclonal antibody STRO-1 identifies a surface antigen expressed by stromal elements within the bone marrow and will not attach to committed progenitor cells (Simmons et al, 1991) however it still lacks specificity to MSC. The lack of a single marker to easily distinguish has led to techniques that involve selecting for MSC based upon rapid adherence to tissue culture plastic and their high proliferative potential in 10% fetal calf serum (FCS) (Koc and Lazarus, 2001), although (Wan et al, 2006) showed that this method removes a non-adherent population of cells that possess mesenchymal characteristics. Despite this loss however the standard procedure remains rapid plastic adherence, a technique that has provided MSC that have ultimately been used to form grafts that have subsequently been implanted successfully into patients (Gong and Niklason, 2008, Matsumura, 2003).

1.3.1.3 Embryonic stem cells

Embryonic stem cells are derived from the inner cell mass of an early embryo (Wolpert, 2006) the first human cell line was created in 1998 (Thomson et al, 1998). These cells are capable of dividing into any of the three germ layers (the developing regions in an embryo) (Donovan and Gearhart, 2001) and are referred to as pluripotent. *In vivo*, the three germ layers are the endoderm (including the gastrointestinal tract and stomach), ectoderm (including the nervous system) and mesoderm (including the muscle, bone and blood). The only cells that embryonic stem

cells are not capable of differentiating to form are those that become extra-embryonic material, such as the placenta. This inability prevents embryonic stem cells from developing into a living organism (Alberts et al, 1994).

There is also suspicion that many tumours contain a small central population of rogue stem cells reproducing uncontrollably (Andrews 2006). Teratocarcinomas which are often found in the reproductive organs of males and females are composed of cells that have been termed embryonic carcinoma stem cells as they seem able to produce all the cells found in an adult organism i.e. they are also pluripotent (Robertson ,1987).

As with mesenchymal stem cells, several markers exist that seem to express strongly in cells that are pluripotent and these include the transcriptional regulators OCT-4 (Nichols et al, 1998), Nanog (Chambers et al, 2003) and Sox 2 (Avilion et al, 2003). However at the current time many of these remain merely potentially useful as little or nothing is known about the role they play in maintenance of pluripotency and self renewal (Draper et al, 2007).

Embryonic Stem Cells being pluripotent theoretically have the potential to form any of the more than 200 cell types found in the mammalian body, however much of this proliferative capacity has not yet been investigated.

Despite this (Yamamoto et al, 2005) showed that Flk-1 (a receptor for VEGF – Vascular Endothelial Growth Factor) positive murine stem cells could be induced to form vascular endothelial cells in vitro by the application of shear stress. This differentiation was characterised by an increase in the expression of VE-cadherin and PECAM-1, and although there was an initial increase in smooth muscle actin (SMA),

this later decreased. This work was later continued (Shimizu et al, 2007) and it was shown that by seeding Flk-1 positive cells onto flexible silicone membranes and exposing them to controlled levels of cyclic strain (4-12% strain, 1Hz, 24 hours) expression of some endothelial markers such as Flk-1 decreased (others such as VE-Cadherin did not) and led to dose –dependant increases in SMA and smooth muscle heavy chain (SMHC).

(Levenberg et al, 2002) derived endothelial cells from human embryonic stem cells expressing PECAM-1. These cells were able to differentiate and form tube structures and when transplanted *in-vivo* into severe combined immunodeficient (SCID) mice, were even able to form microvessels containing mouse blood vessels.

These results indicate that although embryonic stem cells have great potential for use as a raw material in tissue engineering, there is still far too little understanding with regard to what effect a particular chemical or physical impulse will cause upon a cell.

A more long-term problem with the use of embryonic stem cells to form mature cells for use in tissue-engineered blood vessels is the lack of specificity to the patient.

Embryonic stem cells cannot be harvested autologously as they are formed from an embryo of which no cells remain at birth. Attempts have been made to create genetically matched stem cells using a process known as somatic cell nuclear transfer (SCNT). SCNT involves the removal of a nucleus from a cell belonging to the individual who will ultimately be treated and implanting it into an egg cell which has also had its nucleus removed. Such techniques using an established cell line rather

than cells either from or derived from embryos was first used to clone sheep (Campbell et al, 1996) and subsequently several other mammals (Wilmut and Peterson, 2002). Although the cloning of human beings is illegal in most jurisdictions the intent is to use such techniques to give rise to embryos that have the same genetic code as the target patient and harvest cells from the inner mass as with normal embryonic stem cells to create a matched line. To date SCNT in humans and many primates has been unsuccessful, although success was claimed by a group in South Korea (Hwang et al, 2005 *Retracted*) which was later proved false and has not led to the hoped for production of patient specific embryonic stem cells.

A series of recent investigations have led to the formation of cells that possess embryonic characteristics from skin-derived fibroblasts by the addition of four genes Oct $\frac{3}{4}$, Sox 2, Kf4 and Myc in a murine animal model (Yamanaka, 2007) and repeated use of human fibroblasts (Takahashi et al, 2007). Subsequently (Junying et al, 2008) achieved similar successes without the use of Myc, which has been implicated in murine research as a potential cause of cancer, instead using the gene LIN28, which has been implicated in murine research as a potential cause of cancer. After up to 17 months these four lines of induced pluripotent stem cells (iPS) still possessed the morphology of typical embryonic stem cells and possessed a normal karyotype. These cells have not yet been conclusively proven to be embryonic stem cells and hence may behave in ways very different when placed under certain conditions. Mason (2008) points out that Yamanaka and Thomson are at pains to acknowledge introducing genes into cells using disabled viruses can introduce cancer as has happened in France by treating severe immunodeficiency diseases by the sufferers' modified bone marrow cells (Fischer et al, 1990). This step does however at this time seem to provide more

hope of leading to cells that may be patient specific and be used to create tissue engineered blood vessels.

In summary, with mature cells (particularly smooth muscle cells) suffering from a reduced proliferative capacity and embryonic stem cells being simply too recent a development to be sufficiently understood, the most viable cell type for use in the development of tissue engineered artery or bypass grafts that mimic the physiology of native vessels is the mesenchymal stem cell, harvested from the bone marrow. Despite the lack of development in purification techniques and a definite marker extensive the creation of blood vessels using this raw material have been achieved (Matsumura, 2003, Gong and Niklason, 2008).

1.3.2 Cell Culture Media

The growth of adherent mammalian cell cultures requires a complex cocktail of essential amino acids, glucose and growth factors. Common procedure is for a defined medium base such as Dulbecco's Modified Eagle Medium (DMEM) to have foetal calf serum (FCS) added to it. Serum is the liquid component of blood with fibrinogen and clotting factors removed and contains a rich mixture of proteins that allow cells to grow, divide and remain healthy (Freshney, 2000). The addition of FCS is undesirable as it ensures that the resulting medium is not fully defined and given the methods of FCS production and variety of source, experimental conditions cannot be deemed entirely consistent. The animal derived nature of FCS leads to the same concerns as those associated with the use of xenogeneic cells such as disease transmission (Griffith and Naughton, 2002). The DMEM base contains substrates such as glucose and glutamine that the cells can use in respiration to produce energy, grow and proliferate.

It will also often contain a visual pH indicator such as phenol red to indicate an excess concentration of waste product, either necessitating the exchange of the medium or in the case of a contamination, disposal of the flask.

Some success has been achieved with developing fully defined culture medium. (Ludwig et al, 2006) demonstrated the growth of human embryonic stem cells in a defined media that still contained some animal derived components. Despite an entirely animal free media not yet having been developed, the belief within the stem cell community is that this advance will take place soon (Hoffman, 2005).

A major component of wound healing and normal maintenance of all organisms is tissue remodelling. This remodelling is dependant upon a set of growth factors and cytokines. Along with their receptors these factors dictate the type of cell or tissue that will respond and the expression level of their genes will dictate the length of the associated response (Deuel and Zhang, 2000). The most relevant growth factors in the development of blood vessels are endothelial cell growth factor (ECGF), vascular endothelial growth factor (VEGF), endothelin-1 (ET-1), platelet derived growth factor (PDGF) and basic fibroblast growth factor (bFGF).

In terms of the relevance, these growth factors have for the tissue engineering of blood vessels, VEGF a regulator of angiogenesis (Ferrara et al, 2003) has been demonstrated to direct MSC down an endothelial path (Gong and Niklason, 2008, Riha et al, 2007) used cyclic strain to activate PDGF- β and drive murine embryonic stem cells toward forming vascular smooth muscle cells. Seruya (2004) achieved similar results to both of these works, maintaining smooth muscle progenitor cells from muscle as EC using

media containing VEGF and then causing them to differentiate down an SMC pathway by the addition of PDGF- β . bFGF has been shown to stimulate the growth of endothelial cells in denuded arteries and also stimulated growth in quiescent endothelium (in the left carotid denude six week prior to bFGF addition. (Lindner et al, 1990).

These results indicate that growth factors could be highly relevant in the formation of tissue engineered arteries, particularly where progenitor cells such as MSC are involved. Although such factors can encourage division down particular routes, the ideal operation scenario in the long term should be to replicate *in-vivo* conditions to encourage cellular production, leading to the desired differentiation product. Methods such as controlled cyclical strain (Riha et al, 2007) could potentially lead to a much better quality of tissue than merely supplementing the medium with an arbitrary amount of a particular factor.

1.3.3 Polymeric Scaffolds for Tissue Engineering

To form a three-dimensional biological structure, the use of a scaffolding material is usually required. With the exception of the work of L'heureux (1998) most tissue engineering blood vessels have employed some sort of a support scaffold. This scaffold is normally formed from a polymeric or alginate material. As stated by Hutmacher (2000) such a scaffold should possess the following characteristics.

- It should encourage growth
- It should encourage cell adhesion (most mammalian cells are adherent)

- It should ensure adequate distribution of supplied nutrients
- It should be biocompatible
- It should possess a structure that is coherent with the organ/tissue to be grown.
- It should be degradable, i.e. bioresorbable or similar and in breaking down, should not lead to the formation of by-products that are cytotoxic. If the scaffold is not degradable it should not provoke an immune response.

Williams (2003) in expanding upon the term biocompatibility, commented that materials should be selected on the basis of optimal mechanical or physical properties and optimal inertness and the chance of success is highest.

A tissue scaffold can encourage growth by replicating aspects of the natural environment that the cells and developing tissue would experience *in-vivo*. Ensuring a homogenous distribution of cells when seeding encourages growth of cells throughout the scaffold body to produce a distinct three-dimensional structure. A high porosity and surface to area ratio will contribute to this proliferation through the scaffold and also allow the distribution of nutrients to the developing cells and the transport of waste products away (Li et al, 2002, Yang et al, 2001, Hutmacher, 2000).

Aspects such as surface roughness and mechanical strength are examples of such properties that should be carefully controlled (Yaszemski M et al, 1995). Mechanical strength is especially important for the development of hard load-bearing tissue. Often scaffolds for these tissues e.g. bone and other structures composed of softer tissue such

as arteries (Matsumura, 2003) can be dual purpose, allowing development of suitable tissue whilst simultaneously mimicking the tissue until it is fully developed. The mechanical strength of the scaffold and other physical properties should be as close to the original structure as possible and should remain at an appropriate level until the replacement tissue is completely developed (Yaszemski M et al, 1995, Hutmacher, 2000). Strength should not be prioritised at the expense of biocompatibility. Any material intended for transplant *in vivo* must be biocompatible and non-toxic within the human body (Vande Vord et al, 2001).

Ideally any scaffold would gradually break down without producing cytotoxic products (Griffith and Naughton, 2002) at a rate equivalent to the generation of the new tissue/organ. This would provide physical space for further growth and stimulate the formation of a tissue or organ of approximately the same shape as the original Hutmacher (2000). In the case of certain *in-vivo* transplants it is important that certain properties of the scaffold remain until it can be guaranteed that the new tissue has attained the required mechanical strength to carry the weight that will be placed upon it e.g. bone or joint tissue will require some degree of mechanical strength.

It is essential that the cells initially seeded and those that subsequently develop attach strongly to the surface of the scaffold to avoid being displaced by shear effects from nutrient flow (Kim and Mooney, 1998). The scaffold should possess suitable surface chemistry to encourage cell adhesion of appropriate strength. The majority of materials used to modify the surface of such scaffolds are those found within the *in-vivo* ECM such as fibronectin and almost all contain a tripeptide chain (Arginine-glycine-Aspartic acid - RGD) that is critical to binding within the ECM. Components

containing RGD may be either immobilised on the surface of scaffolds or when binding to hydrogels by mixing with the monomers prior to polymerisation (Saltzman, 2000).

Materials that have been used in the production of tissue-engineered arteries include collagen, a key part of the extracellular matrix forming blood vessels. Weinberg and Bell (1986) formed an artery structure from a series of collagen layers containing seeded fibroblast, SMC and EC. Such a structure had an insufficient burst pressure to withstand *in-vivo* stresses. Further improvements have subsequently been made in the design, including increasing collagen concentration (Hirai, 1994), adding sugars to the culture medium to chemically strengthen the collagen matrix (Girton, 2000) and using cyclic strain to encourage cellular led reorganisation of the collagen structure to increase the burst strength to in excess of physiological levels (Seliktar, 2000).

Biodegradable polymers such as poly-L-lactic acid (PLLA), poly-glycolic acid (PGA) and poly-lactide-co-glycolide (PLGA) originated as implanted sutures that dissolved *in-vivo* and have been used for many years (Saltzman, 2000). Because of this use as sutures they are FDA approved and hence highly used in tissue engineering (Teebken and Haverich, 2002). Mooney et al (1995) formed a tube that could be seeded with bovine aortic smooth muscle, by wrapping PGA squares around a Teflon cylinder of 3mm diameter and spraying PLLA or PLGA onto the surface as it was rotated using an atomiser. PGA despite being a versatile material and highly porous will begin to degrade after one day in aqueous solution (Hutmacher, 2000). Mooney et al (1995) found a combination of PGA and PLLA lasted 11 weeks in solution whilst PGA coated with PGLA had lost only 30% mass after 10 weeks. Hutmacher (2000)

comments that the use of such polymers is risky in areas with low vascularisation or blood flow as the build up of byproducts can lead to temporary disturbances where the removal rate is low. This does not affect the ability of such material to be used for tissue engineering blood vessels, as the constant blood transport will transport the degrading polymer to the kidneys at a high rate where it may be excreted. Greisler et al (1993) observed PGA residues leading to the dedifferentiation of SMCS into fibroblast like cells but despite this PGA based scaffolds have been used by several groups within bioreactors designed to produce tissue-engineered blood vessels (Niklason et al, 1999, Hoerstrup et al, 2001, Kim et al, 1999) which may suggest PGA byproduct build up was not the cause (McFetridge and Chaudhuri, 2005).

Hydrogels such as sodium alginate have been used for a variety of biomedical applications (Kuo and Ma, 2001, Mongia et al, 1996). Alginate is a polysaccharide composed of repeating units of gluronic acid (G) and mannuronic acid (M), derived from seaweed and is cheap and abundant (Kuo and Ma, 2001) and biocompatible provided high molecular weight components are eliminated (Zimmerman, 2000). Alginate may be gelatinised by addition of calcium chloride, which causes cross-linking of the polymers. This cross-linked gelatinised form provides a flexible material with which may be moulded to form a variety of 3- dimensional tissue engineering scaffolds. Alginate with covalently bonded RGD groups has been used to augment *in-vivo* soft tissue by injection. When the injected material contained cells it was shown to grow stiffer over a 12-week period indicating cell growth and proliferation (Marler et al, 2000).

Semi-permeable gels have also been created that are intended to limit cell-cell communication and interaction with surrounding tissues; this ensures that the developing organ is contained within experiences the appropriate environmental conditions. It has also been possible to control supply of growth factors to the developing cells by encapsulating them within the hydrogel, ensuring their release as the scaffold breaks down. The intent is to directly link the breakdown of the hydrogel scaffold to the respiration rate of the contained cell (Pachence and Kohn, 2007).

1.3.4 Key steps within a tissue engineering process

Tissue engineering is a multi-stage process with a series of complex integrated steps. The potential scale of operation is very large as the number of patients that may be treated by many of the existing and future potential tissue engineering therapies is of the order of millions. Many of the current products within the market place are manufactured manually (by trained operators within laminar flow hoods) and have undergone limited automation that would permit truly high throughput, although current developments are taking place. The issues with commercialisation of tissue engineering products were highlighted by the bankruptcy of pioneering tissue-engineering companies such as the two main producers of a tissue engineered skin-like substance: Organogenesis and Advanced Tissue Sciences (ATS) in 2002 (Mason, 2003). The former ATS Vice-Chairman Gail Naughton was quoted as saying *“Problems with automation and scaling-up the bioreactors is what has killed the products to date”*.

This observation was echoed in a commercial report published at the time exploring the potential for mass production of tissue engineering products *“Tissue engineering*

has yet to realise its full potential as a platform technology for a wide range of commercial products. This is mainly because current technologies do not allow cost-effective, commercial production of replacement tissues and organs (Anon, 2003).

Since then a number of companies have developed robotic cell culturing systems, which primarily seek to replicate the actions taken by human operators, through the use of automation. Such actions allow standardisation of experimental technique and can be operated without breaks.

The SelecT is an automated robotic system developed for the automation of cell culture by TAP [The Automation Partnership, Cambridge, UK]. With a capacity of 90 T175s or 210 plates (96 or 384 well), the system is capable of harvesting, counting and seeding cells. The system is designed primarily for experimental work and is in no way adapted for tissue or organ growth. With suitable adaptation such a system could however be adapted to provide the steps prior to bioreactor seeding in a tissue engineering or regenerative medicine process. Tecan's Cellerity™ [Tecan Trading AG, Switzerland] is a similar system composed of modular systems such as pipetting, centrifugation that can be combined into an automated cell process. Although the Cellerity differs from the SelecT in its modularity, its application is equally limited to anything more than the initial preparatory steps prior to seeding into the bioreactor.

The following section will discuss the key stages within tissue engineering a blood vessel and both existing and potential automation of the process shown in Fig. 1.4.

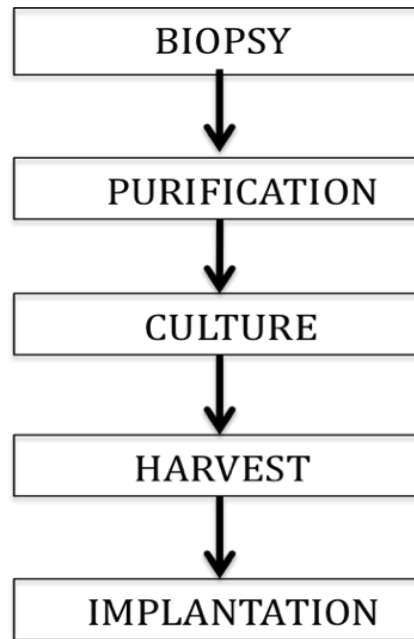


Figure 1.4 Tissue Engineering Process

The growth of an artery by tissue engineering requires that appropriate cells be extracted from the human body by biopsy. Due to the lack of specificity in biopsy, these cells will require purification. Invariably the number of cells post-purification will be insufficient to provide an appropriate seeding volume for growth of tissue and thus *in-vitro* expansion in culture will be required before the replacement organ or tissue may be implanted into the patients.

1.3.4.1 Biopsy

The first stage of tissue engineering a blood vessel is obtaining the cells required. Mature cell types such as EC have been obtained for experimentation from umbilical cord (L'heureux et al, 1998), saphenous vein (Matsumura et al, 2006), or from human patients who have undergone bypass surgery, biopsies of their coronary arteries being taken at that time (L'heureux et al, 2007). SMC have also been obtained from the saphenous vein on occasion (Matsumura et al, 2003) and from the medial layer of bovine aorta (Niklason et al, 1999) although this was not used for human implantation.

More recently most research has moved towards using MSC as the raw material for tissue engineering an artery (Matsumura et al, 2003, Gong and Niklason, 2008).

The nature of the biopsy required to obtain MSC is a bone marrow aspiration or harvest. Bone marrow harvests for the collection of stem cells have taken place for over thirty years and have become routine procedures. The harvesting normally takes place under general anaesthetic in a surgical environment and involves the insertion of a large needle directly into the bone marrow cavity, usually around the hip or lower back area (superior iliac spine) after sterilisation (Matsumura et al, 2003). Bone marrow may then be aspirated from the bones. To collect sufficient material, a number of separate injections are required and the entire procedure normally takes around two hours and acquires a litre of undefined bone marrow material of which the stem cells form just one component. Such a procedure results in discomfort at the site of harvest and may result in complications such as bleeding, infections and in worst cases nerve damage (Bain et al, 2003). The collected material may then be sieved using a nylon cell strainer to remove fat and bone (Matsumura et al, 2003).

An alternative method involving collection of stem cells from the peripheral blood involves the use of a catheter in one or several sites, unlike bone marrow harvesting which has been carried out for several decades (Thomas et al, 1957) this method only arose in the early 1980s (Korbling and Anderlini, 2001).

Bone marrow biopsies carry a large variation in the quality of the product obtained, this variation arises from the doctor making separate injections in a relatively vague region and having little or no idea the location of the most appropriate regions for this patient. This variation in raw material composition translates to variation in process dynamics such as cellular growth rates (Phinney et al, 1999).

Two aspects could be improved to achieve greater standardisation;

1. Improved mapping or modelling of the bone marrow region (Mantalaris et al, 1998). If a more specific location containing a high concentration of stem cells could be established then fewer injections would be required and a greater confidence could be established with regard to the quality of the starting material. A lower number of harvesting injections would also result in a lower risk to the patient.
2. Improved collection of the stem cells. If improved mapping could be coupled with an automated bone marrow collection method possibly involving the use of robotics then the operation would be standardised to a far higher level and consistency would be far higher. Such methods have previously been explored by a number of companies e.g. Harvest Technologies Corporation, Plymouth, MA. (Bottino et al, 1995).

A greater mapping of the region would result in an improved quality of raw material and an automated collection method would reduce human variation introduced into the procedure.

1.3.4.2 Purification

Although clinical trials have taken place using ill-defined cell mixtures such as those to treat coronary heart disease using bone marrow material (Strauer et al, 2002), it is

likely that regulatory and validation requirements will necessitate the separation and subsequent purification of an appropriate well defined cell type before it would receive approval for use in a clinical environment. For this reason cell sorting based upon key cell markers is required. Although MSC are normally selected for by rapid plastic adherence (Koc and Lazarus, 2001) when the markers of these cells are better understood a more formal method of separation would be required.

There are several such separation methods.

FACS (Fluorescence Activated Cell Sorting) is extensively used in immunology to determine the stage of proliferation, differentiation or activation of immuno-competent cell. It has also been used to purify variety of cell types (including neural stem cells) producing GFP (Green fluorescent Protein). Such purification methods would permit separation of an appropriate cell type within a population to allow it to be cultured in isolation (Sergent-Tanguy et al, 2003).

Cells carrying the complementary marker will bind to these beads and concentration may also take place by applying a magnetic field to bring the beads together in a single area (Enroth and Engstrand, 1995). This technique has been applied to separating a type of Embryonic Carcinoma Cells (Embryonic-like stem cells derived from teratocarcinomas) called NTera2 to some effect (Przyborski, 2001). Sterility testing must also take place, the minimum tests required should include mycoplasma and pathogen testing (Stacey et al (2007). Additionally whilst some bacterial contaminations will be clear to the naked eye at an earlier stage, some will be not so

apparent and could lead to cross-contamination with many lines before discovery, potentially risking huge quantities of research work.

Impurity removal may be achieved by washing in Phosphate Buffered Saline (PBS) after separation and purification followed by centrifugation and re-suspension into fresh media (Freshney, 2000).

1.3.4.3 Culture

Before the isolated cells may be inserted into a bioreactor, they must be expanded until the seeding density of $1 \times 10^6 \text{ cell.ml}^{-1}$ of alginate scaffold can be achieved. The first sub-culture or passaging represents an important transition for a culture. It implies that the original culture has expanded to occupy all available substrate and normally the population has become relatively uniform in its growth rate (Freshney, 2000). This expansion takes place in a laboratory setting and for any tissue intended for *in-vivo* implantation must obey current good manufacturing policy (GMP). Biological production processes are obliged to obey strict governmental regulations including the methods, facilities, labelling and storage of the product (Dorresteijn, 1996). To this end each process requires a detailed standard operating protocol (SOP) on record for all steps (Dorresteijn, 1996). During the culture stage, cells from different patients require separate storage in different incubators, with predominantly disposable equipment used to avoid cross contamination during cell handling.

Cells are grown within tissue culture flasks that contain treated bottom surface that encourage cell attachment. Depending upon the cell flask and the cell type required, a

more specific type of coating such as fibronectin or gelatine (Freshney, 2000). The media within these flasks requires constant exchange to limit reduction in substrate concentration and rise in waste concentration. This media exchange also provides an opportunity to determine the rate of metabolism for the growing cells, by measuring the concentration change of various substrates.

1.3.4.4 Harvest and implantation

Martin et al (2004) hypothesised a system that in addition to producing a vascular graft under controlled conditions would monitor the development of the graft and provide the surgical team with data on the development of the graft so that implantation could be scheduled. Although they commented a bioreactor of such complexity being developed to be economical in the near future was unlikely, they did believe this represented the ultimate development. In such a scenario, a coronary artery bypass graft could be performed just as it currently is with the exception that no vein harvesting would be required.

1.4 Bioreactors in tissue engineering

Within this section consideration will be given to the types of bioreactors used for tissue engineering other tissues and finally those within related industries and how such technology may be applied to developing a tissue engineered blood vessel and ultimately designing an integrated environmental control system As outlined by

(Portner et al, 2004) bioreactors are used for a number of different reasons within Tissue Engineering:

- a) Cell proliferation on a small scale, usually for research purposes
- b) Generation of three dimensional tissue constructs
- c) Direct organ support devices

1.4.1 Small Scale cell proliferation

Within this category fall micro-bioreactors for growing suspensions cultures such as those developed at MIT (Zanzotto et al, 2004) and subsequently multiplexed (Szita et al, 2005). These systems often contain at most minimal control systems and are operated in either incubators (which themselves control temperature, carbon dioxide and sometimes oxygen concentration) or bespoke made boxes that behave exactly as an incubator does.

Many incubator stages for viewing live material in real time under the microscope under environmentally controlled conditions can also be best characterised as small-scaled bioreactors and include devices such as those developed by Linkam (Linkam, Surrey, UK) and Nikon (Nikon Instruments Europe B.V). These devices often possess temperature and gas control but still suffer from the feed – starve cycle experienced by static cultures due to a lack of continuous media exchange.

Continuous systems do exist for small-scale cell growth and include hollow fibre and airlift bioreactors (Safinia et al, 2005). Hollow fibre systems possess the advantage of

reducing shear but suffer from issues of scaling due to inconsistencies in gaps between fibres and as with most bioreactors when organ-like cell densities are reached (more than 10^8 cells.ml⁻¹) will suffer from mass transfer limitations (Schonberg and Belfort, 1987).

An alternative system, the airlift bioreactor, although much more able to be scaled effectively suffers from the shear generated by bursting of the bubbles formed from the gas used to sparge the system with oxygen for the developing cells (Sardonini and Wu, 1993). This shear is responsible for cellular damage that impacts cell growth and proliferation.

1.4.2 Generation of three dimensional tissue constructs

Within tissue cultures a key problem is mass transfer through tissue masses as the thickness of biological matter increases (Nerem and Sambinis, 1995). These mass transfer limitations in the right circumstances can lead to necrotic regions forming in tissue engineered materials due to lack of oxygen or nutrient supply (Wohlpert et al, 1991). *In-vivo* such mass transfer limitations do not lead to the formation of necrotic regions due to the extensive vascularisation of the human body (Cassell et al, 2002) and mimicking this vascularisation *in-vitro* is currently one of the greatest challenges limiting the development of large or complex tissue and organs within bioreactors.

It is because of these mass transfer issues that successful tissue engineering products have been limited to relatively simple structures such as skin (Egelstein and Falanga, 1997), blood vessels (L'Heureux et al, 1998) and the bladder (Atala et al, 2006), all

these possess relatively thin walls and can be developed successfully despite limitations of mass transfer.

A number of bioreactors have been developed with the intent of producing a variety of these simple structures e.g. cartilage (Mahmoudifar, 2005), bone (Jannssen et al, 2005), vascular material (Mironov et al, 2003) and even neural material (Sen et al, 2002). These bioreactors are usually used in conjunction with some sort of support scaffold and attempt to mimic *in-vivo* processes such as nutrient supply and waste removal to encourage pockets of cells to proliferate and form three dimensional organ-like structures (Hutmacher, 2000).

Perfusion systems are common in the generation of such constructs as they allow both fresh feeding of medium containing growth factors and the removal of waste products that are often cytotoxic. These perfusion systems tend to take a standard form and incorporate a bioreactor, some method of gas exchanges, media reservoirs and associated pumps.

The majority of perfusion bioreactors that have been successfully employed in tissue engineering are bespoke systems that have been developed within university departments for growth of very specific tissue constructs including heart valves (Hoerstrup et al, 2000), small diameter arteries (Williams et al, 2004) and bone (Cartmell and El Haj, 2005).

Several devices have been adapted to employ mechanical strain on the construct to assist in the development of specific cell structures (Kino-Oka and Taya, 2005),

Cartmell and El Haj, 2005), such devices incorporate the common components in tandem with some method of applying forces to the developing tissues.

Limited development of complex systems for the control of biological parameters has taken place. Minuth et al (2005) identify the key variables as pO_2 , nutrients, electrolytes, ECM, temperature, pH, morphogens and mechanical load, while McFetridge and Chadhuri (2005) specified Temperature, pCO_2 , pO_2 , nutrients and pH must be controlled within set parameters. The methods for achieving such control were respectively not identified and instead the solution was to place their device within a controlled incubator. Such a solution although effective is not useful in the long term as it does not readily lend itself to the scale out required by most market sizes. Additionally incubators experience gradients of temperature and gas concentrations that even at low levels could affect the development of undifferentiated cells such as MSC. (Ellis et al, 2005) stated that *in-vitro* creation of three-dimensional tissues will require well-controlled culture tools but provided no details on how this might be achieved. Kasyanov et al (2005) used a digital pump with a flow-rate range of $28-1700\text{ml}\cdot\text{min}^{-1}$ to which was controlled by a PC connected to a pressure transducer to maintain static pressure at 150mmHg, but resorted to controlling other environmental parameters by designing the system to operate with a standard incubator. Kino-Oka and Taya (2005) showed the future aim of any tissue-engineered bioreactor with a schematic of a radial flow system used to produce antibodies by the Kirin brewery in Japan. This system used a series of continuous control feedback loops linked to invasive probes to maintain environmental properties. pH was measured and maintained by a carbon dioxide mass flow controller, likewise oxygen was measured and kept constant by the action of an oxygen mass flow controller, with

the two being balanced by a third linked mass controller attached to a nitrogen feed. The overall medium flow rate was also controlled to maintain glucose concentration within the system. Although such a system uses invasive probes, the design is very applicable to a tissue engineering system and represents a suitable potential model for a perfusion system such as the VTEB. The ideal long- term goal described by Martin et al (2004) is a system where the surgeon would remove a biopsy from the patient and introduce it to a bioreactor located on site. This bioreactor would contain all required reagents in separate compartments and would automatically isolate, expand, seed and culture the graft. Development would be monitored and surgery scheduled based on estimated delivery time. Although a system of this complexity does not yet exist and its design is based upon purely theoretical ideals, this work will provide a first step towards realising some aspects of this design.

1.4.3 Direct Organ Support Devices

Such devices are relevant to tissue engineering, as many of the control issues are similar to those within tissue culturing devices. Examples of such devices are those used to support Liver function in patients who have suffered failure of that organ referred to as BALs (Bio-Artificial Livers) (Allen et al, 2001). One of the more far-sighted references on such work (Balis et al, 2002) suggested the use of a microcontroller for offline control of parameters such as DOT based upon predictive models. The potential such a system gives for scale-up is one that could be applied on a wider scale to tissue engineering with great effect.

1.4.4 Traditional bioprocessing

The simplest form of cell growth vessel used within the bioprocess or biochemical engineering discipline is one within which there is no dynamic exchange of media contents, a static culture. The vessel for static culture is merely a sunken well in the case of suspension cells or a suitable chemically adapted surface for an adherent culture such as a tissue flask or gas permeable blood bags (Collins et al, 1998). Such systems do not have continuous media exchange and as a result of batch or semi-batch like re-feeding will constantly go through a feast-starve cycle that is in no way representative of *in-vivo* conditions. The absence of mixing in such static 2D systems, gives rise to heterogeneous environmental distributions throughout the system (Collins et al, 1998) and these environmental variations can lead to differences in cell behaviour within the system and reduce reproducibility (Ellis et al, 2005). Additionally, it has become apparent that two-dimensional systems do not necessarily translate to an equivalent three-dimensional cell culture (Weaver et al, 1997, Abbott, 2003) and thus have limitations even as a diagnostic tool of likely behaviour of cells when forming into organs or complex tissues. It is for this reason that dynamic bioreactors are largely seen as the appropriate method of manufacturing any tissue engineered product.

A bioreactor is the general name given to any closed culture environment (usually agitated) that is designed to control at least one environmental parameter of a physio-chemical environment (Ellis et al, 2005) to achieve aseptic feeding and sampling and to automate the process and thus improve reproducibility (Doran, 1995). Some of the first industrial applications of bioreactors were in fermentation and although many

other systems do exist, it is fermentation that has been developed the furthest particularly in the area of process control.

The traditional priorities of fermentations are fundamentally different from those of tissue engineering. Traditional fermentations use the cell as a production facility for a particular intra or extracellular factor (Belter et al, 1998). At the completion of fermentation, in the case of an intracellular product, the cells are disrupted (normally resulting in death) and in the case of extracellular products the cells tend to be filtered out downstream and disposed of as part of the filter cake (Belter et al, 1988). The priority in either case has always been to maximise yield of the desired product. Environmental conditions within the fermenter are optimised for the manufacture of these products and not for the cells, which will either be disrupted or filtered out and disposed of.

It should not be assumed healthy unstressed cells and high product yields are mutually exclusive events during fermentation, indeed much research has taken place to avoid stress in such circumstances (Schweder et al, 2004). In many instances the production of stress products such as heat shock proteins, e.g. chaperones reduces yield of the desired product (Lindquist and Craig, 1988), however the fermenter is often operated in a manner that forces the cell to overproduce the desired factor at the expense of its own health.

The adaptive capabilities of bacteria honed over many years of evolution allow them to respond and adapt to culture conditions in environments such as the laboratory, which are often radically different from the natural habitat (Roszak and Colwell,

1987). Response to such an environmental shift may result in a large increase in desired product yield whilst limiting life span or health of vector. In traditional bioprocessing such a compromise, is deemed acceptable.

Whilst in cell culture the aim is to operate within as tight a tolerance as possible close to the *in-vivo* environment of that cell, the standard approach when carrying out fermentations is to ensure by measurement that the controlled parameter does not fall below a specified minimal level (Stanbury et al, 1999). The extent of control, for example, of oxygen concentration, usually via a feedback loop and an invasive DOT electrode (Stanbury et al, 1999), is to operate above this critical value. Due to the high oxygen demand of bacteria and yeasts (Doran, 1995) and the interest being in the product rather than the cell, the problem of too much oxygen is not one that is likely to be prevalent for fermentation processes. Despite this however mass transfer limitations such as of oxygen and nutrients are an issue in all cell growth systems, in the case of fermentation due to the high growth rates and in the case of tissue engineering, due to the thickness required of living material for many organs.

Mammalian cells are particularly vulnerable to bacterial contamination and the use of antibiotics is not permitted due to the potential for undesirable responses by the immune systems of the recipients due to allergy or idiosyncrasy. Whilst a fermenter is normally made of stainless steel and is sterilised using high-pressure steam (Doran 1995), this level of sterility is not sufficient for a tissue engineering bioreactor and as a result disposable portions tend to be incorporated into the system for those parts that are in contact with the growing cells.

Despite these differences in purpose and strategy, many of the process control demands are the same and include maintaining desired environmental conditions and finding ways to measure cell growth online. In this area fermentation and other areas of bioprocessing are far more advanced than tissue engineering. Although many bioreactors implement simpler control systems, such as two-step and Proportional Integral and Derivative (PID), which respond based upon a set point or perform a mathematical calculation to determine the size of the response based upon the error, much more advanced systems have been theorised.

Siimes and Linko (1995) developed a fuzzy-knowledge based system for the control of baker's yeast production. Fuzzy logic, developed in 1965 (Zadeh, 1983), involves the linking of linguistic statements such as high, low to logical conditions such as 'if' and 'or'. A series of these statements may be formed and by weighting the various statements based on literature or expert knowledge and linking them to numerical ranges a control system may be formed (Konstantinov and Yoshida, 1991). Such a system allows complex systems to be reduced to ranges and combinations of events rather than specific equations and exact relationships, permitting prediction to be made, often with high accuracy. Implementing this approach Siimes and Linko, (1995) were able to identify which growth phase a culture was in and diagnose faults at an early stage.

Konstantinov and Yoshida (1991) observed that fuzzy controllers could be either used to directly control the process, replacing standard controllers (e.g. PID) or in a higher level controller supervising the lower system level which is no different to a standard control system and informing it how to act and when, perhaps by changing the set

point of the controller. Flanagan (1980) used a supervisor to monitor and control the set points of a series of conventional controllers responsible for wastewater treatment. By modifying these set points the overall dissolved oxygen within the system could be controlled effectively.

Intelligent systems using expert knowledge have also been applied to distributed control systems. Flores et al (2000) designed and implemented a system for remote monitoring of wastewater treatment at a number of different locations. This controller was based on an expert system that reduced the output parameters received by the operators to symbolic data that is more easily understood by them, improving the quality and rate of their response. Such a controller reduced start-up time and the attainment of stable conditions from three months to three weeks, a significant decrease. Recent advances have even extended to using neural networks as a tool to predict and control fed batch kinetics (Petrova et al, 1997).

It is vitally important, as with any advancement within science, that the regenerative medicine and associated bioprocessing discipline [tissue engineering] must learn from the experience of other fields (Mason and Hoare, 2006) Many of these advanced control systems will in the future be very relevant to tissue engineering. Distributed control particularly holds great promise for the future scale-out of the bioreactors. Such advances in bioprocessing took place when the limits of controllers such as PID were reached and this is not yet the case in tissue engineering where little or no work in this area has been carried out.

1.5 Control Parameters within tissue engineering bioreactors

Having examined the automation utilised in existing tissue engineering bioreactors and related disciplines such as bioprocessing, it is important to consider which variables require controlling in a biological system.

Major improvements have been achieved in the control of biological production processes. Much of this improvement has been achieved through the development of computerised measurement and control units that have allowed the application of on-line modelling of the process and in doing so improve yield and consistency (Dorrenstijn et al, 1996). Measurement outputs such as Dissolved Oxygen Tension, pH or metabolite concentration can be used to control physiological parameters and regulate substrate feed (Dorrenstijn et al, 1995, Dorrenstijn et al 1996).

The basis of control is largely to produce a standard product through the use of a standard process at a predictable rate. Locher et al (1991) demonstrated that the reproducibility of a bioprocess is directly influenced by the reproducibility of environmental conditions within the bioreactor. The exact parameters that should be measured have become relatively standard within bioprocessing and usually consist of the following:

pH or dissolved carbon dioxide concentration (see section 1.5.1)

Temperature (see section 1.5.2)

Substrates and metabolites (see section 1.5.3)

Dissolved oxygen tension (see section 1.5.4)

1.5.1 pH

pH is a particularly important parameter in mammalian cell culture as it can affect the stability of proteins within the cells and hence the health of the cell. The current philosophy in terms of pH is to keep a culture as close to the physiological pH 6.8-7.5 as possible. Standard medium for the culture of stem cells is normally a basal media such as Dulbecco's modified eagle medium (MEM) or Mesencult (designed specifically for the culture of MSC), containing either a bicarbonate buffer or HEPES (4-(2-hydroxyethyl)-1-piperazineethanesulfonic acid) an organic buffering agent to regulate pH within solution. Bicarbonate buffer is carbon dioxide assisted and requires a certain dissolved carbon dioxide content to maintain a physiologic range. HEPES has the advantage of being independent of such constraints but has a slightly less specific working pH range.

Both of these buffers are used as they possess a pKa optimal for buffering effect around a physiological pH (in the case of bicarbonate this is only the case when physiological carbon dioxide levels are also replicated). Any excursion significantly outside of the stated physiological boundary is likely to indicate:

- i. The environment is no longer suitable for life.

- ii. A contaminating agent may well be present; bacteria divide rapidly and produce large amounts of waste product such as lactate and ammonia – the presence of which is displayed through pH shift.
- iii. The product is likely to be ‘spolied’ i.e. no longer suitable for implantation.
- iv. Progenitor cells may well move down an inappropriate differential pathway (Bernard et al, 2006).

The overriding assertion would seem to be that if a pH change is present that exceeds the range stated as physiological boundary, any sort of further chemical control is inappropriate as the product is no longer viable. Any pH change arising due to the production of waste products should be dealt with by employing some sort of media change system.

A number of methods exist for the measurement of pH within a solution. pH is directly related to the concentration of hydrogen ions by the relationship $\text{pH} = \log_{10}[\text{H}^+]$. Methods such as measuring electrical conductivity and chemical behaviour of solution are thus, the most common methods used to determine pH.

pH electrodes are sensitive to ions such as H^+ as the electrodes voltage output is proportional to the local ion concentration in solution. A pH measurement system consists of such an electrode in tandem with a reference electrode (holds a constant voltage for comparison purposes), these electrodes provide output that may be processed by a pH meter that acts as a transducer; converting the signal from an electrical current, measured in mV to a reading of pH. Often a temperature sensor will be part of the system and also placed in the liquid to allow compensation for the effect

on pH of temperature changes. The disadvantage of such a system is that it is invasive; this can be problematic in environments where high sterility is required, such as those encountered in tissue engineering and regenerative medicine. An additional problem with such electrodes is that due to their size, their operation in small samples is often impossible, again a major issue in fields such as those considered within this body of work.

Fluorescent Sensor spots such as those developed by PreSens (Precision Sensing GmbH, Germany) have a number of advantages over electrodes in being non-invasive, disposable and due to small size; capable of use in small sample volumes. pH mini sensors consist of a planar spot coated in two separate dyes; one, a pH indicator with a short decay, the second, an inert reference dye with a long decay time. When used with a fibre optic cable that acts both as transmitter of light signal and receiver of signals from the spots, the ratio of the emission from both dyes can be converted into a pH value of the solution. The disadvantages of such a system include, the small range of operation relative to an electrode (pH 5-9) although within a cell or tissue culture an excursion from a pH of 7 of a magnitude outside of this range in all likelihood would already be catastrophic and thus does not require accurate measurement. Also the spot over a number of excitations will become bleached and lose sensitivity (www.presens.de)

1.5.2 Temperature

As with similar environmental parameters, the temperature used for most stem cell culture is that experienced physiologically in the human body. Most cell culture takes place in incubators operating at or around 37°C (Freshney, 2000). Normal control methods for this, as stated previously, include operating the bioreactor in a heated chamber either of a bespoke design (Minuth et al, 2005, Balis et al, 2002) or a conventional incubator (Williams and Wick, 2004, Zhao and Ma, 2005, Kino-Oka et al, 2005) as found in cell culture laboratories.

Standard procedure for the measurement of temperature involves the use of thermocouple, which works by creating a circuit of two dissimilar metals. The magnitude and direction of the current within this circuit relates directly to the difference in temperature between the two junctions (Bolton, 2003). In terms of any bioreactor system large temperature fluctuations should ideally be avoided rather than merely controlled, the aim being to ensure the temperature is controlled within specification before it becomes an issue. The most appropriate method to avoid such problems is to operate the incubators within a temperature controlled facility (the standard lab operates at 19-23°C) to minimise fluctuations and for each bioreactor to be stored within a heavily insulated container such as those used in commercial thermally insulated boxes for transport of medical supplies. This box should then incorporate a heating device.

1.5.3 Substrates and metabolism

Respiration represents the method by which energy is produced by cells. This energy is used to drive synthesis of ATP, the “energy currency” of cells. Respiration is predominantly the reaction of oxygen with glucose to form water and carbon dioxide although, other metabolites and waste products are also very relevant thus cell culture typically involves a liquid broth consisting of substrates, metabolites and growth factors. Such a broth is generally referred to as cell culture medium.

These substrates and metabolites consist of glucose (and its waste product lactate) and glutamine (and its waste product ammonia) both of which are key components of cell media. Low concentration components of culture media such as Bone Morphogenic Protein (BMP) are generally ignored in a tissue engineering system, as there is currently no effective method to measure such concentrations rapidly either online or off-line, so their inclusion in the initial medium is normally of a sufficient level to maintain culture for significant periods of time. Pyruvate and glutamate, two cell culture components, are also generally neglected as they are present in much smaller concentrations in cell media. These compounds are produced and consumed at different steps of the Krebs (Citric Acid) Cycle; a key stage in aerobic respiration. Any final measured balance of these two components hence forms a ratio between consumption and production and monitoring such a value and relating it to respiration rate is not practical (Follmer et al, 2006).

1.5.4 Dissolved oxygen tension

Dissolved oxygen tension (DOT) in solution represents one of the key environmental parameters involved in the culture of cells and directly affects their physiological properties. Within any tissue engineering device it is essential that its variation is monitored and, where appropriate, controlled.

Standard policy for most experiments involving mammalian cells is to replicate normal *in-vivo* conditions and use oxygen concentrations comparable to those measured within the relevant part of the human or animal body using invasive techniques such as oxygen electrodes. Within *in-vitro* culture non-invasive measures exist just as with pH (see section 1.5.1) that use a small spot that will fluoresce when excited by a fibre optic cable. This responding fluorescence is retarded by oxygen in solution (Lakowicz and Weber, 1973) between the spot and the fibre optic cable, which also acts as a signal receiver. This signal can then be converted into an oxygen concentration (Precision Sensing GmbH, Germany).

In the case of arteries the appropriate physiological DOT depends upon the location within the body, the further downstream from the lungs the lower the DOT will be. It has been demonstrated that oxygen gradients within the bone marrow may be at least partially responsible for controlling haematopoiesis (the creation of blood cellular components) (Hevehan et al, 2000, Mostafa et al, 2000). Other cell types have also been shown to be affected by oxygen tensions, including adipocytes, the differentiation of which is inhibited under hypoxic conditions (Yun et al, 2002) and

MSCs, the osteogenesis of which is promoted by low oxygen conditions (Lennon et al, 2001).

1.5.5. Representing acceptable ranges of environmental parameters

For a set of multiple related variables, some method must be used to determine what range control variables may operate within for each to allow an overall range to be established.

A useful tool has been developed for representing complex bioprocess design multivariate problems by a graphical representation involving plotting the operational space defined by the system (chemical, physical and biological) and engineering constraints and correlations governing a particular process of operation under consideration (Woodley and Titchener-Hooker, 1996) (Fig. 1.5).

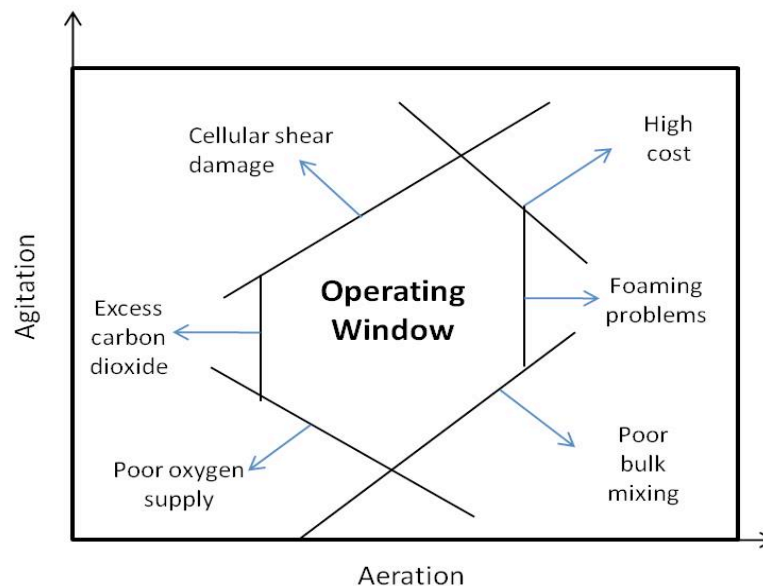


Figure 1.5 Qualitative operating boundaries for an aerobic bacterial fermentation (adapted from Woodley and Titchener-Hooker, 1996).

The window of operation (WOO) is a graphical method of relating two variables together, such as aeration and agitation in a fermenter, and determining the maximum and minimum extents of operation of these two variables. In the examples these extents are determined by parameters such as the maximum amount of aeration that can take place without foaming problems becoming prohibitive.

These windows of operation can be used to determine appropriate compromises where trade-offs must be made between two or more variables and provide an easy method for sensitivity analysis to be performed in this pursuit. Such a method was demonstrated effectively for a range of yeast growth rates within a fermentation and their relation to a set of operating conditions (Zhou and Titchener-Hooker, 1999).

Windows of operation will be used within this thesis to determine appropriate ranges of the control variable and its effect upon parameters such as temperature, pH, oxygen, substrate and metabolite concentration.

1.6 Existing Manufacture of Tissue Engineering Products

The remaining consideration with regard to the creation of a tissue engineered blood vessel is how production may be scaled up from the bench to a level where a demand in the order of millions of patients can be satisfied (Xue and Greisler, 2000).

Within the tissue-engineering field a variety of issues mostly relating to limits of basic scientific knowledge and engineering challenges, are yet to be overcome. For this reason existing tissue engineering products available on the market, have been limited to relatively simple structures that form simple geometric shapes such as skin (thin layer) (Egelstein and Falanga, 1997), blood vessels (thin walled tube) (L'Heureux, 2007) and bladder (thin walled sac) (Atala et al, 2006).

1.6.1 Blood Vessels

As of 2007 an American company Cytograft following animal testing (L'Heureux et al, 2006) with a product named Lifeline™ based on the rolled sheet technology (section 2.1) has entered human clinical trials in Buenos Aires (AV Shunt) and Cambridge, UK (Coronary Artery Bypass Grafts – CABG). Early reports indicate that six patients having undergone dialysis treatment have had cytograft vessels implanted and have been followed for up to 13 months. Of these patients, only one suffered from a non-functional vessel after 12 weeks, due to a thrombogenic failure (forming of a clot within the graft), one died from unrelated causes with a fully functional graft on day 39 and the remaining four at the time of reporting were benefiting from successful implants at between 3 and 13 months post operative monitoring (L'Heureux and McAllister, 2007). It appears that due to autologous nature of the therapy and the small scale of the trials Cytograft is currently still operating a heavily manual process. There is no evidence at the current time that a truly automated production method for creating tissue engineered blood vessels is in operation.

1.6.2 Skin

With several products having successfully proceeded through clinical trials, FDA approval and subsequently establishing positions with the market, bio-artificial skin is commonly regarded as the most successful of all tissue engineered therapies. The development of tissue engineered skin has allowed the wound management process to advance from the passive approach of removing impediments, debriding the wound and allowing natural regeneration (often unsuccessfully) to a more active approach.

Despite this success, these products continue to be limited by their inability to completely mimic the structure and function of skin, and scar formation and wound contraction remain prevalent issues.

Initial success with tissue engineered skin involved its use on burn victims (Eagelstein and Falanga, 1997). As clinicians witnessed success on such patients, treatment for other purposes, such as in the treatment of chronic wounds, was explored (Bello et al, 2001).

The purpose of tissue engineered skin is to restore the structure and function of skin. This requires the presence of an outer keratinocyte layer (major cell type of the dermis to maintain/restore the barrier function, e.g. for water regulation in combination with appropriate dermal components to provide strength, flexibility and function comparable to naturally developed skin.

The major differences between current engineered skin products and the natural substance it is intended to mimic are the absence of structures such as hair follicles and sweat glands (Jahoda and Reynolds, 2001). Such structures are ignored due to arguments that they are not essential to effective healing (an issue contended by Jahoda and Reynolds, 2001) and their inclusion would require a more complex manufacturing process which companies are keen to avoid so that commercial viability can be maintained. A secondary issue with the use of synthetically grown skin is that it can lead to the formation of abnormal scar tissue between the substitute and the patient's own undamaged skin. Particularly in concealed areas such as diabetic

foot ulcers, cosmetic issues are minor compared to a chronic ulcer failing to heal over a period of several years.

The manufacturing techniques used for the production of tissue engineered skin are in large part manual processes. The techniques tend to involve the culture of cells and tissue by trained individuals within clean room laboratories. Dermagraft®, previously produced by Advanced Tissue Sciences [www.advancedtissue.com] and now owned by Advanced Biohealing Inc. [www.AdvancedBioHealing.com] and Apligraf®, produced by Organogenesis [www.organogenesis.com], are both for the treatment of foot and leg ulcers and pressure sores. Both allogeneic therapies involve human cells and animal products such as bovine collagen. Both Organogenesis and Advanced Tissue Sciences suffered extreme financial difficulties in the early 21st century (Tissue Sciences, SEC 8K, 2002) mainly due to difficulties in scalability of the process mainly due to its manual nature (Kemp, 2006, Mason, 2007). Apligraf involved a highly manual process spread over 4 distinct locations (Banks, 2006) Whilst ATS was sold off to Smith and Nephew and has subsequently been bought by ABH, Organogenesis ultimately exited chapter 11 bankruptcy successfully (Organogenesis, SEC 8K, 2003) and has gone on to become a successful company selling around 30,000 units of Apligraf per year and has currently entered clinical trials to determine its efficacy in treating pressure ulcers and Epidermolysis Bullosa (Banks, 2006). At the time of bankruptcy it was reported up to one third of all manufactured discs of skin were contaminated and disposal was required and in 2007 Organogenesis began to roll out an automated process for the production of Apligraf using controlled robotic trays to combat these issues. This process has been designed specifically with the improvement of consistency and waste reduction in mind rather than to increase

product output (Banks, 2006). Other companies such as Ortec (Manufacturers of Orcel®) and Intercytex (launching ICX-pro in 2008) have also only used limited automation to date, an issue which they continue to explore and implement at a slow and controlled rate (Kemp, 2006). Both the owners of bankrupt and currently operating companies within the sector as well as analysts (Anon, 2003) are clear that automation and scalability are essential for the success of a tissue engineered or regenerative medicine product.

1.6.3 Cartilage

Every year around 2 million Americans injure the cartilage in their knees (www.cartiel.com). A number of autologous therapies exist for the treatment of such injuries using the patient's own cells.

The most successful therapy to date has been Carticel® which was the first FDA approved product to reach market within the United States (Wood et al, 2006). The autologous nature of the product has led to a manual process being employed for manufacture. A biopsy of healthy cartilage cells are taken from the patient expanded by manual cell culture and then returned to the surgeon and injected into the knee under a periosteal patch that is stitched over the damaged area.

Such a procedure has a number of concerns including the risk of an uneven distribution of cells within the damaged region and even the unsupported cells leaking from underneath the covered surface. The manual nature of the overall process will affect the consistency and reliability of the material and treatment the patient receives.

The relatively high failure rate of the treatment (Wood et al, 2006) may be related to this aspect.

Attempts have previously been made to develop automated technologies for the treatment of cartilage injuries. Milenium Biologix incorporated aspects of the OSTEO™ bioreactor into their ACTES™ system. The intended function of the ACTES systems was to process a patient's biopsy, culture and expand the cells before seeding them onto an appropriate scaffold and culture the tissue until it was at a suitable stage for implantation, all under automation. This system could be placed and used in a hospital by suitably trained operators (Martin et al, 2004). At the time of writing, unfortunately it appears that Millenium Biologix are no longer operating and their website is no longer active (www.millenium-biologix.com). Despite this failure, the ACTES system has proved to form the basis of a potential long term strategy for the role of bioreactors in tissue engineering (Martin et al, 2004).

1.6.4 Summary

Many tissue-engineering companies have succumbed either to bankruptcy or severe financial difficulties at some point of their operation. This has been in large part due to inadequacies in their largely manual processes, either related to output or consistency of product. The automation of tissue engineering processes subsequent to market launch is a slow and costly procedure, thus the obvious conclusion seems to be that automation must be considered as a key part of product development rather than an afterthought. Mason (2007) characterises this transition in ideology as being analogous to the development of successful Internet companies following multiple bankruptcies

and financial difficulties and christens the current situation as Regenerative Medicine

2.0. Allogeneic products lend themselves much more readily to automation as they bring a consistency of raw material that translates to a consistency in process and product that cannot be as easily achieved with autologous products. For these reasons, it seems likely that, in the long term, provided a suitable method of mitigating the immune response rather than immunosuppressant drugs can be discovered allogeneic materials are likely to become the industry standard. In the short term however autologous products will continue to represent a viable product to deal with a variety of diseases and injuries. The advantage of tissue engineered products is that although they carry a high initial economic cost by solving the underlying injury or problem, in some cases permanently, and reducing the high costs of follow up treatment often directly related to the labour of the treatment they become an attractive alternative to current methods.

1.7 Conclusions

The aim of this chapter was to present a survey of literature that would demonstrate at what stage current technology was with regard to the production of a tissue engineered blood vessel. An overview was given of the underlying biology, existing attempts at producing such vessels and automation of bioreactors within both tissue engineering and related fields. There have been notable successes in both producing a tissue-derived structure from mature cells and creating a structure that mimics the native vessel through the use of mesenchymal stem cells (MSC). The results with tissue engineered skin have shown that the more successful products are those that most closely match the tissue or organ for which they are acting as a replacement.

Mesenchymal stem cells may be the more plausible solution in the short term, as mature cells have limited proliferative capacity, particularly from ageing donors. In the much longer term embryonic stem cells may provide an excellent raw material, however the biology of such cells is little understood and requires much further work before they will provide a viable alternative.

Despite the successes at the bench and small-scale clinical trial level, little or no advance has been made in truly automating the process of creating tissue engineered blood vessels. The progress that has been made, to date, has either neglected the effects of control and the impact subtle changes in local environment may have on immature cells such as MSC or has been applied as applied inappropriate control strategies that have little or no potential for being scaled up. This has severely limited the potential of tissue engineering and regenerative medicine.

1.8 Project aims

The aim of this project was to take the first steps in developing control systems for a developing tissue engineered blood vessel created from mesenchymal stem cells within an alginate scaffold situated in a perfusion bioreactor. Key parameters considered were oxygen concentration, substrate concentration, metabolite concentration and pH, which were required to be maintained within specified ranges. Possible strategies were considered on the basis that the system would ultimately be scaled out and hence any large or expensive pieces of equipment would be inappropriate for use.

Random disturbances can be introduced to test control systems. However it is difficult to implement disturbances that are representative of the type likely to be experienced in normal operation. The solution implemented in this work is to use a surrogate yeast cell line as a diagnostic tool. Yeast is an excellent eukaryotic model and at least 40% of single gene determinants of human heritable diseases find homologues in yeast. It has been used extensively in drug discovery (Hughes, 2002) and particularly in cancer research (Lui and Simon, 2007). In this case yeast's metabolic similarity to human cells can be exploited. Yeast grows and divides at a much higher rate than most human cells and thus if the oxygen and substrate consumption and metabolic waste production of yeast can be effectively controlled, then the system will be sufficient for a bioreactor designed to control the development of a tissue engineered artery.

Chapter 2 Materials and Methods

The aim of this chapter is to describe in detail, techniques, materials and reagents used within the practical work and software packages and solver methods used within the theoretical work.

2.1 Mesenchymal stem cell culture

2.1.1 Cell isolation

Adult human Mesenchymal Stem Cells (MSCs) were provided at stage 2-4 passage (P2-P4) from colleagues working within the Regenerative Medicine Bioprocessing Unit, Dept. Biochemical Engineering. The use of human clinical samples has been approved by the joint University College London and University College London (UCL) Hospital (UCLH) Hospital Ethics Committee of Human Research. These cells were obtained from colleagues working within the Regenerative Medicine Bioprocessing Unit (ReMeBio), Dept. Biochemical Engineering, University College London. The method of isolation of these cells is described below;

A sample size of 10ml (typically 5-10ml was used) of freshly harvested bone marrow was filtered using a 40µm nylon cell strainer (Falcon, Bibby Sterlin, Stone, UK) and then rinsed with an amount equal to the size of the sample of Dulbecco's phosphate buffer solution (DPBS) without calcium and magnesium (Biowhittaker). A 20ml of ficoll of density 1.077g.ml⁻¹ was added to a 50ml centrifuge tube (Corning, NY. USA) and the tube orientated at an angle so that the surface area on the top of the liquid was

maximised. This tube was placed in a suitably balanced centrifuge (5801R Centrifuge, Eppendorf AG, Hamburg, Germany) at 652g for 30 minutes at room temperature with no break applied. This centrifugation caused the desired fraction, the mononuclear cells, to remain at the surface whilst undesirable material, such as red blood cells, was forced to the bottom. The layer of mononuclear cells at the surface were gently aspirated using a pipette (Fisher Scientific, Loughborough, UK) and placed into a second centrifuge tube, rinsed with 40ml of DPBS and centrifuged at 290g for 10 minutes at room temperature with a low brake setting. The supernatant was aspirated off of the resulting cell pellet and discarded and the pellet was resuspended with 5ml of complete MSC media, removed by pipette and injected into a T75 tissue culture flask (Corning, NY, USA). At this point, a further 5ml of complete medium was added. This flask was placed in a humidified incubator at 37°C and 5% Carbon Dioxide concentration (HeraCell 150, Kendro Laboratory Products GmbH, Langensbold, Germany or Galaxy S, RS Biotech Laboratory Equipment Ltd, Irvine, Scotland). Fresh medium was added every 2-3 days and after 2-3 weeks the MSC were sufficiently confluent (ca. 75%) within the T Flask that they were passaged.

2.1.2 Culture Vessel

The stem cells prior to insertion into the bioreactor were grown in polystyrene tissue flasks (Corning, NY, USA). These tissue culture flasks contained a negatively charged, hydrophobic surface to encourage cell attachment. Sizes of these flasks varied from T25 – T150 (25-150cm²).

2.1.3 Culture medium

MSC growth medium was composed of MesenCult (Stem Cell Technologies Inc, Vancouver, British Columbia, Canada) combined with appropriate antibodies, 100U/penicillin.ml⁻¹ of media (Sigma) and 100µl of streptomycin.ml⁻¹ (Sigma) and 1ng.ml⁻¹ recombinant human fibroblast growth factor (rhFGF) (R&D systems, Minneapolis, Minnesota, USA).

2.1.4 Passaging MSCs

MSCs provided by ReMeBio were passaged every 6-7 days with the cells in the flask being divided into three new flasks, when ca. 90% confluency was achieved in T150 culture flasks. Prior to performing cell passaging, the culture medium was examined for colour of pH indicator, presence of cell debris, confluence of cells and morphology.

As a first step, spent medium was aspirated for analysis using the Bioprofile Analyser (Nova Biomedical, UK) to determine glucose, glutamine and lactate and ammonium concentration as an indication of cell health. The bioprofile analyser permits these tests to be carried out in series within a single unit for ca. 300µl of media feed and generates a printout showing the levels of all these metabolites.

Following the media aspiration, the adherent surface was washed with phosphate buffered solution (PBS) to remove any remaining factors such as those from foetal bovine serum (FBS) that can interfere with enzyme activity,

After washing 5ml trypsin-EDTA (0.25%:0.02%) was infused into the culture flask which was then turned horizontally so that it coated the adherent surface and was incubated for 5 minutes in a 37°C 5% CO₂ environment. After 7 minutes hMSC were detached from the base of the flask by tapping it against the open palm of the hand.

Subsequently, enzyme activity was quenched using 10ml media within a 50ml universal flask and centrifuged at 100g for 6 minutes, following which, the supernatant was aspirated off to leave the cell pellet, which was then resuspended in 3ml of media and agitated by pipette. Of this resuspension, 1ml was pipetted into each of three flasks, with 14ml of fresh media subsequently added to each. Finally, these newly seeded flasks were transferred to a 37°C and 5% CO₂ controlled Incubator (HeraCell 150, Thermo Scientific, MA, USA).

2.1.5 Refeeding of MSCs

MSCs were passaged every 6-7 days and cell cultures were also refed in the interim at 3-day intervals. Refeeding is a simple operation and merely involves aspirating spent media (keeping a sample for chemical analysis e.g. glucose, lactate and glutamine) and replacing it with an equivalent amount of fresh media. This refeeding is necessary to replace depleted substrates, consumed by the cells or broken down by thermal degradation at 37°C (glutamine). A build-up of waste products of cellular respiration can prove toxic to the cells and may also lead to a pH shift, which is in itself harmful to the growing cells and such build-ups are also mitigated by media exchange.

2.1.6 Cell Counting and Viability – Trypan Blue Assay

200µl of cell suspension was placed in a 20ml universal tube, with an equivalent amount of 0.4% trypan blue solution. This solution was mixed gently by pipette and allowed to stand for 5 minutes to permit staining. 10 µl of the resulting solution was pipetted into a haemocytometer where stained and unstained cells were counted to form the viable and non-viable cell populations respectively. Multiplying the average number of cells within the quadrants of the haemocytometer by 2×10^4 converts the viable and non-viable cell counts into a concentration per ml.

2.2 Yeast Culture

2.2.1 Yeast extract peptone dextrose (YEPD) broth

Yeast extract peptone dextrose (YEPD) broth is a complete media for yeast culture and contains yeast extract, peptone and dextrose (glucose) and distilled water. 10g of Difco peptone (Sigma) and 5g of yeast extract (Sigma) were added to 450ml of distilled water and autoclaved. 10mg of glucose was added to distilled water and sterile filtered through a 0.2µm cellulose acetate Nalgene filter flask to ensure sterility. This was then added to the autoclaved broth.

2.2.2 Initial Culture

Live baker's yeast was obtained from a master baker (J.Sainsbury and Son, UK) in 1kg units. A 0.5ml pipette tip was used to harvest a small amount of yeast cells, which were cultured in suspension within a 1L shake flask, containing 50ml of yeast extract

peptone dextrose (YEPD) broth, and agitated within an incubated orbital shaker over night (12-16 hours) at 250rpm and then harvested. 50ml volume and 250rpm were selected as operating conditions to ensure oxygen concentration did not fall to zero during cell growth (Talosa et al, 2002).

2.3 Bioreactor System

This system was inherited from previous research (Mason and Town, 2002; Chau, PhD Thesis, UCL, 2008). The general layout is shown in Fig. 2.1 and is of a perfusion design. Fresh feed is pumped into the system to maintain concentration of substrates within the recycle loop and an associate purge ensures the concentration of waste products does not rise indefinitely. An oxygenator within the recycle loop oxygenates the media, which is transported into the bioreactor containing the growing cells

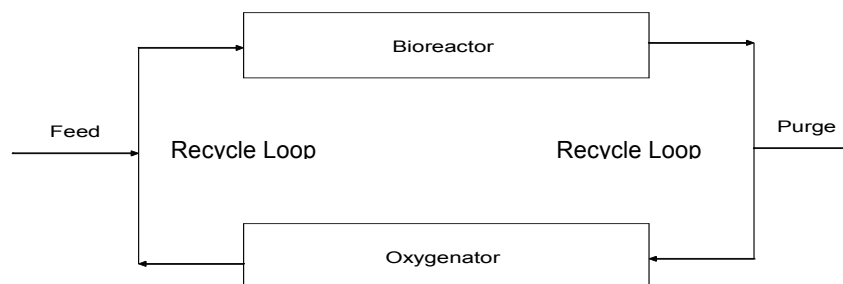


Figure 2.1 General layout of the bioreactor system

The system incorporates a bioreactor, containing the alginate scaffold within which the artery will develop, a membrane oxygenator and a feed and bleed system for providing fresh media and removing build up of waste products.

2.3.1 System fluid transfer (pumps)

The system design necessitates the use of two pumps, one responsible for perfusing fresh feed into the system and one responsible for the movement of media within the recycle loop.

The type of pump selected in both cases was a peristaltic pump. Such a pump was chosen as it is particularly appropriate where the materials being transferred are vulnerable to contamination, such as cell culture medium, and must be kept isolated from the pump housing.

The use of peristalsis as the method of propulsion has an impact upon the type of tubing, which must possess sufficient flexibility to ensure that an appropriate displacement can be created in the tube to force the media forwards. Common materials for such tubing include amongst others Poly Vinyl Chloride (PVC) and silicone rubber. In addition to flexibility the tube must possess sufficient strength to last around six weeks of constant displacement by the peristaltic pump.

Pumps were purchased from Instech laboratories Inc (Plymouth Meeting PA, USA). The Instech P625/900 was selected due to its low flow rates, coupled with accuracy, small size (provides portability which is a pre-requisite for potential future scale-out), and low power demand. Such a pump is especially well suited to battery powered systems which could be useful for future scaling of the bioreactor especially during transport. Although it is likely that this system will go through many iterations of

development before it is suitable for use at a manufacturing scale. However, it is desirable to consider future requirements, even at an early stage.

The feed pump (P625/900, Instech, PA, USA) is designed for operation at moderately low flow rates, as it was anticipated the feed rates would be much lower than the recycle rates. This pump was capable of flow rates of between 1.2ml.hr^{-1} and 24ml.hr^{-1} when used with a 0.031" diameter tube (Instech, Set-up instructions; P625 Peristaltic Pumps).

The recycle pump (P625/141, Instech, PA, USA) operates at higher flow rates than the feed pump within a range of 0.9ml.min^{-1} and 18ml.min^{-1} when used with a 0.093" diameter tube (Instech, Set-up instructions; P625 Peristaltic Pumps).

2.3.2 Tubing

In addition to being appropriately flexible whilst still possessing the inherent structural integrity to be used in tandem with a peristaltic pump there are a number of properties the tubing requires to be used within this body of work.

Given that the gas concentration within the flow will be closely controlled it is vitally important that the tube is as impermeable to gases as possible. Additionally given the biological nature of the material being produced within the bioreactor, it is vital that the tubing does not leech chemicals as plastics commonly do.

The tubing selected to perform this work was the Tygon S-50-HL tubing (Saint-Gobain Performance Plastics Corporation, MA, USA). In addition to meeting the aforementioned criteria Tygon S-50-HL is designed for use in medical and surgical procedures and more specifically for the perfusion of blood in peristaltic systems and meets all requirements of ISO 10993 a standard set relating to biocompatibility of a medical device prior to clinical study.

The values for the pump duties provided by Instech were for silicone tubing, although when tested with the Tygon S-50-HL tubing, they also held true.

2.3.3 Oxygenator

Living cells require oxygen to respire, live and grow. In the case of stem cells the concentration of oxygen carries a separate importance as a signalling molecule.

To enable such control the oxygen must thus be introduced into the system in a regulated manner and the device used to achieve this is a membrane oxygenator (Living Systems Inc., Burlington, VT, USA). This oxygenator is of a membrane bundle design and contains 162 polypropylene fibres of 7.5 centimetres in length with a polycarbonate case. This oxygenator was selected because it had proved successful in previous perfusion bioreactor systems developed within the Department of Biochemical Engineering at University College London. This device contains four fittings (as shown in Fig. 2.2) and oxygen diffuses from the chamber of the device into

the cell culture media as it is pumped through the membrane bundle.

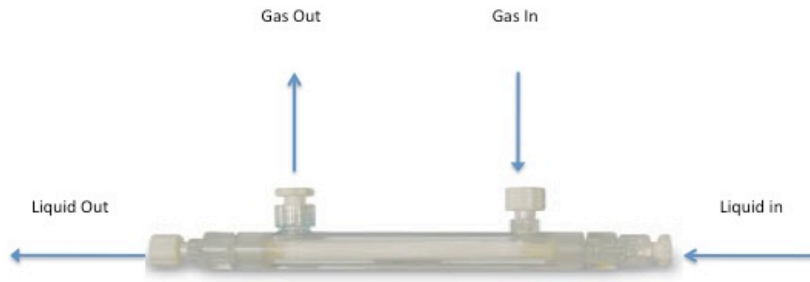


Figure 2.2 OX Miniature Gas Exchange Oxygenator by Living Systems (www.livingsys.com)

2.3.4 Media and Waste Storage

Media and waste were stored in 3L Flexboy clinical bags with Luer locks (Sartorius), which were supplied in sterile condition.

2.3.5 Bioreactor

The perfusion bioreactor design contains a tubular alginate scaffold, containing the cells and created by a reverse coating method (see section 2.3.5.3). The alginate tube is contained within one section of a partitioned insulating container separated from cooled fresh media and waste awaiting disposal (see section 2.3.6). Oxygen sensors within flow chambers form part of the perfusion system (see section 2.3.8) and are positioned between the oxygenator and the alginate tube bioreactor.

2.3.5.1 Alginate Preparation

Manugel DMB high G alginate (ISP Alginate (UK) Ltd Tadworth, UK) was mixed with sterile cell culture grade PBS at a concentration range of 0.5-2.5%w/v. This mixture within a 50ml universal tube was rolled for around 12 hours on a roller mixer (Bibby Stuart Scientific, Stove, UK) to ensure homogeneity.

2.3.5.2 Preparation of cells for mixing with alginate

Mesenchymal stem cells were harvested from tissue culture flasks using the same protocol as for passaging (see section 2.1.4). Post trypsinisation, the resulting suspension was removed to determine cell concentration and then centrifuged in a 50ml centrifuge tube at 100g for 10 minutes. The resulting supernatant was discarded to remove trypsin, which could interfere with cell attachment, and EDTA, which chelates calcium ions and would cause breakdown of the cross-linked alginate scaffold. The cell pellet was resuspended in the required amount of culture medium to achieve a $2 \times 10^6 \text{ cell.ml}^{-1}$ and the same amount of alginate solution to give a final solution of cell concentration $10^6 \text{ cell.ml}^{-1}$ of 50:50 culture -medium and alginate solution. This solution was always used within 30 minutes to form an extruded scaffold.

The same procedure was used to produce alginate scaffolds containing yeast cells, however due to the yeast's higher growth rate seeding concentration was $10^5 \text{ cell.ml}^{-1}$ of 50:50 culture medium and alginate solution.

2.3.5.3 Hydrogel Perfusion Media Preparation

Alginate in solution is normally water-soluble, to cross-link it and form a solid structure that may be used to form a tissue engineering scaffold, a solution containing divalent cations is required. The cross linking solution; CaCl_2 was mixed with sterile cell culture grade PBS at a 2%w/v ratio and sterile filtered through a 0.2 μm cellulose acetate Nalgene filter flask.

2.3.5.4 Alginate Tube Extrusion

The extrusion method developed by Mason and Town (2002) and utilised and modified by Markusen (2005) and Chau (2008) involves reverse coating a precision bore glass cylinder (Glass Precision Engineering, Bedfordshire, UK).

The process involves two steps (see Fig. 2.3).

Step One

Fluid containing a mixture of cells and alginate is injected into a reservoir within the dual inject unit developed by Mason and Town (2002) using a 1ml syringe (Becton Dickinson). The original dual injection unit was a bung with two injection ports, one for the alginate mix and one for the propelling CaCl_2 . A reservoir was created by placing a glass tube over the perfusion inlet in contact with the top surface of the device. The current dual injection unit involves a three way valve connected to a reservoir at the base of glass tube fixed in position on a steel support board with

permanent tubing and three way valves to incorporate quick fitting into the perfusion system. Using a mixture of cells and alginate as the priming solution ensures a homogenous distribution of cells within the scaffold from the beginning. This reservoir surrounds a small plastic sphere (Precision Plastic Ball Company) supported on a central metal cylindrical support.

Step Two

The central metal cylindrical support is a tube connected directly to a 100ml glass syringe (Samco, CA, USA). Following the injection of cells/alginate mixture, the small plastic sphere is propelled on a stream of CaCl_2 at $20\text{ml}\cdot\text{min}^{-1}$.

This stream of CaCl_2 forces the ball and the cell/alginate mix upwards coating the inside of the glass tube as it does so, with the presence of the ball creating the lumen of the tube. CaCl_2 is chosen as the propelling fluid as when it comes into contact with the alginate, it causes the polymer strands to become cross-linked and solidify into a hydrogel scaffold tube containing ready-seeded cells. After cross-linking was complete (ca. 15 minutes) cell culture medium was injected to reduce the CaCl_2 concentration. The resulting cell-alginate tube was matured within the incubator for twelve hours before being placed in series within the bioreactor system.

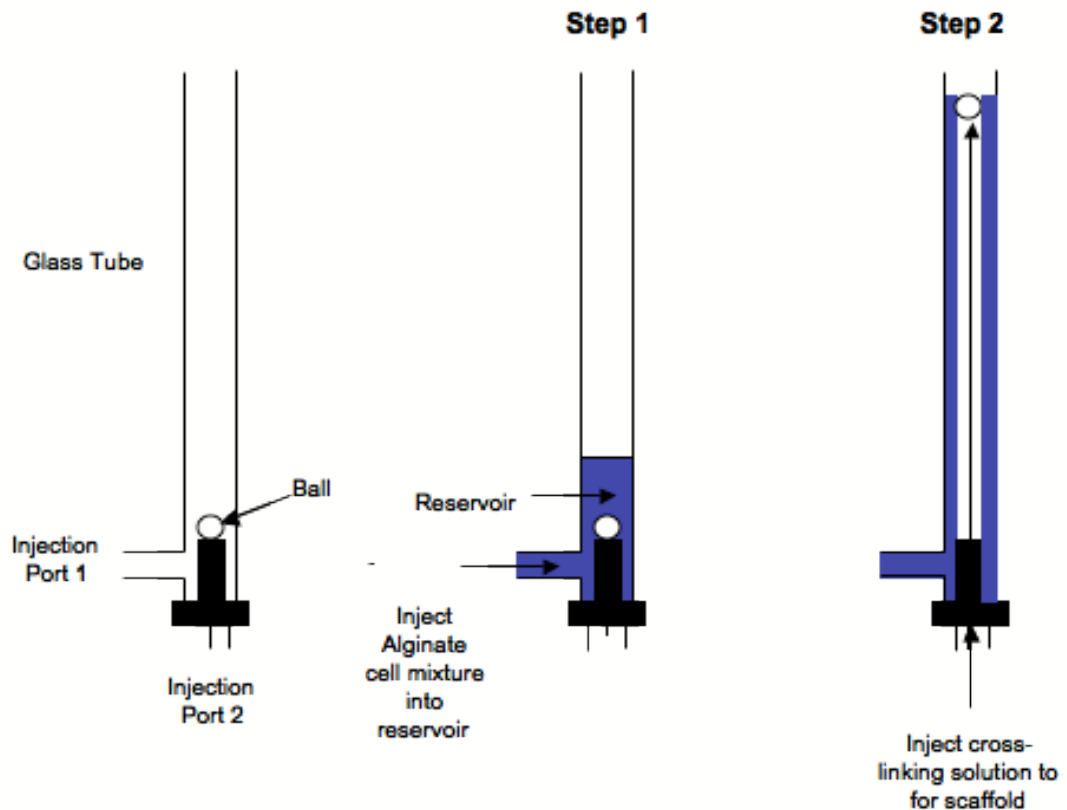


Figure 2.3 Extrusion of alginate scaffold tube

The extrusion of the alginate scaffold takes place by propelling a small ball up the centre of a hollow glass rod on a stream of calcium chloride. When this stream of calcium chloride is propelled through a reservoir of alginate solution, the two liquids will mix together and solidify, progressively coating the inside of the glass rod.

2.3.6 Bioreactor containment and thermal insulation

The VTEB system is contained within an insulating box that is partitioned into a number of separate sections as shown in Fig. 2.4. The walls of the box are dual layered, layer 1 is composed of Ultra High Density (UHD) polystyrene and layer 2 from Normal Density polystyrene. Both layers are of approx 2" giving a total thickness of 4" between the system and the external environment.

Within this insulating container the bioreactor is compartmentalised into three distinct sections. The 4°C section contains the nutrient feed-bag, the waste bag is contained

separately from the cold and warm sections as although temperature control is unnecessary, if it was incorporated into the section controlled at a physiological temperatures, it is likely it would begin to rot due to high bacterial proliferation rates, which is highly undesirable. The bioreactor itself is within the 37°C section so as to match the normal environment an artery would experience when grown in-vivo.

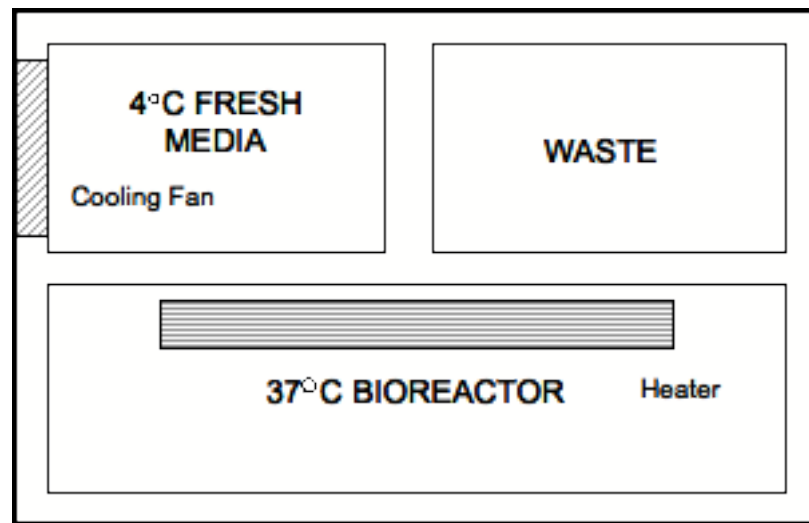


Figure 2.4 Partitioned bioreactor system container

The different sections of the system are partitioned into different regions of a thermally controlled and insulated contained. The alginate scaffold containing the developing artery is controlled at 37 degrees Celsius, human body temperature. Fresh media is controlled at 4 degrees Celsius to limit degradation of active components while waste although stored in a separate compartment is not temperature controlled.

2.3.7 Cooling of fresh feed

Cell Culture media contains a number of components that are thermally unstable. To ensure media remains of suitable composition for the life of the experiments, the bioreactor incorporates a facility for cooling the store of fresh media prior to injection into the system. This required cooling is provided by a thermoelectric assembly that allows heat to be absorbed by a series of heat exchangers equipped with fans

(Supercool, Sweden). This assembly is placed in the external wall of the insulated media chamber of the bioreactor container (see Fig. 2.4).

2.3.8 Oxygen Measurement

Oxygen measurement takes place using fluorescent oxygen spots (see section 1.5.4) that are excited by 2mm polymer optical fibres (Presens), which are also responsible for transmitting fluorescence measurements. Provided the vessel containing the liquid is translucent and non-fluorescent this process can take place non-invasively and will not affect sterility. Measurements from these fibre optic cables are converted into a digital signal by a Fibox-3 system (Presens) that may be processed with a personal computer. A flow chamber was developed by Alfred Ding and Martin Town within the department of biochemical engineering at UCL to allow the media within the recycle loop to flow directly over either one or two oxygen sensitive spots in series. A schematic of this flow chamber is shown in Fig. 2.5.

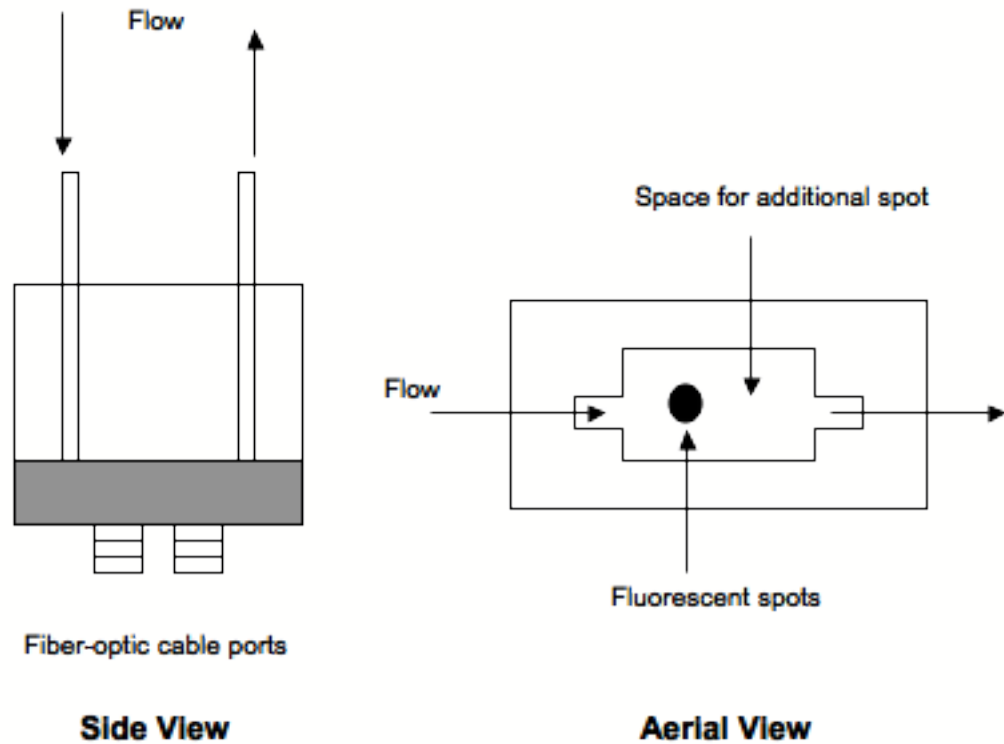


Figure 2.5 Flow chamber for oxygen spots designed by Ding and Town.

The flow chamber allows media flow in and out to be spread evenly over a contained oxygen fluorescent spot. This permits oxygen concentration to be measured.

2.4 Computer modelling

2.4.1 MATLAB

MATLAB (Mathworks, MA, USA) is a numerical software package designed primarily for mathematical analysis. Its name, a portmanteau of Matrix and Lab, relates to the fact that it is most effective when writing programs based upon the manipulation of sets of matrices and tensors.

MATLAB's greatest strength, and one that made it appropriate for use in this work, was its large user population (in excess of 1 million [Mathworks]). MATLAB is capable of forming an interface with most common mathematical software packages used in both industry and academia. For this work these packages included Microsoft Excel (Microsoft Corporation, WA, USA) and Comsol Mutliphysics (Comsol AB, Stockholm, Sweden). Additionally, a number of toolboxes expanding the number of available functions have been designed by users and are supplied commercially or without charge online. The most useful and most extensive of these of these, which is supplied as part of the standard MATLB package, is Simulink. Simulink, which was used extensively to model the bioreactor, is designed specifically for simulating dynamic systems such as the VTEB. Systems to be modelled can be constructed from a number of pre-programmed blocks, each of which provides a graphical representation of a portion of MATLAB code to form the overall model. A screenshot of a simple Simulink program can be seen in Fig 2.6 and in the case of the example permits the use to view and generate a sine wave signal and view the integration of that sine wave signal over a specified time range.

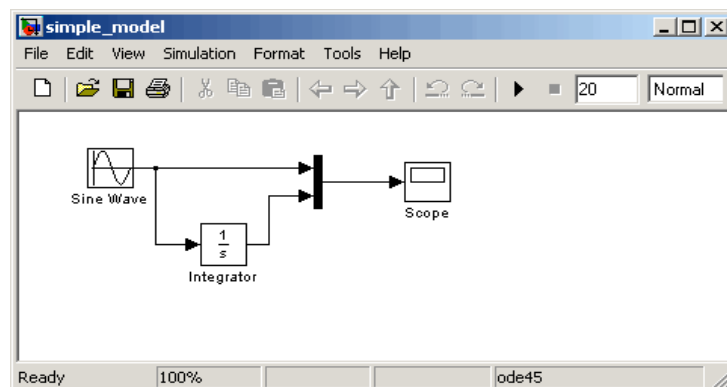


Figure 2.6 A screenshot of a simple simulink program (www.mathworks.com)

2.4.3 Comsol Multiphysics

Comsol Multiphysics 3a (Comsol AB, Stockholm, Sweden) is a finite-element modelling (FEM) package and was used to model the effect of cells growing within the bioreactor. Due to symmetry around the centre line of the tube within the bioreactor it was possible to reduce it to one half of a two-dimensional slice as shown in Fig. 2.7. FEM is a technique for finding approximate solutions to series of partial differential equations (PDEs). Complex, non-linear are broken into smaller regions (finite elements), These regions are solved individually with each solution considering only immediately adjacent regions. This division of a structure into finite elements is referred to as the mesh, with each intersection, a node. A finer mesh yields a more accurate solution. However this accuracy comes at the cost of complexity, computer power and thus greater time to solution. A simple finite element system is shown in Fig. 2.8.

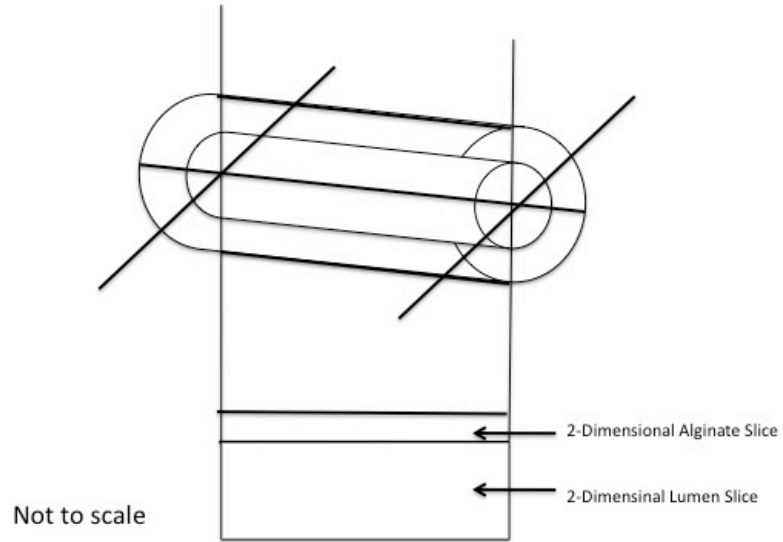


Figure 2.7 Reduction of Cmsol Model from 3D to 2D

The three-dimensional alginate scaffold can be reduced into a two dimensional slice due to symmetry in the 360° angle and also down the central axis.

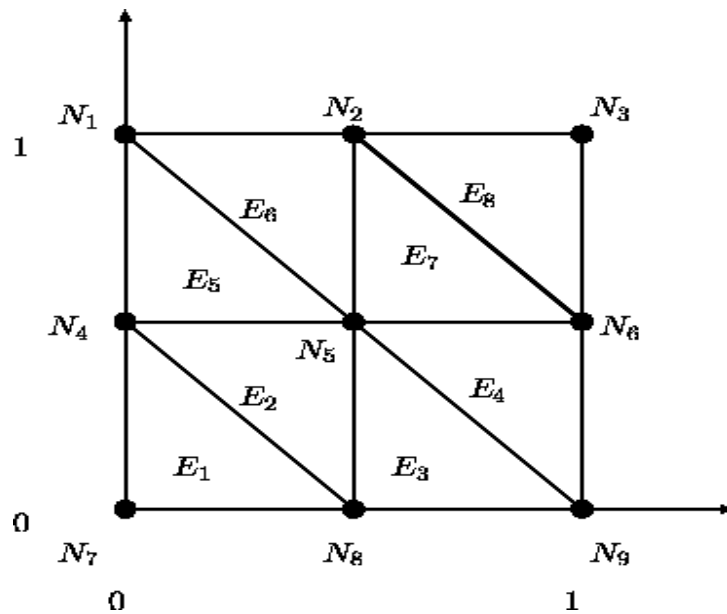


Figure 2.8. A simple example of Finite Element Modelling (FEM)

Finite element modelling allows the division of a non-linear system into a number of finite elements. The mesh dividing up this system is composed of a number of nodes, labelled N_x in the diagram above. Individual finite elements are labelled E_x .

Given the non-linear nature of a number of parameters in the system, the solver method was transient and non-linear, the mesh was refined up to 1800 elements as a balance between accuracy and speed of solution and at each time step Newton iterations were used as the solution method.

Chapter 3 Modelling the Vascular Tissue Engineering Bioreactor (VTEB)

3.1 Introduction

The aim of this chapter is to demonstrate how the tissue engineering system under consideration may be abstracted into a set of discrete components and how each of these components may in turn be represented by a set of equations. Finally it is shown how these equation sets can be used to create a process model suitable for testing control strategies for a number of variables in subsequent chapters.

A process model represents an abstraction of a real system and is by nature simplified to exclude extraneous information. Assumptions are used to achieve such simplification and although the intention is to minimise error and to keep it within acceptable tolerances, it is of vital importance that the limitations of any model are well understood so that is only used to represent appropriately prescribed systems.

The primary step in the development of any model representing a system or a process is to determine the important parameters; constants and variables and equations that characterise the system. Marshall (PhD Thesis, UCL, 1992) whilst exploring the use of comparative reasoning tools and their application to fermentation studies divided the required information into sub-groups as shown in Fig 3.1.

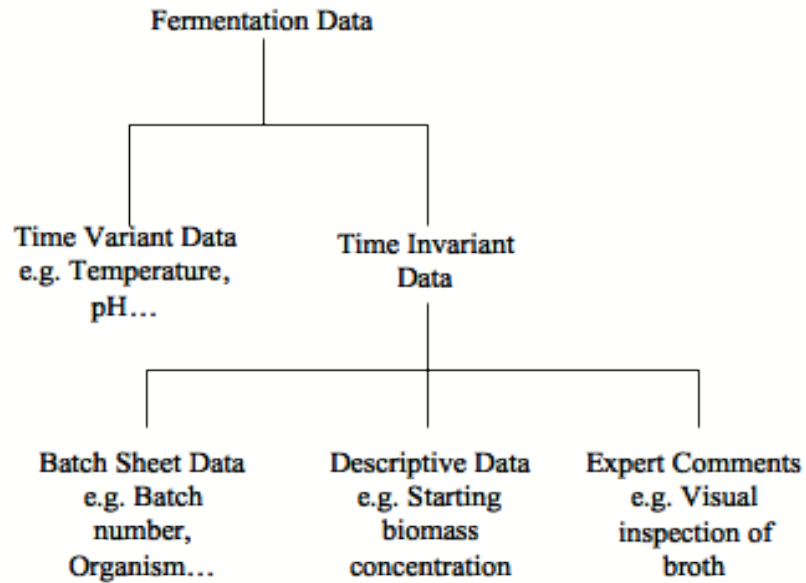


Figure 3.1 Sub-Division of Fermentation Data [Marshall (1992)]

Marshall, 1992 demonstrated that fermentation, a biological process can be divided into time variant and invariant data. The same type of approach can be taken for the tissue engineered artery process.

Fermentation although similar to the operation of a tissue engineering bioreactor is still different in some key respects, as a result both the constituents of each of the subgroups shown in Fig. 3.1 and their values must be determined specifically for the VTEB. The models used in this work have been built using Simulink. Simulink programs are built using time dependant and independent variables, thus a complementary approach to that taken in Fig 3.1 has been adopted for this work.

3.2 Model Variables

The primary grouping of required data is into time variant and time invariant. Time variant data are values that will largely be determined by the model and in an experimental setting will be those parameters that are unknown at outset and are either estimated, monitored or controlled. Such parameters will be specified but will not be assigned a value and are shown in Table 3.1. Time invariant data is usually known or

can be estimated prior to model development or experimentation. It can be subdivided into three categories: batch sheet data i.e. equipment and raw materials used, descriptive data i.e. user imposed conditions and expert comments such as noting that the cells on visual inspection appeared smaller than normal and other factors that may not be recorded under a fully automated analysis.

Table 3.1 Time Variant Data for the VTEB

Temperature
Air flow rate
Oxygen transfer coefficient
pH
Dissolved Oxygen Tension
Dissolved Carbon Dioxide Concentration
Oxygen uptake rate
Cell concentration
Substrate concentration
Waste product concentration
Cell growth rate
Waste production rate
Substrate consumption rate
Substrate breakdown rate
Waste product breakdown rate
Oxygen diffusivity in alginate
Feed flow rate
Recycle flow rate
Shear stress on alginate
Cell viability
Cell physiological state

3.2.1 Batch sheet data

Batch sheets consist of the parameters that would be recorded as standard within a research laboratory book or batch/process logbook. These are normally noted down according to a framework that is generally standard to the institution or company within which the work takes place. For the VTEB the parameters shown in table 3.2 have been chosen. These parameters will have a slight variation depending upon cell source selected as shown in note 2 below. All these parameters are user controlled and will have a known magnitude or value prior to experiment commencement or model development.

Table 3.2 Batch sheet data items

Parameter	Sub Parameters
Batch Number	
Cell Type	
Start date and time	
End date and time	
Medium	Composition Supplier Batch Number
Bioreactor number ¹	
Sterilisation procedure of bioreactor	
Starting Conditions	Temperature, pH,
Feed	Composition
Inoculation	Source ² Cell Seeding Density Passage Number

Notes

1. It is assumed that many VTEBs are operating simultaneously with each carrying a unique identification number
2. If autologous, this will require a full patient history, including age, sex, health, race and medical treatment to date. Additionally a full data trail will be required from cell harvest onwards. If allogeneic, this will require a supplier, batch number and history of storage conditions to date.

3.2.2 Descriptive data (constants)

Descriptive data represents the constants relevant for the dynamic systems within the bioreactor. Such data include maximum possible values for different variables and will assist in both forming equations (as boundary conditions) to model the VTEB and may also be used for assembling diagrams that graphically represent the various operating tolerances of the system (Woodley et al, 1996, Zhou et al, 1999). Several variables have to be estimated using averages from literature such as MSC growth rates which vary between donors. Various attempts have been made to produce the biochemical equivalents of stoichiometric equations for cellular processes and the use of ranges has been required to incorporate this uncertainty. This model has used a similar approach.

Table 3.3 Descriptive Data items

Maximum cell growth rate
Maximum specific cell growth rate
Maximum substrate consumption rate
Maximum substrate degradation rate
Maximum waste production rate
Chemistry of substrate degradation
Maximum waste degradation rate
Chemistry of waste degradation
Yield of cells on substrate
Yield of waste on substrate
Maintenance consumption rates
Maximum cell number
Alginate concentration
Alginate scaffold dimensions
Oxygen diffusivity in medium

3.2.3 Expert comments

Although the temptation due to cost and efficiency is to completely replace human operators with automated machine driven alternatives, the user must not be considered incompetent and instead should be encouraged to apply their knowledge to a system designed to complement rather than replace and allow the user to exercise their expertise more effectively (Marshall, 1992, Dreyfus and Dreyfus, 1986). The weakness of automation lies in its inability to anticipate and although knowledge based learning algorithms (Trilea et al, 2001) and neural network based systems (Zulkeflee, 2007) are being developed for fermentation and other bioprocesses these still struggle to anticipate unusual problems for which the human brain is better suited. An additional risk of excessive reliance upon automation is that in the event of some sort of failure, understanding of how the equipment operates is limited to such a small number of people that potential catastrophes may be impossible to avert (Kletz, 1999). Various human interactions can be incorporated into the control system such as identifying contaminations by the presence of fungal flocks in the outlet stream. These can be useful to identify failure at a pilot stage but are impractical for scaled-out systems as manufacturing scales.

3.2.4 Forming equations

Table 3.3 represents a comprehensive list of unknowns that are required to form an effective and robust model of the VTEB. A list of such values although an essential first step, will in isolation be ineffective without being placed in context through the use of series of equations. The VTEB is a dynamic system within which time variant parameters are constantly changing, often several of these parameters are inter-related

and it is vital that such relationships are defined through the use of appropriate mathematical formulae. The derivation of such formulae requires a logical approach to be taken and the method implemented here is to consider each unit operation within the system as a distinct model. This represents an attempt to simplify the problem by abstracting it into smaller constituent parts that may be solved sequentially and then recombined.

The key control variables within the VTEB are those relevant for cell culture and include: pH, metabolite concentration, waste concentration, and dissolved oxygen tension (DOT). Using the relevant parameters listed in table 3.3, series of equations have been formulated to describe how these variables change in time to form a model.

The VTEB system is a relatively simple process to deconstruct, as it is composed of distinct unit operations (see Fig. 2.1), based around a perfusion bioreactor. Media is pumped through the lumen of the developing artery to supply nutrients and metabolites to the cells contained within.

This media is subsequently passed through a 162-fibre bundle membrane oxygenator where oxygen will diffuse into the media so that this too may be transported through the lumen allowing diffusion into the alginate scaffold, which contains the cells.

The system is of a 'feed and bleed' design, the intent of such a design being to reduce toxic waste product build up through a purge stream and gradually infuse the system with fresh media. The suggested flow rates of the feed and purge streams are relatively small as the cell growth rates are slow hence build up of waste is a gradual process. The various ratios of the purge to the recycle (a function of cell type and bioreactor

operation) can be determined through simulation and will be discussed later in more detail, however it should be noted that a small purge rate relative to the recycle rate has the added benefit that cell factors responsible for encouraging cell growth are permitted to accumulate within the system. However, this also allows toxic waste products to build up, necessitating optimisation of all flow rates.

The VTEB System has been deconstructed into 6 separate parts for analysis;

These six component parts are listed below and illustrated in Fig, 3.7.

- i. Bioreactor
- ii. Oxygenator
- iii. Purge
- iv. Feed
- v. Recycle Part 1
- vi. Recycle Part 2

Each of these sections has been modelled discretely and then incorporated into a final overall model of the VTEB System. Knowing that the main control variables will be dissolved oxygen and metabolic component concentrations, emphasis will be given to deriving equations representing the change of these parameters in relation to other factors such as cell number and flow rate.

3.3 Modelling the oxygenator

The oxygenator is responsible for adding oxygen to the media passing through it at a rate that may be derived from plug flow equations (Metcalf, I.S. 1998). The rate of oxygenation is directly related to; temperature of media, area of exchange to volume ratio, the media flow rate through the system and both the saturation concentration of the media and the existing concentration of oxygen with the media on entry; the difference between these latter two values represents the concentration driving force for mass transfer. The Oxygen Transfer Rate into the media flowing through the oxygenator follows the standard mass transfer equation (3.1, Doran, 1995).

$$\text{OTR} = k_L a (C_L - C^*) \quad (3.1)$$

(OTR is oxygen transfer rate, $k_L a$ is the overall oxygen transfer coefficient, C_L is the concentration of dissolved oxygen in the bulk and C^* is the saturation constant of oxygen in cell culture medium. (Doran, 1995)

$$k_L a = f(T, pH, F_1, a) \quad (3.2)$$

(T is temperature of cell culture medium, F_1 is the flow rate of the bulk liquid through the oxygenator, a is the ratio between surface area and volume).

No cells or living material is present within the oxygenator, thus it is assumed that with the exception of causing a change in oxygen tension it has no further impact upon the composition of the media e.g. metabolic components such as glutamine, glucose or

waste products. Additionally it is assumed that oxygenation of the media is isothermal and hence has no impact upon temperature.

To calculate the oxygen transported into the system in a single pass through the oxygenator the uptake rate between the inlet and outlet of the oxygenator must be determined as outlined in equations 3.3-3.7.

$$\frac{dC_L}{dt} = OTR \quad (3.3)$$

$$\frac{dC_L}{dt} = k_L a (C_L - C^*) \quad (3.4)$$

$$\frac{dC_L}{C_L - C^*} = k_L a \, dt \quad (3.5)$$

$$\ln \frac{C_{L,new} - C^*}{C_L - C^*} = k_L a^* t \quad (3.6)$$

where,

$$t = \frac{V_R}{F} \quad (3.7)$$

The only unknown value within these equations is the overall coefficient of oxygen transfer; the $k_L a$. Experiments have been performed relating this to the bulk flow of the liquid. For these experiments media temperature was assumed to be 37°C as the oxygenator was within a temperature controlled environment and media was perfused through the oxygenator at a variety of flow rates in the absence of cells. By measuring

oxygen accumulation within the system and through the use of equations 3.3-3.7 a relationship between k_La and the flow rate through the oxygenator (recycle rate) was determined as shown in Fig. 3.2.

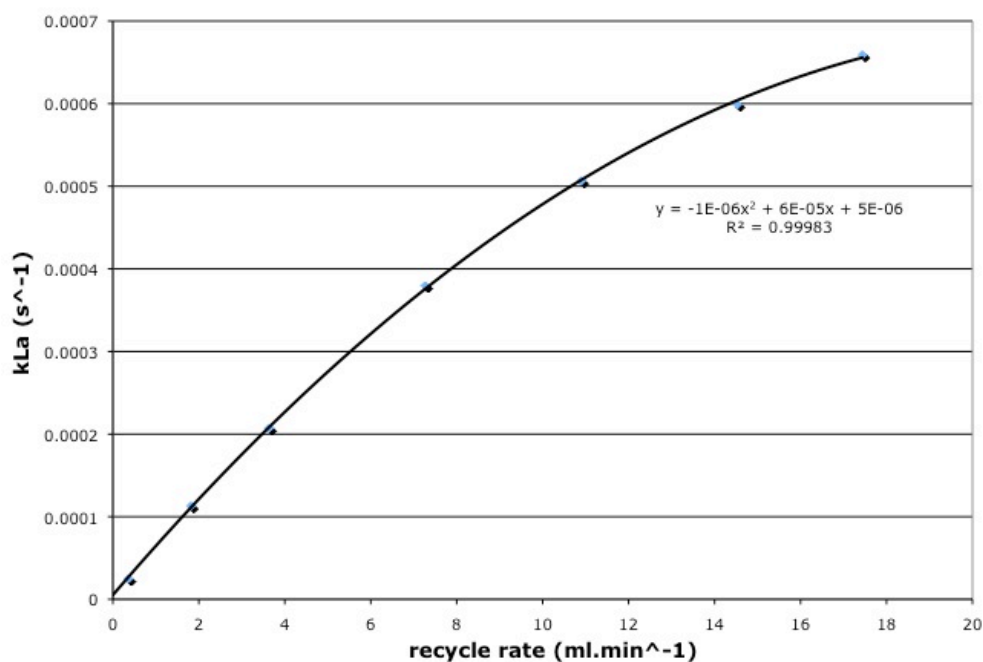


Figure 3.2 Relationship between bulk flow through the oxygenator and the oxygen transfer coefficient.

The oxygen transfer coefficient k_La varies with the rate of flow through the oxygenator. Varying the flow rate through the oxygenator and determining the change in oxygen concentration between input and output for each flow rate allowed determination of this relationship.

By fitting a curve to the empirical data as in Fig, 3.3, an equation can be formed for the relationship between recycle flow rate and oxygen transfer coefficient.

3.4 Modelling the bioreactor

The VTEB is of a bespoke design (Mason and Town, 2002) and is intended to produce a tube like structure approximating to a tissue engineered CABG graft. This structure extrudes a cell-alginate mixture into a polymeric scaffold seeded at inoculation density of cells. The properties of this scaffold such as density and length are of key importance to the modelling of the bioreactor as they affect the porosity of the hydrogel (and thus mass transfer properties and total cell number). These properties are explored in section 3.4.1.

The cells within the scaffold will consume substrates such as oxygen and glucose for use in respiration to allow growth and proliferation. This consumption will vary with the number of cells present in the scaffold. Respiration in addition to producing energy and leading to the production of biomass will also result in waste by-products that are often cytotoxic. This consumption is the prevalent driving force for mass transfer into the scaffold and diffusion is much smaller by comparison. Equations describing the dynamics of the growth and respiration by the encapsulated cells are derived in 3.4.2 and 3.4.3 respectively.

3.4.1 Modelling the alginate scaffold

As outlined in section 2.3.5, cells are grown in the bioreactor within an extruded alginate scaffold. A relationship between the volume and concentration of alginate used in the priming solutions and the scaffold length can be used to determine the density of the scaffold and hence the total cell number present in a scaffold for a given cell number and other properties such as porosity.

Chau (2009) has previously determined a relationship between various alginate properties and the length of the scaffold. In an attempt to replicate results obtained by Chau, the data shown in Fig. 3.3 was obtained relating alginate tube length to initial volume of 1% alginate solution.

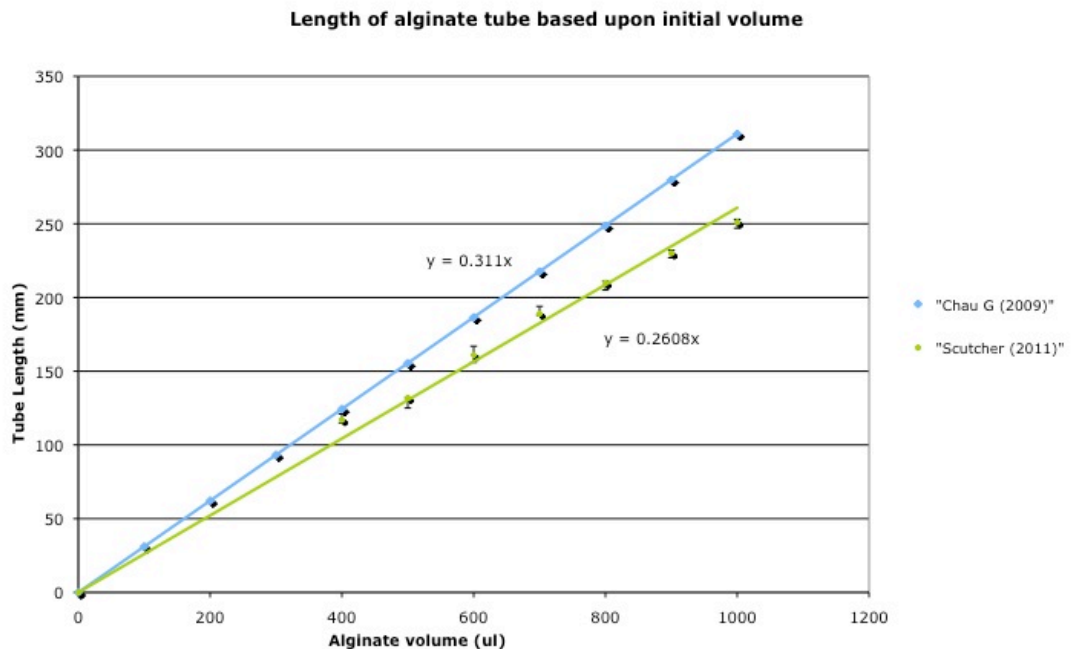


Figure 3.3 Length of alginate tube based upon the priming volume of 1% alginate solution

The length of the alginate scaffold varies with the volume of priming solution. Higher volumes lead to greater lengths.

Clearly this shows a discrepancy and as a result the experiments were repeated several further times, the results still fall within the error bars shown on the Scutcher (2011) data in Fig. 3.3. The variation could be due to a number of factors including variations of alginate source or batch and possibly technique. Despite a satisfactory explanation for the difference not being obtained this thesis is based upon the results obtained by the author of this work.

The alginate concentration within solution will also have an impact upon various parameters of the tube but most ostensibly the length due to increased viscosity increasing resistance to the propelled ball. Fig. 3.4 shows how the length of scaffold is affected by the concentration of the alginate solution used to prime the extrusion device and unsurprisingly the effects of resistance caused by an increased alginate concentration leads to a shorter tube being formed. Scutcher (2011) relates to data obtained during this work.

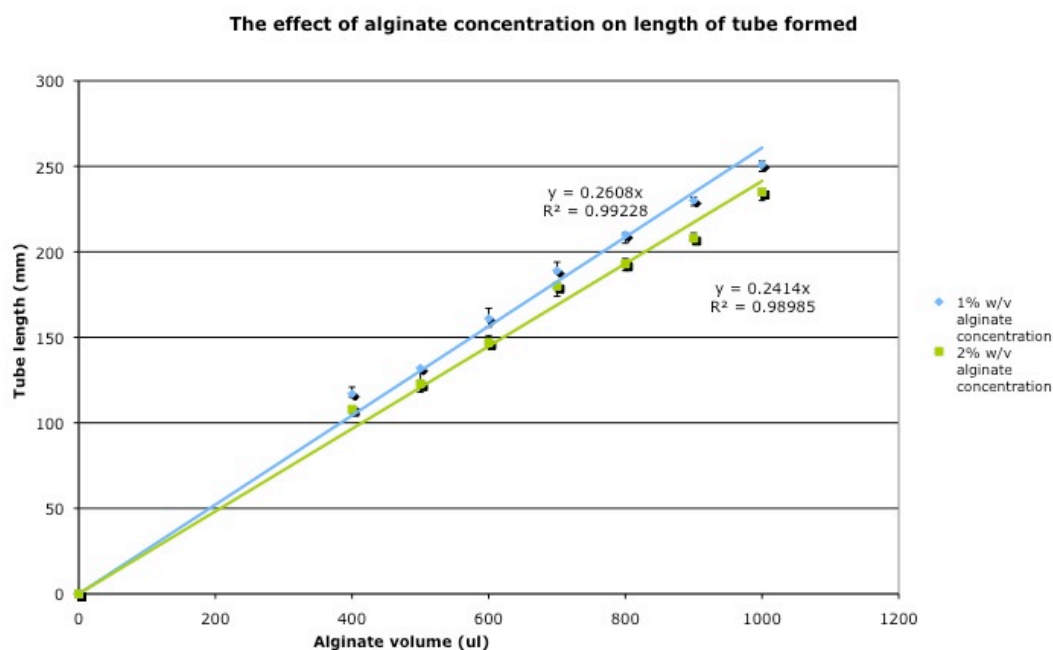


Figure 3.4 Length of alginate tube based upon priming volumes of 1% and 2% alginate solution

Use of the higher concentration alginate, 2%, leads to a shorter scaffold tube length, than use of the 1% concentration alginate. This is due to increased resistances from the higher concentration alginate on the internal wall of the glass rod used in the inverse coating procedure.

The remaining issue regards selection criteria for the concentration of the scaffold. For these experiments a series of scaffolds were formed from alginate of various concentrations. These scaffolds were perfused within the bioreactor for five-day periods and it was found that while the 1% concentration scaffold degraded over time and appeared to erode away, the 2% scaffold was sufficiently robust as to remain intact at the end of the experiment. Interestingly a 3% scaffold appeared to be excessively brittle as it broke in half after two days rather than eroding away. This may be because higher alginate concentrations of alginate result in less homogenous tube formation. This lack of homogeneity means that certain areas of the tube are significantly stronger than others and manifests itself as brittleness. Table 3.4

summarises the parameters determined in this section to allow modelling of the alginate scaffold.

Table 3.4 Alginate scaffold parameters for modelling

Parameter	Value	Source
Alginate scaffold length	0.33m	Assumed
Alginate scaffold conc.	2%w/v	Experimentation
Priming solution volume	1.2ml	Experimentation

3.4.2 Modelling cell growth in the bioreactor

The next stage after determining the properties of the scaffold and prior to establishing the relationship of the various substrate uptake rates to the cell number, a method of modelling the cell growth must be established.

The cell number is determined by the growth rate, which varies with cell type. This growth rate is related to the concentration of the different substrates and directly to whichever of those is limiting (Doran, 1995). Equation 3.8, chosen for modelling cell growth is a standard one used for many types of population growth. One of the most developed areas of modelling that can be considered analogous to the growth of tissue engineered organs is tumour growth. Tumour growth can be modelled using the Verhulst equation (Forys and Marciniak-Czochra, 2003). The Verhulst equation was originally developed for modelling population growth where the growth rate is related to existing population and the amount of available resources (equation 3.8).

$$\frac{dP}{dt} = rP \left(1 - \frac{P}{K} \right) \quad (3.8)$$

P is the population, r is the growth rate and K is the carrying capacity i.e. maximum population.

Equation 3.8 can be solved to give equation 3.9 showing population at any time as a function of time.

$$P(t) = \frac{KP_0 e^{rt}}{K + P_0(e^{rt} - 1)} \quad (3.9)$$

Where P_0 is initial population.

Substituting the general terms for population growth with cell growth variables provides equation 3.10.

$$X(t) = \frac{X_{MAX} X_0 e^{\mu t}}{X_{MAX} + X_0(e^{\mu t} - 1)} \quad (3.10)$$

Where $X(t)$ is the cell growth at time t, X_{MAX} is the maximum cell number with the scaffold, X_0 is the seeding cell number and μ is the specific cell growth rate.

The specific cell growth rate is unique to cell type and may be obtained from the Monod equation (equation 3.11). This equation incorporates terms for the maximum

specific growth rate when all substrates are in excess and terms for the limiting substrate.

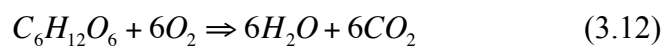
$$\mu = \frac{\mu_{\max} S}{S + K_S} \quad (3.11)$$

Where μ_{\max} is the maximum specific growth rate, S is the concentration of limiting substrate e.g. glucose, sugar, K_S is the Monod coefficient for S, i.e. concentration of S at which μ is one half of its maximum.

For the purposes of this chapter and the relation of the cell growth rate to substrate uptake, the limiting substrate will be assumed to be dissolved oxygen concentration with other substances in excess.

3.4.3 Modelling substrate uptake in the bioreactor

The uptake of the various substrates is directly related as the limiting substance dictates the overall rate of respiration. Equation 3.12 indicates how oxygen and glucose uptake are directly related through the basic equation of respiration:



or



For this reason the relationship between substrate uptake rate (SUR) and cell growth rate is illustrated using oxygen uptake rate (q_{O_2}) in place of SUR; the assumption being that dissolved oxygen concentration is the limiting factor. A similar relationship may be assumed to hold for any substrate that is limiting.

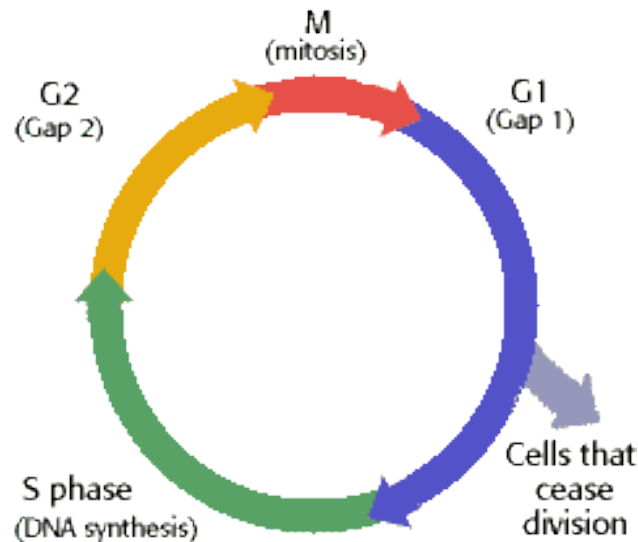


Figure 3.6 Phases of the cell cycle [Adapted from Alberts et al (1994)]

Cell division is composed of four key stages; S – the synthesis phase, G_2 – A gap between S & M phases, M – the mitosis phases and G_1 – A gap between M & S phases. Cells that have ceased dividing and become senescent are often referred to as being in a G_0 phase.

Within a random population of cells, division is almost never synchronous, at any given time a proportion will be operating within a part of the cell cycle and undergoing divisions and the remainder will have left the cycle and have ceased dividing (see Fig. 3.6). It appears that cells undergoing division consume a greater amount of oxygen (Zhao et al, 2005; Gosmann et al, 1988) this is possibly because the energy required to produce the components of a new cell is significantly larger than that required to merely sustain a cell through its normal operation. This greater energy

demand requires a greater level of aerobic respiration to generate it and thus a larger q_{O_2} by the cell is observed.

In the case of the bioreactor, one of the key limiting factors to division will be the available space for the cells as they proliferate. As the maximum cell concentration is reached the proportion of cells dividing will reduce and as such the average q_{O_2} per cell will reduce (Gosmann et al, 1988). q_{O_2} dependant upon cell number and as such must be related to cell growth.

A number of assumptions are made as follows and an equation representing this relationship may be derived (see equation 3.13).

1. Dividing cells consume more oxygen than senescent cells.
2. At any given time, a proportion of cells within a population will be dividing, whilst another proportion are senescent
3. Space limited cells will no longer divide hence cells at high concentration within the alginate scaffold will show a lower average oxygen consumption rate as the senescent proportion begins to dominate.

The single pass oxygen consumption balance between the inlet and outlet of bioreactor can be determined by equation 3.13

$$q_{O_2} = q_{O_2MAX}^{CELL} * \frac{dX}{dt} + q_{O_2MAINTENANCE}^{CELL} * X \quad (3.13)$$

Where q_{O_2} is the oxygen uptake rate (mmol.s^{-1}), $q_{O_2,MAX}$ is the oxygen uptake rate per dividing cell per second ($\text{mmol.cell}^{-1}\text{s}^{-1}$), $q_{O_2,MAINTENANCE}$ is the oxygen uptake rate per senescent cell per second ($\text{mmol.cell}^{-1}\text{s}^{-1}$) and X is the cell number.

For a volume of the bioreactor V_R , equation 3.7 gives the residence time τ , the time required for a single pass.

$$\frac{d([O_2] * V_R)}{dt} = -OUR \quad (3.14)$$

Where; V_R is the volume of the bioreactor, t is the time, $[O_2]$ is the oxygen concentration in the bulk liquid flow. This equation may be rearranged and solved to give equation 3.20.

$$\frac{d[O_2]}{dt} = \frac{-OUR}{V_R} \quad (3.15)$$

$$d[O_2] = \frac{-OUR}{V_R} dt \quad (3.16)$$

$$\int_{[O_2,final]}^{[O_2,initial]} d[O_2] = \int_0^\tau \frac{-OUR}{V_R} dt \quad (3.17)$$

$$[O_2]_{final} - [O_2]_{initial} = C_{outlet} - C_{inlet} = \frac{-OUR}{V_R} \tau \quad (3.18)$$

Therefore the single pass oxygen consumption as a total is given by equation 3.18 *

V_R .

$$\Delta O_{2, SP} = - OUR\tau \quad (3.19)$$

This single pass oxygen consumption may be applied to any limiting substrate and together with equations 3.11 and 3.13 provide the relationships necessary to model cellular growth and the associated consumption of metabolites. These relationships characterise the bioreactor and along with the earlier model derived for the oxygenator constitute a large part of the information required to create a model suitable for testing control strategies. The only remaining requirements to form such a model are equations representing the recycle loop, feed and purge streams and the impact these flows will have upon bulk concentrations within the system.

3.5 Modelling system flows

The major system flows are labelled in Fig. 3.7. The recycle loop represents those portions of the system where the media is transported between the key parts of the system already considered. The only equation required to represent the recycle loop is the residence time or time delay between the media moving between two points (equation 3.20)

$$\tau_D = \frac{V_{RLS}}{F} \quad (3.20)$$

(τ_D is transport delay (s), V_{RLS} is the volume of the recycle loop section between the two points under consideration (ml), F is the recycle rate flow rate ($\text{ml} \cdot \text{min}^{-1}$).

To determine the impact the purge and feed flows have upon the bulk concentrations of oxygen and other metabolites within the system a series of mass balances (Equations 3.21-3.25) have been derived.

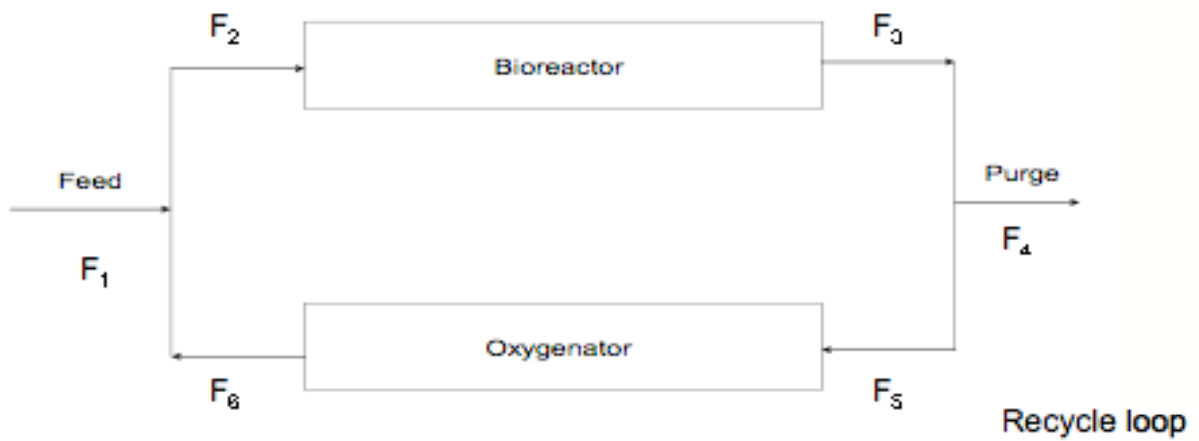


Figure 3.7 Flows within the VTEB system

Feed overall flow rate

$$F_2 = F_1 + F_6 \quad (3.21)$$

Feed substrate component balance

$$xF_2 = xF_1 + xF_6 \quad (3.22)$$

Where x represents the concentration of a component within the flow (mM)

Purge overall balance

$$F_4 = F_5 - F_3 \quad (3.23)$$

Purge substrate component balance

$$xF_4 = xF_5 - xF_3 \quad (3.24)$$

Overall system balance

$$F_1 = F_4 \quad (3.25)$$

These mass balances may be combined with the generation and consumption terms developed in previous sections characterising the oxygenator and the bioreactor to give overall equations for substrate concentration changes in the overall system.

3.6 Overall Model

By combining the separate models that have been developed within this chapter, a set of equations may be collated that represent the overall system. Equations 3.26 to 3.38 represent the necessary information to determine oxygen and other substrate changes within the system (see Fig. 3.8).

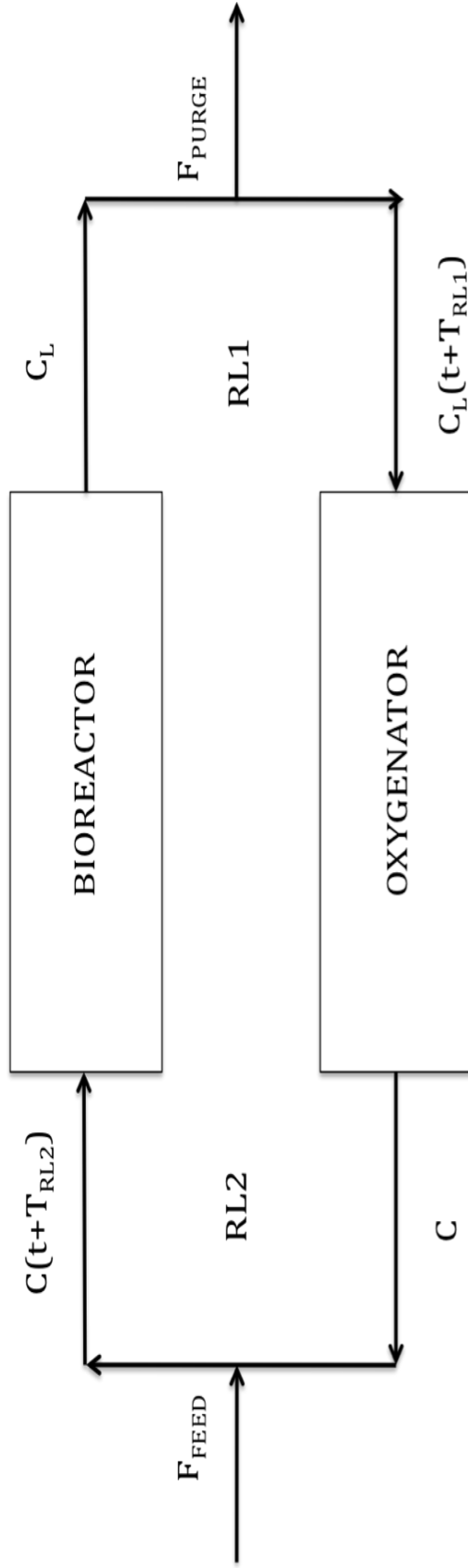


Figure 3.8 Changes in Steady State Dissolved Oxygen Tension Within the Bioreactor System. This diagram illustrates the equations used to model steady state dissolved oxygen tension (DOT) at different fixed points throughout the system. Where C represents oxygen concentration at exit of oxygenator, C_L represents the oxygen concentration at exit of the bioreactor, and T_{RL1} and T_{RL2} represent the time taken for a volume of liquid to pass through the recycle loop **RL1** and **RL2** (labeled), respectively.

The following series of equations (3.26 to 3.38) and starting conditions, derived within the body of this chapter characterises the variables shown in Fig 3.8. All the terms for these equations have been defined previously.

$$\frac{dC_L}{dt} = k_{ov}(C - C^*) \quad (3.26)$$

$$k_{ov} = -10^{-6}F^2 + 6 \times 10^{-5} + 5 \times 10^{-6} \quad (3.27)$$

$$\frac{dC_L}{dt} = \frac{-OUR}{V_R} \quad (3.28)$$

$$OUR = A \frac{dX}{dt} + BX \quad (3.29)$$

$$\frac{dX}{dt} = \mu X \left(1 - \frac{X}{X_{MAX}} \right) \quad (3.30)$$

$$C = C_L - \frac{OUR}{V_R} \tau \quad (3.31)$$

$$\tau_{Oxy} = \frac{V_{Oxy}}{F} \quad (3.32)$$

$$\tau_{Bio} = \frac{V_{Bio}}{F} \quad (3.33)$$

$$\tau_{RL1} = \frac{V_{RL1}}{F} \quad (3.34)$$

$$\tau_{RL2} = \frac{V_{RL2}}{F} \quad (3.35)$$

The required starting conditions are given by equations 3.36 to 3.38.

$$C_L(t=0) \quad (3.36)$$

$$C(t=0) \quad (3.37)$$

$$X(t=0) \quad (3.38)$$

The values for the constant variables contained within these equations are listed in Table 3.5.

Table 3.5 Constants within the overall model for MSC

Constant	Value	Source
$V_{R,1}$	12.26 ml	n/a
$V_{R,2}$	12.26 ml	n/a
$V_{O,2}$	0.549ml	Manufacturer
V_{BIO}	1.151ml	n/a
μ	0.022hr^{-1}	Bruder S.P. et al, 1997
A	Derived in next section	Zhao et al, 2005
B	Derived in next section	Zhao et al, 2005
$X(t=0)$	$10^6 \text{ cells.ml}^{-1}$	n/a
$C(t=0)$	0.079mM.L^{-1}	n/a
$C_L(t=0)$	0.079mM.L^{-1}	n/a
X_{MAX}	Derived in next section	n/a
Monod Constant for oxygen	10^{-6}mol.L^{-1}	Peng and Palsson, 1996

A similar set of equations can be used to determine the concentration of other substrates or metabolites throughout the system but will exclude the terms relating to the oxygenator as this unit has no effect upon the system except in terms of the oxygen concentration.

3.7 Conclusions

This basic VTEB model outlined in this chapter provides a starting point for the development of a control system to maintain environmental conditions within the system. Simultaneously solving the set of differential equations (3.26-3.35) using specified boundary conditions will provide oxygen and substrate curves against time and location in the system. Altering variables within the model allows for control strategies to be tested, using the variation in the oxygen and substrate outputs from the bioreactor to measure success.

Using the model developed in this chapter each control parameter has had a distinct control system designed separately in isolation from the others, DOT (Chapter 4), pH (Chapter 5), and respiratory substrates and waste (Chapter 6). These control systems are ultimately combined into an overall control model (Chapter 7).

Chapter 4 The control of oxygen tension within the VTEB

In this chapter the model developed in the previous section is implemented to determine an appropriate process control strategy for maintaining dissolved oxygen tension (DOT) within appropriate ranges within the vascular tissue engineering bioreactor (VTEB). A strategy is provided for maintaining DOT to allow the proliferation of mesenchymal stem cells (MSC) with the ultimate goal of forming a healthy tissue engineered arterial graft. Methods are also provided for estimating health and developmental state of these grafts non-invasively.

4.1 Introduction

DOT in solution represents a key parameter involved in cell culture, being a key respiratory substrate as well as a signalling molecule. It is thus vital that its variation is both monitored and where appropriate controlled within the VTEB.

Most experiments involving mammalian cells seek to replicate normal *in-vivo* conditions and in the case of DOT, use concentrations comparable to those measured within the relevant part of the body.

For arteries the appropriate physiological DOT depends upon the location within the body, the further downstream from the lungs the lower the DOT will be. In fact the consideration of the *in-vivo* value experienced within an artery is of little importance for this work, rather the *in-vivo* conditions within the source of the progenitor cells and during angiogenesis has been deemed to be of primary concern; i.e. the oxygen tension within the micro-environment of the bone marrow where mesenchymal stem cells are

located and may be harvested from. This is because the work within this thesis will seek to effectively control a bioreactor during the preliminary stages of tissue engineering an artery. This first stage considers the proliferation of MSC throughout a tubular scaffold and attempts to limit differentiation. The second stage that will not be considered within this work will incorporate controlling conditions so as to encourage the differentiation of these MSC into the three layers of a mature artery.

4.1.1 Human mesenchymal stem cells (hMSC)

Low oxygen tension has been shown to be an integral component of the microenvironment of the human mesenchymal stem cell (hMSC), with low concentrations such as 2% leading to higher protein levels and expression of markers such as those of osteoblast and adipocyte cells when compared with culture at 20% O₂ (Grayson et al, 2006).

As the bone marrow is a complex, relatively large structure, the pO₂ is not homogeneous although the average has been measured as 5% (Pennathur-Das and Levitt, 1987) with the maximum concentrations found at the edge of the sinus wall where a venous partial pressure is experienced (Mostafa et al, 2000) It is within the lower pO₂ environment that Mesenchymal Stem Cells (MSCs) exist, along with other progenitor cells, grow and proliferate (Mostafa et al, 2000). Ishikawa and Ito (1988) reported the range of oxygen concentrations within the region of the bone marrow where these undifferentiated progenitor cells reside to be 52.0mm±11.2mmHg (0.069±0.020mmol.L⁻¹). It is this range that provides the boundaries of the oxygen control window.

4.1.2 Yeast

Yeast is a flexible organism with regard to cell metabolism. It does however fundamentally differ from the mammalian cell lines for which it acts as a surrogate, as it produces a diauxic growth curve. When oxygen is limited, yeast cells may switch from an aerobic method of respiration to an anaerobic form, requiring less oxygen and hence causing oxygen to cease to limit growth rate.

In anaerobic cultivation yeast forms ethanol as a by-product. The intention is to operate at a value of DOT that leads to the highest oxygen consumption possible, to represent an effective test of the proposed VTEB control system with the caveat that some value comparable to physiological conditions will be used wherever possible. Baumberger (1939) demonstrated that yeast cells possess a constant respiration rate from 160 mmHg to at least as low as 0.24 mmHg, a similar assertion was made by Winzler (1941) who showed that in the presence of appropriate substrate, the oxygen uptake rate would remain constant to an oxygen concentration of 0.2mmHg. Any operation within this range should not affect the respiration rate of the yeast cells provided substrate concentration is sufficient.

4.1.2 Measurement of dissolved oxygen tension (DOT)

Measurement of DOT was performed non-invasively using PreSens microspots [PreSens GmbH, Germany]. These spots decay with a fluorescence life span proportional to the oxygen concentration within liquid local to the position of the microspot (see Chapter 2). These spots were positioned to measure the DOT at the exit

of the bioreactor as this minimises the delay between the unknown oxygen concentration at that point and any responding control action.

4.2 Methods of controlling DOT within the VTEB

Using the model developed in chapter 3 it is possible to test various control strategies, this section outlines possible methods by which this control can take place and the selection criteria used to determine the most appropriate.

4.2.1 Control mechanism and manipulation of variables

Oxygen transfer across the oxygenator membrane obeys the standard mass transfer equation 4.1.

$$\frac{dC_L}{dt} = k_L a (C^* - C_L) \quad (4.1)$$

The mass transfer coefficient ($k_L a$) of the oxygenator is a function of the flow rate of the gas or the liquid stream flowing through it. Modifying the gaseous side, would involve using a set of gas mass controllers regulating the flow of oxygen, carbon dioxide and a nitrogen balance stream. A feed back loop could be used to link DOT within the system to the mass transfer controllers (MTCs) via an appropriate controller to keep the oxygen within the system at an appropriate set point. A similar approach has been used in previous bioreactors (Altman et al, 2001, Zhao et al, 2005).

The disadvantage of implementing such a system is that it carries a high cost in terms of unit cost and also limits the potential to scale the system. The price of three gas mass controllers whilst not prohibitive is expensive and also adds to the overall complexity of the system – increasing the number of components of which any individual failure will be critical.

The value of the k_La within the oxygenator may be changed in a second way, by altering the flow rate on the liquid side. In a manner analogous to the physiology of a mammal, in the event of an increase in oxygen demand where the heart will work harder, when the oxygen demand of the cells within the alginate scaffold is greater, the pump will increase the flow rate of the culture media. Such a method has the advantages of being relatively cost effective, as the entire required infrastructure already exists within the system. Small oxygen sensing spots [Presens GMBH, Regensburg Germany] are incorporated with the system and used to measure the DOT before and after the alginate scaffold.

If the output from these sensors is processed to specify the speed at which the pump responsible for the recycle rate works, then control can be achieved. This has particular advantage in terms of scalability of the system, as it does not add to the complexity of the system or significantly to the basic unit cost. It is for these reasons, quantified in Table 4.1, that the control parameter for maintaining DOT is the flow rate of the recycle rate.

Table 4.1 Comparing methods of controlling DOT within the VTEB

This table compares the merits of controlling the dissolved oxygen tension (DOT) within the vascular tissue engineered bioreactor (VTEB) by use of either the air-flow rate or the cell culture medium flow rate through the membrane oxygenator.

Parameter	Oxygen Control	Recycle Control
Cost	** (O£1000s)	**** (O£10s)
Complexity Added	**	***
Scale Out	** (Completely new system)	**** (No new equipment)

4.2.3 Types of Controller

The first step in implementing any control strategy is to determine the method of control to be employed. The standard approach is to employ systems in increasing levels of complexity until an acceptable level of tolerance is achieved.

In terms of controller type these are;

1. Two-step Controller. A simple controller such as those attached to a thermostat that heats when the measured temperature is below the set point and turns off heating when it is above.
2. Proportional Controller. The two-step control approach often leads to an oscillatory output, as the response of the controller when the system displays an output below the set point is simply to switch the controlling variable on without any concern for magnitude of response. Proportional control is so-called as it responds to any error in the system with an

increase in the control variable proportional to the size of the error as shown in equation 4.2.

$$P_{out} = K_p e(t) \quad (4.2)$$

(Where: K_p = Constant of proportional control, $e(t)$ = error, P_{out} = Control output)

3. Integral Controller. Proportional control although an improvement on two-step control, will often result in an offset or steady state error whenever the set point is changed mid-process. This is because any change in the set point will mean that the steady state value, which was originally set at a ratio of 50% control action to 0 error will have to have an error value other than 0 to achieve the new set point i.e. an offset (Bolton, 2003). Integral control works so as to eliminate such offsets, by relating the rate of change of the control output to the size of the error as shown in equation 4.3 (Seborg et al, 1989).

$$I_{out} = K_I \int_0^t e(\tau) d\tau \quad (4.3)$$

Where: I_{out} = integral control, t = time, $e(\tau)$ = error, K_I = integral gain

4. Derivative controller. Derivative action anticipates the magnitude of the future error by measuring the rate of change of controlled variables, its derivative (see equation 4.4). Thus, derivative action can improve the dynamic response and achieve superior control. However, the presence of a noisy signal can actually result in inferior control (Willis, 1998).

$$D_{out} = K_D \frac{d}{dt} e(t) \quad (4.4)$$

Where: D_{out} = derivative control, t = time, $e(t)$ = error, K_D = derivative gain

5. Model Predictive Controller. Model reference adaption (Bolton, 2003) is possibly the gold standard of process control strategies. Such a method requires an accurate model of the system to be developed (this is often the barrier to its implementation). This model is run in tandem with the actual controlled system and control strategies can be tested in faster than real-time on the model before being implemented. Such a method is rarely implemented due to the cost, time and immense complexity of developing a model sufficiently accurate. Intelligent and knowledge based systems are a variant of this type of control and have been theorised extensively in literature in diverse areas such as fermentation (Konstantinov and Yoshida, 1991), waste water treatment (Flores et al, 2000) and bioprocesses generally (Guthke et al, 1998).

In terms of the four possibilities this chapter will demonstrate both the effectiveness and weakness of each of the first three strategies using two-step control additionally, prior to implementing proportional and integral control in conjunction. Model Predictive control is beyond the scope of this work, which is a first attempt to determine if the system in its current design is capable of accurate control and if so, implement an initial solution.

A process control diagram of the system is shown in Fig. 4.1 with the measured DOT being compared to the set point and the size of the error being translated by the

controller into a change in pump flow rate. The action of the controller depends both on its type and its set points. Feedback control has been selected in preference to feed forward due to the system's complexity and dynamic nature. Feed forward control is only utilised in situations where the system is very well defined and understood (Seborg et al, 1989).

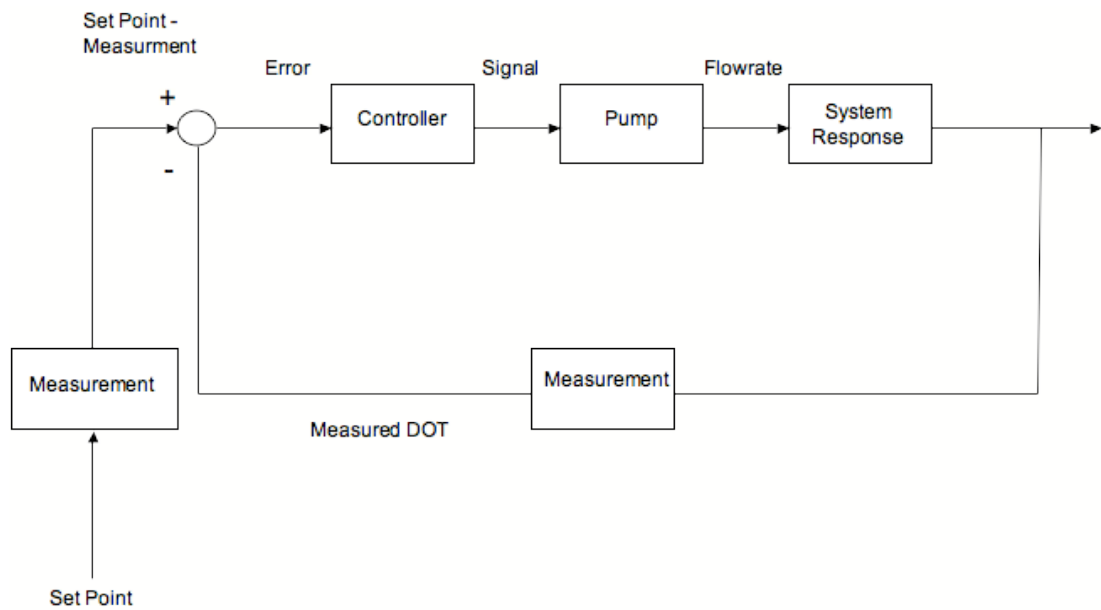


Figure 4.1 Process control feedback loop for DOT

This diagram demonstrates how a feedback control loop responsible for maintaining the dissolved oxygen tension (DOT) within the range $0.079\text{--}0.049\text{mmol.L}^{-1}$ can be deconstructed into a series of unit operations. Each of these unit operations represents a physical, temporal or mathematical aspect of the control loop.

4.3 Determining the capacity of the system and the acceptable range of flow rates

The first stage of defining the control system is determining the acceptable range of rates the recycle loop pump may be operated at. Parameters considered include shear stress, diffusivity of the alginate matrix and cell concentration. A window of operation, a visual tool for presenting acceptable ranges of operating variables, has been employed. This window of operation is created using the model developed in Chapter 3.

4.3.1 Oxygen uptake rate model

The key unknown parameters required to utilise the model of the bioreactor outlined in chapter 3 are those that relate to the relationship between oxygen uptake rate and the cell number (see equation 3.13).

Defining this relationship is of added importance as determining cell number within the bioreactor is essential to determine the health of the developing tissue material and to estimate the likely future delivery day and allow scheduling of surgery for implantation.

The design of the VTEB containing alginate within a glass tube makes sampling to determine cell number almost impossible and continually scanning by some imaging method would prove complex and expensive. The most viable alternative is to infer the cell number by measuring the variation in related parameters such as the

consumption of respiratory metabolites. As OUR is already being measured online in real time to allow its control and is directly related to the cell number it is a suitable candidate provided equations relating it to cell number may be derived.

It has been demonstrated by Gosmann et al (1985) and Zhao et al (2005) that oxygen consumption rate of eukaryotic cells is not constant and reduces as cell concentration increases and space becomes a limiting factor when the cells are encapsulated. This non-constancy ensures that the equations relating OUR and cell number will not be a simple proportional relationship and requires the use of exploratory experimentation. For this work, yeast cells were used both for reasons of time and as they reach maximum cell number within the scaffold in less than 2 days. Scaffold tubes were formed as described in section 2.3.5.2 within the bioreactor and oxygen consumption was measured, when little or no change in oxygen consumption rate was observed between measurements (which were taken at three hour intervals) it was assumed that maximum cell number had been obtained within the scaffold, for each case this took between 33 and 39 hours. Final cell numbers (Fig. 4.2) were obtained by dissolving the scaffold in 1M sodium-citrate solution as the sodium ions interfere with the cross linking and cause the scaffold to dissolve. The resulting solution was neutralised with phosphate buffer solution (PBS) and a cell count was performed with a haemocytometer. The initial seeded concentration was $10^5 \text{ cell.ml}^{-1}$ and the final cell concentration results are shown in Fig. 4.2.

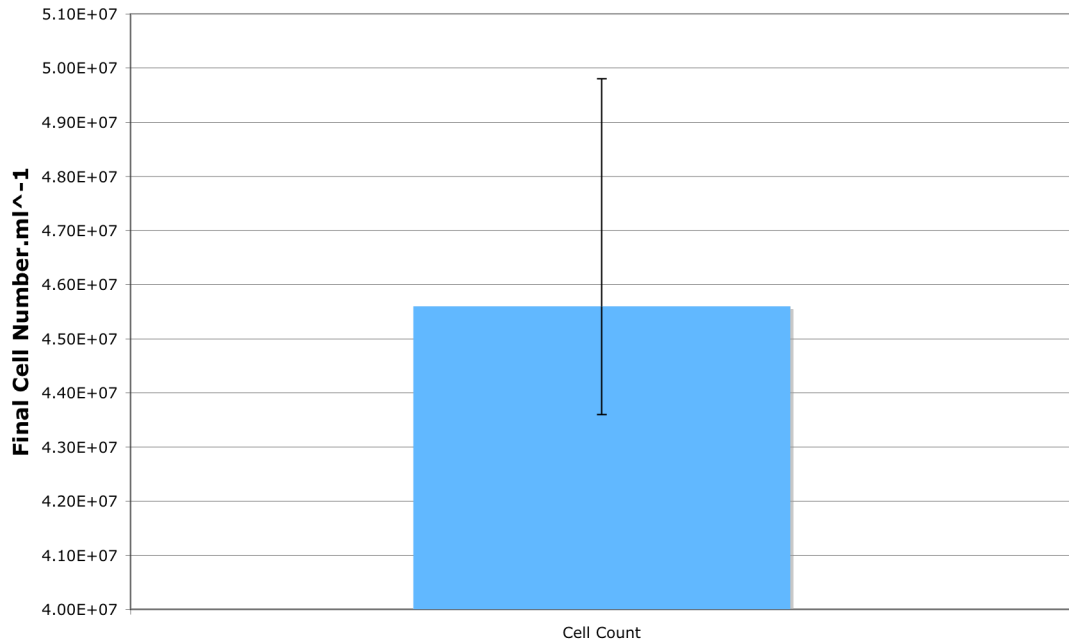


Figure 4.2 Final Yeast Cell Number.ml⁻¹ within Alginate Scaffold

In a series of experiments the final yeast cell number (after 33-39 hours), determined by manual cell count was within the range of 4.3×10^7 - 5×10^7 cells.ml⁻¹.

To determine the relationship between cell number and the oxygen consumption rate, scaffolds were formed and oxygen concentration was measured. Sampling the alginate scaffold to determine cell number is difficult and determining cell number requires sacrifice of the tube. For this reason, Figs. 4.3 and 4.4 are composites of a number of separate experiments. Cell numbers were determined for three-hour intervals and were performed over 39 hour periods to generate growth curves (Fig. 4.3). The consumption rate of these cells was calculated by determining the measured difference in concentration in the bulk flow, between cell counts. This data provided sets for which curves could be fitted and equations derived to determine the necessary equations.

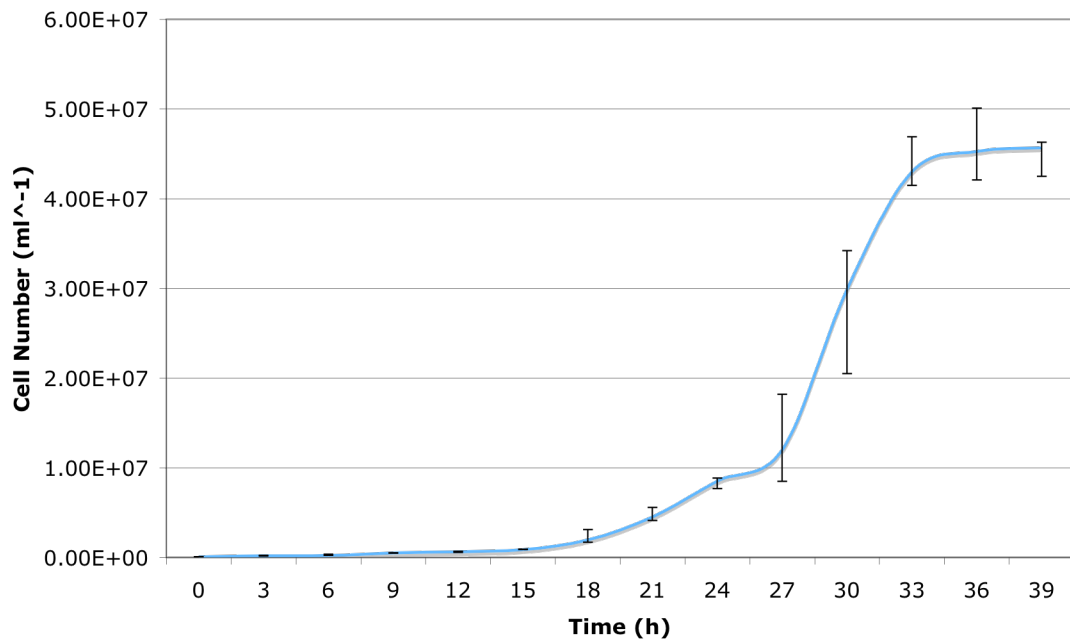


Figure 4.3 Yeast cell growth curves

Cell growth curves for yeast grown in alginate tubular scaffolds undergoing perfusion within the vascular tissue engineering bioreactor were formed from a series of experiments. Due to cell counts requiring sacrifice of the alginate scaffold each point represents a distinct experiment.

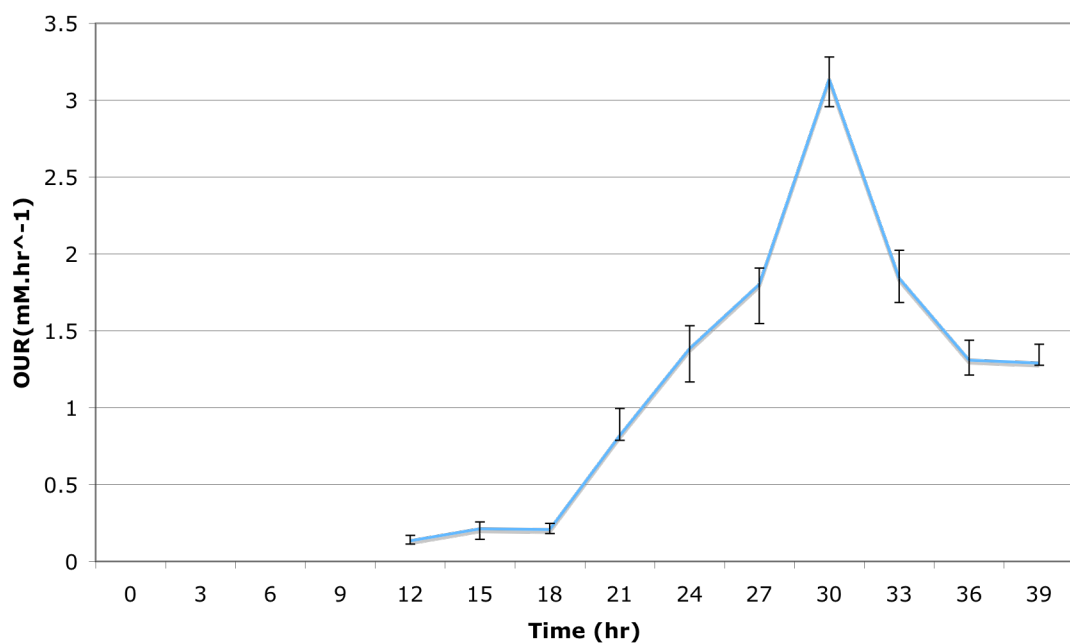


Figure 4.4 Yeast cell oxygen uptake rate curves

Oxygen uptake rates corresponding the yeast growth curves in Fig. 4.3 were determined by the measurement of oxygen concentrations before and after the alginate scaffold. These measurements were obtained using non-invasive fluorescent spots that when excited decay predictably as a function of dissolved oxygen tension (DOT).

By studying Fig. 4.3 and Fig. 4.4 it is clear the relationship between cell number and oxygen uptake rate is not constant and as such equation 4.4 holds true.

$$\text{OUR}/q_{\text{O}_2}(x) \neq \text{cell number} \quad (4.4)$$

OUR is the measured oxygen uptake rate across the bioreactor, mmol.hr^{-1} , q_{O_2} is the oxygen consumption rate, $\text{mmol.cell}^{-1}\text{hr}^{-1}$ and x is the cell concentration, cells.ml^{-1}

These figures demonstrate that as the cell concentration increases the consumption of oxygen per cell decreases. This is likely to be because as space becomes limiting the growth rate reduces more and more cells will enter the G_0 phase of the cell cycle (i.e. cease to divide also referred to as being senescent). This will lead to a reduction in respiration rate and hence oxygen consumption per cell falls.

It seems reasonable to assume that a cell uses more oxygen when dividing than when senescent due to the need to form all the required cellular structures to create the new daughter cell and hence more energy will be required with this coming from respiration.

It is further reasonable to assume that a cell has two different respiration rates depending upon whether it is senescent (G_0) or actively proliferating (Synthesis phase 'S' or Mitosis phase 'M'). Thus, the overall oxygen uptake rate may be assumed to obey an equation composed of two parts; one incorporating oxygen uptake by cells actively producing new cellular material, respiring at a relatively high rate and a

second part representing senescent cells respiring at a relatively low rate. Such an equation is outlined in equation 4.5.

$$OUR = A * \frac{dX}{dt} + B \left(X - \frac{dX}{dt} \right) \quad (4.5)$$

(Where OUR is oxygen uptake rate, A is oxygen consumption rate of proliferating cells, B is oxygen consumption rate of senescent cells, X is cell number and dX/dt is the proliferation rate)

Determining A and B directly is impossible in real time and as such a theoretical method must be adopted so that these values may be inferred. If it is assumed that at the start of the exponential phase, the cells are all proliferating and consuming oxygen at rate A and during the stationary phase all cells are quiescent due to space limitation and thus consuming oxygen at rate B, then these values may be easily derived.

Fig. 4.5 shows how this model compares to an experimentally derived trend with A and B determined to be $1.79 \times 10^{-7} \text{mM.hr}^{-1}$ and $1.30 \times 10^{-8} \text{mM.hr}^{-1}$ respectively. This is based upon Fig 4.5 taking the value at the commencement of the exponential phase and dividing it by the associated cell number to obtain A and repeating the exercise for the values at the end of the exponential phase to obtain B.

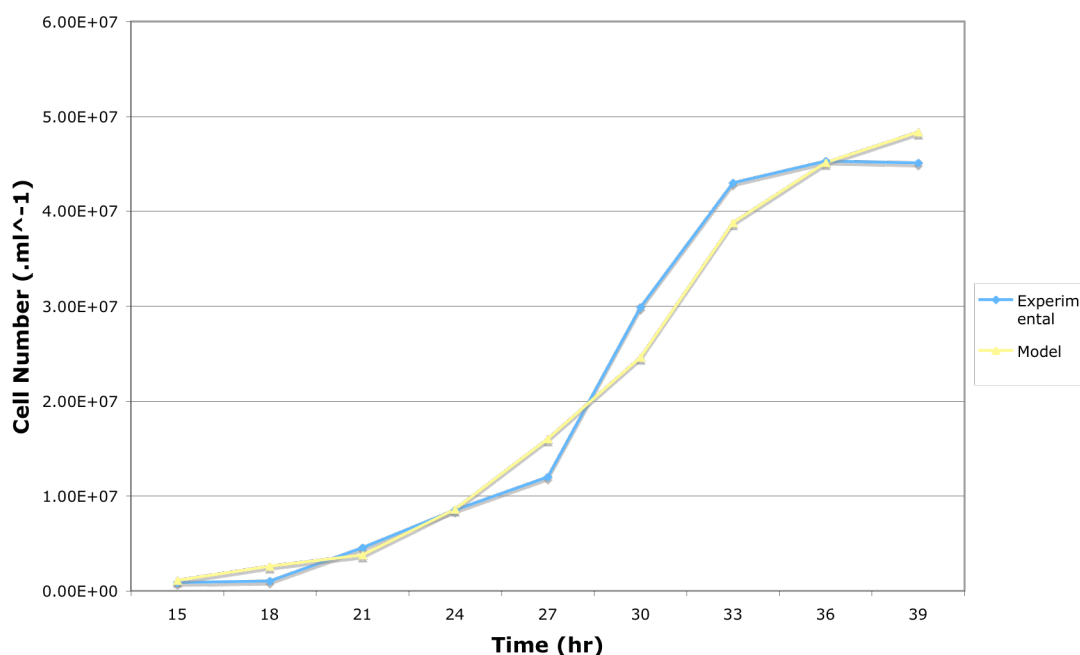


Figure 4.5 Theoretical Model determining cell number (ml⁻¹) within the scaffold based upon oxygen uptake rate.

Our theoretical model using the measured oxygen uptake rate to estimate yeast cell concentration within the alginate scaffold compares favourably with experimental results obtained over a twenty-hour period.

Such a model provides a close fit and a reasonable estimation of the state of the developing graft, as indicated by the cell number and may ultimately be used to estimate the likely delivery time of any developed graft courtesy of curve fitting techniques.

It is possible to estimate A and B for MSC (Mesenchymal Stem Cells) from data provided in Zhao et al (2005) who noted that cells immobilised in alginate consumed less oxygen at higher densities than at the time of seeding (The lower value was $0.0017 \times 10^{-9} \text{ mmol.hr}^{-1}.\text{cell}^{-1}$, while the higher value recorded was $0.012 \times 10^{-9} \text{ mmol.hr}^{-1}.\text{cell}^{-1}$). This data coupled with the method used before provides a suitable estimation of cell number in developing arterial grafts and gives rise to equations 4.6 for yeast and 4.7 for mesenchymal stem cells.

$$OUR = 1.79 * 10^{-7} \frac{dX}{dt} + 1.20 * 10^{-8} \left(X - \frac{dX}{dt} \right) \quad (4.6)$$

$$OUR = 0.012 * 10^{-9} \frac{dX}{dt} + 0.0017 * 10^{-9} \left(X - \frac{dX}{dt} \right) \quad (4.7)$$

Where OUR, is oxygen uptake rate (mM.hr⁻¹), dX/dt is the proliferating cell number and X is total cell number.

4.3.2 Window of operation for dissolved oxygen tension

In-vivo measurements from Ishikawa and Ito, 1998 indicate that the physiological oxygen concentration within the region of the bone marrow stem cells are most likely to be found is between 0.049 and 0.089mmol.L⁻¹ of oxygen. To ensure that concentrations in excess of this value are not experienced the oxygen concentration of the perfused medium within the bioreactor was selected to be 0.079 mmol.L⁻¹. Flow rates based upon this concentration must ensure a minimum concentration of 0.049 at any coordinate within the scaffold must be used. The oxygen concentration's dependence upon mass transfer within the VTEB must be determined. As the oxygen must diffuse from the perfused medium into the alginate scaffold a concentration gradient will exist in two dimensions within the tube (radially and longitudinally).

To determine the range of acceptable flow rates a number of simulations were performed using the Comsol Multiphysics Modeling Package (Comsol, Stockholm, Sweden). The technique used was closely related to that adopted by (Gerontas, PhD Thesis, University of London, 2008) where windows of operation were used to describe oxygen mass transfer within a prototype bioreactor. Gerontas uses standard

diffusion equations obeying Fick's Law and a number of assumptions, as listed in Table 4.2, to obtain equations 4.8 and 4.9.

Table 4.2 Assumptions of model to represent oxygen mass transfer in a prototype bioreactor (Gerontas, PhD Thesis, UCL, 2008).

Gerontas (2008) previously demonstrated how flow could be modelled within a tubular alginate scaffold containing mesenchymal stem cells (MSC). Many of the assumptions used in that work are applicable for the model contained here.

Lumen (Zone 1)	Alginate Scaffold (Zone 2)
Isothermal	Homogenous Suspension
Flow is Laminar, Parabolic and Developed	Oxygen consumption obeys Monod kinetics
No reaction within bulk	No convective transport
Diffusion Coefficient is Constant	Diffusion coefficient is Constant
Diffusion is Fickian	Diffusion is Fickian
Culture medium has equivalent physical properties to water	Oxygen uptake rate by cells is constant

The scaffold is cylindrical so the diffusion equations were used in the form of polar cylindrical coordinates. Equation 4.8 is the continuity equation and represents the mass balance of oxygen within the lumen (zone 1) within the bioreactor while equation 4.9 represents then radial mass balance as oxygen diffuses from the bulk into the alginate scaffold. Diffusion is assumed to be radial only within the scaffold and the outer surface of the scaffold has no transport through it as it is encased within glass.

$$\frac{\partial C_{O_2}^{lumen}}{\partial t} + V_z \frac{\partial C_{O_2}^{lumen}}{\partial z} = D_{O_2}^{LUMEN} \left(\frac{1}{r} \frac{\partial}{\partial r} \left(r \frac{\partial^2 C_{O_2}^{lumen}}{\partial r} \right) + \frac{\partial^2 C_{O_2}^{lumen}}{\partial z^2} \right) \quad (4.8)$$

$$\frac{\partial C_{O_2}^{scaffold}}{\partial t} + V_z \frac{\partial C_{O_2}^{scaffold}}{\partial z} = D_{O_2}^{scaffold} \left(\frac{1}{r} \frac{\partial}{\partial r} \left(r \frac{\partial^2 C_{O_2}^{scaffold}}{\partial r} \right) + \frac{\partial^2 C_{O_2}^{scaffold}}{\partial z^2} \right) + q \quad (4.9)$$

Although windows were developed here using a similar methodology, the underlying model used differed from that of Gerontas in that oxygen uptake rate (OUR) of encapsulated cells was not assumed to be constant based on Zhao et al (2005) for mesenchymal stem cells and Gosmann et al (1985) for yeast cells. In both instances it was demonstrated that as cell concentration rises and proliferation rate falls, the oxygen uptake rate per cell will reduce in all likelihood due to the number of cells switching out of the mitotic cycle into the G_0 static phase increasing until it encompasses the entire encapsulated population. This relationship within the model was defined using equation 4.7.

Dahl et al, (2007) suggested that the minimum concentration of cells required to form a vascular graft would be $1.16 \times 10^8 \text{ cells.ml}^{-1}$. If this is assumed to be correct then the perfusion rate of cell culture media containing $0.079 \text{ mmol.L}^{-1}$ of oxygen on entry to the VTEB must be capable of supporting $1.16 \times 10^8 \text{ cells.ml}^{-1}$ with the concentration of oxygen no lower than $0.049 \text{ mmol.L}^{-1}$ at any point within the scaffold. Such a parameter provides the first lines for the window. Using Comsol Multiphysics, a commercial CFD package, the equations outlined in chapter 3 for cell growth and oxygen uptake were combined with equations 4.7 - 4.10 and solved simultaneously to determine the minimum flow rate permitted for a given cell number to ensure that if DOT is successfully controlled at $0.079 \text{ mmol.L}^{-1}$ at entry the minimum concentration at no point within the scaffold is below $0.049 \text{ mmol.L}^{-1}$

The minimum flow rate capable of achieving adequate mass transfer to support a concentration of $1.16 \times 10^8 \text{ cells.ml}^{-1}$ is $0.095 \text{ ml.min}^{-1}$ and the oxygen concentration throughout the system for this flow rate is shown graphically in Fig. 4.6.

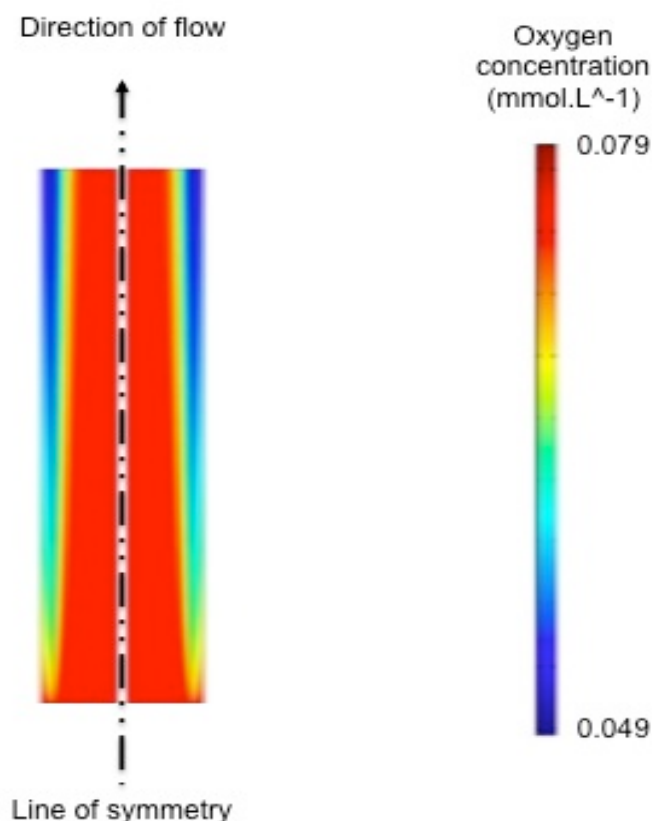


Figure 4.6 Oxygen gradients within the alginate scaffold

Oxygen gradients are shown for cells distributed at a concentration of $1.16 \times 10^8 \text{ cells.ml}^{-1}$ for a recycle flow rate of $0.095 \text{ ml.min}^{-1}$. This flow rate is the minimum possible while still ensuring that at no point within the scaffold is the oxygen concentration below $0.049 \text{ mmol.L}^{-1}$, the lower boundary of *in-vivo* conditions within the bone marrow.

The same type of simulation was run for a range of flow rates up to 20 ml.min^{-1} (the maximum flow rate of the pump) and a window of operation may be formed from the numerical outputs of these simulations and those corresponding to Fig. 4.6. This window is shown in Fig. 4.7 with the acceptable operating range being represented by the bounded region labelled WOO.

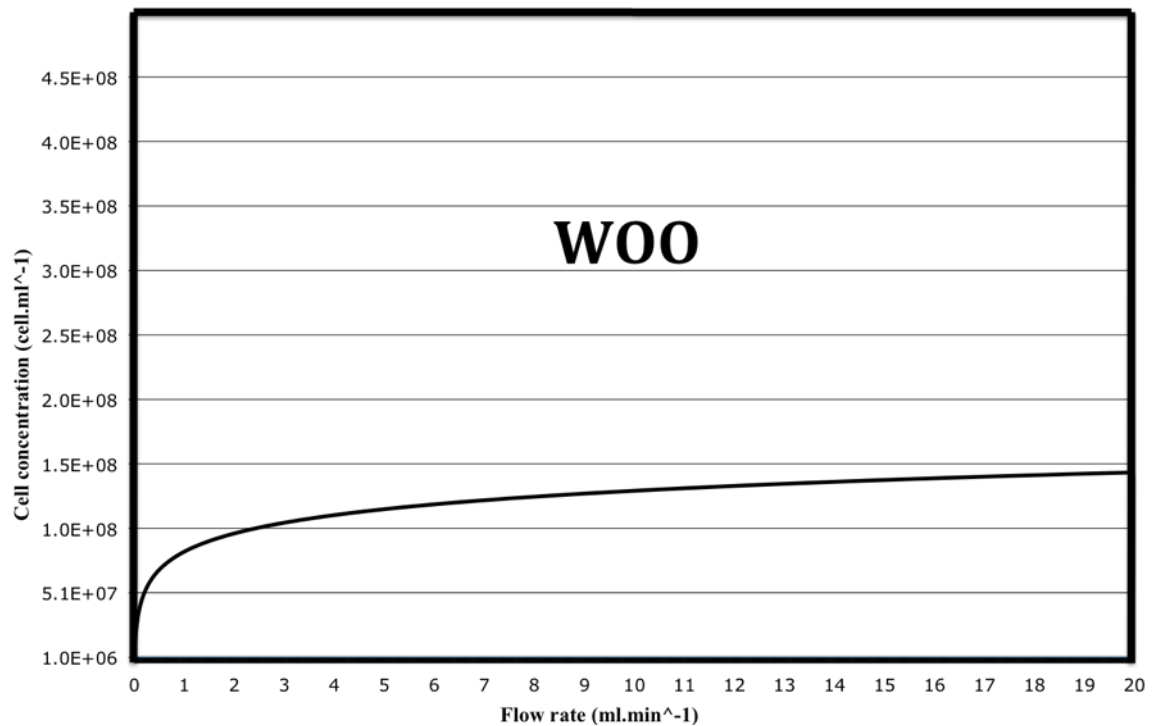


Figure 4.7 Initial window of operation (WOO) relating the flow rate of the recycle stream to the cell concentration within the scaffold.

This WOO applies to maintain an oxygen range of 0.079mM to 0.049mM throughout the scaffold.

Porter et al (2005) showed that mesenchymal stem cells (MSC) within a perfusion bioreactor demonstrated improved proliferation at flow rates exerting shear stresses up to and including 5 dynes. When cells were exposed to shear stresses in excess of this value they demonstrated increased osteogenic tendencies. Differentiation leading to bone lineage is clearly undesirable for cells intended to form blood vessels. Thus, the flow rate through the lumen of the alginate scaffold (recycle rate) should not exceed the value where the shear exerted upon the alginate scaffold wall is equivalent to 5 dynes.

Although alginate is not a rigid material, the scaffold is encased within a glass tube thus it can be assumed to be as such for the purposes of this model. The Reynolds

number for flow at the upper end of the pump's duty ($20\text{ml}\cdot\text{min}^{-1}$) is 1.4×10^{-3} hence the flow can be confidently assumed to be of a laminar nature. Poiseuille's equation (4.10) is valid for steady laminar flow of an incompressible Newtonian fluid through a long straight, rigid smooth, cylindrical tube.

$$\tau = \frac{4\mu}{\pi a^3} Q \quad (4.10)$$

Where τ is shear stress, μ is the viscosity of cell culture medium (assumed to be equivalent to water), a is the cross sectional area and Q is the volumetric flow rate.

Using equation 4.10 it is possible to determine a shear stress of 5 dynes will be exerted by a flow rate through the lumen of $9.4\text{ml}\cdot\text{min}^{-1}$. Thus $9.4\text{ml}\cdot\text{min}^{-1}$ represents a new extent of the window of operation.

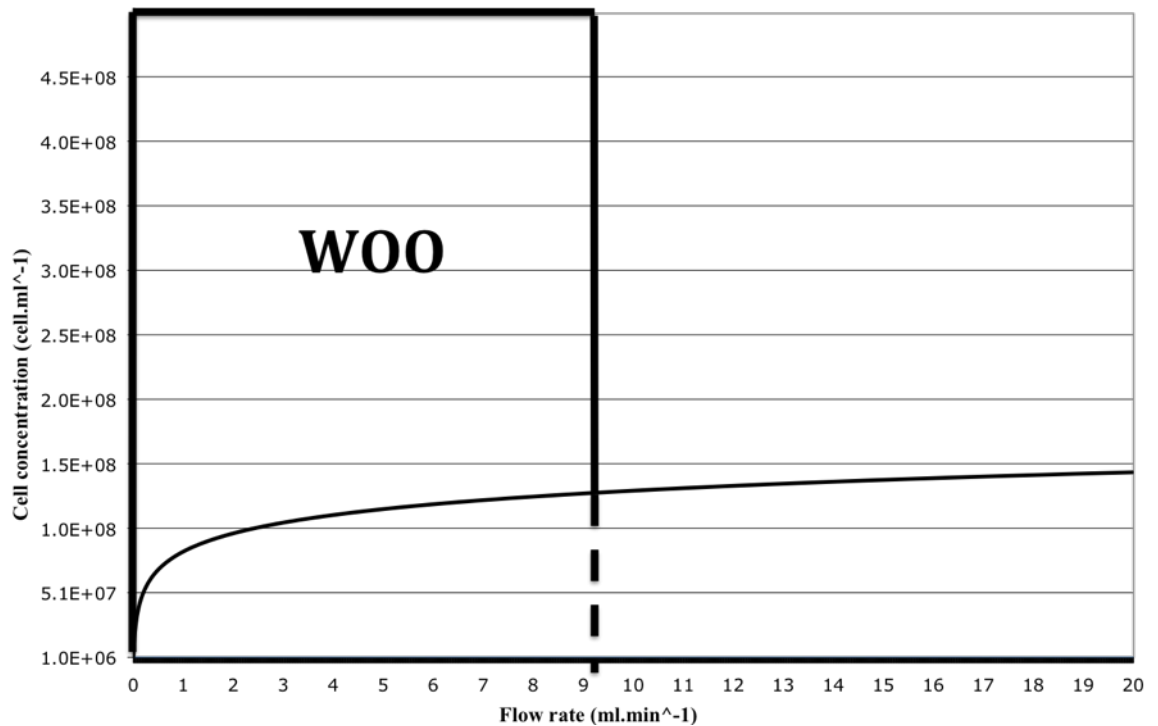


Figure 4.8 Enhanced window of operation (WOO) incorporating shear stress
When shear stress is considered an upper limit is placed on the recycle rate of $9.4\text{ml}\cdot\text{ml}^{-1}$. This constricts the WOO to the bounded region shown.

Fig 4.8 shows the final window of operation for the growth of MSC within the VTEB with permitted recycle loop flow-rates within the range $0.02 - 9.4 \text{ ml} \cdot \text{min}^{-1}$ (depending upon cell number). This window although informative is only valid where the entrance concentration of oxygen is effectively controlled at $0.079 \text{ mmol} \cdot \text{L}^{-1}$ and as such discounts the impact of other steps within the process and effectively considers the VTEB in isolation. The oxygen concentration within the system also depends upon the rate of transport into the system by the oxygenator and also flow in from the feed and out in the purge.

The form these equations take will depend upon the strategy used to achieve the required DOT from the oxygen concentration at the start, for this there are two possible options.

1. The media should be sparged with nitrogen to remove all dissolved oxygen and then re-oxygenated to the desired concentration prior to being fed into the bioreactor.
2. Sparge the oxygen from the media using nitrogen and re-oxygenate by flowing it around the system very rapidly to raise the oxygen tension to the desired value after the start up of the bioreactor with a fresh feed and purge flow rate of zero.

The second of these two alternatives has been selected with the intention being to circulate prior to introducing the seeded bioreactor. This method ensures the correct

oxygen concentration of 0.079mmol.L⁻¹. The implementation of this sparging strategy means that the oxygen concentration of the fresh feed is 0mmol.L⁻¹.

A mass balance on oxygen around the system (equation 4.11) includes terms for oxygen flow in, oxygen flow out, oxygen consumption in the bioreactor, and a term for transport in the oxygenator.

$$x_{in}F_F - x_{exit}F_F - OUR + k_{OV}(x_{exit} - C^*) = 0 \quad (4.11)$$

Where, F_F is the fresh feed rate, x_{in} is the concentration of oxygen on entry to the oxygenator, x_{out} is the concentration of oxygen on exit from the oxygenator, k_{OV} is the mass transfer coefficient for oxygen within the oxygenator, OUR is the oxygen uptake rate of the cells within the bioreactor, C^* is the saturation constant of oxygen in cell culture medium.

$$0 - x_{exit}F_F - OUR + k_L a(x_{exit} - C^*) = 0 \quad (4.12)$$

$$OUR = 0.012 * 10^{-9} \frac{dX}{dt} + 0.0017 * 10^{-9} \left(X - \frac{dX}{dt} \right) \quad (4.13)$$

The oxygen transfer coefficient, $k_L a$, for the oxygenator obeys equation 4.14 as shown in Fig. 3.2.

$$k_L a = -1e - 06F_R^2 + 6e - 05F_R + 5e - 06 \quad (4.14)$$

Substituting equation 4.14 into equation 4.12 gives equation 4.15.

$$k_L a(x_{exit} - C^*) = (-1e - 06F_R^2 + 6e - 05F_R + 5e - 06)(x_{exit} - C^*) \quad (4.15)$$

Finally, combining equation 4.13 and 4.15 gives the overall oxygen mass balance (see equation 4.16).

$$\begin{aligned}
& -x_{exit}F_F - 0.012 * 10^{-9} \frac{dX}{dt} + 0.0017 * 10^{-9} \left(X - \frac{dX}{dt} \right) + (-10^{-7} F_R^2 + 6 * 10^{-6} F_R \\
& + 5 * 10^{-7})(x_{exit} - C^*) = 0
\end{aligned} \tag{4.16}$$

This overall mass balance (equation 4.16) shows that the oxygen concentration within the system is a function of both the fresh feed 'F_F' and recycle rate 'F_R' as well as the cell concentration and the proportion of cells that are proliferating versus those that are senescent.

Having already determined the theoretical range of the recycle rate, it is now possible to calculate an equivalent range for the fresh feed rate. This range can be determined using equation 4.16. The lower boundary is determined by substituting the minimum recycle rate (0.1ml.min⁻¹), the minimum cell concentration (10⁶cells.ml⁻¹) and the lower oxygen consumption rate (0.0017mmol.cell⁻¹.s⁻¹) into equation 4.16. The upper boundary may be determined similarly by substituting the maximum recycle rate (9.4ml.min⁻¹), the maximum cell concentration (1.16*10⁸cells.ml⁻¹) and the higher oxygen consumption rate (0.012mmol.cell⁻¹.s⁻¹) into equation 4.16. The results for the evaluation of these equations can be used to form a window of operation as shown in Fig 4.9.

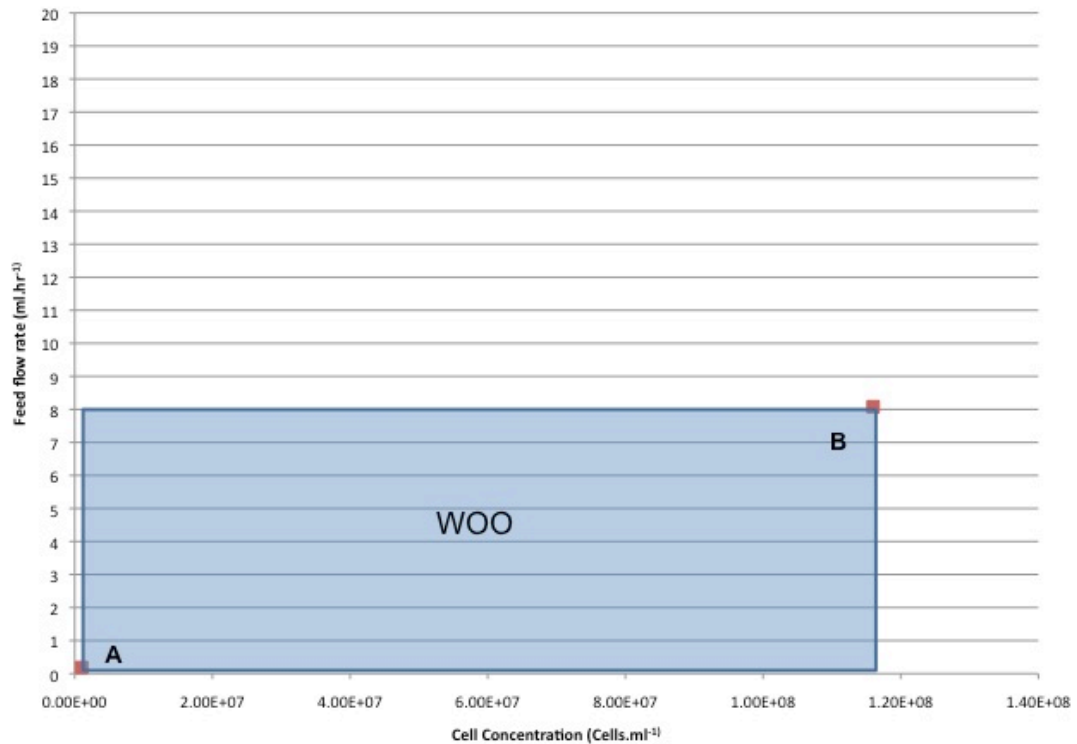


Figure 4.9 Window of Operation relating cell concentration and feed rate

The range of possible fresh feed rates is a function of cell concentration within the alginate scaffold and the recycle rate within the bioreactor system. This window of operation demonstrates that the range of acceptable fresh feed rates varies between 0.19ml.hr^{-1} (A) and 8.08ml.hr^{-1} (B).

4.4 Designing process controllers

Using the windows of operation shown in Figs. 4.8 and 4.9 it is possible to design process controllers. The simplest form of a process controller is the two-step controller where the recycle rate pump is instructed to work at a different flow rate depending upon whether the measured DOT falls above or below a set value.

The position of the sensor for measuring the DOT is most sensibly at the exit of the bioreactor (Fig. 4.10) as this is the point closest to the region where control of oxygen concentration is most important. It is placed near the exit rather than the inlet as the control system chosen is a feedback loop due to the complexity and dynamic

nature of the system. The set point for the exit of the bioreactor flow within the bulk has been set at 0.079mmol.L^{-1} and at low flow rates the time delay through the system to any other point of the system further from the cell scaffold will affect the rate of control response unfavourably.

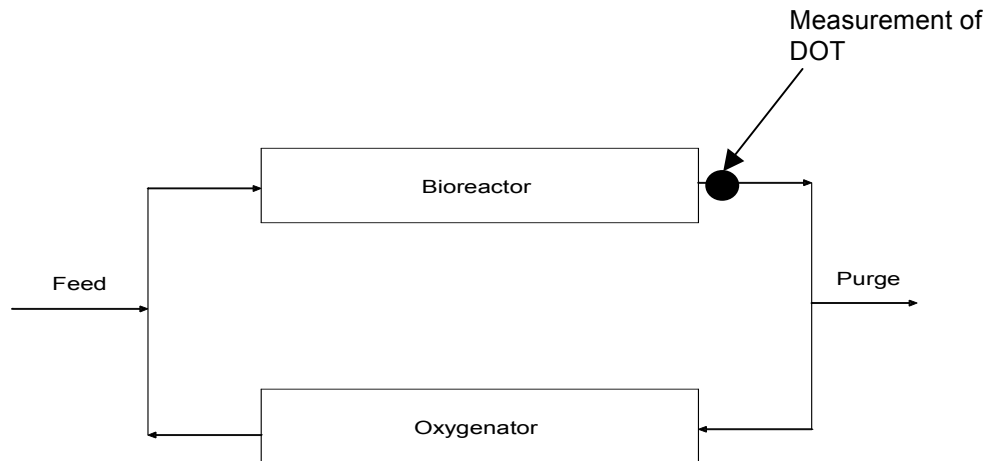


Figure 4.10 Location of DOT sensor within the system

The sensor responsible for measurement of the dissolved oxygen tension (DOT) shall be located at the exit of the bioreactor containing the alginate scaffold and the developing cells.

4.4.1 Two-step controller

A two-step controller is the simplest form of controller. It is designed to overact when the system is operating at a value below a user-specified set point and under-act when the system is below the same set point. Two-step controllers are not sophisticated and generally lend themselves to simple processes where gradual changes take place and the inconvenience of oscillations and relatively large time delays are insignificant compared with keeping the system simple and cost effective.

To illustrate this case, a two-step controller for the VTEB has been designed. For this model, the system normally operates at 0.1ml.min^{-1} and is only activated when the

concentration falls below 0.074mmol.L^{-1} , at which point the controller changes the flow rate of the recycle loop to 9.4ml.min^{-1} . This flow rate is maintained until a concentration of 0.079mmol.L^{-1} is attained. At this time the controller is deactivated and the flow rate returns to 1ml.min^{-1} . 9.4ml.min^{-1} and 1ml.min^{-1} were selected as the two steps of the controller. These values were selected as it has already been determined that 0.1ml.min^{-1} and 9.4ml.min^{-1} represent the range of acceptable recycle flow rates. A two-step controller takes no account of error magnitude so thus it is common for such controllers to over-react and become unstable.

Such a control strategy is illustrated in Fig. 4.11 and Fig. 4.12. These figures present a two-step flow rate change and the associated oxygen concentration trend, respectively. These trends are symptomatic of a two-step controller, oscillating around the set point of the controller, 0.079mmol.L^{-1} .

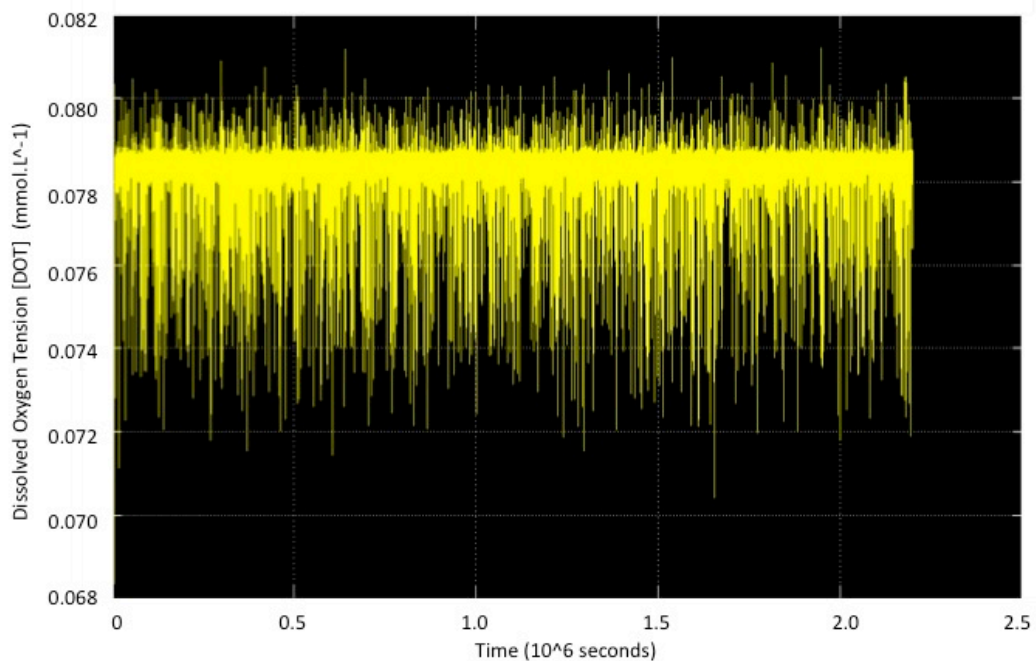


Figure 4.11 Two-step Control of DOT at the exit of the tissue engineered artery support scaffold

This control took place over a time period where the artery developed to a cell concentration in excess of 1.1 billion cells per ml of alginate scaffold and the model incorporated random noise into the measured signal received by the two-step controller. The fresh feed rate was constant at 3.0ml.hr^{-1} of culture medium and all substrates other than oxygen were kept in excess. Waste concentrations were not considered. The DOT set point is 0.079mmol.L^{-1} at the exit of the bioreactor.

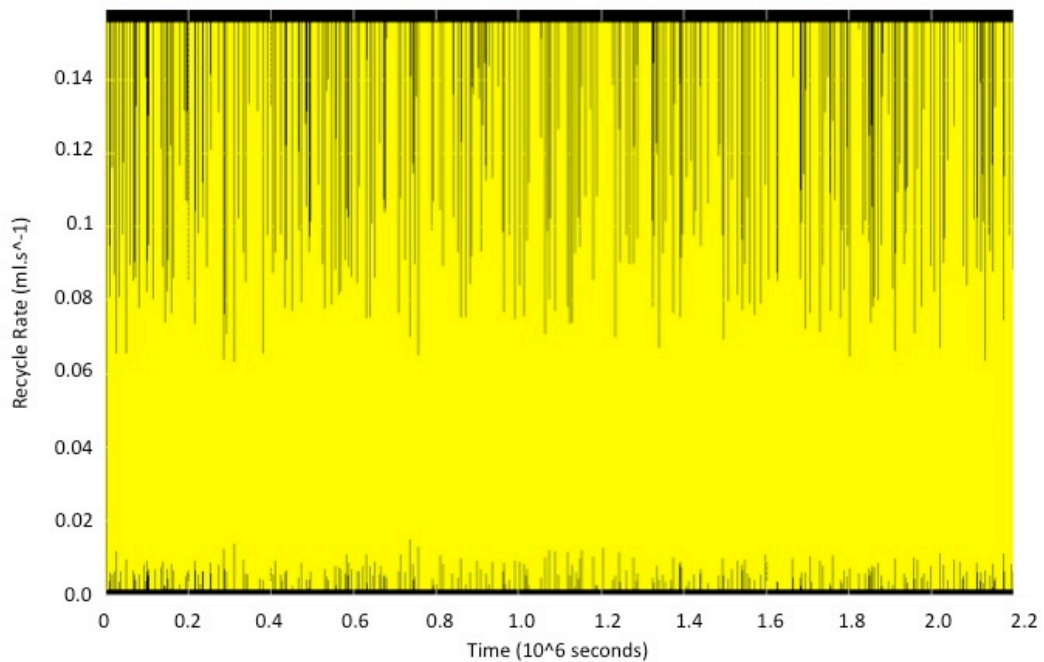


Figure 4.12 Flow Rate of Two-Step Controlled Recycle Stream
This controlled recycle rate relates to the controlled DOT shown in Fig. 4.11.

Given the relative ineffectiveness of such a controller in a system such as the VTEB where much closer control is desirable, more sophisticated controllers such as Proportional-Integral (PI) are required.

4.4.2 Proportional-Integral (PI) controller

The PI controller is widely used in industrial application. Before designing the PI controller, the transfer of the function will be given as follows. Equations 4.17 - 4.26 represent the derivation of a transfer function relating DOT concentration at the exit of the bioreactor to recycle loop flow rate. Equation 4.17 represents a mass balance neglecting cell growth terms. For the purposes of determining the transfer function cell growth and the associated oxygen uptake has been treated as a disturbance entering the system to modify the oxygen concentration undesirably.

$$V \frac{dx}{dt} = F_{in}x_{in} - F_{out}x_{out} + k_L a(C^* - x_{out}) \quad (4.17)$$

Where: V is the system volume, F_{in} is the fresh feed flow rate, F_{out} is the purge flow rate, x_{in} is the concentration of oxygen in the feed, x_{out} is the concentration of oxygen in the purge, $k_L a$ is the overall mass transfer coefficient in the oxygenator, C^* is the saturation constant of oxygen within cell culture medium, x is the concentration of oxygen within the system and t is time.

Knowing that the fresh feed flow rate is equal to the purge flow rate (4.18) and that the concentration of oxygen within the feed is 0 (4.19) gives equation 4.20.

$$F_{in} = F_{out} = F \quad (4.18)$$

$$\frac{V}{F} \frac{dx}{dt} = x_{in} - x_{out} + \frac{k_L a(C^* - x_{out})}{F} \quad (4.19)$$

$$\frac{V}{F} \frac{dx}{dt} + x_{out} = \frac{k_L a(C^* - x_{out})}{F} \quad (4.20)$$

Assuming that the controller is effective and the exit concentration from the bioreactor is at a steady state allows equation 4.21 to be formed.

$$\frac{V}{F} \frac{dx}{dt} + x_{out} = \frac{(C^* - x_{out}^{ss})}{F} k_L a \quad (4.21)$$

Where: x_{out}^{ss} = the steady state concentration on exit from the bioreactor

$k_L a$ is a non-linear term and has the potential to complicate the system, however on examination, the relationship between $k_L a$ and recycle rate (See Fig. 3.3) has the potential to be linearised. It has already been determined that the maximum recycle flow rate cannot exceed 9.4ml and the curve relating to $k_L a$ will approximate to a linear relationship within this range. This linearisation is shown in Fig. 4.13.

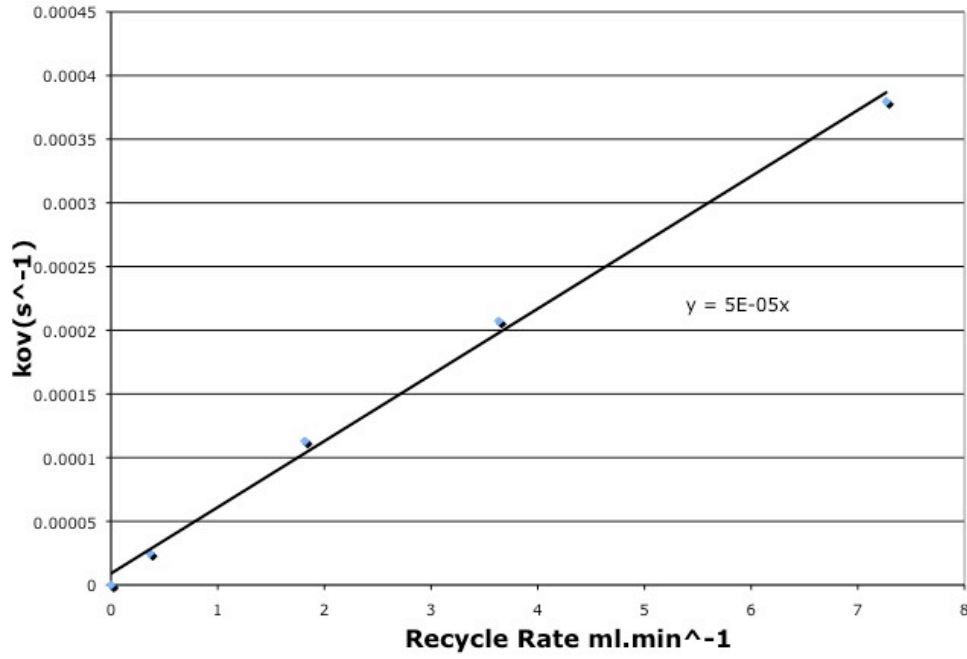


Figure 4.13 Linearization of the relationship between overall oxygen transfer coefficient, $k_{L,a}$, within the oxygenator and the recycle rate.

Substituting this linearised term of $k_{L,a} = 5 \times 10^{-5} F_R$ into equation 4.22 gives the overall relationship between change in oxygen concentration, recycle rate and feed rate.

$$\frac{V}{F} \frac{dx}{dt} + x_{out} = \frac{(C^* - x_{out}^{ss})}{F} (5 \times 10^{-5}) F_R \quad (4.22)$$

Assuming the feed rate is constant performing a Laplace Transform on equation 4.22 generates a transfer function that characterises the dynamic nature of the system.

$$\delta x(s) = \frac{\frac{(C^* - x_{out}^{ss})}{F} (5 \times 10^{-5})}{\left(\frac{V}{F}\right)s + 1} \delta F_R(s) \quad (4.23)$$

Assuming a feed rate of $0.1 \text{ ml} \cdot \text{hr}^{-1}$ and a steady state exit concentration of $0.079 \text{ mmol} \cdot \text{l}^{-1}$ allows this transfer function to be used to calculate the gain of a proportional controller. The gain of this transfer function is thus 0.1098 and relates a change in recycle rate to a change in oxygen concentration. Given this transfer function has been determined without giving consideration to cell growth significant tuning is required.

Proportional controllers work by multiplying the error between a set point and the measured value by this gain. A Simulink program was used to model the system and is outlined in Appendix 1. Using 0.10 as the initial gain and using trial and error to minimise the offset that is inherent in the use of a proportional controller the most effective value was determined to be 15. To eliminate noise within the system and prevent excessive control the mean average of the oxygen concentration over five minute intervals was used to determine the error rather than a point value. This served to smooth the data and eliminate any random outlying values arising for some reason and having a negative effect on the control of the system. The controlled recycle rate is shown in Fig. 4.14, the associated oxygen concentration, at the exit from the bioreactor, is shown in Fig. 4.15 and the cell growth rate curve, within the bioreactor, is shown in Fig. 4.16.

Fig. 4.16 demonstrates the disadvantage of using a proportional controller, which generates a response directly related to the magnitude of the measured error. Such a controller will always have an offset from the desired set point as the generated response falls away to 0 linearly as the error falls to 0. It can also result in both

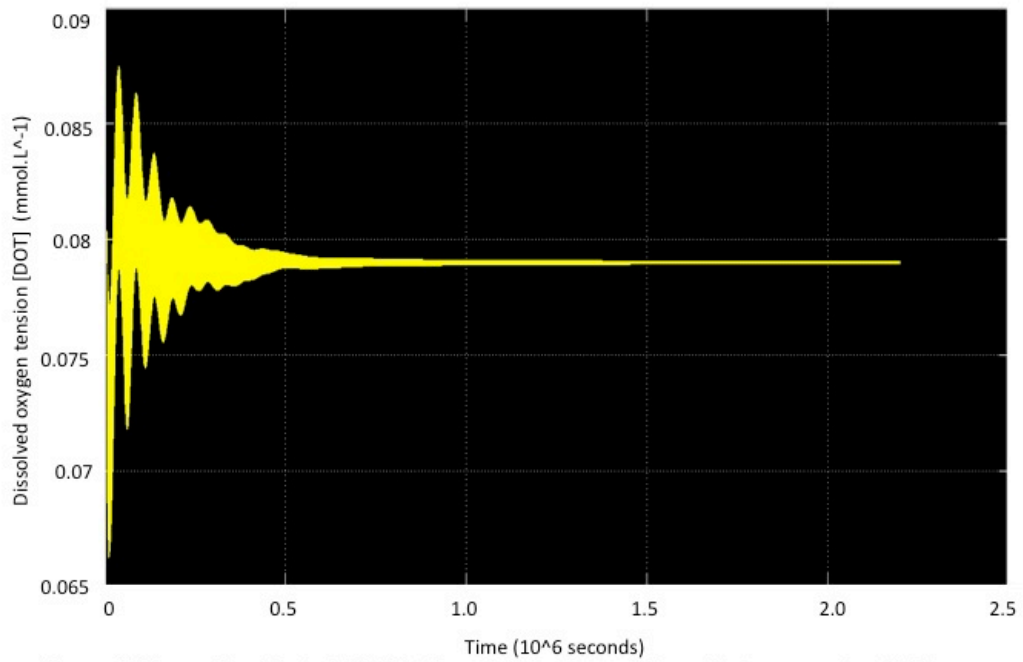


Figure 4.14 Proportional Control of DOT at the exit of the tissue engineered artery support scaffold

This control took place over a time period where the artery developed to a cell concentration in excess of 1.1×10^8 cells per ml of alginate scaffold and the model incorporated random noise into the measured signal received by the P controller. The fresh feed rate was constant at $1.0 \text{ ml} \cdot \text{hr}^{-1}$ of culture medium and all substrates other than oxygen were kept in excess. Waste concentrations were not considered. The DOT set point is $0.079 \text{ mmol} \cdot \text{L}^{-1}$ at the exit of the bioreactor.

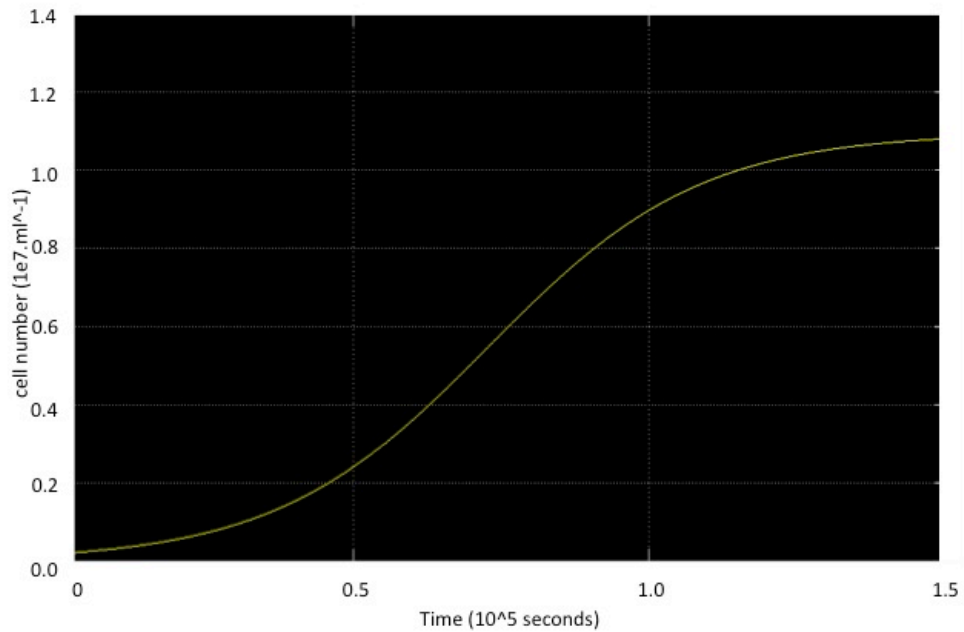


Figure 4.15 Cell growth within alginate support scaffold related to Fig 4.14

A cell growth curve modeled as outlined in Chapter 3. This cell growth curve related to the DOT shown in Fig. 4.14 and the recycle rate shown in Fig. 4.15.

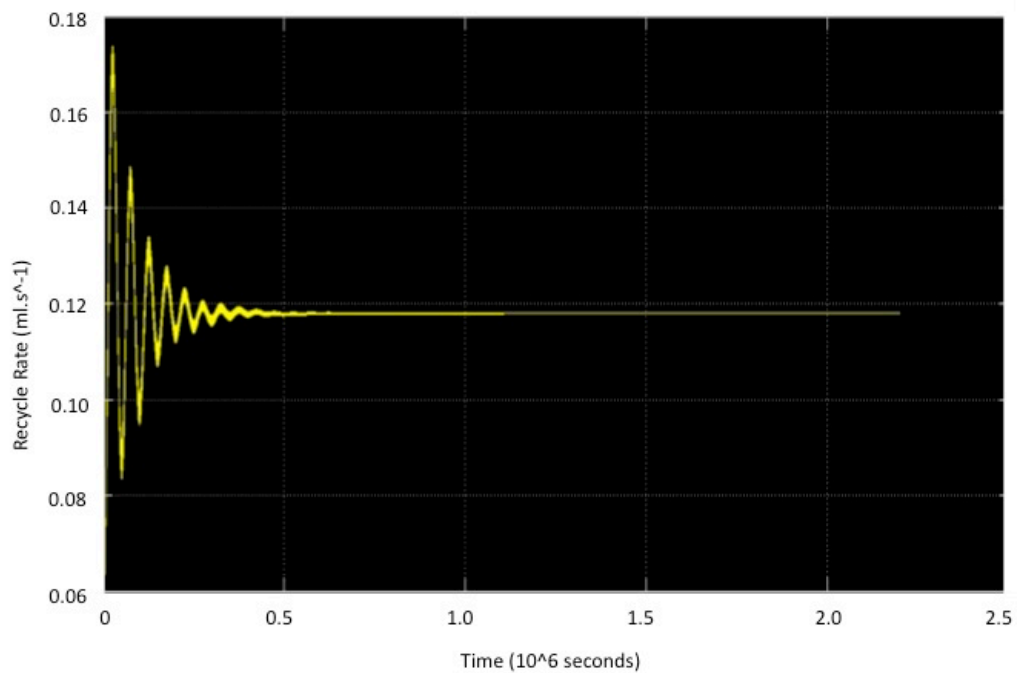


Figure 4.16 Flow Rate of Proportional controlled Recycle Stream
This controlled recycle rate relates to the controlled DOT shown in figure 4.14

overshoot and undershoot of the desired set point, as the controller does not respond effectively to the rate at which the error increases or reduces. A proportional integral (PI) controller generates a response equal to the integral of the error over time and thus even when the measured error approaches zero, the PI controller will still have a response output to eliminate the offset generated by a proportional controller in isolation. Given the large delays and slow response inherent in the VTEB system, it is not surprising to find the integral time is a large value. After using an initial value equivalent to $0.1 \times \text{Gain}$, the optimum value was determined, by tuning to be $1e-3$ and generated controlled recycled rate and dissolved oxygen tension trends as shown in Figs. 4.17 and 4.18, respectively.

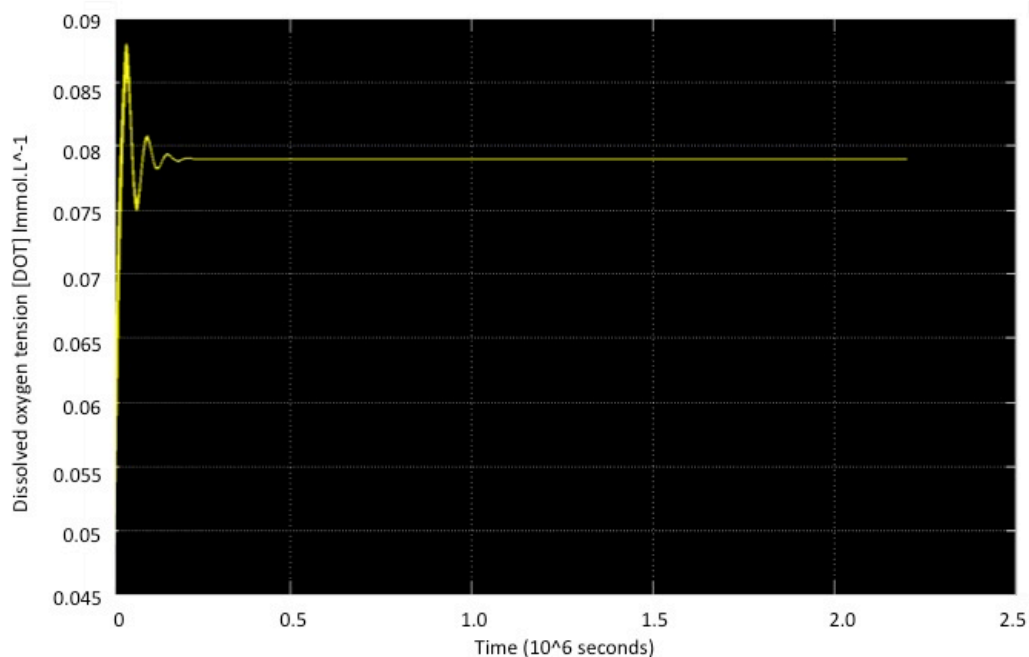


Figure 4.17 Proportional and Integral Control of DOT at the exit of the tissue engineered artery support scaffold This control took place over a time period where the artery developed to a cell concentration in excess of 1.1 billion cells per ml of alginate scaffold and the model incorporated random noise into the measured signal received by the PI controller. The fresh feed rate was constant at $3.5 \text{ ml} \cdot \text{hr}^{-1}$ of culture medium and all substrates other than oxygen were kept in excess. Waste concentrations were not considered. The DOT set point is $0.079 \text{ mmol} \cdot \text{L}^{-1}$ at the exit of the bioreactor.

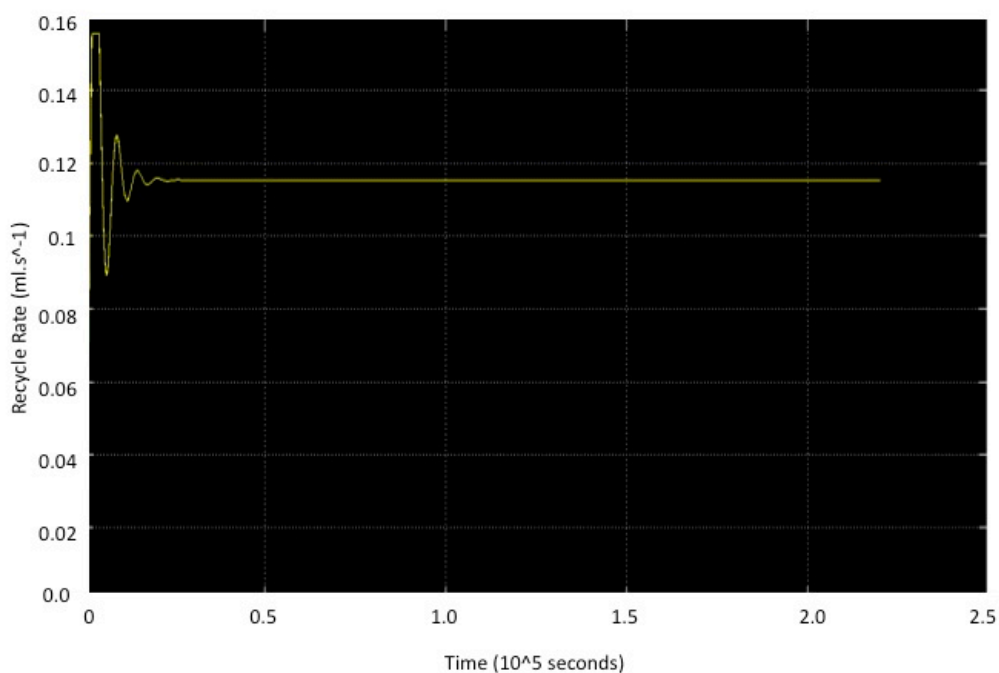


Figure 4.18 Flow Rate of Controlled Recycle Stream This Controlled Recycle Rate relates to the controlled DOT shown in Fig 4.17.

These results serve to indicate that the oxygen concentration within the bioreactor system may be controlled successfully by a control loop incorporating a sensor at the bioreactor's exit and a proportional and integral controller linked to a pump responsible for the flow of media within the recycle loop. Many of the values incorporated into the model used to determine this control loop are not certain and have been assumed or taken from literature. For this reason sensitivity analysis should be carried out to determine the effect a change on these parameters will have upon the proportional integral (PI) controller's effectiveness.

4.4.3 Testing the control system

Two assumed values within the model have had sensitivity analysis performed on them, the growth rate of the cells and the oxygen uptake rate. For a growth rate of +10% of the specified value and oxygen uptake of +10%, for both senescent and proliferating cells, the controlled DOT trend is shown in Fig. 4.19. This trend demonstrates that the control system developed is capable of maintaining the dissolved oxygen tension at the bioreactor exit even if there are 10% errors in both the assumed cell growth rate and the assumed oxygen consumption rate.

4.5 Conclusions

This chapter has shown that it is possible to derive windows of operation for the vascular tissue engineered bioreactor (VTEB) within which oxygen concentration may feasibly be controlled. These windows have been used in conjunction with the model

developed in chapter 3 to demonstrate that it is possible to control

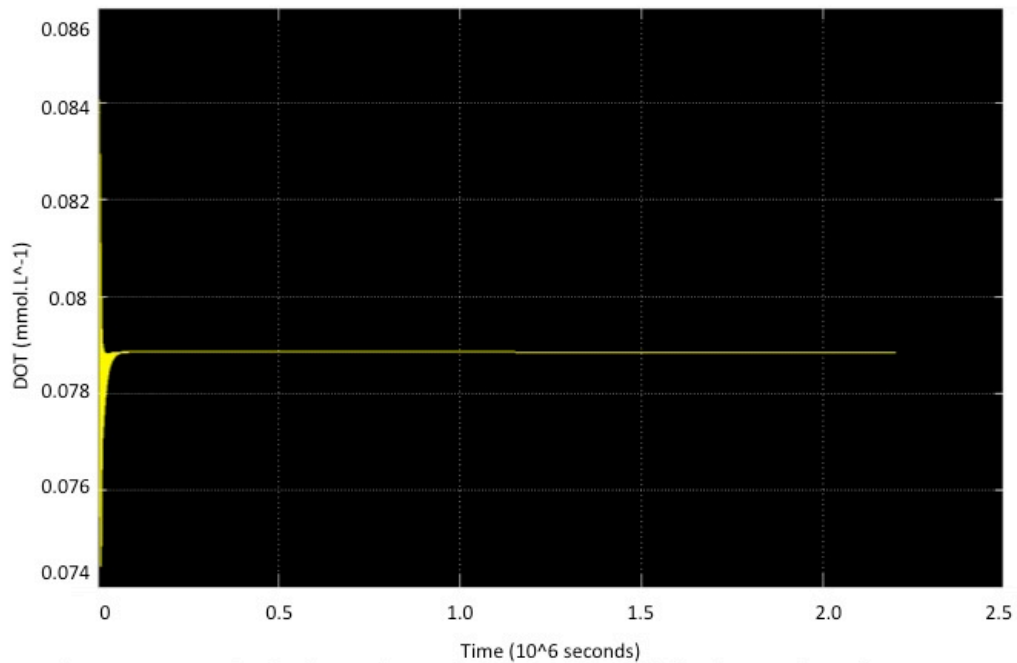


Figure 4.19 Proportional and Integral Control of DOT at the exit of the tissue engineered artery support scaffold This control took place over a time period where the artery developed to a cell concentration in excess of 1.1 billion cells per ml of alginate scaffold and the model incorporated random noise into the measured signal received by the PI controller. The fresh feed rate was constant at $7.0 \text{ ml} \cdot \text{hr}^{-1}$ of culture medium and all substrates other than oxygen were kept in excess. Waste concentrations were not considered. The DOT set point is $0.079 \text{ mmol} \cdot \text{L}^{-1}$ at the exit of the bioreactor.

the dissolved oxygen within the VTEB. PI controllers simulated within a relevant software package have been demonstrated to provide superior maintenance of DOT when compared with two-step or proportional control and provide sufficient control to grow a graft within currently estimated *in-vivo* tolerances, even when some parameters are modified. More complex control techniques are discussed in Chapter 7 when oxygen control is considered not in isolation as it has been here but as part of a more complex strategy along with metabolite concentrations and variables such as pH and full integration between feed and recycle loop controllers.

Additionally, methods have been developed that allow the use of the oxygen consumption rate by the cells within the bioreactor to estimate the cell number online. This estimation of cell number may be used both to estimate the health of the culture

and also estimate likely delivery time by fitting the generated growth curve to the expected trend.

Chapter 5 pH within the VTEB system

5.0 Introduction

Most mammalian cell lines grow at a pH of 7.2-7.4. The consumption of glucose and other substrates coupled with waste production such as lactic acid can influence this pH, which necessitates constant media change when cells are grown in static culture. In a perfusion system where media exchange continuously takes place this is less of an issue provided the system is operated within a suitable range of flow rates that ensure pH does not fall below 7.2 or exceed 7.4.

5.1 Cell Media Buffers

The by-products of cellular metabolism are not exclusively cytotoxic and include growth factors that are beneficial to cell division and stimulate proliferation, for this reason constant media change is not ideal and most cell media contain buffers that are capable of keeping pH constant in the presence of small amounts of acidic or basic chemicals.

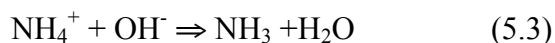
Chemical buffers work upon the principal of a reversible chemical reaction between a compound and its conjugate ion such as ammonia and ammonium chloride (see equation 5.1)



In the presence of an increased concentration of H^+ ions the reaction balance will move to the left hand side (see equation 5.2).



In the presence of an increased number of OH^- ions the balance of the reaction will move to the right (see equation 5.3).



Different buffers are effective within different ranges of pH, this is dictated by the dissociation constant of the acid K_A , i.e. the equilibrium ratio between the compound and its conjugate (see equation 5.4).

$$K_A = \frac{[H^+]_{eq}[A^-]_{eq}}{[HA]_{eq}} \quad (5.4)$$

The pH of a solution is directly related to the K_A value of a solution by the Henderson-Hasselbach equation (Atkins, 1998), (see equations 5.5-5.6).

$$pH = pK_A + \log_{10} \frac{[A^-]}{[HA]} \quad (5.5)$$

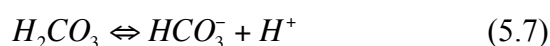
$$pK_A = -\log_{10}[K_A] \quad (5.6)$$

A buffer is most effective at a pH equivalent to its pK_A and its effective range under normal conditions is generally considered to be its $pK_A \pm 1$.

There are two common chemical buffers used in mammalian cell culture the sodium bicarbonate (NaHCO_3) and HEPES systems.

5.2 Bicarbonate Buffer

The bicarbonate buffer system is analogous to one of the main buffering systems present in the blood. Its prevalence in use within cell culture media stems from its advantages of being cheap, non-cytotoxic and being a physiological system. There is even some possibility it may have some nutritional benefit (Freshney, 2000).



Despite these benefits the bicarbonate buffer has a pK_A of 6.1 and as such is not an effective buffer at the required physiological pH required by mammalian cells of 7.2-7.4.

To achieve such a pH bicarbonate buffered media must be used within an environment where the carbon dioxide is controlled at a concentration up to 100 times higher than that found in the air (normally 5% within an environmentally controlled incubator). Such a situation is similar to that experienced in the human body where carbon dioxide is a waste product of respiration and is carried in solution within the blood to the lungs where it may be excreted.

The presence of this carbon dioxide moves the equilibrium of the reaction towards the left hand side and increases the pH of the solution to a less acidic value i.e. the required physiological value of 7.4.

Due to the relative weakness of the bicarbonate buffer and also the risk of contamination, medium incorporating this buffer often contains the visual indicator, phenol red, which appears a distinct colour depending upon the pH of the solution.

Table 5.1 Phenol red colour variation with solution pH

pH	Colour
>7.8	Purple
7.6	Pink
7.4	Red
7.0	Orange
6.5	Yellow
<6.5	Lemon Yellow

5.3 HEPES buffering system

A common alternative to the bicarbonate buffering system is HEPES. HEPES in comparison to bicarbonate buffer is a very strong buffer within the physiological range 7.2 – 7.4. The reason that HEPES has not become the prevalent buffer in cell culture is because it is much more cytotoxic especially for certain cell lines which may not be grown in solutions containing it. An additional disadvantage of HEPES is that in comparison to bicarbonate it is far more expensive. For these reasons DMEM containing bicarbonate is commonly used in static cell culture, being changed at 1-2 day intervals, and it is selected for tissue engineering arteries within the VTEB. Although bicarbonate is a weaker buffer than HEPES, given it is sufficient to ensure buffering capacity for 48 hours within a static culture it is deemed acceptable for a perfusion system with continuous media exchange.

5.4 Calculating the window of operation for pH versus lactic acid concentration

The bicarbonate buffer, within the cell culture medium, is capable of ensuring the pH in solution is constant for low levels of acid or base, but cannot achieve this indefinitely.

The standard concentration of bicarbonate buffer within Dulbecco's Modified Eagle Medium (DMEM), a common basal media, is 44mM, however to determine pH of the buffer it is necessary to know the ratio of bicarbonate ion to carbonic acid. Under normal conditions the pH of bicarbonate buffer is 6.1, equivalent to its pK_A , however in a carbon dioxide controlled environment the pH is 7.4.

To determine the ratio H_2CO_3/HCO_3^- at a pH of 7.4 the Henderson-Hasselbach equation can be used;

$$7.4 = 6.1 + \log_{10} \frac{[HCO_3^-]}{[H_2CO_3]} \quad (5.8)$$

$$[H_2CO_3] + [HCO_3^-] = 44mM \quad (5.9)$$

From these two equations it is possible to form equation 5.10 and determine the concentration $[HCO_3^-]$ as 41.88mM and then from substitution into equation 5.9 $[H_2CO_3]$ as 2.11mM.

$$7.4 = 6.1 + \log_{10} \frac{44 - [H_2CO_3]}{[H_2CO_3]} \quad (5.10)$$

Glycolysis is the first stage of respiration within a mammalian cell. Respiration is the process by which glucose is broken down to release energy for the cell to use. Glucose is initially broken down into pyruvate, which is ultimately converted into lactate. The lactate, which forms lactic acid on passing into solution, is one of the agents primarily responsible for pH shifts in cell culture medium. With the values determined using

equations 5.8-5.10 it is possible to determine the amount of lactic acid that will produce a change in pH of undesirable magnitude.

The physiological pH range is generally considered to be between 7.2 and 7.4 and it is this range that determines the limits of the pH window of operation.

Again using the Henderson-Hasselbach equation it is possible to determine the amount of lactic acid that would be required to shift the pH beyond this acceptable range. For a system at the lower limit of the pH range 7.2; we have.

$$7.2 = 6.1 + \log \frac{[HCO_3^-]}{[H_2CO_3]} \quad (5.11)$$

$$[H_2CO_3] + [HCO_3^-] = 44mM \quad (5.12)$$

Using the same approach as employed previously it can be shown that the presence of lactic acid causes the buffer equilibrium to move to the left hand side with $[H_2CO_3]$ now equal to 3.24mM and $[HCO_3^-]$ 40.76mM.

For a pH shift from 7.4 to 7.2, the concentration of H_2CO_3 has changed by 3.24mM-2.09mM = 1.13mM due to an addition of a stoichiometrically equivalent amount of protons from lactic acid, this relationship is shown visually in Fig. 5.1, forming a window of operation for pH versus lactic acid concentration.

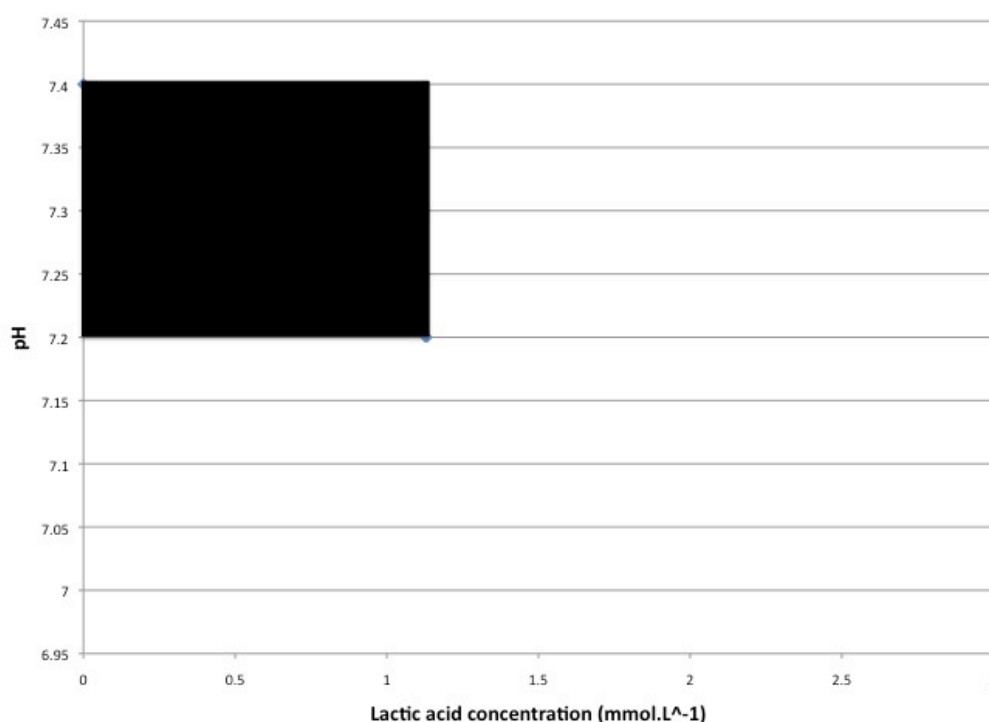


Figure 5.1 Window of operation for pH versus lactic acid concentration

To determine an operating window of pH versus control variable the method of control must first be established. Given that media exchange will provide fresh buffer for controlling pH, the most appropriate method of control is regulating the rate of the fresh feed/purge both to provide fresh buffer and remove the responsible chemicals from the system.

The operating window can thus be formed by plotting pH against the feed flow rate (the control variable). This requires a value for the lactic acid production rate for each cell type of interest.

To obtain appropriate values for embryonic stem cells and mesenchymal stem cells, a set of data obtained from literature has been used and is outlined in Table 5.2.

Table 5.2 Data required for calculating lactate production rate by cells

	MSC	Reference
Glucose consumption rate	$1.46 \pm 0.92 \times 10^{-10}$ g.cell ⁻¹ .hr ⁻¹	Markusen JF (2005)
Lactate yield on glucose	2mol.mol ⁻¹	Zeng A et al (1998)

As stated in the previous chapter on the control of oxygen within the VTEB (Chapter 4), it is known that a cell density of between 1×10^8 cells.ml⁻¹ and 5×10^8 cells.ml⁻¹ are required for a functional tissue engineered artery.

With a cell population of 5×10^8 cells.ml⁻¹ the total cell number within the tissue-engineering scaffold (volume 1.2ml [2s.f.]) will be 5.8×10^8 cells [2s.f.]. The production rate of lactic acid per mesenchymal stem cell (MSC) is 2.79×10^{-13} mmol.s⁻¹.cell⁻¹ based on the glucose consumption provided by Markusen (2008) and the lactate yield on glucose from Zeng A, et al (1998) (See table 5.2). Thus the lactate production rate of 5.8×10^8 MSC can be determined to be 2.6×10^{-4} mmol.s⁻¹ (2s.f.). Given 5×10^8 cells.ml⁻¹ is the maximum concentration for an arterial graft 2.6×10^{-4} mmol.s⁻¹ (2s.f.) represents the maximum likely production rate of lactic acid within the alginate scaffold (even though as stated in chapter 4 as cell density increases, respiration rate falls and an increasing number of cells become senescent, the lactate production is likely to fall dramatically).

5.5 Single pass pH window of operation

As there are two controlled flow rates within the vascular tissue engineering bioreactor (VTEB) two separate windows of operation are required. The first and simplest of these relates the flow rate within the recycle loop i.e. the flow through the bioreactor with the pH drop between the points shown in Fig. 5.2. The window in this case designates flow rates required to ensure that the pH drop across the bioreactor does not exceed 0.2 (7.4-7.2).

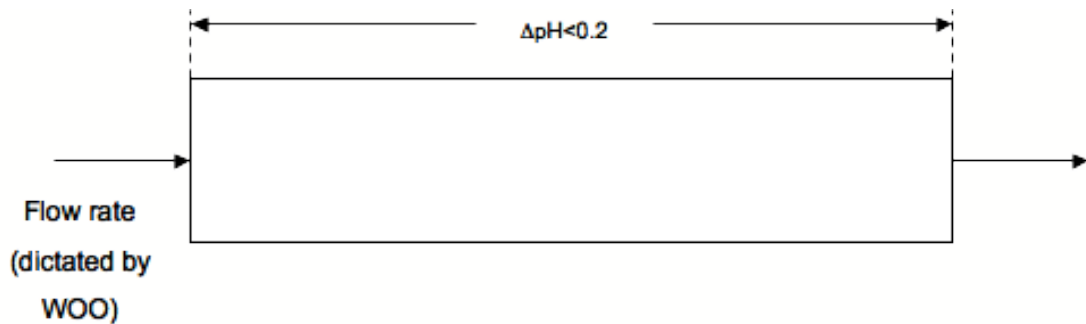


Figure 5.2 Single pass pH change across the alginate scaffold containing mesenchymal stem cells (MSC).

The minimum single pass flow rate through the bioreactor can be determined by relating the lactate production rate of the cells to the amount of lactate required to cause a pH change that falls outside of the acceptable range. i.e. <7.2 and determining the amount of time such a change would occur in. This relationship is shown in equation 5.13. This time can then be related to flow rate using equation 5.14.

$$\frac{\text{concentration_of_lactate_to_cause_pH} < 7.2}{\text{rate_of_concentration_change_from_cells}} = \tau \quad (5.13)$$

$$\tau = \frac{V_R}{v_t} \quad (5.14)$$

(τ is residence time (s), V_R is reactor volume (ml) and v_t is the flow rate within the recycle loop (ml.s⁻¹))

The size of the single pass window of operation relating pH to the recycle rate is dependent upon both the cell type and the number of cells present. As the number of cells increase during arterial growth and development the required flow rate will increase. This required flow rate can be determined from equation 5.15, formed by combining equations 5.13 and 5.14 and this equation can be used to relate cell number to recycle rate as shown in Fig. 5.3 on a logarithmic plot.

$$\frac{V_R * n * LPR}{\text{concentration_of_lactate_causing_pH} < 7.2} = v_t \quad (5.15)$$

(V_R = reactor volume (ml), n = cell number,

LPR=lactate production rate (mmol.cell⁻¹s⁻¹))

Equation 5.15 can be used to relate cell number to the minimum recycle rate as shown in Fig. 5.3. The minimum required recycle flow rates are less than 0.1ml.min⁻¹ for all cell concentrations below the target required for a tissue engineered blood vessel (1.16*10⁸ cells.ml⁻¹) as discussed in chapter 3. These minimum flow rates can be readily achieved in conjunction with the window of operation derived in chapter 3 for the control of dissolved oxygen tension (DOT). This DOT window permitted recycle rates of between 0.1 and 9.33 ml.min⁻¹. This range will ensure pH remains within an acceptable range.

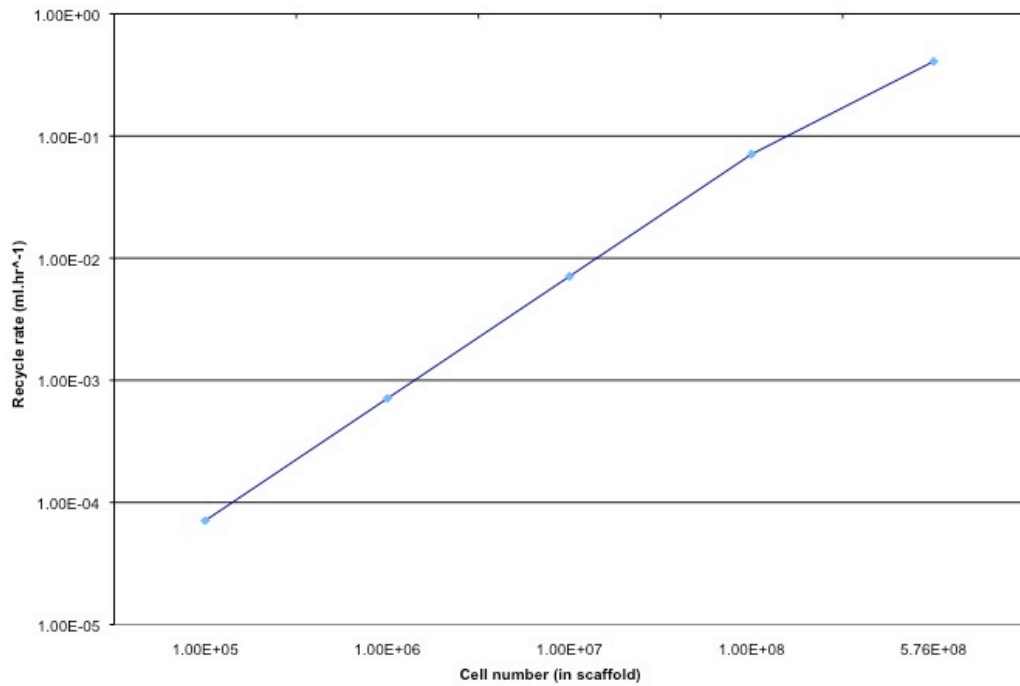


Figure 5.3 Logarithmic plot of mesenchymal stem cell number present in scaffold and minimum recycle rate flow rate required to ensure pH change across the bioreactor falls within an acceptable range

5.6 Continuous pH window of operation

The second controlled flow rate within the VTEB is that responsible for the fresh feed of media into the recycle loop. The relationship between the two windows within the system is shown in Fig. 5.4.

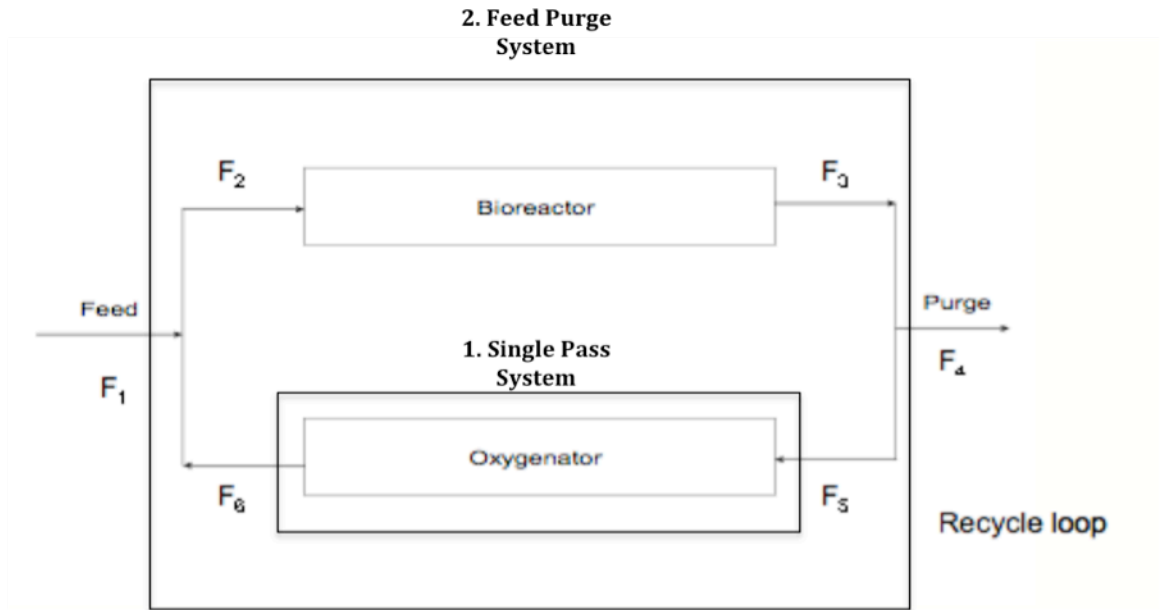


Figure 5.4 Controlled flow rates within the VTEB System

The concentration of lactate within the feed to the system can be considered to be 0. For the purposes of calculating the window the concentration within the exit stream must be large enough to ensure the pH remains above 7.2. Such a concentration has already been determined as 1.13mM of lactate. Knowing this value a conventional mass balance (equation 5.16) may be used to create a window of operation relating cell number to fresh feed flow rate.

$$x_1 F_1 - x_4 F_4 + LPR * n = 0 \quad (5.16)$$

(x_1 = inlet concentration of lactate, F_1 = fresh feed rate of cell culture medium, x_4 = outlet concentration of lactate, LPR = lactate production rate per cell, n = cell number)

It can be assumed that the concentration of lactate within the fresh feed is zero, hence equation 5.16 becomes equation 5.17.

$$LPR * n = x_4 F_4 \quad (5.17)$$

Using equation 5.17, it is possible to develop a window of operation for MSCs relating fresh feed flow rate to cell number. Plotting equation 5.18 allows the formation of such a window as shown in Fig. 5.6

$$\frac{2.79 * 10^{-13} * n}{1.13 * 10^{-3}} = F_2 \quad (5.18)$$

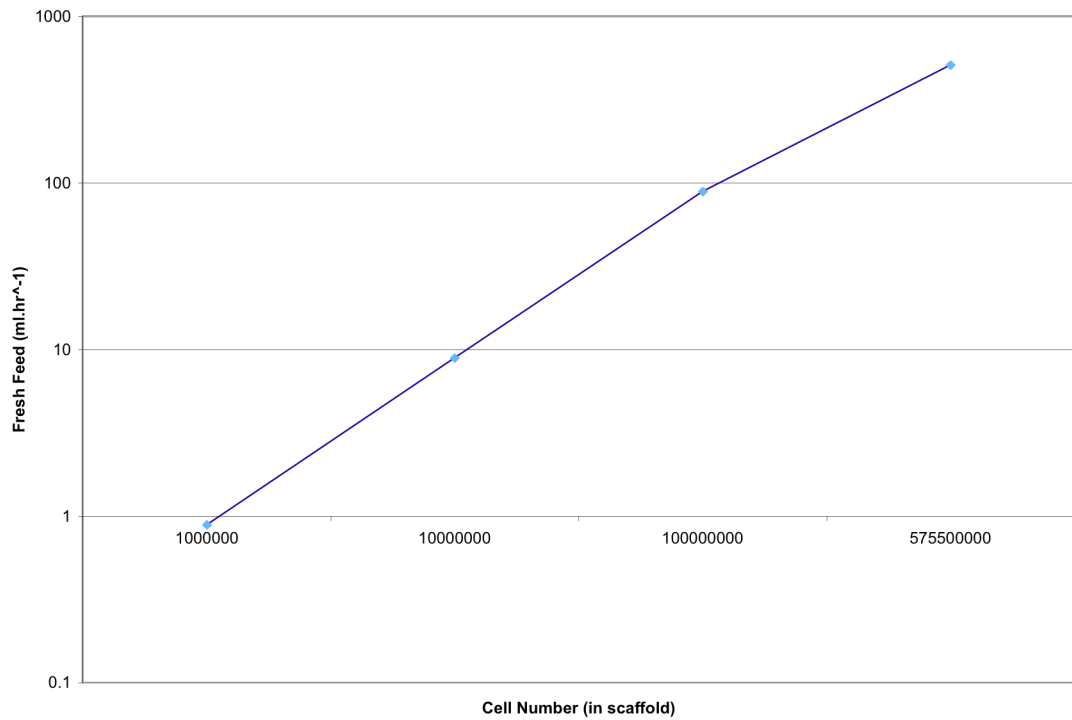


Figure 5.6 Continuous window of operation for pH for mesenchymal stem cells.

5.6 Conclusions

The purpose of this chapter was to determine if the pH of the cell culture medium should play a role within any control strategy employed to maintain metabolite and dissolved oxygen concentration within the bulk flow of a perfusion vascular tissue engineering bioreactor (VTEB).

Equations have been derived in this chapter that allow the creation of two windows of operation. The first of these windows relates the flow rate of the recycle stream and cell number to pH. The second of these windows relates the flow rate of the fresh feed stream and cell number to pH. It has been demonstrated no account need be taken of the effect changes in the flow rate of the recycle stream will have on pH even at maximum cell number. However, changes in fresh feed flow rate have been shown to have an impact on pH within the system. Ultimately, the overall control strategy will need to take account of pH when using the fresh feed flow rate as a control variable.

A further point is that these equations have not taken account of ammonia production and the effect this may have in balancing the pH. In addition to the production rate of ammonia being low in comparison to that of lactate, these equations were derived to indicate the most extreme example of pH changes that could arise within the system. Such an assumption does of course provide a future opportunity for further optimisation of any final control system.

Chapter 6 Process Control of Respiratory Substrates

The aim of this chapter is to investigate how to control the inlet flow rate to achieve various requirements on two key substrates: glucose and glutamine; and on two key waste products lactate and ammonia. Feasible flow rates will be defined based on components' mass balance in the system.

6.1 Glucose

As stated previously respiration is predominantly based around the reaction of glucose with oxygen (6.1), as such its concentration in cell culture media is highly relevant to respiration rate.



i.e.

oxygen + glucose \rightarrow carbon dioxide + water

The fresh media used to culture mesenchymal stem cells contains 6 mmol.L⁻¹ and a maximum acceptable drop of 2 mmol.L⁻¹ to give a concentration of 4 mmol.L⁻¹ has been chosen as a reasonable range. The flow rates required to achieve this will vary depending upon the cell number present in the alginate scaffold. (Markusen, 2005) provides a value of $1.46 \pm 0.92 \times 10^{-10}$ g.cell⁻¹.h⁻¹ (2.25×10^{-13} mmol.cell⁻¹s⁻¹) for the glucose consumption rate of mesenchymal stem cells (MSCs). Using this value a series of equations may be formed that can be used to derive the flow limits required to ensure glucose stays in the range $4 \times 10^{-2} - 6 \times 10^{-2}$ mmol.ml⁻¹. A mass balance across the system gives equation 6.2.

$$F_1 x_1 \Delta t - F_4 x_4 \Delta t - UTR * N \Delta t = 0 \quad (6.2)$$

Where cell number is calculated by;

$$N = n * V_S \quad (6.3)$$

Where F_1 is inlet flow rate (ml.h^{-1}), F_4 is outlet flow rate (ml.h^{-1}), x_1 is medium glucose concentration (mmol.ml^{-1}), x_4 is exit glucose concentration (mmol.ml^{-1}), N is total cell number, n is cell concentration (cell.ml^{-1}), V_S is volume of alginate scaffold, UTR is glucose uptake/consumption rate ($\text{mmol.cell}^{-1}.\text{s}^{-1}$).

The volume of the bioreactor is $1.151 \times 10^{-6} \text{ m}^3$ given by equation 6.4.

$$V_S = \pi(R_2^2 - R_1^2)L \quad (6.4)$$

Where R_2 is the external radius of the alginate scaffold and R_1 is the internal radius of the alginate scaffold

$$V_S = \pi((2 * 10^{-3} \text{ m})^2 - (1.7 * 10^{-3} \text{ m})^2) * 0.33 \text{ m} = 1.151 * 10^{-6} \text{ m}^3 \quad (6.5)$$

Implementing the condition that the concentration within the purge stream cannot be less than $4 \times 10^{-2} \text{ mmol.ml}^{-1}$ gives equation 6.6 which may be rearranged as shown in equations 6.7 and 6.8 to form 6.9.

$$x_2 = \frac{F x_1 - UTR * N}{F} \geq x_{\min} \geq 4 * 10^{-2} \text{ mM ml}^{-1} \quad (6.6)$$

$$F x_1 - UTR * N \geq x_{\min} F \quad (6.7)$$

$$F(x_1 - x_{\min}) \geq UTR * N \quad (6.8)$$

$$F \geq \frac{UTR * N}{x_1 - x_{\min}} \quad (6.9)$$

Where x_1 is $6 \cdot 10^{-2} \text{ mmol.ml}^{-1}$, x_{\min} is $4 \cdot 10^{-2} \text{ mmol.ml}^{-1}$, UTR is $2.25 \cdot 10^{-13} \text{ mmol.cell}^{-1} \text{ s}^{-1}$, n is $10^6 - 10^8$ and V_S is 1.15 ml

Equation 6.9 may be used to determine a window of operation for glucose that ensures that glucose concentration within the bulk flow remains within $0.04 - 0.06 \text{ mmol.ml}^{-1}$. This window is shown in Fig. 6.1 and the flow rate must be equal or above the plotted line to achieve the appropriate glucose concentration.

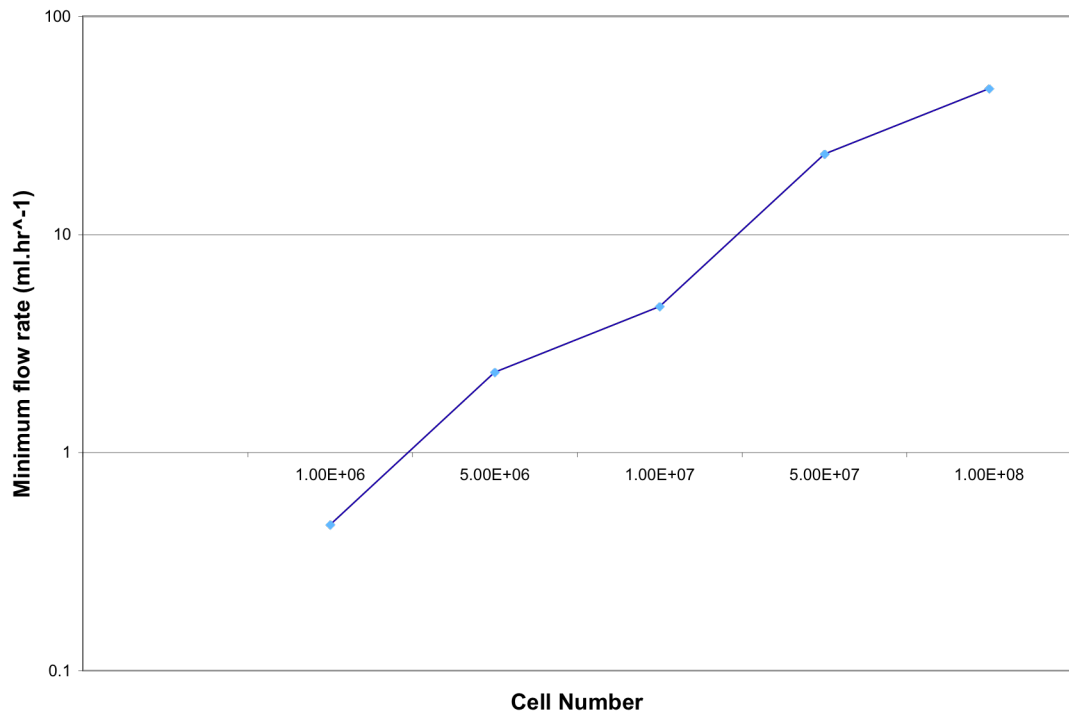


Figure 6.1 Window of operation for glucose concentration 4-6mmol.L⁻¹

The minimum flow rate required is directly proportional to the cell number within the alginate scaffold. This log graph demonstrates the possible feed flow rates for a given cell number. Control action must take place at a value equal to or exceeding the curve.

The required flow rates to maintain glucose within the range $4-6 \text{ mmol.L}^{-1}$ range from 0.5 to 47 ml.h^{-1} depending upon cell number, thus as the graft develops, the required feed rate of media will need to increase to maintain glucose concentration within acceptable limits.

6.2 Lactate

Lactic acid is the primary product arising from the breakdown of glucose. Normal blood lactate concentrations fall in the range 1-3mM providing an appropriate range for the window of operation. Zeng et al (1998) provided a conversion ratio of 1: 2 for glucose to lactate meaning that one mole of glucose consumed gives rise to 2 mole of lactate. This information allows an estimate of the lactate production rate to be made giving a value of $2 \times UTR = 4.56 \text{ mmol.cell}^{-1}\text{s}^{-1}$. The lactate concentration in the fresh feed and the system at time zero is assumed to be 0 mmol.ml^{-1} and will increase and change over time. The lactate concentration over time must be determined and the appropriate flow rate selected to keep the concentration less than 3 mmol.ml^{-1} .

Based on the mass balance across the system for a given Δt

$$x_1 F_1 \Delta t - x_4 F_4 \Delta t + k_L N \Delta t = 0 \quad (6.10)$$

Where it is known that feed rate is equal to purge rate and assumed that lactate concentration in the feed is 0. F_1 is the fresh feed flow rate, F_4 is the purge stream flow rate, x_1 is the concentration of lactate in the feed stream, x_4 is the concentration of lactate in the purge stream, k_L is the production rate of lactate ($\text{mmol.cell}^{-1}.\text{s}^{-1}$),

$$x_4 F = k_L N \quad (6.11)$$

Where $F = F_1 = F_4$

$$x_4 = \frac{k_L N}{F} \leq 3 \quad (6.12)$$

$$F \geq \frac{k_L N}{3} = \frac{2}{3} (-UTR) N \quad (6.13)$$

Using equation 6.13 the flow rates required to ensure a lactate concentration equal to or below $3 \times 10^{-2} \text{ mmol.L}^{-1}$ can be determined. The production rate of lactate, which varies with cell concentration provides figure 6.2, a window of operation for lactate.

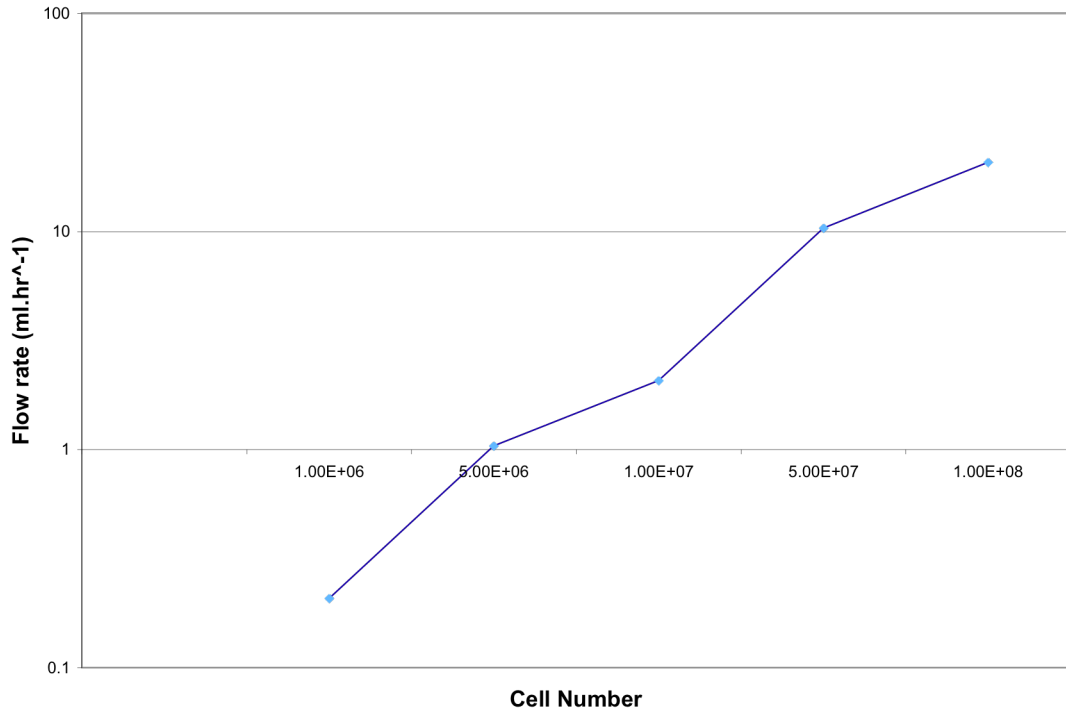


Figure 6.2 Window of operation for lactate concentration 0-3mmol.L⁻¹

The minimum feed flow rate required is directly proportional to the cell number within the alginate scaffold. This log graph demonstrates the possible feed flow rates for a given cell number. Control action must take place at a value equal to or exceeding the curve.

The required flow rates to ensure lactate concentration does not exceed 3mM are lower (0.21 ml.h^{-1} to 20.7 ml.h^{-1}) than those required to maintain glucose concentration (0.5 to 47 ml.h^{-1}). This indicates that it is likely that lactate will not need to be considered in the overall model. For a given cell number the flow rate required to maintain glucose concentration will always be higher than that required to maintain lactate concentration.

6.3 Glutamine

Cell culture medium typically contains glutamine; a major energy and nitrogen source for mammalian cells in culture (Thilly, 1986, Ozturk and Palsson, 1990).

Of the four chemicals under consideration (glutamine, glucose, lactate and ammonia), glutamine is arguably the most interesting as unlike the others, it is not thermally stable in cell culture medium (Glacken, 1986, Ozturk and Palsson, 1990). This thermal instability means that unlike glucose, even in the absence of significant cellular growth glutamine concentration will fall considerably over time. The difference between actual glutamine uptake rate (including thermal degradation) and apparent glutamine uptake rate can be up to 200% (Ozturk and Palsson, 1990).

This instability is linked to temperature and is the major justification for storing cell culture medium within a refrigerated environment and for providing it with a finite shelf life.

This thermal instability is of concern as the design of the Vascular Tissue Engineering Bioreactor (VTEB) as the circulating media is kept at a controlled temperature of 37°C. This fact alone ensures that degradation kinetics form a key variable in any system being designed to control metabolic concentrations. Ozturk and Palsson (1990) demonstrated that a number of factors influenced such breakdown kinetics *in-vitro* and included temperature, media type, presence of foetal bovine serum (FBS) (although not in Dulbecco's Modified Eagle Medium; DMEM).

The relevance of media type relates to the presence of phosphate ions and bovine serum contains enzymes such as glutimases. Unsurprisingly as glutamine is an amino acid the pH the cell culture is stored at will also play a role in its breakdown.

Ozturk and Palsson (1990) using curve fitting stated the relationship between the degradation constant of glutamine and pH (see equation 6.14).

$$\ln k_G = a + b * pH \quad (6.14)$$

Where k_G is the coefficient of degradation (s^{-1}), b is the specified constant, a is the specified constant)

Based upon DMEM maintained at 37°C the degradation constant is equivalent to; $k_G = 6.03 * 10^{-7} s^{-1}$.

To determine the change of glutamine concentration, the thermal degradation must be combined with the consumption of glutamine by the cells present as part of a mass balance around the system. Zeng et al (1998) showed that the ratio of glutamine consumption to glucose consumption falls between 0.2 and 0.5 $mol.mol^{-1}$.

Based on the mass balance for a given Δt ,

$$F_1 x_1 \Delta t - F_4 x_4 \Delta t - UTR * GGR * N \Delta t - k_G x_4 V_s \Delta t = 0 \quad (6.15)$$

Where F_1 is the fresh feed rate, F_4 is the purge rate, UTR is the glucose uptake rate, GGR is the ratio of glucose uptake to glutamine uptake, N is the cell number in the scaffold, k_G is the degradation coefficient for glutamine, x_1 is the fresh feed concentration of glutamine, x_4 is the purge stream concentration of glutamine, V is the volume of the entire system and t is time

As feed rate is equal to purge rate ($F_1 = F_4 = F$) this equation may be simplified to;

$$(F + k_G v_s) x_4 = F x_1 - UTR * GGR * N \quad (6.16)$$

$$x_4 = \frac{F x_1 - UTR * GGR * N}{F + k_G v_s} \geq x_{\min} \quad (6.17)$$

$$F x_1 - UTR * GGR * N \geq F x_{\min} + k_G v_s x_{\min} \quad (6.18)$$

$$F(x_1 - x_{\min}) \geq UTR * GGR * N + k_G v_s x_{\min} \quad (6.19)$$

$$F \geq \frac{UTR * GGR * N + k_G v_s x_{\min}}{x_1 - x_{\min}} \quad (6.20)$$

Equation 6.20 can be used to plot flow rate ranges that may be implemented to ensure glutamine concentration remains between a chosen range of 3mmol.L^{-1} and 4mmol.L^{-1} for all ratios of glucose conversion to glutamine conversion. This window is shown in Fig. 6.3.

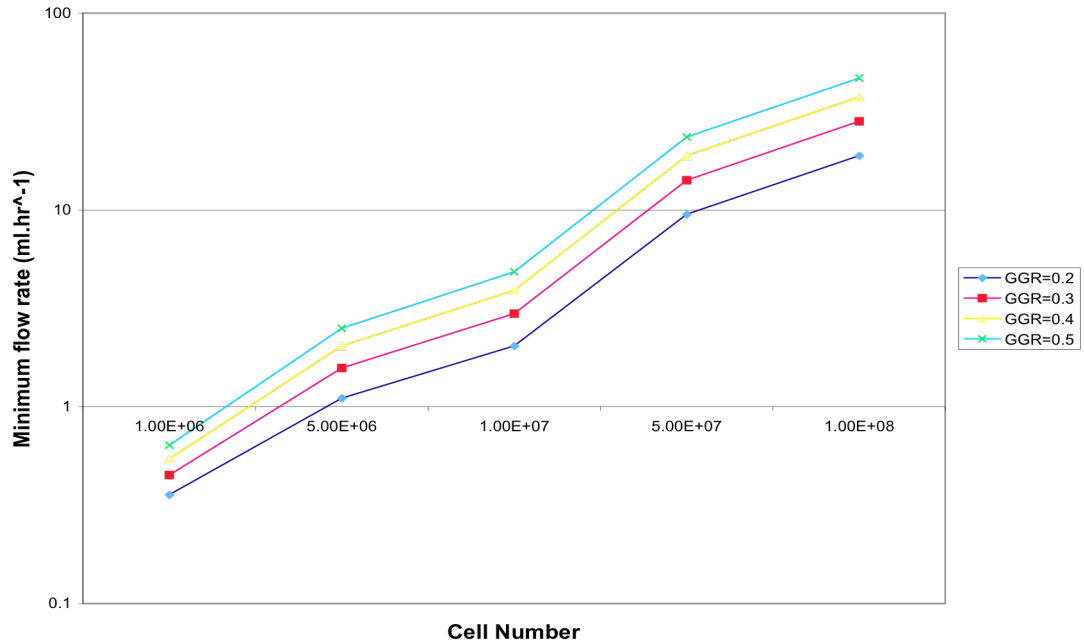


Figure 6.3 Window of operation for glutamine concentration 3-4mmol.L⁻¹

The minimum feed flow rate required is directly proportional to the cell number within the alginate scaffold. This log graph demonstrates the possible feed flow rates for a given cell number and for a range of theoretical ratios of glucose uptake to glutamine uptake. Control action must take place at a value equal to or exceeding the curve.

These results indicate that except at low cell densities the required flow rates do not exceed those required to maintain glucose. This indicates that with the exception of when the cell number is low, provided glucose is controlled, glutamine will also remain within specification.

6.4 Ammonia

The main product of glutamine breakdown is ammonia (the other being pyrrolidone carboxylic acid). The presence of ammonia can inhibit cell growth and cause cell death or morphological changes due to toxicity. Mirabel et al, 1987 showed that 72 hours culture in ammonia concentrations of 6 mmol.L⁻¹ reduced cell numbers

significantly when compared with control populations. For the purposes of this study a value of 6mM was used as a control set point.

Zeng et al (1998) provided a conversion rate for ammonia to glutamine of 0.8, using this value and the 6 mmol.L⁻¹ limit for ammonia production allows the formation of a window of operation in a similar fashion to the other metabolites. A mass balance (6.21) over the system allows derivation of equations (6.22 – 6.27) that may be used to create such a window (Figure 6.4).

Based upon the mass balance for a given Δt

$$x_1 F \Delta t - x_4 F \Delta t + k_a N \Delta t = 0 \quad (6.21)$$

The feed concentration of ammonia is assumed to be 0

$$x_1 = 0 \quad (6.22)$$

Zeng et al, 1998 provided a coefficient of ammonia production to glutamine conversion of 0.8.

$$k_a = UTR * AGR \quad (6.23)$$

This can thus be related to glucose consumption rate

$$AGR = GGR * 0.8 \quad (6.24)$$

and substituted into the mass balance, which may be rearranged.

$$x_4 F + UTR * GGR * 0.8 * N = 0 \quad (6.25)$$

$$x_4 = \frac{UTR * GGR * 0.8 * N}{F} \quad (6.26)$$

$$F \geq \frac{0.8 * UTR * GGR * N}{x_{\min}} \quad (6.27)$$

As a range of values exists for possible consumption rates of glutamine and ammonia is a product of its breakdown a number of possible values also exist for the production rate of ammonia.

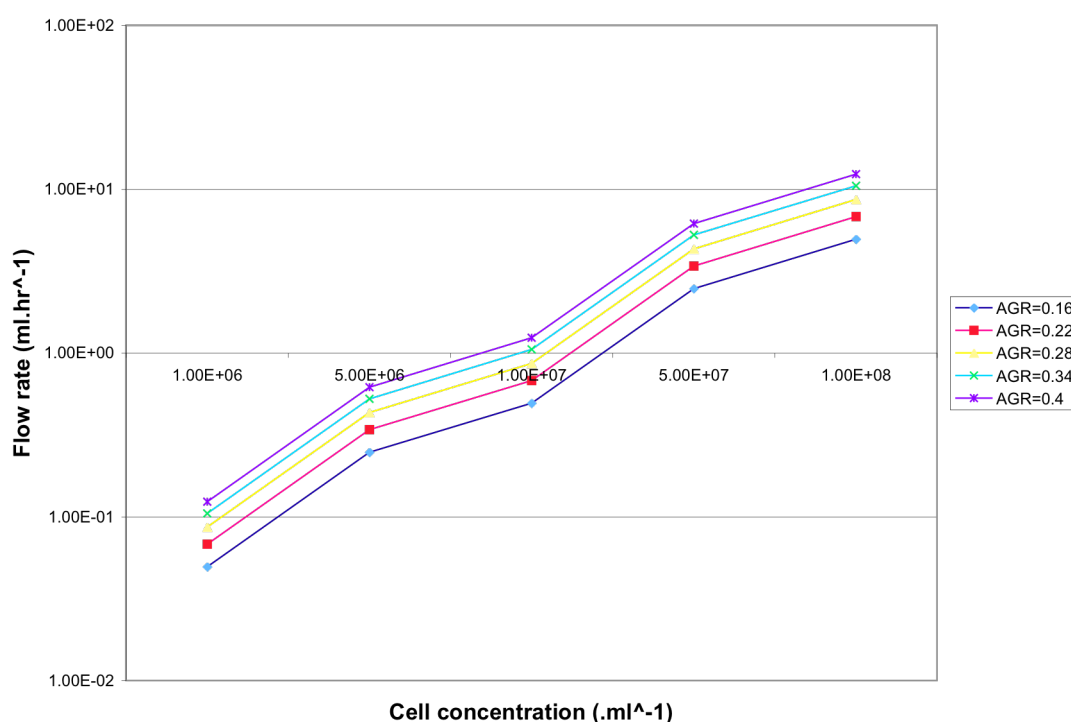


Figure 6.4 Window of operation for ammonia concentration 0-6mmol.L⁻¹

The minimum feed flow rate required is directly proportional to the cell number within the alginate scaffold. This log graph demonstrates the possible feed flow rates for a given cell number for a range of glutamine to ammonia conversion ratios. Control action must take place at a value equal to or exceeding the curve.

The minimum flow rates required to ensure the ammonia concentration is between 0 and 6mmol.L⁻¹ are much lower than for any of the three other considered metabolites. It can be said with reasonable certainty that ammonia can be neglected in terms of the eventual overall control strategy, as other metabolites will have to be very far out of specification before ammonia exceeds 6mmol.L⁻¹ in concentration.

6.5 Combination of metabolic windows of operation

Combining figures 6.1-6.4 provides an overall metabolic window of operation taking into account glutamine, glucose, lactate and ammonia concentrations within the bulk flow. This window shown in Fig. 6.5 show that the waste products lactate and ammonia may be ignored as the flow rates required to ensure they remain within acceptable concentration limits are much lower than those required to maintain glucose and glutamine.

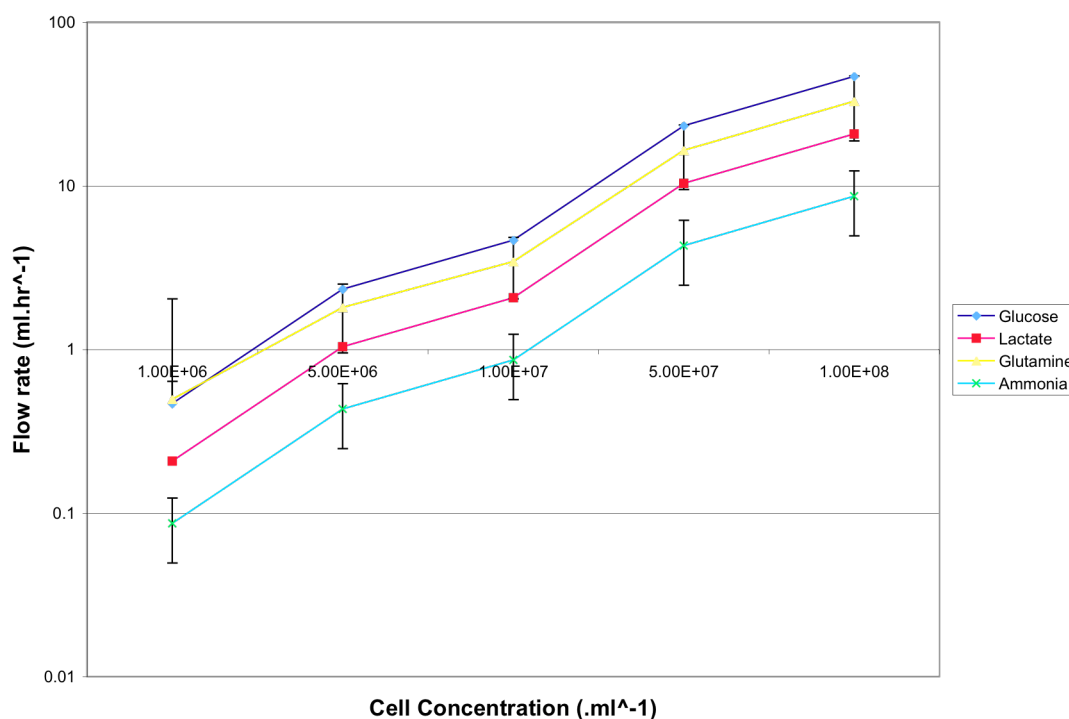


Figure 6.5 Overall metabolic window of operation

Combination of windows of operation for the two substrates, glucose and glutamine, and the two metabolic waste products, ammonia and lactate demonstrates that where glucose is controlled the other three will also be controlled indirectly with the exception of low cell numbers where glutamine control will be dominated. The error bars shown indicate the range of ammonia and glutamine based upon the ranges indicated in figures 6.3 and 6.4.

The flow rate window of operation is dictated by glucose or glutamine concentration which itself depends upon cell number as at low concentrations within the scaffold

thermal degradation rate of glutamine becomes significant when compared with the consumption rate by the mesenchymal stem cells. Figure 6.6 demonstrates that this cross over takes place at a very low cell concentration not much higher than that at the time of seeding, where the GGR is taken to be 0.35 (the middle of the suggested range, Zeng et al (1998), below this cell concentration glutamine dominates and above this glucose concentration dominates. For this reason it can be assumed that only glucose requires to be controlled to maintain the concentrations of the two substrates: glucose and glutamine and the two metabolites: lactate and ammonia. For any minimum flow rate to maintain glucose, lactate and ammonia concentrations will be below specified limits.

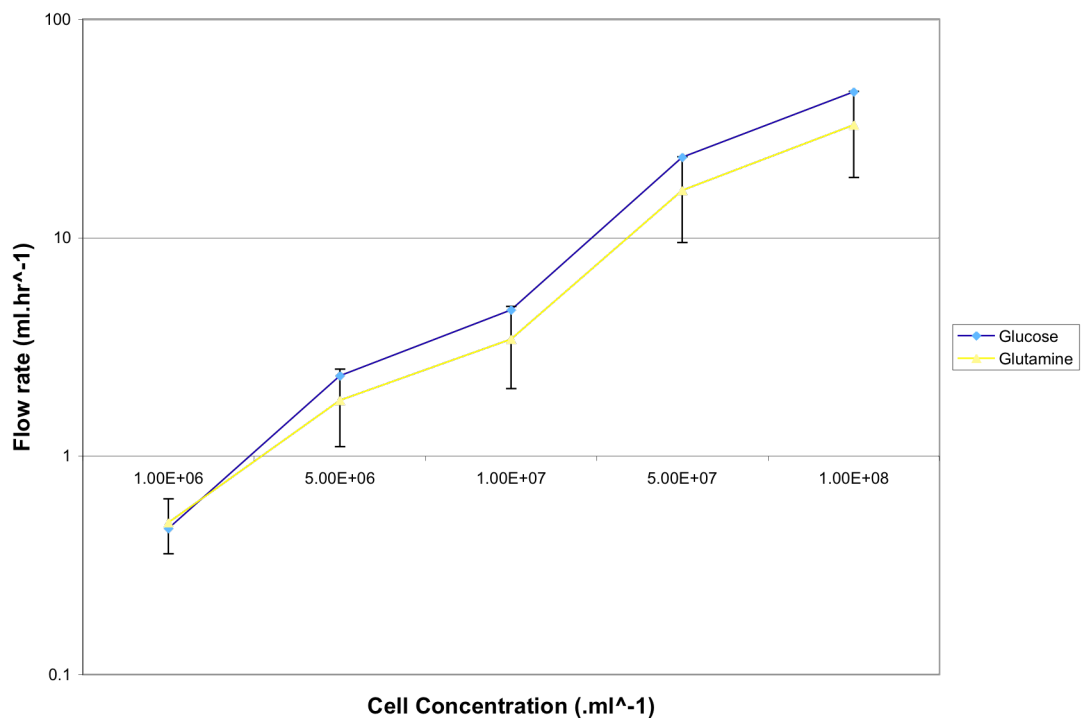


Figure 6.6 Glutamine vs. Glucose domination on window of operation

The importance of considering glutamine control and glucose control only applies at low cell concentrations. When the average ratio of glucose uptake to glutamine uptake is assumed, glutamine control is not of concern. Thus, in this work glutamine control is neglected.

6.6 Process control

Using the windows of operation process control loops can be set up to control the metabolite concentrations within the bulk flow. It has already been determined that if glucose is controlled, glutamine, lactate and ammonia concentrations may be neglected and assumed to be controlled within specifications. The oxygen was considered to be controlled effectively at 0.079mmol.L^{-1} and not vary on entry to the bioreactor.

Work on developing a controller to maintain the oxygen concentration in solution has demonstrated that two-step controllers are inappropriate for use within this system as due to the delays inherent in the system the response is too slow to prevent large oscillations. For this reason proportional integral (PI) control was tested from the outset. Indications were that irrespective of the value assigned to the gain, control of this nature was quite unstable.

The solution was to use a gain that was proportional to the cell number estimated by the oxygen uptake rate as stated in the previous section and thus varied in time. Gains above 2.9 were unstable so the gain was specified as 2.9 divided by the maximum cell number to give a gain value of $2.519 \times 10^{-8} X$ where X is the estimated cell number based upon oxygen consumption rates (outlined in Chapter 3). By dividing the maximum stable gain by the maximum cell number, the risk of instability was minimised, as the overall gain cannot exceed 2.9. Integral control was estimated at $0.1 \times \text{Proportional gain}$. As with the model of oxygen control in Chapter 4, a model of control of substrate concentrations was created in Simulink. This model is outlined in

Appendix 2. The results of the controller within the model are shown in Fig. 6.7 and 6.8. Fig. 6.7 shows that this proportional integral controller leads to good maintenance of the glucose concentration. However, there is considerable offset. The associated fresh feed rate responsible for controlling this DOT is shown in Fig. 6.8 and has a sigmoidal shape. This is expected as the gain varies in a sigmoidal shape due to its relation to the estimated cell number. The offset indicates that further tuning of the controller is required. Final results were obtained for a controller with a proportional gain of 1×10^{-3} and an integral time of 1×10^{-5} (see Fig. 6.9 and 6.10). Although the response of the system still has offset, increasing the gain further results in instability of the type characterised in Fig. 6.11.

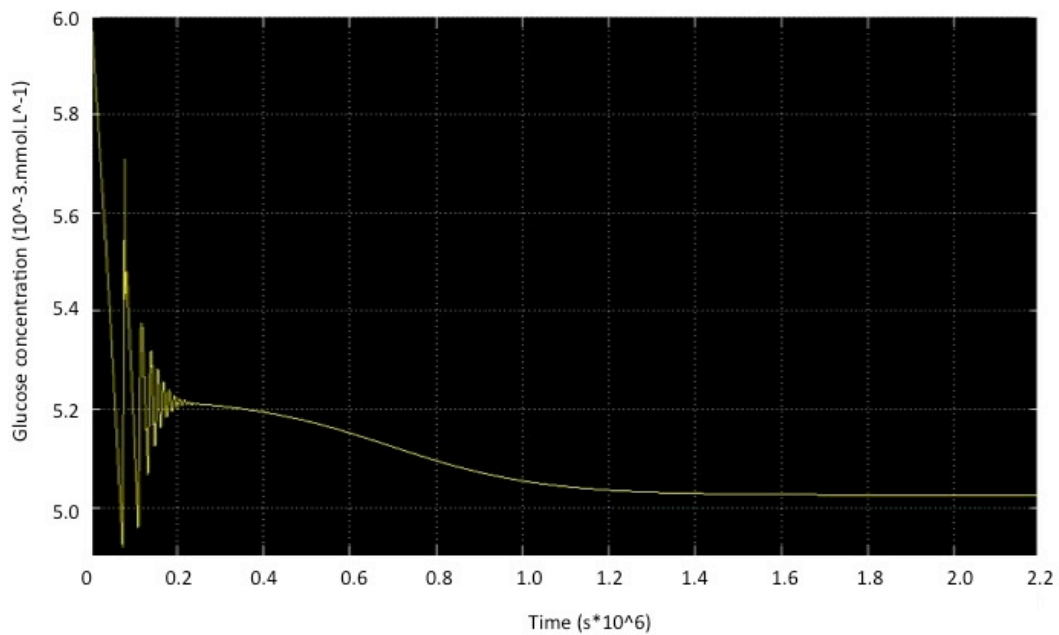


Figure 6.7 Glucose control achieved with untuned PI controller

Proportional constant ' P ' = $2.9 \times 10^{-8} \cdot X$, where X is cell concentration, and Integral time ' I ' estimated using $I = 0.1 \cdot P$. Control is achieved however there is considerable offset from the desired set point of 5.5 mmol.L^{-1} . This indicates tuning is required.

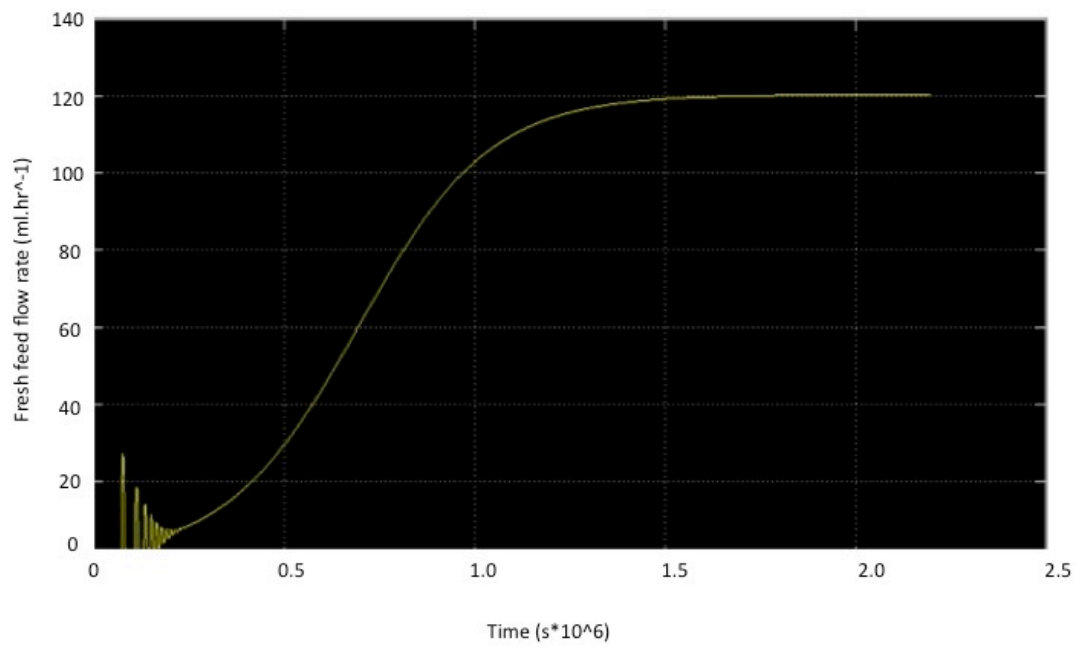


Figure 6.8 Feed flow rate control associated with figure 6.7

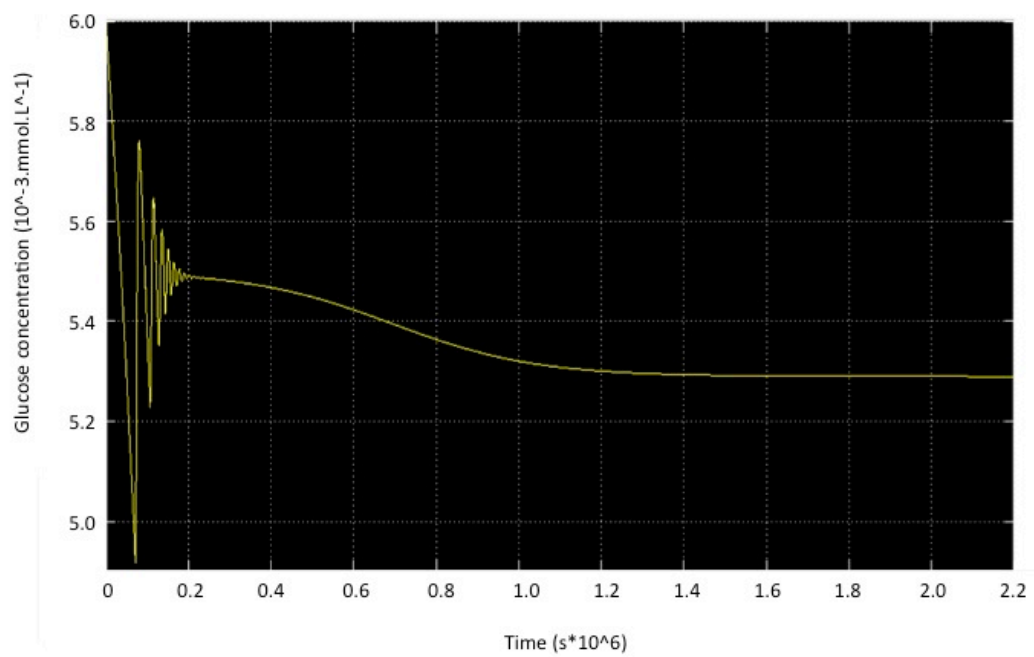


Figure 6.9 Glucose concentration achieved by tuned proportional integral feed rate controller
Proportional gain of $1 \cdot 10^{-3} \cdot X$, where X is cell number, and Integral time of $1 \cdot 10^{-5}$ achieve the optimal control possible using this system.

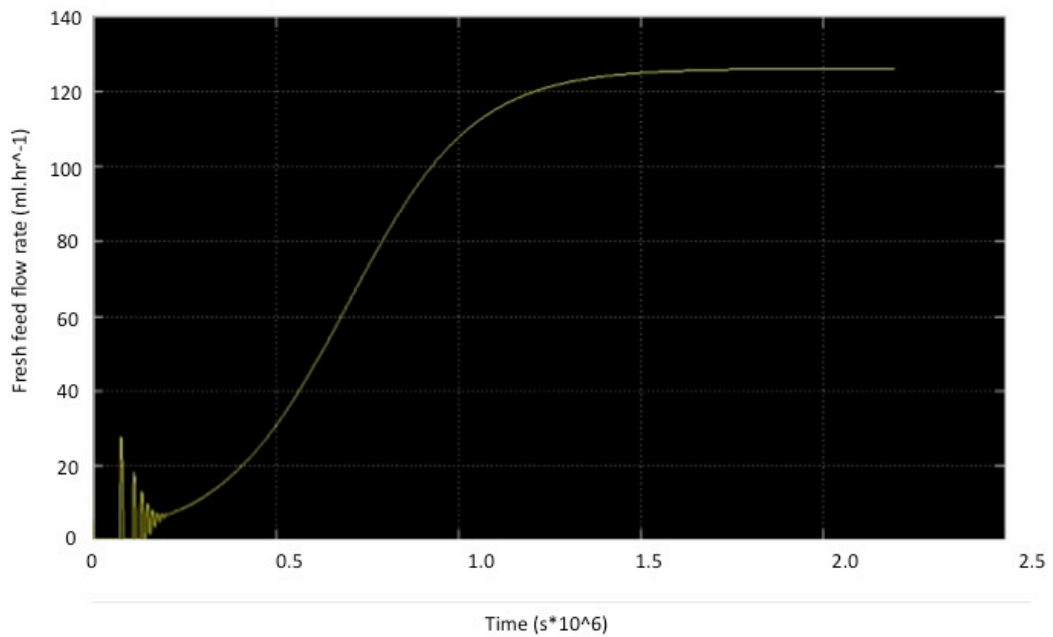


Figure 6.10 Proportional integral feed rate controller action associated with the glucose concentration in figure 6.9. Proportional gain of $1 \cdot 10^{-3} \cdot X$, where X is cell number, and Integral time of $1 \cdot 10^{-5}$ achieve the optimal control possible using this system. The control response is S shaped due to the association with cell number

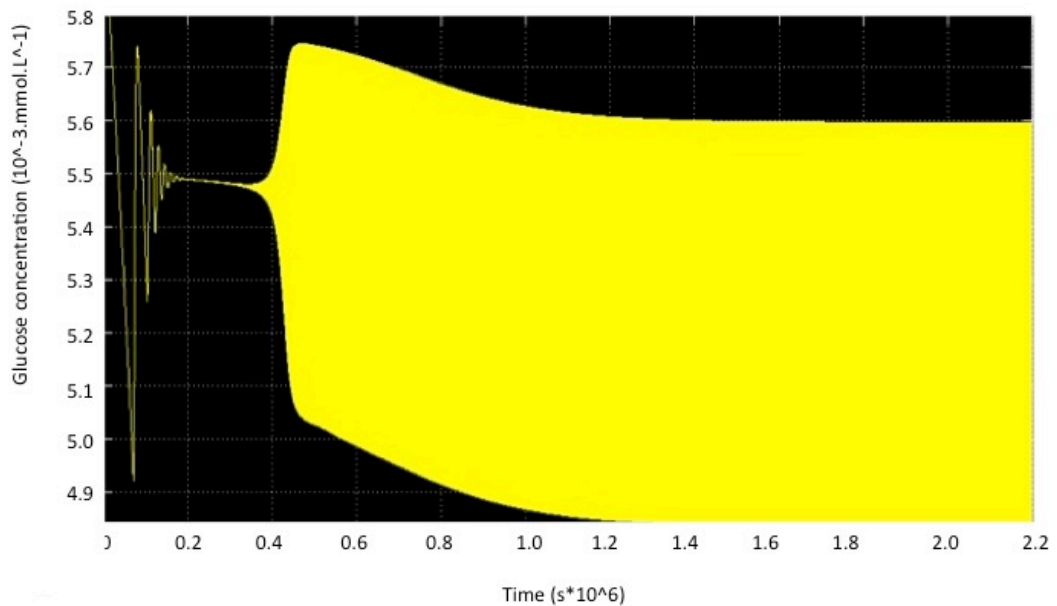


Figure 6.11 Instability of glucose concentration due to excessive gain of feed rate controller. Increasing the gain further than in figure 6.10 does not result in improved control, rather it introduces instability into the system

The strength of this control system at maintaining concentration well within the specified boundaries, despite the offset means that attempts to improve this controller further will not be made. The next stage in the process will be integrating this proportional controller with the Proportional Integral (PI) controller developed in Chapter 4 to maintain dissolved oxygen tension.

6.7 Conclusions

The work contained within this chapter has demonstrated that of the four key metabolites under consideration, merely controlling one (glucose) with the specified boundaries will ensure the other three (lactate, ammonia and glutamine) remain within specifications. The only exception to this relationship is at low concentrations close to the seeding number $10^6 \text{ cell.ml}^{-1}$ where glutamine dominates, rather than glucose. Given that this only takes place at the outset of the graft development this has been neglected. A control model has thus, been created for glucose based on measurement of glucose in the exit concentration of the purge stream being compared to a set point and the resulting error being processed by a proportional integral (PI) controller.

After early difficulties with the stability of the controller, a solution was found that linked an estimated cell number to the gain which changed in time rather than being constant. The results of this controller although showing a small offset as is characteristic of a proportional controller have sufficient stability that no further improvement is needed prior to its unification with the oxygen control model.

Chapter 7 Overall Process Control

In this chapter a possible technique for integrating the previously developed control systems for the dissolved concentrations of three key substrates and two metabolites in the process of creating a tissue engineered artery; glucose, glutamine, oxygen, lactate and ammonium is presented. Appropriate modifications to inlet conditions are performed and an overall strategy is implemented that will maintain the ranges of all five compounds within physiological boundaries.

7.1 Introduction

In Chapter 4, a control strategy using the flow rate of culture medium within the recycle loop was demonstrated that would maintain dissolved oxygen tension within the physiological range of mesenchymal stem cells. This control system made no consideration of any other parameters within the system with the exception that temperature remained constant at the physiological 37°C. All feed substrates and metabolites were considered to be in excess and the feed flow rate was maintained as a constant. In Chapter 6 a similar approach was taken and the concentration of two key substrates and two metabolites was considered, feed components glucose and glutamine and their respective waste products lactate and ammonia. For this control system the oxygen concentration was assumed to be controlled at 0.079mmol.L⁻¹. Although the model was not constructed independently of oxygen dependence it took no account of the effect a variation in oxygen concentration would have on metabolite consumption or production. To determine whether the environmental conditions of the vascular tissue engineering bioreactor (VTEB) in its current incarnation may be effectively controlled these two separate and distinct systems must be combined and

integrated to determine if further strategy modifications are necessary. An additional window was constructed for pH. The minimum flow rates required by the pH window (Chapter 5) are much lower than those required to keep the concentrations of glucose and glutamine within specification and can thus be neglected.

7.2 Comparing windows of operation

A window of operation has been derived for the fresh-feed and recycle streams' flow rates so as to maintain a DOT of 0.079mmol.L^{-1} (see Fig 4.9) at the exit of the bioreactor. The fresh feed rates are low due to the absence of oxygen within the culture medium; higher flow rates would result in the oxygen concentration falling below 0.079mmol.L^{-1} .

Separately Fig. 6.5 provides the lower limit of a window of operation representing the minimum permissible feed flow rate for the four feed metabolites against cell number for each of the four chemicals.

It is clear from examining these two figures that the two separate control systems, developed independently, for oxygen and feed substrates cannot be integrated. The fresh feed rates required to maintain the feed substrate concentrations are far in excess of the maximum permissible flow rates that will maintain the DOT without violating the limits placed upon the recycle loop flow rate by the windows of operation derived in Chapter 4. The conclusion must be that the current operating conditions require that a decision be made whether either the concentration of oxygen or the feed substrates

are controlled within the physiological limits. It is not possible to maintain conditions within all specified tolerances hence the operating conditions must be modified.

7.3 Modification of operating conditions

A number of opportunities for modifying the operating conditions exist including increasing the limit upon the recycle flow rate, increasing the concentration of the substrates within the feed and increasing the dissolved oxygen concentration within the feed.

Increasing the permitted range of the recycle rate and thus expanding the window of operation is not possible, as stated in Chapter 4 higher shear rates have been shown to lead to the formation of osteoblasts, progenitors of bone cells (Portner et al, 2005). Formation of such cells would render any tissue-engineered graft useless and thus cannot be allowed.

Increasing the concentration of the glucose and glutamine within the feed is a potential solution, as lower fresh feed rates would then be required to maintain specified tolerances for these substrates. By increasing feed concentration of glucose from 6mmol.L^{-1} to 12mmol.L^{-1} and glutamine from 4mmol.L^{-1} to 8mmol.L^{-1} (assuming a ratio of glutamine uptake to glucose uptake of 1:0.35 moles) the required feed rate drops dramatically (see Fig. 7.1).

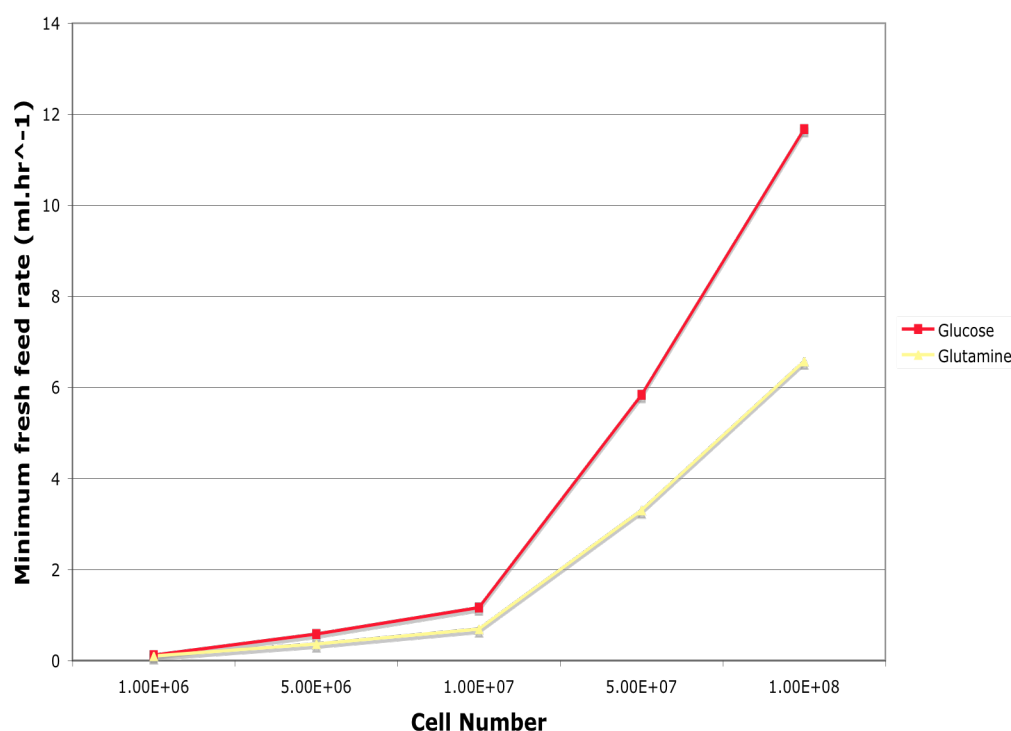


Figure 7.1 Minimum fresh feed rates required to maintain glucose and glutamine concentrations for feed composed of 12mmol.L⁻¹ glucose and 8mmol.L⁻¹ glucose within specification.

Although these flow rates are not sufficient to allow the maintenance of the dissolved oxygen concentration within acceptable parameters (see Fig. 4.9), they do indicate that a small concentration adjustment can bring about a change in required feed rate equivalent to an order of magnitude. Unfortunately the effect these reduced feed flow rates have upon the concentration of one of the waste products, lactate is prohibitive.

Figure 7.2 shows that for the reduced fresh feed flow rates, lactate concentration will significantly exceed the specified limit of 3mmol.L⁻¹. Ammonia is unlikely to breach

its upper limit of 6mmol.L^{-1} under these conditions, but potentially could if the ratio of glucose uptake rate to the ammonia production rate is high.

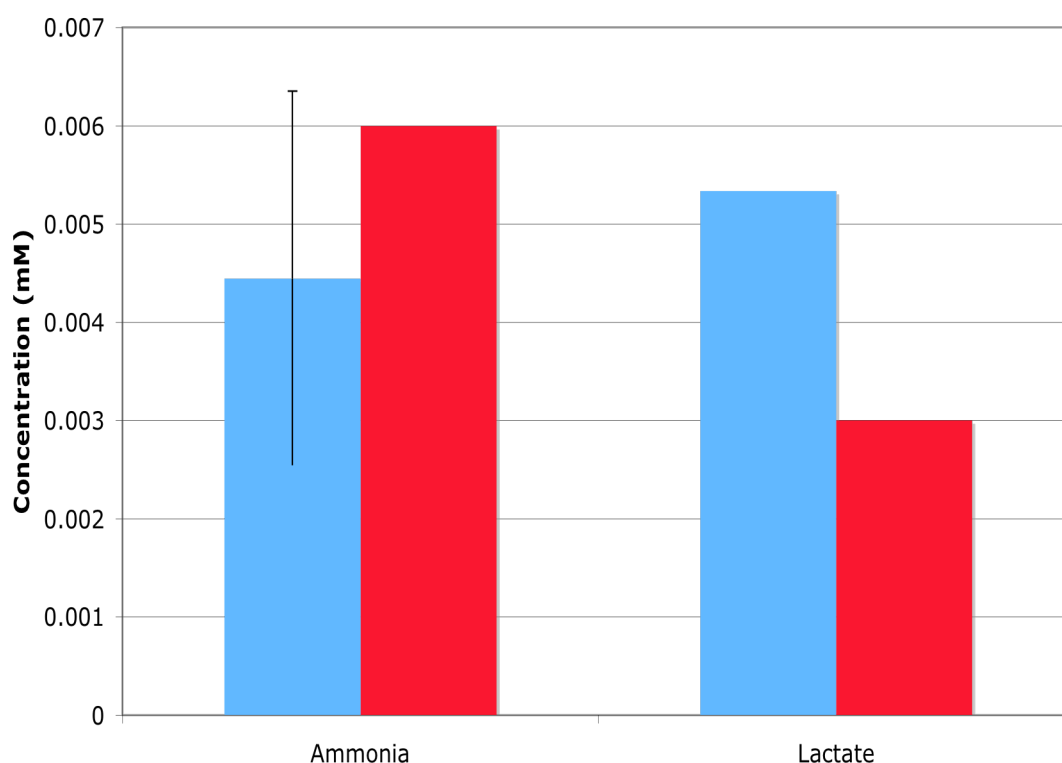


Figure 7.2 Concentration of lactate and ammonia for decreased feed rates

Blue represents desired concentration, red represents specified maximum concentration, error bars on ammonia represent maximum and minimum ratio for glucose uptake rate to ammonia production rate.

Given that the feed rates were not reduced sufficiently to allow oxygen concentration to be maintained and the concentration of lactate began to limit, it is clear that increasing the concentration of the feed is not sufficient to solve the problem. Any method that requires reduction of the fresh feed rate is not appropriate as the concentration of the waste products lactate and ammonia will always exceed specifications. The curve of feed flow-rate against cell number for lactate shown in Fig. 6.2 represents the absolute minimum feed flow rates that may be achieved by modulating the concentrations of the fresh feed metabolites. If the concentration of

glucose is increased to 8.5mmol.L^{-1} the minimum flow rates required to maintain glucose concentration can be reduced to those required for lactate. Fig. 7.3 shows the minimum glutamine concentrations required to allow operation equivalent to the lactate window. The error bars represent variation in the ratio of the glucose uptake rate to the ammonia production rate.

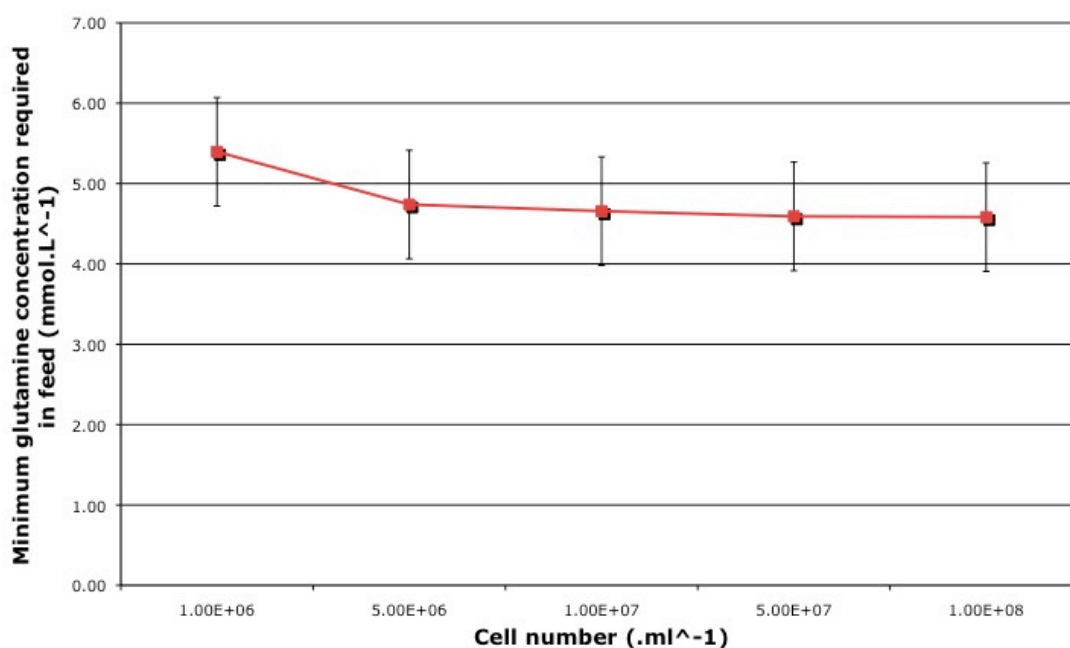


Figure 7.3 Minimum concentration of glutamine required in the fresh feed

This concentration ensures fresh feed/purge flow rates that maintain both lactate and glutamine within specified levels.

By using a fresh feed composed of 6mmol.L^{-1} glutamine and 8.5mmol.L^{-1} glucose rather than the originally specified recipe containing 4mmol.L^{-1} and 6mmol.L^{-1} , the trend of minimum values for fresh feed against cell number changes to that shown in Fig. 7.4.

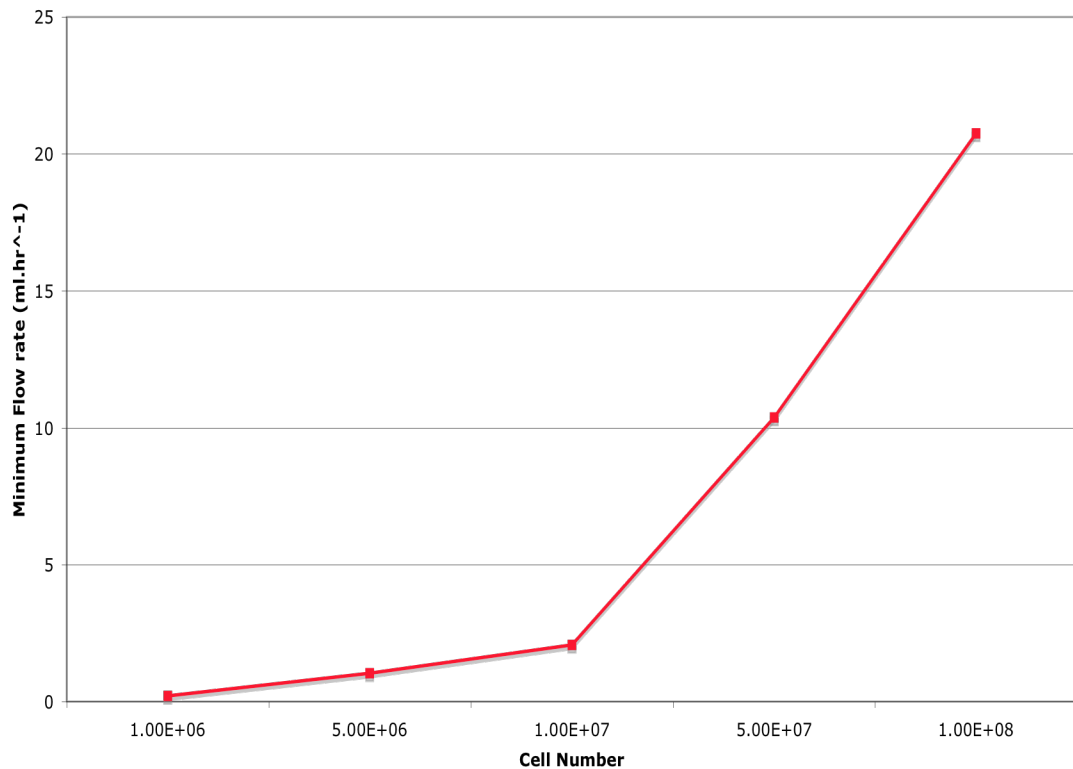


Figure 7.4 Minimum flow rate required to maintain concentration restraints for richer culture medium.

This curve represents the minimum fresh feed flow rates of the new media composition to ensure the two substrates, glucose and glutamine, and the two metabolite, lactate and ammonia, remain within specifications.

This new window shown in Fig. 7.4 although sufficient to maintain fresh feed metabolites still does not allow for operation of the bioreactor at that will maintain the oxygen concentration.

The remaining option to achieve this integrated control is to increase the concentration of dissolved oxygen within the fresh feed, this has the advantage of permitting higher fresh feed rates that can supply sufficient glucose and glutamine, purge excessive ammonia and lactate and not dilute the oxygen concentration below physiological limits. By varying the oxygen concentration it is possible to determine what oxygen

feed concentration is required to permit operation within the same range of fresh feed flow rates specified by the feed metabolite windows of operation. For fresh feed containing a range of oxygen concentrations Fig. 7.5 shows the windows of possible feed rates for varying recycle rate.

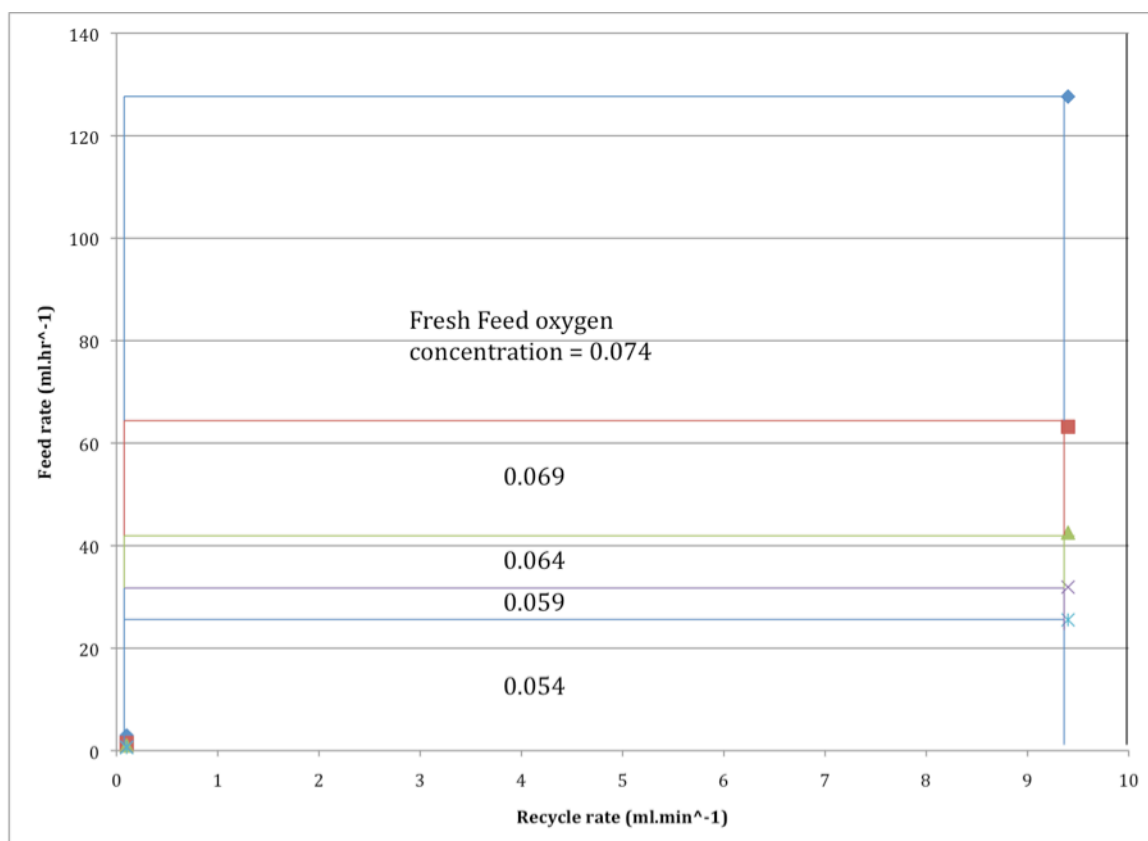


Figure 7.5 Windows of Operations (WOOs) relating recycle rate to feed flow rate for a variety of oxygen concentration.

A series of WOOs show how the range of acceptable fresh feed flow rates increases with the oxygen concentration of the fresh feed.

The Windows of Operation (WOOs) in Fig. 7.5 represent systems where the fresh feed stream contains a range of dissolved oxygen tensions. Together, Fig. 7.5 and 7.4 demonstrate that the fresh feed rate in an integrated system may be controlled in a way that maintains both the specified oxygen and feed metabolite concentrations. Table 7.1

summarises the changes made in operating conditions to allow an integrated control model to be created.

Table 7.1 Modifications to system operating conditions to allow models developed in chapters 4 and 6 to be integrated.

Changing the properties of the feed stream allows the windows of operation for the substrates and oxygen to overlap permitting a unified control system to be developed.

Metabolite	Previous concentration in fresh feed (mmol.L ⁻¹)	Revised concentration in fresh feed (mmol.L ⁻¹)
Glutamine	4	6
Glucose	6	8.5
Oxygen	0	0.054

7.4 Integrated Control Model

Using the new operating conditions (see table 7.1) that have been demonstrated to allow integrated control, the first stage of creating a unified model is to determine which parameters are cross-linked, so that results obtained are truly representative of the process system in its entirety. A new Simulink model was created for this simulation, combining the models developed in Chapter 4, for oxygen, and in Chapter 6, for the respiratory metabolites. This combined model is outlined in Appendix 3.

Fig. 7.6 represents the inputs and outputs of the two models and how these should be cross-linked to combine the oxygen model (see chapter 4) and the feed metabolite model (see chapter 6). The oxygen control loop controls the recycle loop rate to maintain the oxygen concentration within the bioreactor and the value this controller take within the metabolite system.

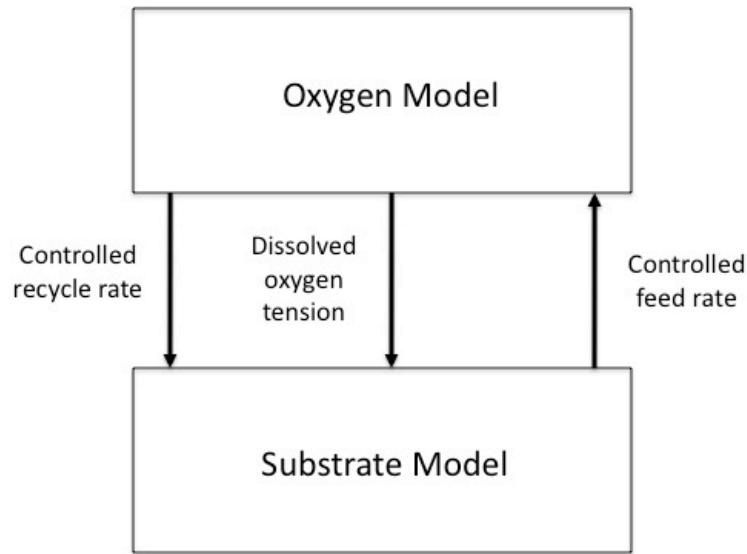


Figure 7.6 Integration of oxygen model (see chapter 4) and substrate model (see chapter 6) into a single model.

The fresh feed rate will also affect the recycle rate controller within the oxygen system although this effect is indirect as the effect of the feed rate on the dissolved oxygen tension (DOT) requires the recycle rate to rise to compensate. The oxygen concentration at any time is required by the metabolite control model to determine the consumption rate by the cells as the metabolic reactions are all cross-related.

The interaction of these variables requires some new terms to be included within the integrated model that were not part of either of the two constituent parts.

This combined model must take account of the interaction of the glucose and oxygen consumption, as at any given time either substrate may be responsible for limiting the cell growth rate. Equation 7.1 represents the Verhulst equation for cell growth and equation 7.2 shows how the growth rate is dependant upon the concentration of a limiting substrate, both of these equations were implemented in Chapter 4.

$$\frac{dX}{dt} = \mu X \left(1 - \frac{X}{X_{\max}} \right) \quad (7.1)$$

Where X is the cell concentration (.ml^{-1}), μ is the specific growth rate (s^{-1}) and X_{\max} is the maximum cell concentration (.ml^{-1}),

$$\mu = \mu_{\max} \frac{S}{K_S + S} \quad (7.2)$$

Where S is the substrate concentration (mM), K_S is the half saturation constant for the substrate (mmol.L^{-1}), μ is the maximum specific growth rate (s^{-1}).

In a situation where there are two limiting substrates such as in this integrated model equation 7.3 applies.

$$\mu = \mu_{\max} \frac{C_G}{K_G + C_G} * \frac{C_{O_2}}{K_{O_2} + C_{O_2}} \quad (7.3)$$

Where C_G is the glucose concentration (mM), K_G is the half saturation constant for glucose (mM), μ is the maximum specific growth rate (s^{-1}). C_{O_2} is the oxygen concentration (mM) and K_{O_2} is the half saturation constant for oxygen.

Zeng et al (1998) stated that the ratio of consumption of glucose to oxygen is 1mol.mol^{-1} hence the uptake rates should be equivalent.

Equation 7.3 has been implemented within the unified model to simultaneously model the effect of glucose and oxygen concentrations on the cell growth rate. A further term is included in the integrated model to acknowledge that it is not possible to pre-gas the media with oxygen to a high accuracy. This variation in accuracy introduces noise into

the system and was represented within the integrated model by a term for random variation in oxygen concentration between 0.044 and 0.064mmol.L⁻¹ (the desired value is 0.054mmol.L⁻¹).

Testing the unified model including these new terms provides the control trends for the recycle loop flow rate and fresh feed rate and the measured values of oxygen and glucose are shown in Fig. 7.7-7.10. These figures show that the changes in the operating conditions have been sufficient to allow both systems to work in unison without further tuning being required. The unified model of the bioreactor has successfully demonstrated that both the glucose and the oxygen concentration in solution may be controlled by modulated changes in the feed and recycle loop flow rates.

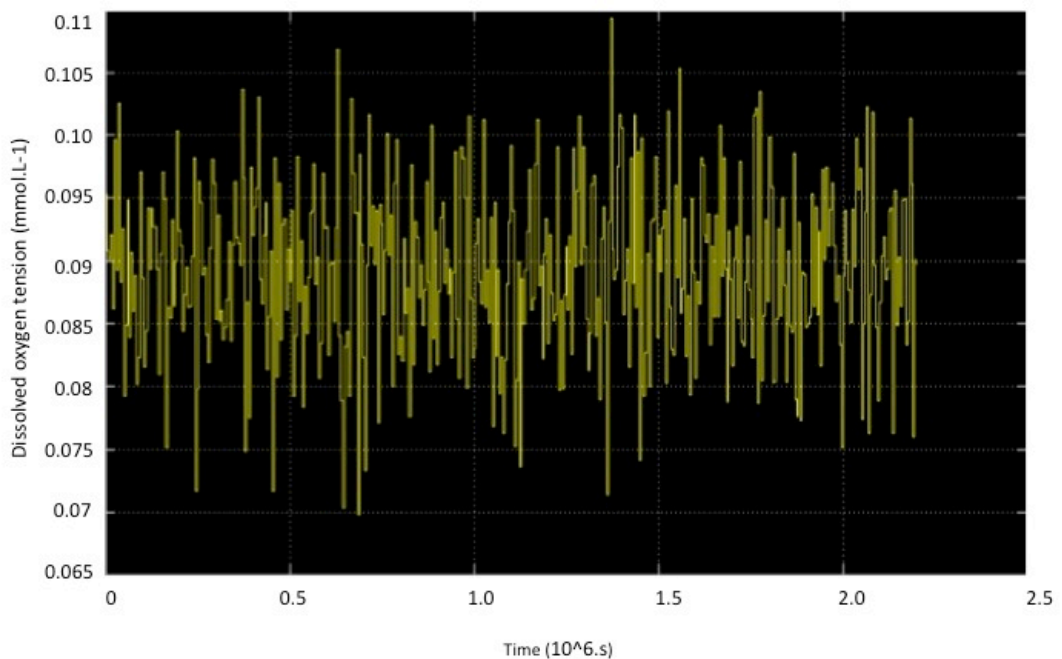


Figure 7.7 Controlled dissolved oxygen tension (DOT) trends, at exit of bioreactor, within overall combined model

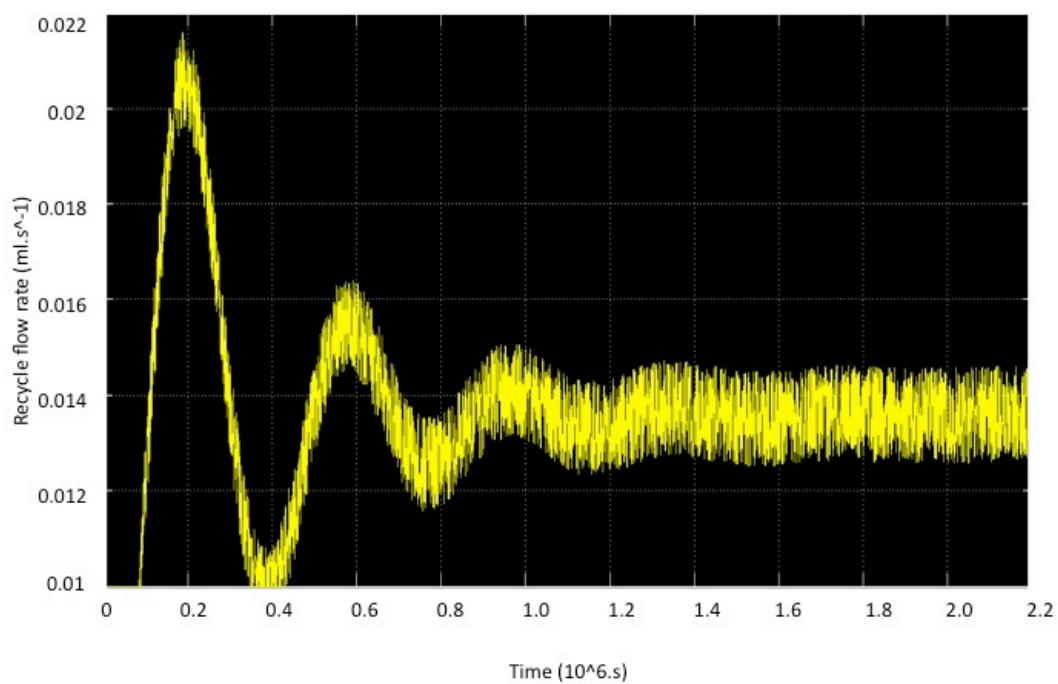


Figure 7.8 Controlled recycle flow rate, in overall control system, into bioreactor system

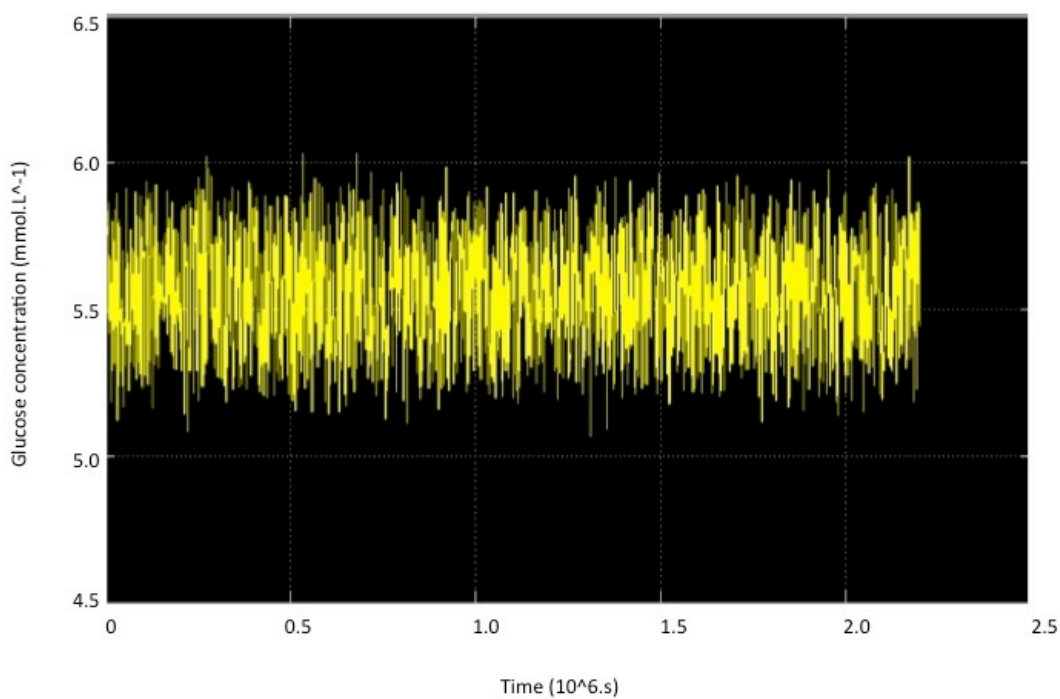


Figure 7.9 Controlled glucose concentration trends, at exit of bioreactor, within overall combined model

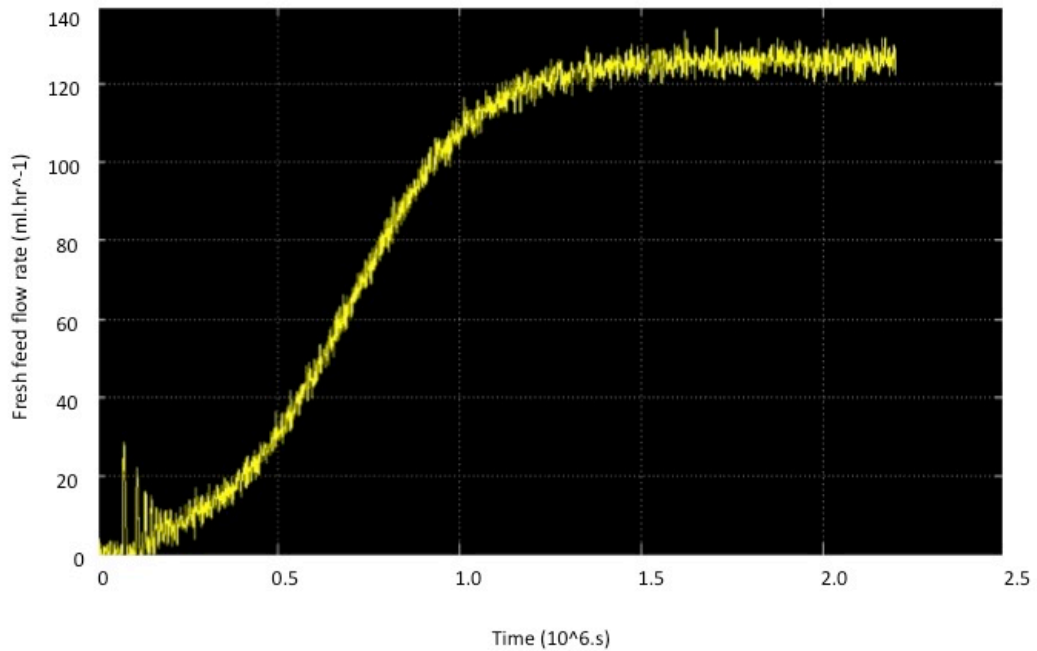


Figure 7.10 Controlled fresh feed flow rate, in overall control system, into bioreactor system

7.5 Conclusions

The aim of this chapter was to bring together the separate models derived for oxygen, substrates and waste products and pH. Earlier work has shown that lactate, glutamine and ammonia could be neglected where glucose was controlled successfully and the same was also true for pH. This meant that the final unified system was only required to maintain control of two substrates, oxygen and glucose.

The windows of operation developed for these two substrates in earlier chapters were shown to be incompatible and changes in the operating conditions were required to overcome this. The feed concentrations of oxygen, glucose and glutamine were increased. These increases enabled the creation of a window within which all five substrates could be controlled within specified ranges.

Control was possible with the two systems unified as shown in Fig. 7.6 and the results in Fig. 7.7 - 7.10 show that although there are oscillations within the system glucose and oxygen concentrations are broadly controlled. Given the complex inter-relationship between all the parameters this must be considered a successful outcome. A unified model for the control of a bioreactor containing cells developing into the first stage of a tissue engineered bypass graft has been proposed.

Chapter 8 Conclusions and Further Work

A model for the control of a bioreactor system designed to produce tissue engineered arterial grafts has been developed in this work. The model has been used to control the oxygen, substrate and waste levels within the system.

8.1 Bioreactor system

Using a combination of scientific literary sources and empirical data, a model was developed to describe the dynamics of the bioreactor system.

The model was divided into subsystems: oxygenator, bioreactor, recycle loop, feed and purge. These subsystems were subsequently integrated together. This unification provided a representation of the dynamic system suitable for modelling changes in the dissolved concentrations of substrates and waste products and was suitable for determining the possibilities for environmental control.

One of the key issues with the design of the bioreactor system was an inability to determine cell number online for any given time. This coupled with the variability of the oxygen uptake rate depending upon cell density provided a considerable obstacle to predicting the cell number in real time.

Yeast cells which grew rapidly compared with mammalian cells were utilised as an example of a eukaryote cell to determine how oxygen uptake rate decreases as the cell density increases and how oxygen uptake rate is related to the cell number in this

work. This relationship provided crucial information for the control of the bioreactor system. This had the secondary benefit of allowing cell number to be estimated online from the oxygen consumption rate. Estimation of cell number online allows the health of the graft to be estimated. If oxygen uptake rate falls unexpectedly potential problems with the graft may be detected. Delivery time of a developing artery may also be determined, this allows scheduling of surgery for a recipient of the graft.

8.2 Dissolved oxygen tension (DOT) process control

Control of the flow rate within the recycle loop, containing the membrane oxygenator, was utilised to maintain oxygen tension within the alginate scaffold. Oxygen tension was maintained at a value analogous to the *in-vivo* concentration within the bone marrow regions where mesenchymal stem cells may be isolated.

A computational fluid dynamics (CFD) software package was used to determine the minimum flow rate within the recycle loop to ensure that the oxygen tension within the scaffold remained at physiological concentrations. This minimum flow rate varied with cell number and increased as the graft developed, at any given time it represented the minimum possible rate at which the controller could instruct the recycle rate to operate.

A window of operation for the bioreactor was formed using this minimum flow rate coupled with shear stress limitations. This window provided the maximum and minimum flow rates that could be implemented by the controller. The simplest form of controller, the two-step, was insufficient for maintenance of DOT. Thus, a

Proportional and Integral (PI) controller was investigated using the software package, Simulink. For the development of these controllers it was assumed that all other substrates were in excess and oxygen was the only limiting factor. A transfer function was formed using a mass balance and linearisation of the non-linear terms to describe the input-output relationship between the recycle flow rate and the oxygen concentration at the exit of the bioreactor. This transfer function provided a first approximation of the system and by using online Ziegler-Nichols techniques and finally trial and error the PI controller's parameters were selected. This control was capable of ensuring DOT remained within a physiological range. Thus, it is demonstrated that recycle loop control is sufficient to control DOT when oxygen is the only variable requiring control.

8.3 Metabolic compound process control

Key substrates within the cell culture medium were identified as glucose and glutamine. The key waste products were the by-products of their breakdown, lactate and ammonia. Approximate relationships between these four components of cellular metabolism were obtained from Zeng et al (1998). The fresh feed flow rate was chosen as the control parameter for maintenance of the four components. Windows of Operation were determined for each component using similar methods to those used for the control of the oxygen concentration. The combination of the four resultant Windows of Operation demonstrated that, with the exception of at very low cell numbers, glucose control would simultaneously ensure that glutamine, lactate and ammonia would also be controlled appropriately. Under the assumption that oxygen was controlled at a constant level of 0.079mmol.L^{-1} , a gain that incorporated a term for

cell number was used. A proportional controller was used to achieve glucose control. Cell number was estimated using the model for cell growth. Dissolved oxygen tension was maintained constant at 0.079mmol.L^{-1} . The output from the cell growth model fed directly into the proportional controller. Changes in the cell growth model output led to a change in the value of the controller gain as the graft developed and allowed superior control to be achieved.

Simulations were performed using Simulink and it was demonstrated that it is viable to use control of the fresh feed flow rate by proportional control to maintain glucose within specified boundaries and thus, also the glucose, glutamine, and lactate concentrations when the oxygen concentration is maintained at 0.079mmol.L^{-1} .

8.4 Overall system control model

Combining the oxygen and metabolite models without prior modification was not possible. The fresh feed flow rates required by the metabolic control system, particularly at higher cell numbers, required recycle rates far in excess of those permitted by the Window of Operation for the dissolved oxygen concentration. The solution was to use pre-gassed rather than sparged fresh medium and also to increase feed concentrations of glucose and glutamine. The oxygen concentration selected was 0.054mmol.L^{-1} . However a lack of possible accuracy in the gassing of cell culture media ensures that there would be considerable variation and as such a term was included within the model to set the value randomly within the range $0.044\text{--}0.064\text{mmol.L}^{-1}$. This variation introduced noise into the system but did not prevent successful control of the dissolved oxygen by the PI controller. Glucose and glutamine

concentrations within the fresh feed were increased from 4 to 6 and 6 to 8.5 mmol.L⁻¹, respectively. Combination of the two models, with these new parameters, permitted simultaneous control of the concentrations of glucose, glutamine, lactate, ammonia and oxygen.

Although this model has demonstrated a possible theoretical strategy for the control of a number of environmental parameters within a tissue engineering bioreactor, the solution is far from comprehensive. This model contains a number of limitations. It is based upon a set obtained from empirical data and peer reviewed literature and it involves a number of assumptions. Stem cell biology remains in its infancy, since tissue engineering was first coined as a phrase, only very simple materials, such as skin, have been approved by the US FDA (Food and Drug Administration) for use as a treatment in humans. The exact definitions of stem cell sub-populations, such as mesenchymal stem cells (MSC), remain controversial and the methods used to isolate such populations are ill defined and require much further development. This lack of definition ensures that assumed values for metabolic and growth rates of such cells are merely estimates and are subject to revision as the field advances. However, the shortage of viable alternatives that are capable of matching the effectiveness of the organs and tissues that we are born with, ensure that this field will move forwards. To achieve the production scale of tissues and organs required to meet the demand of an ageing population demands that methods of production be considered in parallel as the biological knowledge advances. Tissue engineered material designed for use in human patients will need to be produced in a regulated, controlled and replicable manner. This type of process will be demanded by government regulatory agencies to ensure the safety of patients. It is thus, vital that control engineering is explored within the

context of tissue engineering and this thesis provides a first step. Concerns of scale have been considered and methods that provide solutions to these problems have been explored. A solution to controlling a number of biological parameters within a bioreactor for the development of a tissue engineered blood vessel has been demonstrated.

8.5 Future Work

As a first step this body of work provides numerous opportunities for further work and investigation. One key area is how process control can be designed to accommodate changes in cellular metabolic demand as immature cell types differentiate into more mature cell types. Environmental conditions responsible for causing stem cell populations to differentiate down particular pathways require much further research before this will be possible. However once the biology is better understood, the creation of sophisticated mathematical models will be possible. Such models, likely based around non-linear dynamics and population modelling, will provide powerful tools for the development of a wide variety of control systems that can both drive development of tissues and organs and allow their healthy development prior to implantation within patients. Ultimately bioreactors for use in tissue engineering are likely to have two distinct stages of production. In the case of a tissue engineered blood vessel, the first will be the proliferation of an immature cell type such as MSC throughout the scaffold, allowing the initial formation of a tube structure. It is a control system for this stage, that this thesis has focused upon. The second stage will expose the MSC cells to controlled environmental conditions that encourage the

conditions that lead to the development of a healthy artery composed of three distinct layers of connective tissue, muscle, and a lining of endothelial cells.

For the development of a control system used within this thesis many of the required values have been obtained from literature in good faith and are normally founded upon *in-vivo* conditions. Further research is required to determine if *in-vivo* conditions are indeed truly the most appropriate.

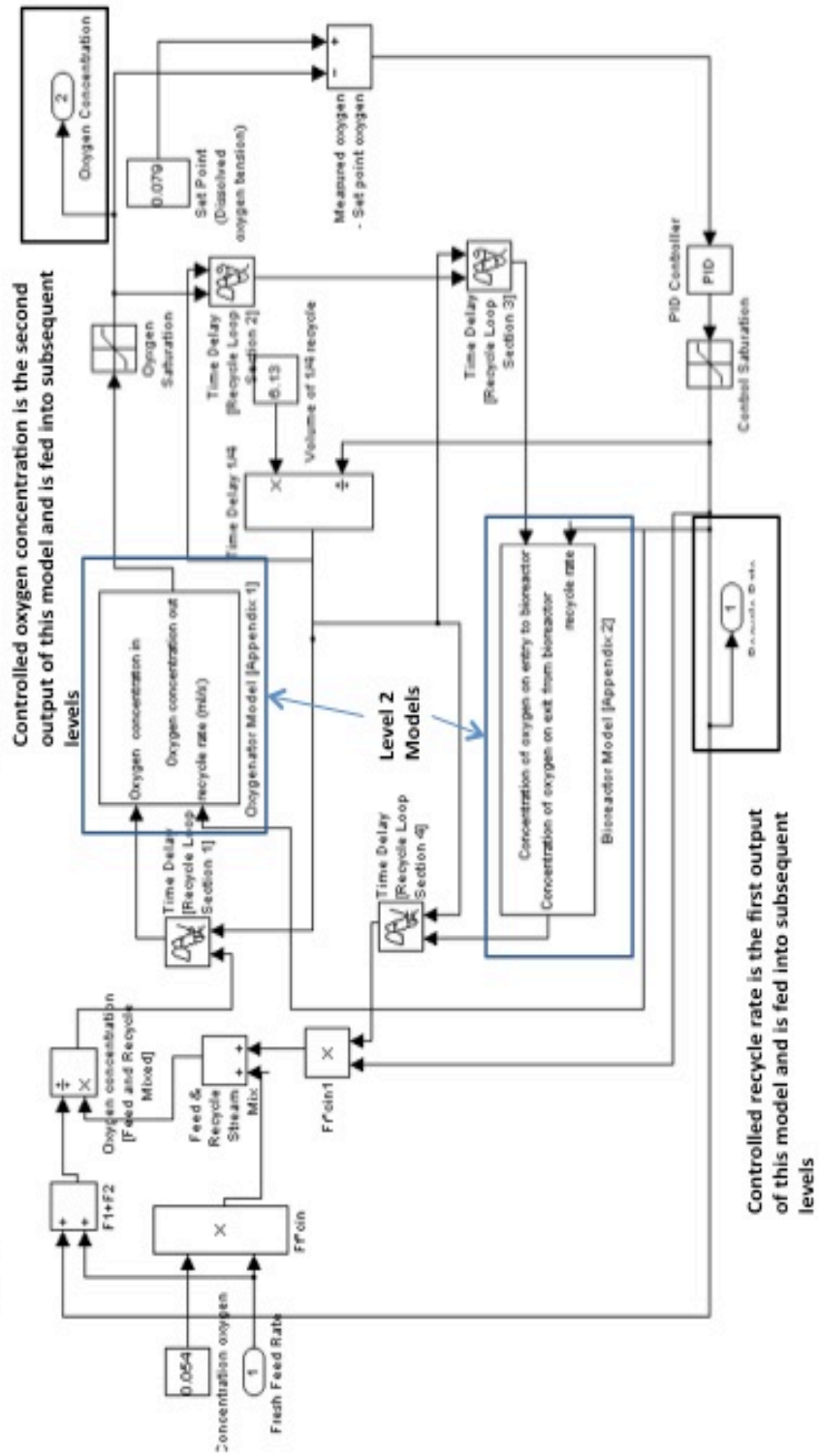
With regard to the design of the vascular tissue engineering bioreactor (VTEB) used within this work, it requires further improvement before it can become an effective method of producing tissue engineered arterial grafts. Sterility remains a large issue, the use of antibiotics being unsuitable to tissue engineered materials due to the risk of allergic or idiosyncratic responses, the masking of cryptic infections that can become resistant later and because of possible effects upon cell growth and/or proliferation. Full automation of the system requires incorporation of steps such as cell handling and tube extrusion although such concerns remain low priority for the foreseeable future.

The work performed in this thesis demonstrates the possibility and the complexities in developing environmental control of bioreactors used for tissue engineering. As a greater understanding of the biology of stem cells is attained the control methods discussed here may be implemented to allow the production of arterial grafts for use in the treatment of a variety of medical conditions. The advancement of stem cell biology will allow tissue engineering and cell therapy to realise the hope of curing underlying disease rather than merely treating the symptoms.

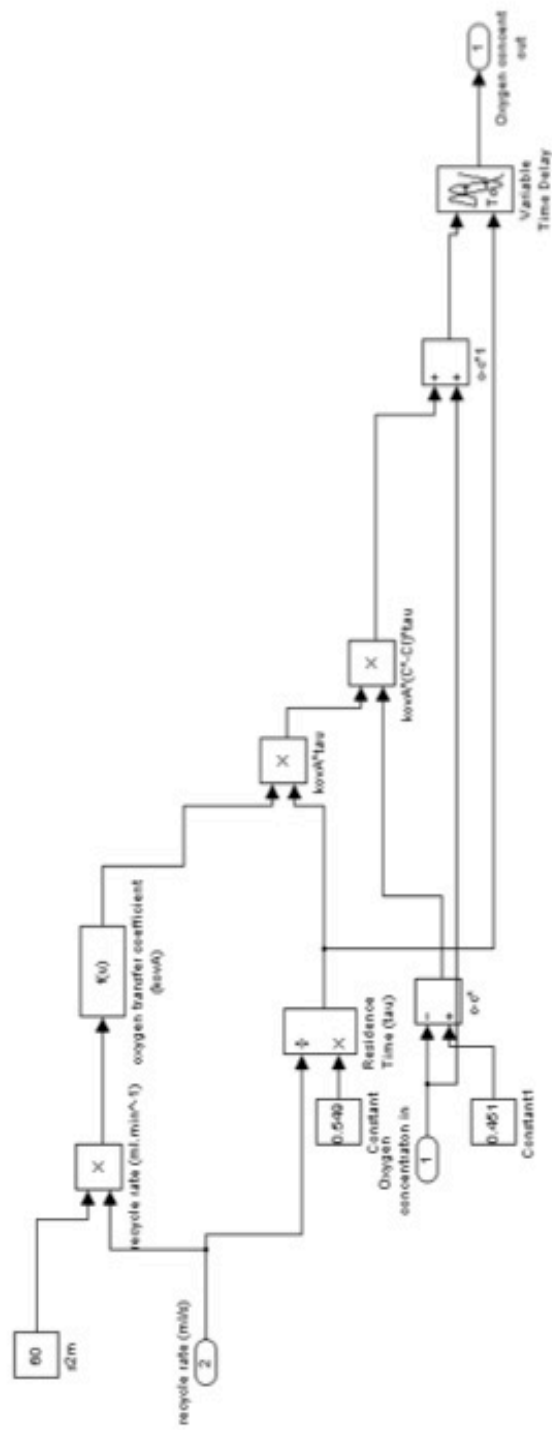
Appendices

These Appendices include the Simulink models used to produce the results presented and discussed within the main thesis. Appendix 1 incorporates the two levels of the model used to develop oxygen control for the bioreactor (See chapter 4). Appendix 2 incorporates the two levels of the model used to develop substrate control for the bioreactor (see chapter 6). Finally, Appendix 3 shows how these two models interacted to model the overall control system developed for the bioreactor (see Chapter 7).

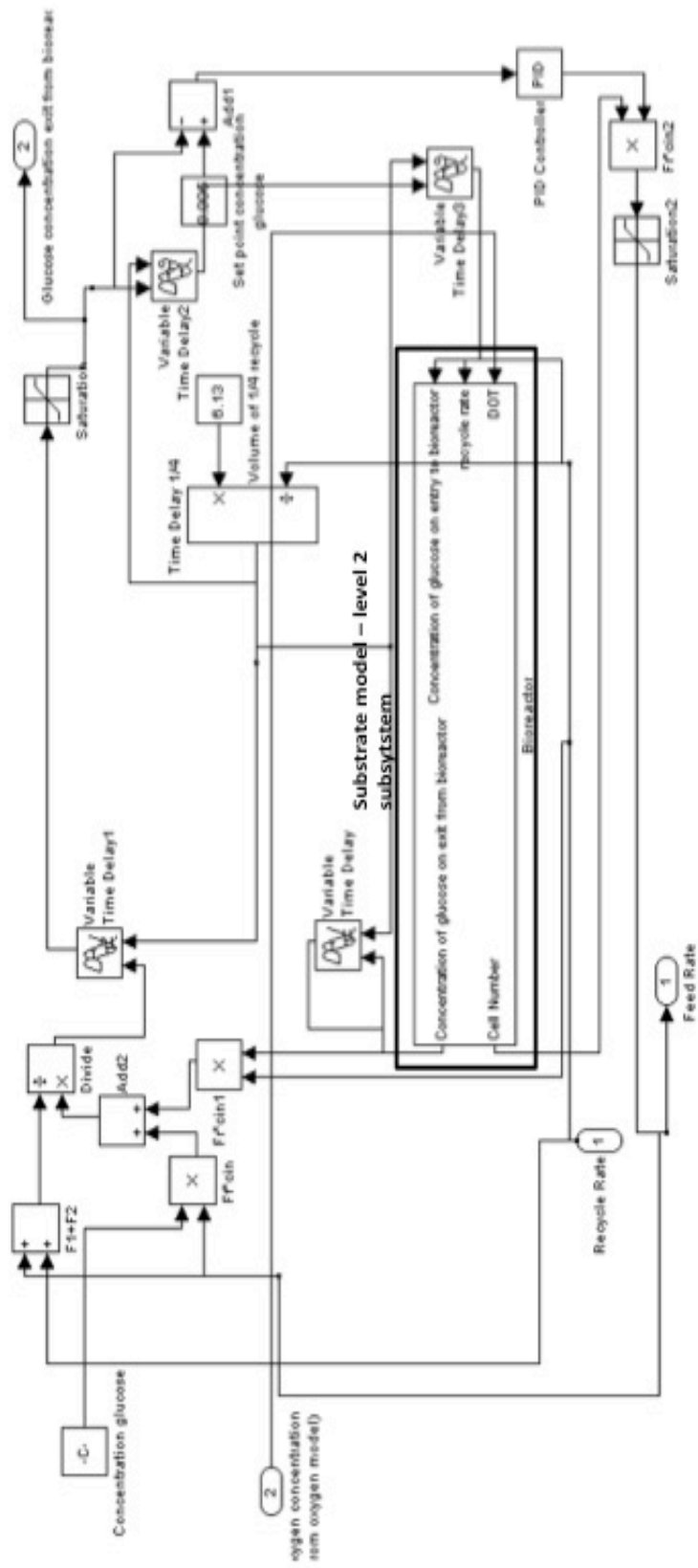
Appendix 1: Oxygen model-level 1



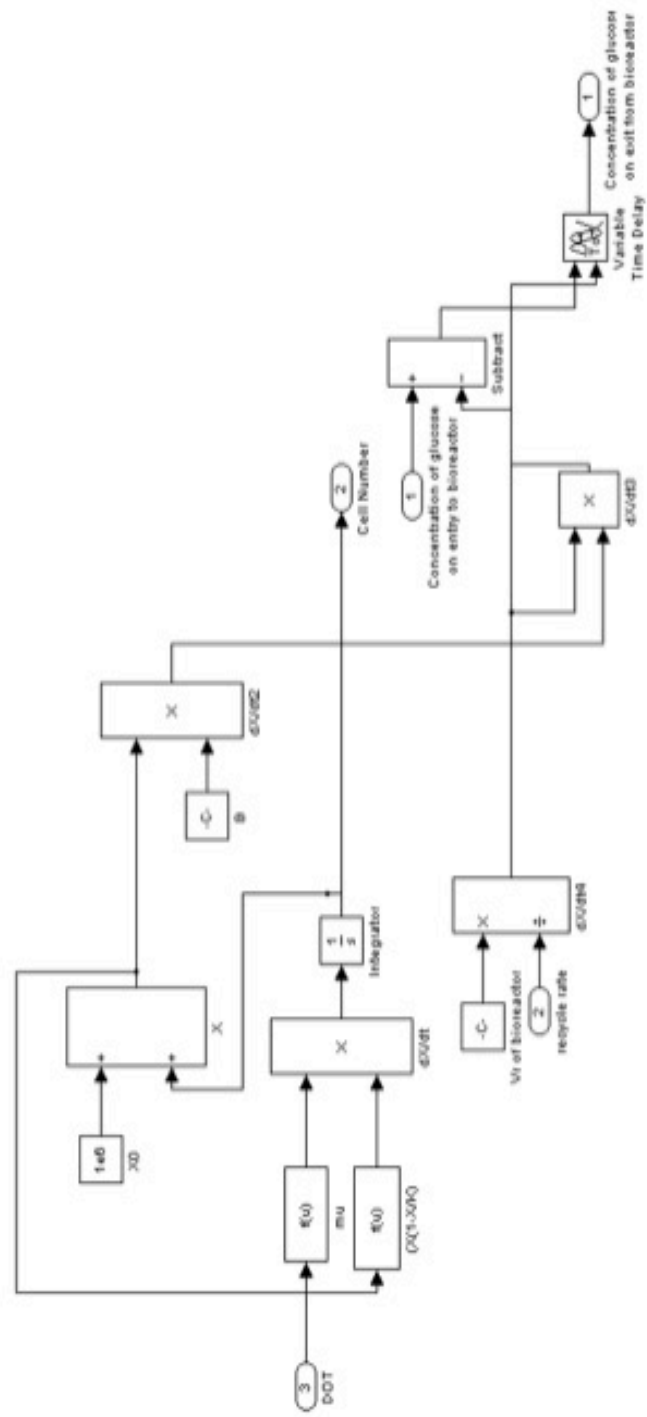
Appendix 1: Oxygen model-level 2 (oxygenator)



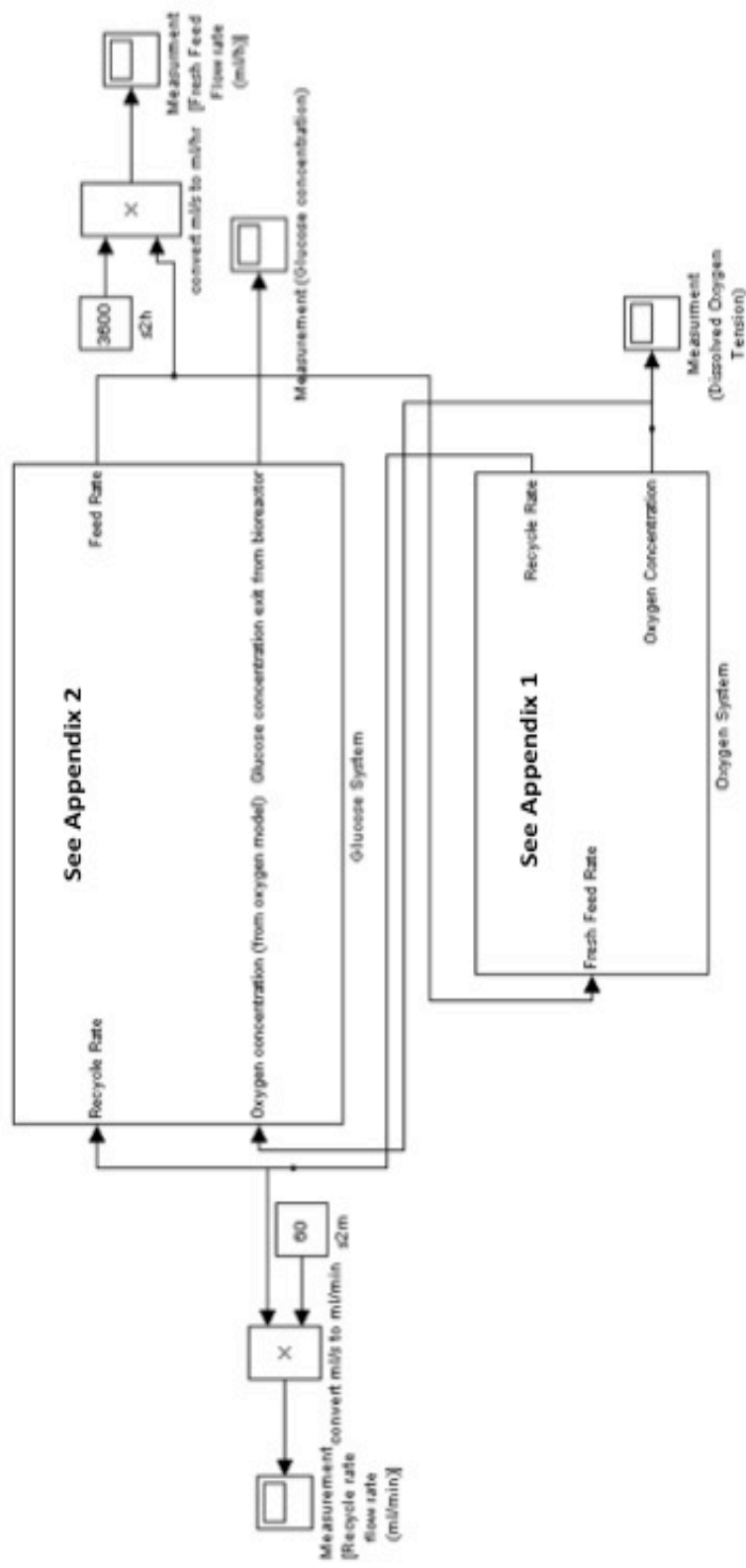
Appendix 2: Substrate model-level 1



Appendix 2: Substrate model level 2 (bioreactor)



Appendix 3: Overall Model Top level



References

- Abbott, A. (2003) Cell Culture: Biology's New Dimension. *Nature* 424: 870-872
- Abedin, M., Tintut, Y., Demer, L.L. (2004) Mesenchymal Stem Cells and the Artery Wall, *Circulation Research*, 95: 671-676
- Activated Cell Sorting (FACS): A Rapid and Reliable Method to Estimate the Number of Neurons in a Mixed Population. *Journal of Neuroscience Methods* 129(1): 73-79.
- Alberts, B., Bray, D., Lewis, J., Raff, M., Roberts, K., Watson, J.D. (1994), *Molecular Biology of The Cell*, 3rd Edition, Garland, New York.
- Allen, J.W., Hassanein, T., Bhatia, S. (2001) Advances in Bioartificial Liver Devices. *Hepatology* 34(3): 447-455
- Altman, G.H., Lu, H.H., Horan, R.L., Calabro, T., Ryder, D., Kaplan, D.L. (2002) Advanced Bioreactor with Controlled Application of Multi-Dimensional Strain for Tissue Engineering. *Journal of Biomechanical Engineering* 124(6): 742-749
- Andrews (2006) The Selfish Stem Cell *Nature Biotechnology* 24(2): 325-326
- Angelini, G.D., Newby, A.C. (1989) The Future of Saphenous Vein as a Coronary Artery Bypass Graft. *European Heart Journal* 10: 273-280
- Anon (2003), Clinica's Market Briefing September 2003: Tissue Engineering – Ready for Mass Production?

Atala, A., Bauer, S.B., Soker, S., Yoo, J., Retik, A. (2006) Tissue-engineered Autologous Bladders for Patients Needing Cystoplasty. *The Lancet* 367(9518): 1241-1246.

Atkins PW (1998) *Physical Chemistry* 6th Revised Edition, Oxford University Press, UK.

Avilion, A.A., Nicolis, S.K., Pevny, L.H., Perez, L., Vivian, N., Lovell-Badge, R., (2003) Multipotent cell lineages in early mouse development depend on SOX2 function. *Genes Development* 17:126-140.

Bain, B.J. (2003) Bone Marrow Biopsy Morbidity and Mortality. *Br. J. Haematol.* 121(6):949-951.

Balis, U.J., Yarmush, M.L., Toner, M. (2002) Bioartificial Liver Process Monitoring and Control Systems with Integrated Systems Capability. *Tissue Engineering* 8(3): 483-498

Banks, S. (2006) Director of Production, Organogenesis, *Private Communication*.

Baumberger, J.P., Leong, H.C., Neville, J.R., (1967) Oxygen Delivery Rate of Human Blood, *Journal of Applied Physiology* 23(1): 40-46

Bello, Y.M., Falabella, A.F., Egelstein, W.H. (2001) Tissue-engineered Skin. Current Status in Wound Healing. *American Journal of Clinical Dermatology* 2(5): 305-13

Belter P.A., Cussler, E.E., Hu, W-S. (1988) Cell Disruption *Chapter 3*, In:

Bioseparations; Downstream Processing for Biotechnology . John Wiley and Sons, New York *Bioengineering* 58(5): 530-537

Bolton, W. (2003) *Mechantronics: Electronic Control Systems in Mechanical and Ectrical Engineering* 3rd Edition, Pearson Prentice Hall, Harlow, England 45-47

Bottino, R., Linetsky, E., Selvaggi, G., Kong, S.S., Qian, T., Ricordi, C. (1995) Automation of Human Vertebral Body Bone Marrow Harvest. *Annals of the New York Academy of Science* 770: 364-365.

Bourassa, M.G., Enjalbert, M., Campeau, L., Lesperance, J. (1984) Progression of Atherosclerosis in Coronary Arteries and Bypass Grafts: Ten Years Later. *The American Journal of Cadiology* 53(12): 102C-107C

Boyd, A.S., Higashi, Y., Wood, K.J. (2005) Transplanting Stem Cells: Potential Targets for Immune attack. Modulating the immune response against embryonic stem cell transplanatation, *Advanced Drug Delivery Reviews*, 57: 1944-1969

Bruder, S.P., Jaiswal, N., Haynesworth, S.E., (1997) Growth Kinetics, Self Renewal and the Osteogenic Potential of purified hMSCs during extensive subcultivation and following cryopreservation. *Jounral of Cellular Biology* 64: 278-294

Burnstock, G., (1998) Release of vasoactive substances from endothelial cells by shear stress and purinergic mechanosensory transduction. *Journal of Anatomy* 195: 335-342

Campbell, K.H.S., McWhir, J., Ritchie W.A., Wilmut, I. (1996) Sheep Cloned by Nuclear Transfer From a Cultured Line. *Nature* 380:64-66

Cartmell, S.H., El Haj, A.J. (2005) Mechanical Bioreactors for Bone Tissue Engineering. In: *Bioreactors for Tissue Engineering: Principles, Design and Operation*, Chaudhari, J., Al-Rubeai, M. editors. Springer 193-208

Cassell, O.C., Hofer, S.O., Morrison, W.A., Knight, K.R. (2002) Vascularization of Tissue-Engineered Grafts: The Regulation of Angiogenesis in Reconstructive Surgery and in Disease States. *Brit J Plast Surg.* 55:603-610.

Chambers, I., Colby, D., Robertson, M., Nichols, J., Lee, S., Tweedie, S., Smith, A. (2003) Functional Expression Cloning of Nanog, A Pluripotency Sustaining Factor In Embryonic Stem Cells. *Cell* 113: 643 – 655.

Chau G. (2009) Tube-forming device design for the production of cell-integrated alginate tubes. *PhD Thesis*, University College London, University of London.

Collins, P.C., Nielsen, L.K., Patel, S.D., Papoutsakis, E.T., Miller, W.M. (1998) Characterization of hematopoietic cell expansion, oxygen uptake and glycolysis in a controlled stirred-tank bioreactor system. *Biotechnology Progress* 14(3): 466-472

Cox, J.L., Chiasson, D.A., Gottlieb, A.I. (1991) Stranger in a strange land: the pathogenesis of saphenous vein graft stenosis with emphasis on structural and functional differences between veins and arteries. *Progress in Cardiovascular Diseases* 34(1)-45-68.

Davies P.F., (1995) Flow mediated endothelial transduction *Physiological Review* 75(3): 519-560

Deans, R.J., Moseley, A.B., (2000) Mesenchymal Stem Cells: Biology and Potential Clinical Uses *Experimental Haematology* 28: 875-884

Deuel, T.F., and Zhang, N. (2000) Growth Factors In: *Principles of Tissue Engineering*, Second Edition, Lanza, R, Langer, R, Vacanti, J. editors. Academic Press, San Diego 129-141.

Deutsch. M., Meinhart, J., Fischlein T., Presiss, P., Zilla, P. (1999) Clinical Autologous In-Vitro Endothelialization of Infrainguinal ePTFE Grafts in 100 Patients: A 9-Year Experience. *Surgery* 126: 847-855

Donovan, P.J., Gearhart J. (2001) The End of the Beginning for Stem Cells, *Nature* 414: 92-97.

Doran, P.M., (1995) *Bioprocess Engineering Principles*, Academic Press, San Diego.

Dorresteyjn, R.C., Harbrink Numanm, K., De Gooijer, C.D., Tramper, J., Beauvery, E.C., (1995) Application of Software Sensors in Animal Cell Culture, In: *Proceedings of JAACT 1995, Lizuka, Japan*

Dorresteyjn, R.C., Wieten, G., Van Santen, P.T.E., Philippi, M.C., De Gooijer, C.D., Tramper, J., Beauvery, E.C. (1996) Current Good Manufacturing Practice in Plant

Automation of Biological Production Processes, *Cytotechnology* 23:19-28

Draper, J.S., Seguin C.A., Andrews, P.A., (2007), Phenotypic Analysis of Human Embryonic Stem Cells, In: *Human Embryonic Stem Cells: The Practical Handbook*, Sullivan, S., Cowan, C.A., Eggan, K., editors, John Wiley and Sons, Ltd.

Dreyfus. H., Dreyfus, S. (1986) Why computers never think like people. *Technology Review*. 89:42-61.

Eagelstein, W.H., Falanga, V. (1997) Tissue Engineering and the Development of Apligraf®, a Human Skin Equivalent. *Clinical Transplantation* 19(5): 894-904

Ellis, M., Jarman-Smith, M., Chaudhari, J.B. (2005) Bioreactor Systems for tissue engineering a four-dimensional challenge, In: *Bioreactors for Tissue Engineering: Principles, Design and Operation*, Chaudhari, J., Al-Rubeai, M. editors. Springer 1-18

Enroth, H., Engstrand, L. (1995) Immunomagnetic Separation and PCR for detection of *Helicobacteria pylori* in water and stool specimens. *Journal of Clinical Microbiology* 8: 2162-2165

Ferrara, N., Gerber H., LeCouter, J. (2003) The Biology of VEGF and its receptors, *Nature Medicine* 9(6): 669-676

Fischer, A. (1990) European Experience of Bone-Marrow Transplantation For Severe Combined Immunodeficiency. *The Lancet* 336, 8719:850-854.

Flanagan, M.J., (1980) On the application of approximate reasoning to control of the activated sludge process. *Proceedings of the Joint Automatic Control Conference, San Francisco* 1: TA6-C

Flores, J. Arcay, B. Arias, J. (2000) An Intelligent System for Distributed Control of an Anaerobic Wastewater treatment process. *Engineering Applications of Artificial Intelligence* 13: 485-194.

Forys, U., Marciniak-Czochra, A. (2003) Logistic Equations in Tumour Growth Modelling. *Int. J. Appl. Math. Comput. Sci.* 13(3):317-325.
four transcription factors, *Cell proliferation* 41(Suppl. 1): 51-56.

Freshney, R.I. (2000) *Culture of Animal Cells: A Manual of Basic Technique*, Fourth Edition, Wiley-Liss, New York.

Galotto, M., Berisso, G., Delfino, L., Podesta, M., Ottagio, I., Sallorso, S., Durfour, C., Ferrara, G.B., Abbondandolo, A., Dini, G., Bacigalupo, A., Cancedda, R., Quarto, R. (1999) Stromal Damage as a Consequence of High Dose Chemo/Radiotherapy in Bone Marrow Transplant Recipients. *Experimental Hematology* 27(9): 1460-1466

Gerontas, S. (2007) Bioreactor Design For the Controlled Formation of Engineered Tissues. *PhD Thesis*, University College London. University of London.

Girton T.S., Oegema, T.R., Grassl, E.D., Isenberg, B.C., Tranquillo, R.T., (2000) Mechanisms of Stiffening and Strengthening in Media-Equivalents Fabricated Using Glycation. *Journal of Biomechanical Engineering* 122(3): 216-233

Glacken, M.W., Adema, E., Sinskey, A.J. (1988) Mathematical Description of Hybridoma Culture Kinetics: 1. Initial Metabolic Rates *Biotechnology and Bioengineering* 32: 491-506

Gong, Z., Niklason, L.E., Small-diameter human vessel wall engineered from bone-marrow-derived mesenchymal stem cells (hMSCs) *The Federation of American Societies for Experimental Biology (FASEB) Journal* 22: 1635-1648

Gossman, B., Rehm, H.J. (1985) Oxygen Uptake of Microorganisms entrapped in Ca-Alginate *Applied Microbiology and Biotechnology* 23(3-4): 163-167

Grayson, W.L., Zhao, F., Izadpanah, R., Bunnell, B., Ma, T. (2006) Effects of Hypoxia on Human Mesenchymal Stem Cells Expansion and Plasticity in 3D Constructs. *Journal of Cellular Physiology* 207:331-339.

Greisler, H.P., Henderson, S.C., Lam, T.M. (1993) Basic Fibroblast Growth factor Production in-Vitro by Macrophages exposed to Dacron and polyglactin 910. *Journal of Biomaterials Science, Polymer Edition*. 4(5): 415-430

Griesler, H.P. (1990) Interactions at the Blood/Material Interface, *Annals of Vascular Surgery* 4(1): 98-103

Griffith, L., Naughton, G.K., (2002) Tissue Engineering- Current Challenges and

Expanding Opportunities, *Science* 295: 1009-1014

Grodin, C.M., Campeau, L., Lesperance, J., Enjalbert, M., Bourassa, M.G. (1984) Comparison of Late Changes in Internal Mammary Artery and Saphenous Vein Grafts in Two Consecutive Series of Patients 10 Years After Operation. *Circulation* 70(3) Part 2: 1208-1212.

Guthke, R., Schmidt-Heck, W., Pfaff, M. (1998) Knowledge Acquisition and Knowledge Based Control in Bioprocess Engineering. *Journal of Biotechnology* 65(1): 37-46

Hevehan, D. (2000) Physiologically Significant Effects of pH and Oxygen Tension on Granulopoiesis *Experimental Haematology* 28(3): 267-275

Hirai, J., Kanda, K., Oka, T., Matsuda, T., (1994) Highly Orientated, Tubular, Hybrid Vascular Tissue for Low Pressure Circulatory System. *Transactions of the American Society of Artificial Internal Organs*, 40: M383-388.

Hoerstrup, S.P., Sodian, R., Sperling, J.S., Vacanti, J.P., Mayer, J.E. New Pulsatile Bioreactor for in-vitro formation of tissue engineered heart valves. *Tissue Engineering* 6(1): 75-59

Hoerstrup, S.P., Zund, G., Sodian, R., Schnell, A.M., Grunenfelder, J., Turina, M.I. (2001) Tissue Engineering of Small Caliber Vascular Grafts. *European Journal for Cardio-thoracic Surgery* 20:164-169

Hoffman, L.M., Carpenter, M.K. (2005) Characterization and Culture of Human Embryonic Stem Cells, *Nature Biotechnology* 23(6): 699-708

Hutmacher, D.W. (2000) Scaffolds in Tissue Engineering Bone and Cartilage, *Biomaterials* 21: 2529-2543

Hwang, W.S. , Roh, S.I., Byeong, C.L., Kang, S.K., Kwon, D.K., Kim, S., Kim, S.J., Park, S.W., Kwon, H.S., Leww, C.K., Lee, J.B., Kim, J.M., Ahn, C., Paek, S.H., Chang, S.S., Koo, J.J., Yoon, H.S., Hwang, J.H., Hwang, Y.Y., Park, Y.S., Oh, S.K., Kim, S.H., Park, J.J. (2005) Patient-Specific Embryonic Stem Cells Derived From Human SCNT Blastocysts. *Science*. 308, 5729:1777-1783.

intensivecare.hsnet.nsw.gov.au Accessed January 13th, 2010.

Ishikawa, Y., Ito, T. (1988) Kinetics of Hemopoietic Stem Cells in a Hypoxic Culture. *European Journal of Haematology*. 40(2):126-129

Jahoda, C.A.B., Reynolds, A. (2001) Hair Follicle Dermal Sheath Cells: Unsung Participants in Wound Healing 358(9291): 1445-1448

Janssen, F.W., Oostra, J., van Oorschot, A., Clemens, A., van Blitterswijk, A. (2005) A Perfusion Bioreactor System Capable of Producing Clinically Relevant Volumes of Tissue-Engineered Bone: In vivo Bone Formation Showing Proof of Concept. *Biomaterials* 27(3):315-323

Ji, G., O'Brien, C.D. Feldman, M., Manevich, Y., Lim, P., Sun, J., Albelda, S.M., Kotlikoff, M.L. (2002) PECAM-1 (CD-31) regulates a hydrogen peroxide-activated nonselective cation channel in endothelial cells. *Journal of Cell Biology* 157(1):173-184

Junying Y., Vodyanik, M.A., Smuga-Otto, K., Antosiewicz- Bourget, J., Frane, J.L., Tian, S., Nie, J., Jonsdottir, G.A., Ruotti, V., Stewart, R., Sluvkin, I.I., Thomson, J.A. (2008) Induced Pluripotent Stem Cell Lines Derived From Human Somatic Cells, *Obstetrical and Gynecology Survey* 63(3): 154-155

Kasyanov, V., Sistino, J.J., Trusk, T.C., Markwald, R.R., Mironov, V. (2005) Perfusion Bioreactors for Cardiovascular Tissue Engineering (2005), In: *Bioreactors for Tissue Engineering: Principles, Design and Operation*, Chaudhari, J., Al-Rubeai, M. editors. Springer 285-307

Kemp (2006) London Regenerative Medicine Network Presentation, , Guy's Campus, Kings College London, 19th January, 2006.

Kim, B.S., Mooney, D.J. (1998) Development of Biocompatible Synthetic Extracellular Matrices for Tissue Engineering. *Trends in Biotechnology* 16(5): 224-230.

Kino-Oka, M., Taya M., (2005) Design and Operation of a Radial Flow Bioreactor for Reconstruction of Culture Tissues, In: *Bioreactors for Tissue Engineering: Principles, Design and Operation*, Chaudhari, J., Al-Rubeai, M. editors. Springer 115-133

Kletz, T.A., (1999) The Origins and History of Loss Prevention. *Process Safety and Environmental Protection*. 77(3):109-116.

Koc , O.N., Lazarus, H.M., (2001) Mesenchymal Stem Cells: Heading into the Clinic. *Bone Marrow Transplantation* 27: 235-239

Korbling, M., Anderlini, P. Peripheral Blood Stem Cell Versus Bone Marrow Allotransplantation: Does the Source of Hemaopoietic Stem Cells Matter? *Blood* 98(10): 2900-2908.

Kostatinov, K.B., Yoshida, T., (1992) Knowledge-based control of fermentation, *Biotechnology and Bioengineering* 39: 479-486

Kuo, C.K., Ma, P.X. (2001) Ionically cross-linked alginate hydrogels as scaffolds for tissue engineering: Part 1. Structure, Gelation rate and Mechanical Properties. *Biomaterials*, 22: 511-521

L'heureux N., (2007) Tissue-Engineered Blood Vessel for Adult Arterial Revascularization, *New England Journal of Medicine*, 357: 14.

L'heureux, N., Duserre, N., Konig, G., Victor, B., Keire, P., Wight, T.N., Chronos, N.A.F., Kyles, A.E., Gregory, C.R., Hoyt, G., Robbins, R.C., McAllister, T.N. (2006) Human tissue-engineered blood vessels for adult arterial revascularisation. 12(3) 361-365

L'heureux, N., Paquet, S., Labbé, R., Germain, L., Auger, F.A. (1998) A completely biological tissue-engineered human blood vessel, *The Federation of American Societies for Experimental Biology (FASEB) Journal* 12: 47-56.

L'Heurux, N., McAllister, T.N. (2007) Tissue-Engineered Blood Vessel for Adult Arterial Revascularization. *New Eng. J. Med.* 357(14):1451-1453.

Lakowicz, J.R., Weber, G. (1973) Quenching of Fluorescence by Oxygen. A Probe for Structural Fluctuations in Macromolecules (1973) *Biochemistry* 12(21): 4161-4670

Lamm, P., Juchem, G., Milz, S., Schuffenhauer, M., Reichart, B. (2001) Autologous Endothelialized Vein Allograft *Circulation* 104: I-108-I-114

Langer, R., Vacanti, J.P. (1993) Tissue Engineering, *Science*, 260: 920-926

Lennon D.P., Edmison, J.M., Caplan, A.I, (2001) Cultivation of Rat Marrow-Derived Mesenchymal Stem Cells in Reduced Oxygen Tension. Effects on in-vitro and in-vivo Osteochondrogenesis; *Journal of Cellular Physiology* 187(3): 345-355

Levenberg, S., Golub, J.S., Amit, A., Itskovitz-Eldor, J., Langer, R. (2002) Endothelial Cells Derived From Human Embryonic Stem Cells. *Proceedings of the National Academy of Sciences of the United States of America* 99(7): 4391-4396

Li, W., Tuli, R., Okafor, C., Derfoul, A., Danielson, K.G., Hall, D.J., Tuan, R.S. (2002) A Three-Dimensional Nanofibrous Scaffold for Cartilage Tissue Engineering

Using Human Mesenchymal Stem Cells, *Biomaterials* 26(6): 599-609

Lindner, V., Majack, R.A., Reidy, M.A. (1990), Basic Fibroblast Growth Factor Stimulates Endothelial Regrowth and Proliferation in Denude Arteries, *Journal of Clinical Investigation*, 85: 2004-2008

Lindquist, S., Craig, E.A. (1988) The Heat Shock Proteins, *Annual Review of Genetics* 22: 631-677

Locher, G., Sonnleiter, B., Fiechter, A., Automatic Bioprocess Control. 2. Implementations and Practical Experiences, *Journal of Biotechnology* 19: 127-144

Ludwig, T.E., Levenstein, M.E., Jones, J.M., Berggren, W.T., Mitchen, E.R., Frane, J.L., Carndall, L.J., Daigh, C.A., Conard, K.R., Piekarczyk, M.S., Llanas, R.A., Thomson, J.A. (2006) Derivation of human embryonic stem cells in defined conditions, *Nature Biotechnology* 24(2):185-7

Madden, R.L., Lipkowitz, G., Browne, B., Kurbanov, A. (2004) Experience with cryopreserved cadaveric vein allografts used for haemodialysis access. *Annals of Vascular Surgery* 18(4): 453-458

Mahmoudifar N., Doran, P.M., Tissue Engineering of Human Cartilage in Bioreactors Using Single and Composite Cell-Seeded Scaffolds. *Biotech, Bioeng.* 91(3):338-355.

Mantalaris, A., Keng, P., Bourne, P., Chang, A.Y.C., Wu, J.H.D. (1998) Engineering a

Human Bone Marrow Model: A Case Study on ex-vivo Erythropoiesis, *Biotechnology Progress* 14(1):

Markusen, J.F. (2005) Growth and Characterization of Cells Used to Design a Tissue Engineered Blood Vessel. *PhD Thesis*, University College London, University of London.

Marler, J.J., Guha, A., Rowley, J., Koka, R., Mooney, D., Upton, J., Vacanti, J. (2000) Soft-Tissue Augmentation with Injectable Alginate and Syngeneic Fibroblasts. *Plastic and Reconstructive Surgery* 105(6): 2049-2058

Marshall, C. (1992) The Design and Implementation of Comparative Reasoning Tools For Fermentations. *PhD Thesis*, University College London. University of London

Martin, I., Wendt, D., Heberer, M. (2004) The Role of Bioreactors in Tissue Engineering, *Trends in Biotechnology* 22(2): 80-86

Mason, C. (2003) Automated Tissue Engineering; A Major Paradigm Shift in Health Care, *Medical Device Technologies*, January/February 2003: 16-17

Mason, C. (2007) Regenerative Medicine 2.0 *Regenerative Medicine* 2(1): 11-18

Mason, C. (2007) The Time Has Come to Engineer Tissues and Not Just Tissue Engineer, *Regenerative Medicine* 1(3): 303-306.

Mason, C., Hoare, M. (2006) Regenerative medicine bioprocessing: the need to learn from the experience of other fields, *Regenerative Medicine* 1(5): 615-623

Mason, C., Town, M.A. (2002) Methods for forming hardened sheets and tubes. Patent #WO 02/077336 (Geneva World Intellectual Property Organisation).

Mason, C.M., (2008) Stem Cell Prospects, *New Scientist* 2640: 24

Matsumura, G., Hibino, N., Ikada, Y., Kurosawa, H., Shin'oka, T. (2003) Successful Application of Tissue Engineered Vascular Autografts: Clinical Experience. *Biomaterials* 24: 2303-2308.

Mavromastis, K., Fukai, T., Tate, M., Chesler, N., Ku, D.N., Galis, Z.S. (2000) Early Effects of Arterial Haemodynamic Conditions on Human Saphenous Veins Perfused Ex-Vivo. *Arteriosclerosis, Thrombosis and Vascular Biology* 20(8): 1889-1895

McFebridge, P.S., Chaudhari, J.B. (2005) Design of Vascular Graft Bioreactors, In: *Bioreactors for Tissue Engineering: Principles, Design and Operation*, Chaudhari, J., Al-Rubeai, M. editors. Springer 269-283

Metcalf, I.S. (1997) Chemical Reaction Engineering. *Oxford University Press*.

Minuth, W.W., Strehl, R., Schumacher, K. (2005) Microreactor Optimisation for Functional Tissue Engineering, In: *Bioreactors for Tissue Engineering: Principles, Design and Operation*, Chaudhari, J., Al-Rubeai, M. editors. Springer 19-45

Mirabet, M., Navarro, A., Lopez, A., Canela, E.I., Mallol, J., Lluís, C., Franco, R. (1997) Ammonium Toxicity in Different Cell Lines. *Biotechnology and*

Mironov, V., Kasyanov, V., McAllister, K., Sherrell, O., Sistino, J., Markwald, R. (2003) Perfusion Bioreactor for Vascular Tissue Engineering with Capacities for Longitudinal Stretch 14(3): 340-347

Mongia, N.K., Anseth, K.S., Peppas, N.A. (1996) Mucoadhesive poly (vinyl alcohol) hydrogels produced by freezing/thawing processes: Applications in the development of wound healing systems. *Journal of Biomaterials Science, Polymer Edition* 7(12): 1055-1064.

Mooney (2001) Nimble Progenitors Rescue Vascular Grafts, *Nature Medicine* 7(9): 996-997

Mooney, D.J., Baldwin, D.F., Suh, N.P., Vacanti, J.P., Langer, R. (1995) Novel Approach to Fabricate Porous Sponges of Poly(D,L-Lactic-co-glycolic acid) without the use of organic solvents. *Biomaterials* 17(14): 1417-1422

Mostafa, S.S., Miller, W.M., Papoutsakis, E.T., (2000) Oxygen Tension Influences Differentiation, Maturation and Apoptosis of Human Megakaryocytes, *British Journal of Haematology* 111: 879-889

Naughton, G.K., (2002) From Lab Bench to Market, Critical issues in Tissue Engineering, *Annals of the New York Academy of Sciences* 961: 372-385

Nerem R.M., Sambanis, A. (1995) Tissue Engineering: From Biology to Biological Substitute, *Tissue Engineering* 1(1): 3-13

Newman, P.J., (1997) The Biology of PECAM-1. *Journal of Clinical Investigation* 99(1): 3-8.

Nichols, J., Zevnik, B., Anastassiadis, K., Niwa, H., Klewe-Nebenius, D., Chambers, I., Scholer, H., Smith, A. (1998). Formation of Pluripotent Stem Cells in the Mammalian Embryo Depends upon the POU transcription factor Oct4. *Cell* 95: 379 – 391.

Niklason, L.E., Gao, J., Abbott, W.M., Hirschi, K.K., Houser, S., Marini, R., Langer, R. (1999) Functional Arteries Grown in Vitro, *Science* 284: 489-493.

Niklason, L.E., Langer, R.S. (1997) Advances in Tissue Engineering of Blood Vessels and Other Tissues, *Transport Immunology* 5: 303-306

Nwasokwa, O.N., (1995) *Coronary Artery Bypass Graft Disease*, *Annals of Internal Medicine*, 123(7): 528-533.

Oswald, J., Boxberger, S., Jorgensen, B., Feldmann, S., Ehninger, G., Bornhauser, M., Werner, C. (2004) Mesenchymal Stem Cells Can be Differentiated into Endothelial Cells In Vitro. *Stem Cells* 22(3):377-384.

Owens, G.K. (1995) Regulation of Differentiation of Vascular Smooth Muscle Cells. *Physiological Reviews* 75:487-517

Ozturk, S.S., Palsson, B.O. (1990) Chemical Decomposition of Glutamine in Cell Culture Media: Effect of Media Type, pH and Serum Concentration. *Biotechnology Progress* 6:121-128

Pachence, J.M., Kohn, J.(2000) Biodegradable Polymers In: *Principles of Tissue Engineering*. Lanza, R.P., Langer, R., Vacanti, J. editors. Academic Press, San Diego.

Peng, C., Palsson, B.O. (1996) Determination of Specific Oxygen Uptake Rates in Human Hematopoietic Cultures and Implications for Bioreactor Design. *Annals of Biomedical Engineering* 24:373-381

Pennathur-Das, R., Levitt, L. (1987) Augmentation of in-vitro human marrow erythropoiesis under physiological oxygen tension is mediated by monocytes and T lymphocytes. *Blood* 69(3): 899-907

Petrova, M., Koprinkova, P., Patarinska, T. (1997) Neural Network modelling of fermentation processes: Microorganisms cultivation model. *Bioprocess Engineering*, 16:145-149.

Phinney, D.G., Kopen, G., Righter, W., Webster, S., Tremain, N., Prockop, D.J. (1999) Donor Variation in the Growth Properties and Osteogenic Potential of Human Marrow Stromal Cells, *Journal of Cellular Biochemistry* 75: 424-436

Pittenger, M.F., Mackay, A.M., Beck, S.C., Jaiswal, R.K., Douglas, R., Mosca, J.D., Moorman, M.A., Simonetti, D.W., Craig, S., Marshak, D.R., (1999) Multilineage Potential of Adult Human Mesenchymal Stem Cells. *Science* 284:143-147

Portner, R., Nagel-Heyer, S., Goepfert, C., Adamietz, P., Meenen, N.M. (2005) Bioreactor Design for Tissue Engineering, *Journal of Bioscience and Bioengineering* 100(3): 235-245

Powers, D.E., Millman, J., Almedia, J.P.M.M, Colton, C.K. (2006) Culture Under Reduced Oxygen Dramatically Increases Differentiation of Murine Embryonic Stem Cells into Cardiomyocytes, *American Institute of Chemical Engineers Conference 2006*,: Tissue Engineering Section (11).

Przyborski, S.A., Morton, I.E., Wood, A., Andrews, P.W. (2001) Developmental Regulation of Neurogenesis in the Pluripotent Human Embryonal Carcinoma Cell Line NTERA-2. *European Journal of Neuroscience*. 12(10):3521-3528

Riha, G.M., Wang, X., Wang, H., Chai, H., Mu, H., Lin, P.H., Lumsden, A.B., Yao, Q., Chen, C. (2007) Cyclic Strain Induces Vascular Smooth Muscle Cell Differentiation From Murine Embryonic Mesenchymal Progenitor Cells *Surgery* 141(3): 394-402

Robertson, E.J. (1987) Teratocarcinomas and Embryonic Stem Cells: A Practical Approach. *Oxford: IRL Press*.

Robinson, B.I., Fletcher, J.P., Tomlinson, P., Allen, R.D., Hazelton, S.J., Richardson, A.J., Stuchberry, K. (1999) A Prospective Randomized Multicentre Comparison of Expanded Polytetrafluoroethylene and Gelatin-sealed Knitted Dacron Grafts for Femoropopliteal Bypass. *Cardiovascular Surgery* 7: 214-218.

Rosenborg, N., Martinez, A., Sawyer, P.N., Weslowsky, S.A., Postlthwait, R.W., Dillon, M.L., (1966) Tanned Collagen Arterial Prosthesis of Bovine Carotid Origin in Man. *Annual Surgery* 164:247.

Roszak, D.B., Colwell, R.R., (1987) Survival Strategies of Bacteria in the Natural Environment, *Microbiological Reviews* 51(3): 365-379

Safinia, L., Panoskaltsis, N., Mantalaris, A. (2005) Haemopoietic Culture Systems. In: *Bioreactors for Tissue Engineering: Principles, Design and Operation*, Chaudhari, J., Al-Rubeai, M. editors. Springer 309-334

Saltzmann, W.M., (2000) Cell Interactions with Polymer. In: *Principles of Tissue Engineering*, Second Edition, Lanza, R., Langer, R., Vacanti, J., editors, Academic Press 221-235.

Sardonini, C.A., and Wu, Y-J. (1993) Expansion and Differentiation of Human Haemopoietic Cells From Static Cultures Through Small-Scale Bioreactors. *Biotechnology Progress* 9: 131-137

Schey, H.M. (1997) *Div, Grad, Curl and All That – An Informal Text on Vector Calculus*. 3rd Edition, W.W. Norton and Company, New York.

Schonberg, J.A., Belfort, G. (1987) Enhanced Nutrient Transport in Hollow Fiber Perfusion Bioreactors: A Theoretical Analysis. *Biotechnology Progress* 3(22): 80-89

Schweder, T., Hecker, M. (2004) Monitoring of Stress Responses. *Advances in Biochemical Engineering and Biotechnology* 89: 47-71

Seborg, D.E. (1989) *Process Dynamics and Control* 1st Edition. John Wiley & Sons.

Seliktar, D., Black, R.A., Vito, R.P., Nerem, R.M. (2000) Dynamic Mechanical Conditioning of Collagen-Gel Blood Vessel Constructs Induces Remodelling In-Vitro (2000) *Annals of Biomedical Engineering*

Sen, A., Kallos, M.S., Behie, L.A. (2002) Passaging Protocols for Mammalian Neural Stem Cells in Suspension Bioreactors *Biotechnology Progress* 18: 337-345

Sergent-Tanguy, S., Chagneau, C., Neveu, I., Naveilhan, P. (2003) Fluorescent

Seruya, M., Shah, A., Pedrotty, D., Du Laney, T., Melgiri, R., McKee, J.A., Young, H.E., Niklason, L.E. (2002) Clonal Population of Adult Stem Cells: Life Span and Differentiation Potential. *Cell Transplantation* 13(2): 93-101

Shanahan, C.M., Weissberg, P.L., Metcalfe, J.C., (1993) Isolation of Gene Markers of Differentiated and Proliferating Vascular Smooth Muscle Cells. *Circulation Research* 73:193-204

Shimizu, N., Yamamoto, K., Obi, S., Kumagaya, S., Masumura, T., Shimano, Y., Naruse, K., Yamashita, J.K., Igrashi, T., Ando J. (2007) Cyclic Strain Induces Mouse Embryonic Stem Cell Differentiation Into Vascular Smooth Muscle Cells by Activating PDGF receptor β . *Journal of Applied Physiology* 104: 766-772.

Shin'oka, T., Imai, Y., Ikada, Y. (2001) Transplantation of a Tissue-Engineered Pulmonary Artery. *The New England Journal of Medicine* 344(7): 532-533

Siimes, T., Linko, P., Von Numers, C., Nakajima, M., Endo, I. (1995) Real-Time Fuzzy-Knowledge-Based Control of Baker's Yeast Production, *Biotechnology and Bioengineering*, 45: 135-143

Simmons, P.J., Tork-Storb, B. (1991) Identification of Stromal Cell Precursors in Human Bone Marrow by a Novel Monoclonal Antibody, STRO-1. *Blood* 78(1): 55-62

Stacey, G.N., Cobo, F., Nieto, A., Talavera, P., Healy, L. (2006) The development of 'feeder' cells for the preparation of clinical grade hES cell lines: Challenges and Solutions. *Journal of Biotechnology* 125(4): 583-588

Stanbury, P.F., Hall, S.J., Whitaker, A. (1999) *Principles of Fermentation Technology*. Butterworth-Heinemann, Oxford, UK.

Stock, U.H., Vacanti, J.P. (2001) Tissue Engineering: Current State and Prospects. *Annual Review of Medicine* 52:443-451

Strauer, B.E., Brehm, M., Zeus, T., Kosterling, M., Hernandez, A., Sorg, R.V., Kogler, G., Wernet, P. (2002) Repair of Infarcted Myocardium by Autologous Intracoronary Mononuclear Bone Marrow Cell Transplantation in Humans. *Circulation* 106: 1913-1918.

Szita, N., Boccazzi, P., Zhang, Z., Boyle, P., Sinskey, A.J., Jensen, K.F. (2005) Development of a multiplexed system for high-throughput bioprocessing, *Lab on a Chip* 5: 819-826

Takahashi, K., Tanabe, K., Ohnuki, M., Narita, M., Ichisaka, T., Tomoda, K., Yamanaka, S. (2007) Induction of Pluripotent Stem Cells from Adult Human Fibroblasts by Defined Factors. *Cell* 131: 1-12.

Talosa, L., Kostov, Y., Harms, P., Rao, G. (2002) Noninvasive Measurements of Dissolved Oxygen in Shake Flasks. *Biotechnology and Bioengineering* 80(5): 594-597

Teebken, O.E., Haverich, A. (2002) Tissue Engineering of Small Diameter Vascular Grafts, *European Journal of Vascular and Endovascular Surgery* 2: 475-485

Thilly, W.G. (1986) *Mammalian Cell Technology*, Butterworth, Boston.

Thomas, E.D., Lochte, H.L., Lu, W.C., Ferrebee, J.W. Intravenous Infusion of Bone Marrow in Patients Receiving Radiation and Chemotherapy. *New England Journal of Medicine* 257: 491-496

Thomson, J.A., Itskovitz-Eldor, J., Shapiro, S.S., Waknitz, M.A., Swiergiel, J.J., Marshall, V.S., Jones, J.M. Embryonic Stem Cell Lines Derived from Human Blastocysts (1988), *Science* 282: 1145-1147

Trelea, I.C., Titica, M., Landaud, S., Latrille, E., Corrieu, G., Cheruy, A. (2001) Predictive modeling of brewing fermentation from knowledge-based to black-box models. *Mathematics and Computers in Simulation* 56(4-5):405-424.

Tzima, E., Irani-Tehrani, M., Kiosses, W.B., Dejana, E., Schultz, D.A., Engelhardt, B., Cao, G., DeLiseer, H., Schwartz, M.A., (2005) A mechanosensory complex that mediates the endothelial cell response to fluid shear stress, *Nature* 437(15):426-431.

Vande Vord, P.J., Matthew, H.W.T., De Silva, S.P., Mayton, L., Wu, B., Wooley, P.H. (2002) Evaluation of the biocompatibility of a chitosan scaffold in mice. *Journal of Biomedical Materials Research* 59: 585-590.

Vestweber, D., Cadherin V.E. (2008) The major endothelial adhesion molecule controlling cellular junctions and blood vessel formation. *Arteriosclerosis, Thrombosis and Vascular Biology* 28:223-232.

Vorhees, A.B., Jaretski, A., Blakemore, A.H. (1952) The Use of Tubes Constructed

From Vinyon 'N' Cloth in Bridging Arterial Defects. *Annual Surgery* 135:332-336.

Wan, C., He, Q., McCaigue, M., Marsh, D., Li, G. (2006) Nonadherent Cell Population of Human Marrow Culture is a Complementary Source of Adult Human Mesenchymal Stem Cells. *Journal of Orthopaedic Research* 24(1): 21-8

Weaver, V.M., Petersen, O.W., Wang, F., Larabell, C.A., Briand, P., Damsky, C., Bissell, M.J. (1997) Reversion of the Malignant Phenotype of Human Breast Cells in Three-Dimensional Culture and In Vivo by Integrin Blocking Antibodies, *Journal of Cell Biology*, 137(1): 231-245

Weinberg, C.B., Bell, E., (1986) A Blood Vessel Model Constructed From Collagen and Culture Vascular Cells *Science* 231: 397-400

Williams, C., Wick, T.M. Perfusion Bioreactor for Small Diameter Tissue-Engineered Arteries, *Tissue Engineering* 10(5/6): 930-941

Williams, D. (2003) Revisiting the Definition of Biocompatibility, *Medical Device Technology*, October 2003: 10-13

Willis M.J. (1998) Proportional-Integral-Derivative Control.

http://www.appdigitech.com/PID_doc.pdf Accessed 13th January, 2010.

Wilmut, I., Peterson, L.A. Somatic Cell Nuclear Transfer (cloning) efficiency (2002) (online) (<http://www.roslin.ac.uk/public/webtablesGR.pdf>)

Winzler, R.J., (1941) The Respiration of Baker's Yeast at Low Oxygen Tension.
Journal of Cellular and Comparative Physiology, 17(3): 263-276

Wohlpert, D., Gainer, J., Kirwan, D. (2001) Oxygen Uptake by Entrapped Hybridoma Cells, *Biotechnology and Bioengineering* 37(11): 1050-1053

Wolpert, L., Smith, J., Jessell, T., Lawrence, P., Robertson, E., Meyerowitz, E. (2006)
Principles of Development 3rd Edition, Oxford University Press, Oxford, UK.

Wood, J.J., Malek, M.A., Frassica, F.J., Polder, J.A., Mohan, A.K., Bloom, E.T., Braun, M.M, Cote, T.R. (2006) Autologous Cultured Chondrocytes; Adverse Events Reported to the United States Food and Drug Administration *The Journal of Bone and Joint Surgery*, 88:503-507.

Woodley, J.M., Titchener-Hooker, N.J. (1996) The Use of Windows of Operation as a BioProcess Tool, *Bioprocess Engineering* 14: 263-268

www.advancedbiohealing.com

www.advancedtissue.com (In-active)

www.bristol.ac.uk/biochemistry/stephens/ypd.pdf

www.carticel.com

Xie, L., Wang, D.I., (1993) Fed-Batch Cultivation of Animal Cells Using Different Medium Design Concepts and Feeding Strategies. *Biotechnology and Bioengineering* 43: 1175-1189

Xue, L., Greisler, H.P., Blood Vessels, In: *Principles of Tissue Engineering*, Second Edition, Lanza, R, Langer, R, Vacanti, J. editors. Academic Press, San Diego 427-446.

Yamamoto, K., Sokabe, T., Watabe, T., Miyazono, K, Yamashita, J.K., Obi, S., Ohura, N., Matsushita, A., Kamiya, A., Ando, J., (2005) Fluid Shear Stress Induces Differentiation of Flk-1 positive embryonic stem cells into vascular endothelial cells in vitro. *American Journal Physiology - Heart and Circulatory Physiology* 288: H1915-1924

Yamanaka, S., (2007) Induction of pluripotent stem cells from mouse fibroblasts by

Yang, S., Leong, K., Zhaohui, D., Chua, C. (2001) The Design of Scaffolds for Use in Tissue Engineering. Part 1. Traditional Factors. *Tissue Engineering* 7(6): 679-689

Yaszemski, M.J., Payne, R.G., Hayes, W.C., Langer, R.S., Aufdemorte, T.B., Mikos, A.G. (1995) The Ingrowth of New Bone Tissue and Initial Mechanical Properties of a Degrading Polymeric Composite Scaffold, *Tissue Engineering*, 1(1): 41-52

Yeager, R.A., Hobson, I.I., Robert, W., Lynch, T.G., Jamil, Z., Lee, B.C., Jain, K., Keys, R. (1982) Analysis of factors influencing patency of polytetrafluoroethylene prostheses for limb salvage. *Journal of Surgical Research*. 32(5):499-506.

Yun, Z., Maecker, H.L., Johnson, R.S., Giaccia, A.J. (2002) Inhibition of PPAR-gamma2 Gene Expression by the HIF-1 Regulated Gene DEC1. *Developmental Cell*. 2(3):331-341.

Zadeh, L. (1983) The Role of Fuzzy Logic in the Management of Uncertainty in Expert Systems. *Fuzzy Sets and Systems* 11(1-3):197-198

Zanzotto, A., Szita, N., Boccazzi, P., Lessard, P., Sinskey, A., Jensen, K.F. (2004) Membrane Aerated Microbioreactor for High-Throughput Bioprocessing, *Biotechnology and Bioengineering* 87(2): 243-254

Zeng, A., Hu, W., Deckwer, W. (1998) Variation of Stoichiometric Ratios and Their Correlation for Monitoring and Control of Animal Cell Culture. *Biotechnology Progress* 14: 434-441

Zhao, F., Pathi, P., Grayson, W., Xing, Q., Locke, B.R., Ma, T. (2005) Effects of Oxygen Transport on 3-D Human Mesenchymal Stem Cell Metabolic Activity in Perfusion and Static Cultures: Experiments and Mathematical Model. *Biotechnology Progress* 21: 1269-1280.

Zhou, Y.H., Titchener-Hooker, N.J., (1999) Visualising Integrating Bioprocess Designs through “Windows of Operation”. *Biotechnology and Bioengineering* 65: 550-557

Zimmerman, U., Mimietz, S., Zimmerman, H., Hillgartner, M., Schneider, H., Ludwig, J., Hasse, C., Haase, A., Rothmund, M., Fuhr, G. (2000) Hydrogel-Based Non Autologous Cell and Tissue Therapy. *BioTechniques* 29(3) 564-581

Zulkeflee, S.A., Aziz, N. (2007) Control Implementation in Bioprocess System: A Review, *International Conference on Control, Instrumentation and Mechatronics Engineering (CIM'07)* 28-29 May 2007, Johor Bahru, Johor, Malaysia.